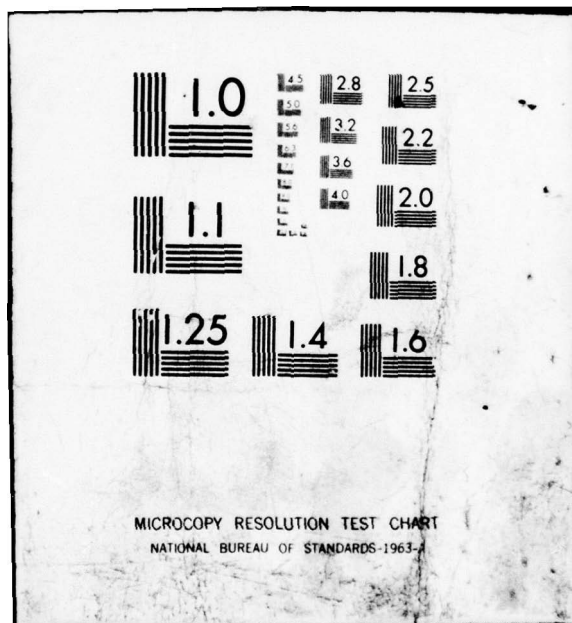


AD-A062 746

UNITED TECHNOLOGIES RESEARCH CENTER EAST HARTFORD CONN F/G 13/10
LIGHTWEIGHT PROPULSION SYSTEMS FOR ADVANCED NAVAL SHIP APPLICAT--ETC(U)
NOV 78 S C KUO, T L HORTON, H SHU, C W DEANE N00014-77-C-0735
UNCLASSIFIED NL

1 OF 3
AD
AD 82746





~~LEVEL~~ UTRC Report R78-952979-4
(12)

LIGHTWEIGHT PROPULSION SYSTEMS FOR ADVANCED NAVAL SHIP APPLICATIONS

PART II - CONCEPTUAL DESIGN AND RELIABILITY ANALYSIS

ADA062746

Annual Technical Report
November 1978

Simion C. Kuo - Principal Investigator

Travis L. O. Horton

Ho-Tien Shu

Charles W. Deane

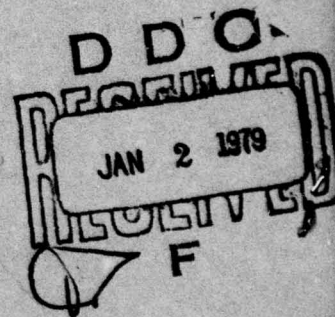
Earl R. Fisher

THIS DOCUMENT IS BEST QUALITY PRACTICABLE.
THE COPY FURNISHED TO DDC CONTAINED A
SIGNIFICANT NUMBER OF PAGES WHICH DO NOT
REPRODUCE LEGIBLY.

Prepared for

The Office of Naval Research, Arlington, Virginia

Under Contract No. N00014-77-C-0735



DDC FILE COPY

UNITED TECHNOLOGIES
RESEARCH CENTER



EAST HARTFORD, CONNECTICUT 06108

This document has been approved
for public release and sale; its
distribution is unlimited.

77-06-78-1

78 12·1 040

DISCLAIMER NOTICE

**THIS DOCUMENT IS BEST QUALITY
PRACTICABLE. THE COPY FURNISHED
TO DDC CONTAINED A SIGNIFICANT
NUMBER OF PAGES WHICH DO NOT
REPRODUCE LEGIBLY.**

(14) UTRC Report R78-952979-4

LIGHTWEIGHT PROPULSION SYSTEMS FOR ADVANCED NAVAL SHIP APPLICATIONS.

PART II - CONCEPTUAL DESIGN AND RELIABILITY ANALYSIS.

(9) Annual Technical Report

(11) November 1978

(12)

(12) 263p.

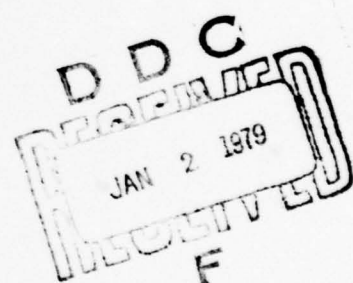
(10) Simion C. Kuo - Principal Investigator

Travis L. O. Horton,

Ho-Tien Shu

Charles W. Deane

Earl R. Fisher



Prepared for

The Office of Naval Research, Arlington, Virginia

Under Contract No. N00014-77-C-0735

**UNITED TECHNOLOGIES
RESEARCH CENTER**



EAST HARTFORD CONNECTICUT 06108

409252

77-05-78-1

78 12 · 1 040

UNITED TECHNOLOGIES RESEARCH CENTER



East Hartford, Connecticut 06108

R78-952979-4

Lightweight Propulsion Systems
for Advanced Naval Ship Applications
Part II - Conceptual Design and
Reliability Analysis

Annual Technical Report

A handwritten signature in black ink, appearing to read "Simion C. Kuo".

Dr. Simion C. Kuo
Principal Investigator
(203) 565-8758

Prepared for:
The Office of Naval Research, Arlington, Virginia
Under Contract No. N00014-77-C-0735
Mr. M. Keith Ellingsworth, Program Monitor

November 7, 1978

This document has been approved
for public release and sale; its
distribution is unlimited.

Lightweight Propulsion Systems for Advanced
Naval Ship Applications - Part II -
Conceptual Design and Reliability Analysis

TABLE OF CONTENTS

	<u>Page</u>
FOREWORD.	1
SUMMARY	2
RESULTS AND CONCLUSIONS	4
INTRODUCTION.	6
REFERENCES.	9
PHASE II-1 - HEAT SOURCE CHARACTERISTICS AND INTEGRATION PROBLEMS . .	10
1.1 State of the Art of Fossil-Fired Heaters.	10
1.2 Heater System Parametric Analyses	17
1.3 Heater System Compatibility and Integration Problems. . . .	23
1.4 Preferred Heater System	25
REFERENCES.	26
PHASE II-2 - SELECTION AND DEFINITION OF REFERENCE PROPULSION SYSTEM.	44
2.1 Ship Type Selection	44
2.2 Propulsion System Size and Installation Limitations	46
2.3 Baseline Propulsion System Selection.	48
2.4 Requirements for Baseline Propulsion System	52
REFERENCES.	54
PHASE II-3 - CONCEPTUAL DESIGN OF CLOSED-CYCLE HELIUM TURBINE PROPULSION SYSTEM	66
3.1 CCGT Component Design Conditions.	66
3.2 Turbomachinery Conceptual Design.	66

FOREWORD

The work described herein was performed by the United Technologies Research Center (UTRC) under Contract N00014-77-C-0735. Dr. Simion C. Kuo is the Principal Investigator for this contract. Included among those who assisted in performing this work were Messrs. T. L. O. Horton, E. R. Fisher, W. R. Davison, and Drs. H. T. Shu and C. W. Deane, all of UTRC. Mr. Sydney D. Parker and co-workers at Pratt & Whitney Aircraft Group/GPD prepared a conceptual design drawing for the reference 80,000-shp helium turbomachinery based on preliminary design data generated by UTRC. Mr. F. H. Boenig of Power Systems Division, United Technologies Corporation provided valuable comments and expert assistance on helium turbine design requirements. Additionally, Professor P. Mandel of MIT and J. J. Henry, Inc. provided valuable consulting services on advanced Naval ship characteristics and propulsion system integration requirements.

As a special work task (Phase II-6), an ONR/UTRC-sponsored fact-finding trip was made by S. C. Kuo to Japan for the purpose of discussing the latest development and crucial technical problems relating to open- and closed-cycle gas turbines, ship propulsion systems, gas-cooled nuclear reactors, and energy research at major heavy industry corporations and selected government agencies. An executive summary report, UTRC Report R77-952972-1, summarizing the major trip findings was submitted to ONR, November 1977.

The contract program was initiated with the Office of Naval Research on August 15, 1977, and the Technical Monitors of the program for ONR were LCDR William R. Seng from August 1977 to May 1978 and Mr. M. Keith Ellingsworth thereafter. Valuable guidance and comments received from Mr. Ellingsworth, LCDR Seng, and Mr. John R. Satkowski, Director, Power Program at ONR are gratefully acknowledged.



Lightweight Propulsion Systems
for Advanced Naval Ship Applications --
Part II - Conceptual Design and Reliability Analysis

SUMMARY

This report presents the results of conceptual design studies and reliability analyses as part of a comprehensive study program to evaluate the technological and economic feasibility of utilizing open- and closed-cycle gas turbines integrated with fossil or nuclear heat sources for providing advanced lightweight propulsion power for future Navy capital ship applications. The level of technology considered is that judged by the Contractor to be available during the 1990's.

The state-of-the-art for fossil-fired heaters was reviewed, and a heater system configuration most suitable for integration with the closed-cycle gas turbine for lightweight ship propulsion applications was selected. Subsequently, parametric performance, size, and weight analyses were performed for the selected heater system, and the problems of integrating the heater with the power conversion system aboard a Naval ship were investigated.

Utilizing a "Benefit-Matrix" screening process, a conceptual high-speed destroyer with maximum/cruise speeds of 50/20 knots was selected as the reference ship type, and an 80,000-shp closed-cycle helium turbine (two needed) was selected from the candidate baseline closed-cycle engines identified earlier (Part I - System Studies) to provide propulsion power for the high-speed destroyer. The conceptual design of the 80,000-shp propulsion power system, including material selection, component designs, engineering drawings, and weight estimates for the turbomachine, heat exchangers, and ducting was performed with technical support from the Pratt & Whitney Aircraft Group/GPD, United Technologies Corporation in the area of turbomachine detailed design drawings.

Based on the hull dimensions and structural arrangement provided by Professor P. Mandel of MIT, the preliminary propulsion system layout aboard the conceptual high-speed destroyer was prepared with consulting support from J. J. Henry, Inc., particularly in the area of shipboard constraints and interface requirements for Naval ships. Figures showing the engine room locations, power conversion system layout, and overall propulsion system integration with the ship are presented. The operational characteristics of the propulsion system using selected power level control methods were investigated.

The reliability characteristics of the reference 80,000-shp closed-cycle helium gas turbine power conversion system were predicted, and they were compared with those estimated for conventional steam turbine power systems in ship propulsion applications. These reliability estimates were made based on a methodology formulated using the block diagram approach which incorporated appropriate adjustment factors and various means allowable for improving reliability characteristics through realistic maintenance schedules and power system reconfiguration. The estimated reliability values are presented in figure form to show their sensitivity to variation in repair/replacement criteria and reconfiguration time allowed.

The major observations and conclusions for the fact-finding trip to Japan as reported in an executive summary report UTRC Report R77-952972-1 issued to ONR are reproduced in this report as Appendix B.

The study program was conducted by the Energy Conversion Systems group at UTRC under Contract N00014-76-C-0735 from the Power Program Branch of the Office of Naval Research, Arlington, Virginia.

RESULTS AND CONCLUSIONS

1. Fossil-fired closed-cycle gas turbines using helium heater designs which incorporate aircraft-derivative technology offer the potential of lightweight propulsion systems for improving mission capabilities of advanced Navy capital ships.
2. The performance capability of the reference closed-cycle gas turbine (CCGT) propulsion system will be limited by the temperature capability of the helium heater; this limit is currently approximately 816 C (1500 F) for land-based systems with normal plant lifetime (30 years). A helium heater operating at this temperature in the marine environment is expected to have a shorter lifetime, perhaps less than 30,000 hours.
3. For Naval propulsion applications, helium heater designs incorporating disposable hot-sections may be employed to achieve higher turbine inlet temperatures or increased overall system lifetime.
4. A parametric design study of the size and weight characteristics of various helium heaters leads to the conclusion that implementation of aircraft derivative technologies in a hot-gas generator/hot-gas boiler type (rather than the conventional combustion-chamber type) would be imperative to achieve a lightweight design suitable for Naval ship applications.
5. The preferred helium heater system selected for the reference 80,000-shp CCGT propulsion system has a specific weight of approximately 2.7 Kg/kW (4.5 lb/shp), and a heater thermal efficiency of 87.5 percent; the overall package of the heater system has a length of 10 m (33 ft) and a diameter of 4.9 m (16 ft).
6. A conceptual high-speed destroyer (approximately 4000-ton displacement) capable of 50/20 knots max/cruise speed was identified to benefit the most from implementing the CCGT lightweight propulsion system.
7. A closed-cycle helium turbine power conversion system which produces 59.7 MW (80,000-shp) on a single output shaft would be most suitable for providing propulsion power (two units needed) for the conceptual high-speed destroyer in the 1990's.
8. The reference 80,000-shp closed-cycle helium turbomachine design incorporating aircraft derivative technology is relatively compact and lightweight compared with the industrial-design helium turbines; at a specific weight of 0.16 Kg/kW (0.26 lb/shp), the reference CCGT is regarded as suitable for lightweight propulsion system applications.

9. The tube-in-shell type of heat exchanger with small, bare tubes is selected for the design of the three heat exchangers on the basis of reliability and of being compact and lightweight. The distributed type of heat exchanger design is chosen (over integrated designs such as wrap-around) to facilitate maintainability, thereby improving reliability. The heat exchanger package (regenerator, precooler, and intercooler) weighs 0.92 kg/kW (1.53 lb/shp).
10. The conceptual-design 80,000-shp CCGT propulsion system is compact enough to be installed in the engine room allocated without severe integration problems with other propulsion system components; the locations and sizes of the engine rooms were specified in accordance with the Naval requirements for ship stability and floodable length.
11. The start-up, reverse-thrust, and other operational characteristics of the reference closed-cycle gas turbine propulsion system meet the requirements projected for the conceptual high-speed destroyer. Only a small heater and a small helium circulator are needed to keep the recuperator warm to avoid excessive thermal stress during the rapid start-up.
12. A lightweight propulsion system using closed-cycle helium gas turbines could be more reliable than the conventional steam turbine propulsion system for both conventional and high-speed destroyer applications.
13. The power conversion system reliabilities calculated allowing neither repair/ replacement nor alternate operating configurations are 0.42 for the CCGT system and 0.10 for the conventional steam turbine system.
14. Both the closed-cycle gas turbine and the conventional steam turbine power conversion systems must rely on alternate operating configurations to achieve high mission reliabilities above the 0.90 level; without the power system reconfiguration, the reliability ranges would be 0.4 to 0.83 for the CCGT system and 0.1 to 0.4 for the steam turbine system, depending on the types of repair/ replacement schedules implemented.
15. While introducing the routine at-sea repair/replacement maintenance practice would drastically improve the reliability of both the closed-cycle gas turbine and conventional steam turbine power systems (by approximately 0.15 to 0.35 depending on reconfiguration time allowed), implementation of more stringent maintenance practice with major repair/replacement at sea would achieve only a small (less than 0.1) improvement in reliability.

INTRODUCTION

For Navy planners to successfully meet future challenges, understanding the potential for lightweight ship propulsion (LWSP) systems, their technological and economic feasibilities, and the level of efforts and time required to bring about a practical system would appear a crucial issue indeed. Lighter propulsion systems can be beneficial to Naval ship performance in many ways, including improved strategic and tactical operational capabilities resulting from increased speed and/or endurance time, increased payload or reduction in ship size and cost, as well as independence from refueling in foreign ports. Recently, there have been many debates in Congress and elsewhere on the fate of the surface effect ship (SES) design and of large nuclear-powered aircraft carrier construction programs; many studies have been performed on the relevance of various advanced Naval vehicle types (Refs. 1, 2, and 3). The necessity for such studies has stemmed partly from demands for better ship performance, mission capability, payload, and cost effectiveness, and partly from increasing uncertainties in the future Naval fuel demand/supply situation. Regardless of ship type, the mission capabilities and cost effectiveness of a Naval ship often depend significantly on the specific weight, performance, reliability and cost characteristics of the propulsion system utilized.

Previous advancements in marine propulsion systems have often resulted from changes in the type of fuel available. As fuel type changed successively from wood to coal, from coal to oil, and recently from oil to nuclear fuels, new concepts in propulsion systems have evolved. Naval propulsion systems have traditionally relied on coal- or oil-burning steam turbines while most current commercial and some Naval ships are powered by lower power diesel engines which are more efficient, noisier, and less flexible. While the question has arisen whether diesel engines would be displaced by nuclear propulsion systems using steam turbines, open-cycle gas turbines also have been recognized as being capable of providing lightweight, quiet, and responsive propulsion for Naval combat ships (Ref. 4 and 5). Despite some operational problems and relatively short lifetimes, the open-cycle gas turbine system is certain to receive continued attention for selected applications. However, factors such as environmental impact, safety, fuel availability, and cost effectiveness for oil-fired and nuclear-powered system concepts have been undergoing close re-examination triggered by the nuclear controversy and the increasingly uncertain future oil supply. Therefore, the future Naval fleet may have to operate efficiently on a number of energy sources - all the traditional sources plus potential new ones such as synthetic fuels, or even fluidized coal beds (Ref. 6).

Such diversity of fuel types could lead to a very complex Naval fleet operation, particularly if different propulsion systems were used for each fuel type. Thus, propulsion system commonality would simplify many aspects of fleet

operation while improving mission flexibility as well. Although conventional steam turbine systems offer such multi-fuel capability because of external combustion, they are too massive for small (less than 6000 tons displacement) high-performance ship propulsion applications. In this context, the closed-cycle gas turbine appears to offer considerable advantages since it is easily adaptable to various heat sources, fossil or nuclear, and since it has been demonstrated to operate efficiently and reliably. Recent technological advances in land-based power generation systems using the CCGT concept (Refs. 7, 8, and 9) would indicate that it is prudent to assess its feasibility for Naval ship propulsion applications, particularly through conceptual design studies and reliability analysis.

Unlike the land-based constant-speed powerplants, turbomachinery designs for the CCGT propulsion system must be harmonized with the transmission type as well as the thruster operating requirements, particularly in terms of shaft RPM which represents another variance from the land-based powerplants in terms of performance, weight, reliability, and economic characteristics. Furthermore, to develop a practical propulsion system layout, the physical dimensions and possible limitations inherent with the propulsion system components must be identified, and their integration with a selected ship type must be investigated.

Although many of the land-based CCGT plants have been operating reliably, with some accumulating over 110,000 hours (Ref. 7), the reliability of light-weight CCGT propulsion systems operating in the marine environment aboard high-speed ships will definitely suffer. Furthermore, the CCGT propulsion system envisioned for lightweight propulsion applications would operate at a turbine inlet temperature of 816 C (1500 F), which is well above existing plant temperatures limited to approximately 700 C (1300 F) designed decades ago. This increased turbine inlet temperature would also contribute to additional uncertainties regarding system reliability. It should be mentioned that despite several conceptual design studies attempted in the past (Refs. 8, 10, and 11), no practical closed-cycle propulsion engine has ever been installed and operated aboard a ship; and thus marine operational experience is totally lacking. Therefore, in this follow-on study of lightweight propulsion systems, it is timely to undertake, based on the results of Part I System Analysis (Ref. 12), a conceptual design of a reference 80,000-shp CCGT propulsion system for applicable Navy ship (high-speed destroyer) installations and to project expected levels of operational reliability to enable an overall feasibility assessment for this type of lightweight propulsion system.

Therefore, a conceptual design and reliability analysis were performed for a 59.7 MW (80,000-shp) CCGT system as installed in a conceptual high-speed destroyer hull capable of 50 knots maximum speed. The work reported herein is the second part of an ONR-sponsored study program to assess the technological feasibility and reliability of CCGT propulsion systems for advanced Naval ship

applications. The work performed in the Part I study was first extended to include estimates for the characteristics and integration problems of appropriate heat sources. Then, a reference ship type and propulsion system were selected to establish the constraints and design specifications for the preliminary conceptual design which followed. The conceptual design defined the aeromechanical characteristics for all the critical power conversion system components including: fossil-fueled heater, helium turbomachinery, heat exchangers, ducting, and major accessories. From this conceptual design, the CCGT-LWSP system was designed for installation within the confines of a refined estimate for a 50-knot destroyer hull form. Preliminary operational characteristics were also estimated for this installation.

Finally, to assess one of the most important Naval operational characteristics, reliability, a detailed study was made to evaluate the probability of success of a selected mission (mission reliability) for both the CCGT-LWSP and a conventional steam turbine propulsion system. A comparison was made of these two systems which included the consideration of many varied philosophies of operation which might typically occur in the Navy application. The results will allow future comparisons to be made between the CCGT and other propulsion systems by a separate, relative comparison of the new system to the conventional steam system.

The results of the Part II - Conceptual Design and Reliability Analysis, are presented in this report in five sections. An appendix is also included for detailed coverage of analytical procedures used to perform the reliability analyses. Phase II-1 presents the heat source characteristics and integration problems. Phase II-2 defines the selected reference propulsion system. Phase II-3 describes the preliminary conceptual design, while Phase II-4 presents the system layout and preliminary operational characteristics of this design, as installed in the selected ship type. The last Phase II-5, presents the reliability evaluation followed by an appendix which expands upon this subject.

REFERENCES

1. Rainey, P. G.: Basic Ocean Vehicle Assessment. Naval Engineers Journal, April 1976.
2. Kehoe, J. W.: Warship Design - Ours and Theirs. Naval Engineers Journal. February 1976.
3. Goldman, R., and R. Peterson: Planning and Development for a New Generation of Gas Turbine Propelled Ships in the U.S. Navy. ASME Paper 74-GT-158.
4. DeBiasi, V., and I. W. Sawyer: Worldwide Status of the Marine Gas Turbine. ASME Paper 70-GT-44, 1970.
5. Rains, D. A., and R. J. d'Arey: Considerations in the DD963 Propulsion System Design. Naval Engineers Journal, August 1972.
6. MacIntyre, K. R.: Ship Fuels - Alternatives to Oil. Paper presented to Royal Institution of Naval Architects in London, and excerpted in Motor Ship Magazine article "Ex-King Coal May Reign Again," January 1978.
7. Kuo, S. C.: Recent Development of Closed-Cycle Gas Turbines and Gas-Cooled Reactors in West Germany and Switzerland. UTRC Report No. R76-952566-2, October 1976.
8. Kuo, S. C.: Status of Technological Development of Gas Turbines, Nuclear Reactors, and Naval Shipbuilding in Japan - An Executive Summary. UTRC Report No. R77-952972-1, November 1977.
9. Boenig, F. H., and R. I. Strough: HTGR Direct Cycle Turbomachinery Technology, Final Program Report prepared for General Atomic Co., Report No. PSD-R-106, September 1976.
10. Anon.: 16,000-shp Closed-Cycle Gas Turbine for Marine Propulsion, Escher Wyss Report, 1950.
11. Rackley, R. A.: Marine Closed Gas Turbine and LNG Refrigeration System Study - Part I, Closed Gas Turbine Marine Power Systems, Marad Report No. MA-RD-920-175003, June 30, 1974.
12. Kuo, S. C., T. L. O. Horton, and H. T. Shu: Lightweight Propulsion Systems for Advanced Naval Ship Applications -- Part I -- Systems Studies. UTRC Report No. R77-952566-5, submitted to ONR, May 1977.

Lightweight Propulsion Systems for Advanced Naval Ship
Applications--Part II - Conceptual Design and Reliability Analysis

PHASE II-1

HEAT SOURCE CHARACTERISTICS AND INTEGRATION PROBLEMS

The state of the art of fossil-fired heat sources suitable for integration with closed-cycle helium gas turbines was reviewed, and candidate heater systems selected for the lightweight ship propulsion application were characterized with respect to performance, size, and weight.

1.1 State of the Art of Fossil-Fired Heaters

A comprehensive survey was performed to identify the state of the art of various fossil-fired air and helium heater designs and technologies including: the conventional combustion chamber (i.e., boiler types) (Refs. 1 and 2); the hot-gas generator/hot-gas boiler (Refs. 3 and 4); fluidized beds (Refs. 5 and 6); the configuration with moving ceramic packing (Ref. 7); and the compact shell-and-tube design (Refs. 8 to 10).

Conventional combustion chamber heaters have been used to heat the working fluid (air) in many closed-cycle turbine plants with ratings which range from 2,300 to 14,300 kW. Generally, these units incorporate a two-pass design arranged vertically, where the combustion chamber with top-mounted burners constitutes the first (downward) pass. Typically, a single row of tubes surrounds the gas path to form the radiation section. The heat transfer surface of the convection section is located in the second (upward) gas pass, and above this is located the air preheater. The working fluid from the air inlet header mainfold flows through the heater tubes in cross counter-flow to the combustion gases in the convection section and then is collected in an outlet header manifold. From this point, the working fluid flows parallel to the combustion gas flow downward through the radiation section, whereupon it is collected into a pipe leading to the turbine. As noted in Ref. 3, the combustion-chamber type of heater tends to be bulky because of three major factors: (1) only half of the heating surfaces of the combustion chamber walls are utilized since the outside half of the surface is not exposed to the hot gases; (2) the amount of heat transferred by radiation is small in comparison with that transferred by convection because of the small temperature difference between the combustion gases and heater tubes

in the radiation section; and (3) the shape of the convection heating surface is governed by the dimensions of the combustion chamber. Examples of the combustion-type air heaters are those in the Toyotomi plant in Japan (a 2000-kW natural-gas-fired CCGT unit) with dimensions at approximately 13.5 x 8.5 x 4 meters; and the Ravensburg plant in Germany (a 2300-kW light-oil-fired CCGT unit) with dimensions of approximately 20 x 8 x 4 meters. Although the overall dimensions depend on many factors which include tube arrangement, cycle pressure loss, and fuel, the conventional combustion chamber heater design does not appear to be attractive for a lightweight ship propulsion system because of its size.

A modification of the conventional combustion chamber design is called a hot-gas generator/hot-gas boiler, and an example of its use is the helium heater for the Oberhausen II plant in Germany. In this type of system, the combustion takes place at nearly adiabatic conditions within a refractory-lined combustion chamber called the hot-gas generator. In the Oberhausen II design, the burner and air intake are located at the front face, the hot flue gases leave the chamber at the rear, and heat is transferred to the tube bundles by both convection and gas radiation (Refs. 4 and 11). The basic idea behind the development of this type of combustion system was to separate the combustion process from the heat transfer process. This design not only eliminates practically all flame radiation but also reduces the volume of the overall heater system by some 30 to 40 percent relative to the conventional combustion-chamber type discussed above. In the Oberhausen II helium heater, Incoloy 807 tubing is used for the high-temperature heat-exchanger surfaces. The outer diameters of the tubes range between 31.8 and 63.5 mm, and wall thicknesses are approximately 3 mm. The maximum allowable metal temperature of 800°C (1472°F) was selected to provide a design lifetime of 100,000 hours. The weight of tubing alone is approximately 100 tons (2.98 lb/shp), the overall dimensions, including the air preheater, are approximately 17.5 x 12.5 x 8 meters, and the overall heating efficiency is 92.2 percent. The concept of separating the combustion process from heat transfer process to reduce the overall heater size has a positive impact on the current study.

The fluidized bed furnace and heater system is currently being used in over 200 domestic installations to roast pyrite ores and in over 100 additional domestic systems to incinerate industrial wastes and sludge from sewage plants. In addition, there has been an extensive amount of experience with the use of fluidized bed systems, both in industrial processes (particularly the catalytic cracking and reforming of gasoline) and in experimental coal combustion systems coupled with steam boilers. The advantage of using fluidized bed systems is that the heat transfer coefficient on the gas side of the fluidized bed is 3 to 5 times that on the gas side of conventional combustion chamber systems. The increase in heat transfer coefficient would be even greater if a pressurized fluidized bed or a shallow fluidized bed were employed. In terms of present

shipboard propulsion system applications, the disadvantages of the fluidized bed heater system include: (1) complicated control system requirements for startup, shutdown, and load changes; (2) unsteady or unpredictable performance characteristics due to the change of bed surface level accompanying pitch, roll, shock, and vibration during normal ship operation; (3) added weight represented by the bed material; and (4) the high pressure drop in the combustion chamber which would degrade the heater efficiency. Because of these factors, the fluidized bed concept will not be considered further during the present parametric study. A similar conclusion was also drawn for the moving ceramic packing-type gas heater concept (Ref. 7).

The three experimental shell-and-tube helium heater designs, described in detail in Refs. 8, 9, and 10, represent a significant departure from commercial practices for gas heating. To meet the heat transfer requirement within a fixed volume, the helium heater design for the advanced test reactor (ATR) design of Ref. 8 utilized a two-stage heater of concentric tubular heating elements where the gas flowed through the inside of the heating element tubes. The first-stage heating element material was Nichrome, while the second-stage heater element material was molybdenum. A 110-kW electric element was used to heat the helium from 815.5°C (1500°F) to 1148.9°C (2100°F) at a pressure level of 24.13 bars (350 psi). This configuration had been installed in the model loop and was operated successfully for 1600 hours at helium exit temperatures of 1093.3°C (2000°F) to 1148.9°C (2100°F) during most of its operating time. Except for identifying possible tube material selections, no other application was found for this experimental system.

The helium heater developed by the Rocketdyne Division of the Rockwell International Corporation (Ref. 9) was designed to heat helium from approximately 500°C (932°F) to 815.5°C (1500°F) at a pressure of 1000 psi for testing of a power conversion loop of a regenerative helium Brayton cycle suitable for use in a nuclear reactor power plant. The general requirements and design criteria of the Rocketdyne system are quite similar to those of the lightweight ship propulsion study except that the helium volume in the heater and the pressure drop through the heater more closely match those of a nuclear system. A heater system cycle configuration similar to Configuration II in Fig. 1.1 was employed in the Rocketdyne heater performance analysis and component design except that the hot gases leaving the combustor were diluted by the compressor discharge air instead of air from the heater exit. This configuration not only limits the heater efficiency but also requires increased air/gas flow through each component. In the Rocketdyne heater design, which contains 349 Variflux concentric-tube assemblies per module, the pressurized combustion gases (at about 50 psi, or a compression ratio of 4.3) flow through the inner tube, and the high-pressure helium flows through the annular passage (approximately a 0.25 in. gap) between the inner and outer tubes. Inconel 617 was selected for the inner tubes (25.4-mm ID and 38.1-mm OD), while Inconel 800 was selected for

outer tubes (50.8-mm ID and 53.34-mm OD). The combustor, which is designed to accommodate two-stage combustion in order to reduce NO_x emissions, is joined to the heater tube assemblies to form a helium heater module. Either fuel oil or natural gas can be burned, and with fuel oil the overall heater system efficiency has been calculated to be 75.5 percent. Each heater module (which includes a combustor, a flame shield, and a helium heater) is approximately 9.75 m (32 ft) in length and 1.98 m (6.5 ft) in diameter and approximately 52,514 kg (115,000 lbs) in weight for an energy output of 55,669 kW (52,778 Btu/sec) per unit.

In the marine gas turbine study of Ref. 10, Garrett/AiResearch presented an analysis and a conceptual design for a 20,000-shp CCGT engine helium heater system. The cycle configuration considered is similar to that shown in Configuration IV of Fig. 1.1. This type of heater system is derived essentially from the open-cycle gas-turbine concept, and instead of producing mechanical energy or thrust from an expansion turbine or a nozzle, the heat energy of the combustion gas is transferred to another working fluid of the power conversion system through a heat exchanger which is defined as the heater in the present study. In general, this type of heater system consists of four major components: the air compressor or blower with mechanical drive; the fuel combustor; the heater; and the air preheater (optional). A compressor or a blower is required not only to draw in the combustion air but also to enhance the combustion process and to allow a reduction in the size, weight, and capital cost of the heater. A small gas generator from an open-cycle gas turbine can be easily modified and used as the air compressor. The air preheater (if it were needed) would be a low-temperature and low-pressure, gas-to-gas heat exchanger, and consequently, would not be a critical component. The combustor and the high-temperature heater, however, are the two most critical components in the present system because a specific type of fuel and precisely controlled operating conditions are required in addition to specifically imposed external constraints. Further discussion of the development status of these two components is presented below.

Combustor

It appears that combustion chambers developed for the open-cycle gas turbine engines can be modified to provide heat-input to the CCGT systems. If natural gas or liquid distillate fuels were specified, only minor modifications to the combustion chambers used in aircraft gas turbine engines would be required; use of a residual oil would require adoption of single or multiple combustors developed for industrial gas turbines. The differences in combustor design arise from the fact that residual fuels have a higher carbon-to-hydrogen ratio, a higher viscosity, and a higher carbon content than do distillate fuels.

The high carbon-to-hydrogen ratio of residual fuels increases the radiant energy heat release (low luminometer number) to the combustion chamber walls

as well as increased carbon formation tendency for deposition when compared to the combustion of distillate fuels. Furthermore, inadequate fuel atomization of residual fuels caused by high viscosity can lead to poor spray patterns and particle dispersion, and in turn, these can produce long flames which could impinge on the combustor walls. Both single and multiple combustors have been used successfully for industrial gas turbines burning residual fuel. Single combustion chambers are generally favored by European industrial gas turbine manufacturers (Ref. 11) especially for high-powered turbines. The single combustion chamber encompasses a reverse-flow chamber having a single fuel nozzle located in a swirl-type air register. This configuration, which has been used as a standard design by Brown Boveri for many years, usually is found as a free-standing configuration, placed vertically with the air entry on one side and the hot-gas discharge vertically downward. The English Electric and DeLaval Ljungstrom Turbine Company units also utilize large, simple, vertical chambers in their units rated at 6,000 kW and above. Based on their many years of experience, Brown Boveri claims (Ref. 12) that a wide variety of fuels can be burned in these combustors with only minor modifications required to the fuel nozzle which is located in the center of the primary-air intake to assure proper air-fuel mixing.

Considerable effort in the United Kingdom was also expended by Ruston & Hornsby, Ltd. and the National Gas Turbine Establishment (NGTE) on the elbow- and vortex-type of single combustion chambers where the residual air used for mixing is introduced at right angles to the primary air and fuel. The turbulence produced by the right-angled entry of the secondary air assists in the combustion in the main chamber. The vortex-type combustion chamber in which the walls provide vortex flow of air and fuel was developed by NGTE (Ref. 14) as a method of providing sufficient time for complete combustion of the individual residual oil particles and as a device to contain the ash formed during combustion. However, the development of the vortex-type chamber was abandoned when later developments with conventional combustion chambers proved that adequate mixing and combustion could be achieved even with the heaviest fuels.

American manufacturers of residual-oil-burning gas turbines, principally General Electric and Westinghouse, have favored multiple combustion chamber designs. These chambers (as many as 12 are used for a single turbine) follow aircraft engine practice by employing bands of holes in the flame tube to introduce the primary air for combustion in approximately stoichiometric quantities. Secondary air for wall cooling and exit temperature control is then added through additional holes in the last two-thirds of the combustor. Both GE and Westinghouse use reverse-flow configurations to keep the chamber length as short as possible.

In selecting optimum combustor dimensions, it should be recognized that excessive heat losses may be increased in attempting to achieve complete combustion. Although 100 percent fuel combustion could be achieved by allowing greater residence time, the percentage heat loss from the combustor would increase, and the exit gas temperature would decrease. An optimal combustor geometry (the length/diameter ratio) which could achieve good mixing of fuel and oxidizer and also minimize heat losses can only be determined experimentally from the operating conditions of mass flow rate, pressure, temperature, stoichiometric ratio, maximum residence time, and heat loss.

Materials for combustion containment are of two major types: metals and refractories. Several varieties of metals can be used for combustion containment depending on the nature of the environment, size of containment, and economic considerations. Included are copper and copper alloys, high-alloy steels, and high-nickel alloys. Each has unique properties of thermal conductivity, high-temperature strength, and immunity to stress-corrosion cracking. Although copper has seen considerable application in small-scale, clean-fuel combustors, it will probably be replaced by austenitic stainless steels and high-nickel alloys as combustor sizes are increased. Stress-corrosion cracking can occur in these latter two classes of materials; for example, the stainless steels are highly prone to stress-corrosion cracking due to attacks by the chlorides in salt water. Although the same is true for some high-nickel alloys, other grades exhibit rather high resistance to chloride attack. In general, there appears to be an adequate selection of state-of-the-art metals to meet design requirements. Most refractory materials can provide good resistance to erosion. However, other properties of refractory materials may be more important than their ability to withstand erosion. These include such factors as the ability to withstand thermal stresses developed during heat-up and cool-down, and high-thermal gradients across the component parts during steady-state operation.

High Temperature Heater

The selection of combustion chamber type depends not only on the helium heater characteristics but also on other environmental constraints. Requirements of the helium heater include the ability to heat helium to temperatures of 1,500°F or higher; to operate at helium pressures of 600 psia or higher; to attain fast thermal response compatible with the load variation requirements; to be compact, lightweight, and in low cost; and to display high reliability and reasonable maintainability. There is no existing heat exchanger which can satisfy all these requirements. Various design models (Refs. 15 to 19) have been proposed and investigated, including the Rocketdyne dual-concentric-tube "Vari-flux" helium heater, the Garrett AiResearch multipass crossflow tube/shell helium heater, the Bobcock Atlantique compact plate heat exchanger, the General Electric composite tube crossflow air heater (coal-fired), and the Sulzer EVO

helium heater. Except for the EVO heater which has been operating since 1974, all these heaters are in varying stages of development.

The critical problems encountered in helium heater design include the material selection, the design to achieve uniform temperature, high-temperature fabrication, and the thermal expansion problems in both the tubes and the headers. The selection of material depends on the size and weight requirements, lifetime constraints, and cost characteristics. The most important factor which should be considered in any system with this type of (indirect-fired) heater is the temperature and/or material limitations imposed by the vanadium, sodium, and other harmful ash elements in the fuel. In many respects, these limitations are similar to those imposed on present-day steam systems used in central power stations and marine propulsion. Because of this, the upper steam temperature limit in residual-oil-fired marine applications is presently about 510 to 540°C, while that in coal-fired central power station steam systems is restricted to temperatures of 565 to 595°C. Field and laboratory tests have indicated that the corrosion caused by the ash in burning fuels increases rapidly as metal temperatures exceed 595°C. In oil-fired boilers, magnesium-based additives can be added to the fuel before or during combustion to suppress excessive ash corrosion at temperatures as high as 705°C. Shields have been used successfully in some operational boilers where liquid-ash corrosion has occurred. However, the appreciable reduction of heat transfer (by 25 to 30 percent) limits the use of shields.

For metal temperatures above 700°C, the use of additives and/or more corrosion-resistant materials such as nickel-base alloys would be required. The materials commonly used for the heater are Inconel 800, Inconel 617, Hastalloy X, and Nb-1Zr. Prices of these materials vary from \$1.7 to \$28 per foot for typical 19 mm (OD) tubing. Another important cost factor is the header fabrication which could run as high as \$60 per tube when Nb-1Zr is used. The GE composite tube used in demonstration tests consists of an Inconel liner inside a silicon carbide sheath. At combustion-gas temperatures above 1090°C, the silicon carbide sheath is strong enough to contain the pressurized gases while the Inconel acts as a seal to prevent leakage. The ceramic outer sheath also provides a corrosion-resistant barrier to the coal ash (and presumably would also be suitable for oil ash) and hence permits turbine inlet temperatures as high as 926.7°C to be attained. Another study conducted by the Navy also indicates that the use of an indirect-fired gas turbine power plant using compact heat exchanger surfaces in the heater offers a possible solution to the sulfidation problem.

The technological advancements associated with the various heater designs reviewed to date provide a guideline for parametric performance analyses and component size and weight estimates of the lightweight fossil-fired heater systems. These are discussed in the following section.

1.2 Heater System Parametric Analyses

The criteria and general requirements for selecting candidate fossil-fired heat source configurations are summarized in Table 1.1. A heater which would satisfy these criteria and requirements aimed at achieving lower specific weight and higher shock resistance represents a significant departure in design approach when compared with conventional practices of steam boilers and gas heaters for a chemical process plant.

1.2.1 Alternate Heater System Configurations

Based on the results of a literature survey, four candidate configurations (I, II, III, and IV) were selected for parametric performance analyses. These are depicted in Fig. 1.1.

In general, the fossil-fired heater required in a closed-cycle gas turbine ship propulsion system consists of seven components: an air intake; an air compressor or blower with mechanical drive; a fuel combustor; a turbine to drive the compressor; a gas heater; an air preheater (optional); and a gas uptake. The required air filtration and exhaust gas sound proofing equipment are included in the intake and uptake components. A compressor or blower is used not only to supply the combustion air but also to enhance the combustion efficiency in the combustor to reduce the size, weight, and capital cost of the overall heater system.

Configuration I of this study is based on the open-cycle gas turbine system. In this configuration, the heat of combustion is transferred to the helium working fluid through a heat exchanger (helium heater) instead of being used to produce power via a power turbine. The Configuration I system has the advantages of simplicity and a maximum utilization of the existing technologies and equipment which should reduce the development cost and shorten the time schedule. However, the large air/gas flow through each component would mean that bigger and heavier equipment (which would have higher capital costs) would be required.

Configuration II is a modified form of Configuration I wherein a part of the combustion gas is recirculated from the helium heater exit to dilute the hot combustion gas leaving the combustor. There are two major advantages to this approach: (1) the intake-air and uptake-gas flows would be reduced substantially (about 50 percent) which would reduce the sizes of intake duct, compressor, air preheater, and uptake duct; and (2) the combustor can be operated close to the stoichiometric combustion condition to improve the overall thermal efficiency since the hot gas can always be diluted to a desirable temperature by the recirculating gas.

The thermodynamic temperature-entropy (T-S) diagrams (Frame (a) of Fig. 1.2) for these configurations indicate that the gas temperature exhausted from the uptake duct might still be high because the maximum air preheater effectiveness is limited by the compressor exit temperature. A modification of Configuration II is embodied in Configurations III and IV. In addition to the two advantages discussed before, Configuration III and IV should further improve the cycle thermal efficiency and also reduce the turbine size. In Configuration III, the recirculation gas is directed from the exit of the air preheater back to the mixer to dilute the hot combustion gas from the combustor. In Configuration IV, the recirculating gas is extracted from the heater exit and recirculated back to the main stream as in the previous case.

The temperature-entropy diagram for Configurations III and IV is shown in frame (b) of Fig. 1.2. Although the recirculating and mixing processes using air to dilute the hot gas to a desired temperature level are not shown, these processes can be imagined as those describing paths between the state point 6 (or 7) to a point along the process from point 4 to point 5.

1.2.2 Parametric Performance Analyses

Before parametric performance analyses could be undertaken, two basic ground rules had to be established: (1) integration requirements with the power conversion system (i.e., thermal capacity, helium inlet and outlet conditions, and mass flow rate) must be identified initially; and (2) the parameters (and their applicable ranges) which might significantly affect the heater performance must be identified.

In order to establish the first ground rule, the results presented in the Part I System Studies (Ref. 20) were reviewed. It is well known that the cycle thermal efficiency increases as the regenerator effectiveness is increased. However, the pressure drop and the size (and hence, cost) of the regenerator also increase as effectiveness increases. The larger pressure drop will adversely affect the cycle efficiency. An optimal regenerator effectiveness can be determined from the trade-off between cycle efficiency (incorporating the effect of increasing pressure loss) and the system capital costs. It should be mentioned that when the regenerator effectiveness increases, the sizes of heater and precooler decrease. Taking these observations into consideration, the UTRC computer programs developed for closed-cycle gas turbine cycle performance and component conceptual design analyses were modified to incorporate the relationships among the heat transfer coefficient, working fluid physical properties, heat exchanger geometry alternatives, and pressure loss characteristics. By combining the thermodynamic performance program with the component sizing programs, the overall cycle pressure loss variation and their resultant cycle thermal efficiencies for various regenerator effectiveness could be computed through an iteration process to satisfy both the thermodynamic conditions and the

mechanical design conditions specified for the system component. A series of system optimization studies were undertaken for 59,680-kW (80,000 shp) helium CCGT power conversion system (Ref. 21), and these results were used as part of the inputs for heater system performance analyses (Table 1.2). The parameters and their applicable ranges which would significantly affect the heater system performance are also summarized in Table 1.2.

A range of pressure ratios from 3.0:1 to 5.0:1 was selected for the turbo-compressor which supplies the combustion air in the heater system. This range of pressure ratios can be achieved by a single-stage centrifugal compressor at a mechanical efficiency of approximately 75 percent or by an axial flow compressor (incorporating 3 to 4 stages) at a mechanical efficiency of approximately 88 percent. The combustion air pressure loss was estimated to be in the range of 4 to 10 psi to provide reasonable designs for the air preheater and the helium heater. During these optimization studies, it was observed that the effect of pressure loss on the helium heater thermal efficiency is less significant than on the component size and weight characteristics; this effect is discussed in a subsequent section of this report.

The maximum helium temperature leaving the helium heater is dictated by the maximum allowable metal temperature of the heater. Since ceramic core heaters are not likely to withstand the high shock and vibration encountered during naval operations, it was assumed that a superalloy metal heat exchanger will be required, and that the maximum metal temperature could not exceed 982.2°C (1800°F). Finally, the temperature of combustion gas, which will not only affect the heater cycle efficiency but also will control the intake and uptake air/gas flow, was assumed to be in the range from 1204.4°C (2200°F) and 2200°C (4000°F). The selection of the lower limit temperature of 1204.4°C was based on the consideration of heater metal temperature limitation in the flow path downstream of the turbine for Configuration I; whereas, the selection of 2200°C applies that in Configurations II, III and IV. These assumptions are based on the observations that: (1) the maximum temperature rise across the combustor is approximately 1750°C (3150°F) at stoichiometric condition with the combustion of marine diesel fuel; and (2) the selection cycle pressure ratio ranges between 3.0:1 and 5.0:1. As mentioned earlier, the hot gas in Configurations II, III and IV can always be diluted to the desirable temperature by the recirculated gas; furthermore, a higher combustion gas temperature would be beneficial in reducing the component size.

The maximum air preheater effectiveness is normally affected by the allowable cycle pressure loss limitations. Through the use of the State-of-the-Art Performance Program (SOAPP), an automatic balancing of the allowable cycle pressure loss, the helium inlet and exit temperature differences, and the fraction of recirculation gas required was established to obtain the maximum attainable air preheater effectiveness for improved heater cycle thermal efficiency.

The thermal properties of the combustion products formed when Marine Diesel Fuel (MDF) is burned is based on a simplified chemical reaction model developed and incorporated into the SOAPP program. The MDF properties were obtained from ONR (Ref. 22), and for reference, these are tabulated in Item A of Table 1.3. The simplified chemical reaction model presented in Table 1.4 contains the constants C_1 , C_2 and C_3 which were calculated from the MDF properties. For a selected helium heater thermal capacity and the given temperature differences between the combustion gas and the helium gas at the inlet and outlet stage, the SOAPP program computes the required fuel-air ratio based on the lower heating value of Marine Diesel Fuel. The computed fuel-air ratio was then transferred to the simplified chemical reaction model to calculate the percentage of excess air, and the mole fraction of each constituent. The validity of this simplified model has been checked (to a level of about 99.7 percent accuracy) by comparing its results with those obtained from a more comprehensive computer program (Ref. 23) which was developed by the Utilities Power Systems Group of UTRC for a coal gasification study.* A sample result of the computed equilibrium composition of combustion gas is presented as Item B of Table 1.3. These data have been used in helium-heater and air-preheater design and reliability analyses, and they will continue to be used whenever the need arises.

Based on the use of the two ground rules, the SOAPP model, and the simplified chemical reaction model program, the performance results shown in Figs. 1.3 and 1.4 were obtained. Figure 1.3 presents comparisons of heater system efficiencies as a function of helium inlet/gas exit temperature difference and combustion gas temperature (which has been converted into fuel/air ratio) for a heater inlet temperature and cycle pressure loss. The results indicate that Configuration III and IV indeed are superior to the other two configurations. Similar conclusions can also be drawn from Fig. 1.4 which shows the comparison of intake air flow rates as a function of the same independent variables.

The effects of cycle pressure drop and air-preheater effectiveness on the heater performance for Configurations III and IV are shown in Figs. 1.5 and 1.6 for air/gas flow rate and heater efficiency, respectively. Figure 1.5 indicates that more intake air flow and uptake gas flow would be needed to achieve the required propulsion power when the cycle pressure drop decreases. The difference between the uptake and intake flow is the fuel flow required. The results presented in Fig. 1.6 indicate that increased system pressure drop would provide improved heater efficiency. However, the requirement that the uptake discharge

* This latter program is called Equilibrium Model for Coal Gasifiers and was developed based on Gibb's free energy to calculate the equilibrium composition of mixture of gases and a solid. The program was implemented on UNIVAC 1110 system and cannot be easily linked to the SOAPP program which is processed on the IBM 360 system. Consequently, it was decided to develop a simplified model to couple with the SOAPP program for the overall heat source system performance analyses.

pressure must exceed one atmosphere would limit the maximum attainable pressure drop. For example, a system having the overall pressure drop greater than 15.5 percent would be unable to discharge combustion gases through its uptake, and therefore, such a system would not be feasible. On the other hand, for a system pressure drop less than or equal to nine percent, efficiency would be lowered, and the system would be very bulky and heavy; therefore, it too would not be attractive. It becomes obvious that the applicable overall cycle pressure drop for the LWSP fossil heater system should fall in the range of from 10 to 15 percent. The effects of compression ratio on the component size and weight were found substantial, and these are discussed in the next section.

1.2.3 Parametric Size, Weight and Cost Estimates

Component design point specifications (inlet and exit temperature, pressure, and mass flow rate) identified from the heater system cycle analyses were used as input data to estimate the heater system size and weight characteristics from the component conceptual design programs. Subsequently, the results from the component design program were used as input data for the cost model to estimate the overall system cost.

An axial flow turbocompressor was chosen to circulate the air and combustion gas because of its superior isentropic efficiency in comparison with centrifugal-type machines. Design parameters such as rotational speed, blade tip speed, stage work coefficient, flow coefficient, and exit swirl angle were estimated through a series of computer calculations which allowed reasonable blade sizes, hub-tip ratios, and stress levels to be attained. In the air preheater and helium heater designs, counterflow shell-and-tube-type heat exchangers were selected for analysis because of their high reliability and outstanding structural integrity. In order to reduce the heater size and weight, tube sizes of 6.35 mm and 8.89 mm OD (0.25 and 0.35 inches) were chosen for air preheater and helium heater, respectively. However, design safety factors of 3.0 and 4.5, respectively, were used to assure the high reliability. Modular construction where each module consists of 85 tubes provides minimum modular volume (Ref. 24). All 85 tubes would be attached by means of welded-joints to a two-inch tube at each of their ends; in turn, the two-inch tubes of each module would then be attached to the tubesheets. In view of naval operating requirements, the combination of tube-end-welding and rolled expansion joint may be the best tube-to-tubesheet attachment for long-term, trouble-free service.

Material selections for each component had to be specified at this point in the program to provide the necessary basis for the stress analyses. It should be emphasized that whereas the material selection depends on the component operating conditions, it also dictates the component size and cost. However, detailed material selection have to be reviewed later during the conceptual design phase descriptions. For the present parametric analysis, tentative selections

were: for the low-temperature sections (such as intake and uptake components), low carbon steel, and for the high-temperature sections (such as combustor, mixer, helium heater tubing and shell), Inco 718 and/or Hastalloy X. AISI 410 was selected for compressor airfoils and disks, and Udimet 700 and AMS 5718 was chosen for turbine airfoils and disks, respectively. For air preheater tubing and shell, AISI 347 and AISI 4340, were used.

Both distributive and semi-integrated heater system concepts were investigated. The distributive system is the most desirable from reliability, maintainability, and weight balance viewpoints, while the semi-integrated system is more attractive from system compactness and weight viewpoints. Although the distributive heater system concept has been selected for use in the final propulsion system layout, the semi-integrated concept was also investigated to provide a comparison of the overall size and weight for different heater cycle configurations. The semi-integrated heater systems for Configuration III and IV are shown in Figs. 1.7 and 1.8. The results of the analysis are presented in Figs. 1.9 to 1.11.

Figure 1.9 shows the effect of allowable cycle pressure loss on the overall heater system thermal efficiency, size, and weight at the maximum attainable air preheater effectiveness for the 59,680-kW (80,000-shp) engine of Configuration IV. If pressure loss were increased from 8 to 16 percent (from 4 psi to 8 psi), the thermal efficiency would decrease from 91.2 percent to 87.4 percent, while the specific weight would decrease from 3.7 to 2.70 kg/kW (6.08 to 4.44 lb/shp) as shown in the lower frame of Fig. 1.9. Similarly, the upper frame of Fig. 1.9 shows the decreases in length and diameter with increased pressure loss. From these results, a reference heater system can be selected based on trade-offs among the efficiency, size and weight. Similar results were also obtained for Configuration III. To facilitate comparisons between Configurations III and IV, the results are presented in terms of efficiency, size, weight, and cost as a function of heater efficiency in Figs. 1.10 and 1.11.

Figure 1.10 shows that the performance of Configuration IV is better than that of Configuration III when both are compared at the same geometrical sizes. In other words, Configuration IV still represents a more attractive heater system for the present application. For the Configuration IV system, the overall heater length ranges from 32 to 38 feet and its diameter from 10 to 14 feet for acceptable heater efficiencies. These dimensions could conceivably be reduced through appropriate rearrangement of each component within the package if a more detailed conceptual design of the heater system were undertaken. However, this activity is beyond the scope of the present study.

Figure 1.11 shows the estimated weight and cost characteristics of the overall heater systems including the intake (duct, silencer, and demister) and

uptake (duct, silencer and eductor). The total heater weight would vary from 2.13 to 3.40 kg/kW (3.5 to 5.6 lb/shp) if Configuration IV were considered.

The individual component costs were obtained with assistance from the UTRC cost estimating computer model which includes the compressor, combustor and mixer, turbine and recirculating fan, casing, inlet and outlet guide vane, bearings, fuel control, air preheater, helium heater, intake and uptake systems, and control systems. The overall system cost was estimated by summing these component costs and multiplying by a factor of 1.20 which includes an allowance for the cost of assembly plus other items such as insulation, etc. The results are shown in the lower frame of Fig. 1.11. Again, it can be seen that from the point of view of total system cost, Configuration IV is more attractive than is Configuration III. It is concluded that the heater system represented by Configuration IV should be selected as the candidate system to meet the integration requirement for the ship type selected.

1.3 Heater System Compatibility and Integration Problems

The design of the fossil heater system for the closed-cycle gas turbine depends to a considerable extent on the application. In contrast to systems associated with land-based power generation stations, the integration of the heater system with: 1) a selected power conversion system; 2) a particular ship type; and 3) the marine environmental requirements, imposes additional constraints on the selection of heater cycle configurations and design conditions. Although the parametric performance analyses conducted in this program and discussed in the previous section for all four configurations have been based on a power conversion system rating of 59,680-kW (80,000-shp) CCGT engine, the preliminary performance analyses and size and weight estimates indicated that Configurations I and II cannot meet the compact, lightweight, and high reliability requirements considered in this study. Between Configurations III and IV, the latter appears to be more attractive for naval ship propulsion application.

In selecting a candidate heater system, potential problems which could accompany the integration of the propulsion engine (power conversion system) and the ship powered by this LWSP system should also be investigated. These are discussed below.

1.3.1. Integration with Propulsion Engine

There are two very critical problems in terms of integrating the heater system with the propulsion engine. These two problems are: 1) the need to minimize the length of duct and the bends between the recuperator exit and the heater inlet and between the heater exit and the high pressure turbine inlet; and 2) the requirement to provide adequate thermal response to the propulsion engine when the propulsion load changes. As a solution to the integration problem, the

distributive heater concept (discussed in a previous section) can be employed, and each component of the heater system can be properly arranged and designed to meet the integration requirement. Addressing the thermal response problem, since the turbine inlet temperature (TIT) of the propulsion engine will remain essentially constant because of the inherent characteristics of inventory control, the temperature of the combustion gas entering and leaving the heater should be as close to their design point as possible. This can be accomplished by a control device which would properly correlate the following major parameters: 1) the mass flow rate of the propulsion engine; 2) the fraction of the recirculation gas inside the heater loop; 3) the fuel/air ratio; and 4) the mass flow rate of the combustion air. It is expected that because the temperature at each key point throughout the entire propulsion engine system (heater system and power conversion system) will not change when the propulsion load is varied, the thermal efficiencies of the heater system and the power conversion system should not decrease significantly. Based on the same reasoning, the rate of the thermal input variation required in response to the change in load demand should not cause any severe temperature-related component failure. On the other hand, the thermal input response which occurs during the start-up period will be different primarily because this response rate is controlled by thermal stress (or temperature rise per minute) of materials selected for the heater system. This cold-iron start-up response cannot be determined without detailed component conceptual design which is beyond the scope of the current program.

1.3.2 Integration With Ship

The integration problem with the ship cannot be fully determined without knowledge of the type of ship to be selected and at the very least, a preliminary conceptual design of the heater system. The following discussion is based on the results from the above system parametric performance and preliminary component parametric design analyses.

The three major problems of integrating the heater system with the ship are those associated with: 1) the available engine room space; 2) the combustion air intake and gas uptake subsystem characteristics; and 3) the heater efficiency and the fuel supply system capability and requirement.

In an effort to determine the available engine room space, a reference ship type had to be selected. For the present study, a high-speed destroyer (HSD) ship type displacing 3,500-to 4,000-metric tons, and providing maximum and cruise speeds of 50 and 20 knots, respectively, was selected as a reference ship for propulsion system integration and layout studies. Based on the results of a ship analysis (Ref. 24), the maximum engine room dimensions available for the heater system and the propulsion engine including reduction gearbox were approximately 13 meters in width and 14 to 16 meters in length. These dimensions provided a guideline for selecting the candidate heater system.

The results of Fig.1.5 indicate that the mass flow of air intake for Configuration IV (which has been identified to be the most promising configuration among those four configurations shown in Fig. 1.1) varies from 68.5 to 70.0 Kg/sec (151.0 to 154.3 lb/sec) and that of the exhaust gas varies from 72.0 to 73.5 Kg/sec (158.7 to 162.0 lb/sec). When the component size limitation and the heater efficiency requirements are considered, the mass flow rate of the intake air and the exhaust gas of the candidate heater system would be approximately 69 Kg/sec (152 lb/sec) and 75 Kg/sec (166 lb/sec) respectively. These air and exhaust gas flow rates are slightly less than half of those needed in the DD963 propulsion systems. In the present parametric performance and design analyses of heater system (Section 1.2.2), the pressure losses in the intake and uptake components were assumed to be the same as those used in the DD963 system design. Therefore, no major integration problem would be expected in terms of the intake and uptake design and installation.

Finally, the candidate heater system also must satisfy the minimum heater efficiency requirement which is the most important factor in estimating the fuel capacity and the ship endurance. It is obvious that a heater system which can provide better heater efficiency and which will not exceed the size limitation should be selected. One of the heater design requirements (Table 1.1) is that a candidate heater system must be able to achieve a heater efficiency equal to or greater than 85 percent.

1.4 Preferred Heater System

Combining the heater system design criteria, the performance requirements, and the component size limitation, a preferred heater system can be selected from Fig. 1.9. The cycle definition of the selected preferred fossil-fired heater system is shown in Fig. 1.12. The overall length and diameter of this selected system are approximately 10 and 4.9 meters (33 and 16 ft) respectively, its specific weight is about 2.7 Kg/kW (4.5 lb/shp), its overall cycle pressure loss is 15 percent, and its cycle thermal efficiency is 87.5 percent.

REFERENCES

1. Hass, W.: Air Heater, Heat Exchanger and Cooler for CCGT Plant. Closed-Cycle Gas Turbines for All Fuels, Escher Wyss, 1969.
2. Bammert, K. and E. Nickel: Design of Combustion Chambers of Heaters for Transmission of the Primary Heat of Closed-Cycle Gas Turbines, ASME Paper No. 66-GT/CLC-1, March 1966.
3. Bienz, J. and H. N. Sharan: Hot Gas Generator/Hot Gas Boiler - A New Combustion System for Producing Steam and Heat. Sulzer Technical Review, 1/1973.
4. Bammert, K.: Layout and Present Status of the Closed-Cycle Helium Turbine Plant Oberhausen, ASME Paper 74-GT-132.
5. Fraas, A. P., et al: Design Study for Coal-Fueled Closed Cycle Gas Turbine System for MIUS Application, IECEC '75 Record, pp. 260-268.
6. Brown, D. H., et al: Energy Conversion System Alternatives Study (ECAS), General Electric Phase II Final Report, Vol. II, Part 2, Closed Turbine Cycles, NASA-CR-134949, December 1976.
7. Pomerantsev, V. V., et al: Results of Laboratory, Commercial and Design Investigations of Air Heater with Moving Ceramic Packing, Thermal Engineering, Vol. 23-3, 1976.
8. Evans, R. J.: A Two-Stage 2100 F Helium Gas Heater for the ATR Model Gas Loop, Eng. Development Dept., Pacific Northwest Lab., Richland, Washington, November 1966.
9. Larson, V. R., S. V. Gunn, and J. C. Lee: Helium Heater Design for the Helium Direct Cycle Component Test Facility, AIAA Paper No. 75-1262, October 1975.
10. Rackley, R. A.: Marine Closed Gas Turbine and LNG Refrigeration System Study, Vol. I - Closed Gas Turbine Marine Power Systems, Report No. MA-RD-920-75003.
11. Tipler, W.: Combustion in European Industrial Gas Turbine, ASME Paper No. 61-WA-82 presented in New York, December 1961.
12. Kind, C.: The Behavior of Gas Turbine Combustion Chambers While Burning Different Fuels, ASME Paper 60-GTP-10 presented in Houston, Texas, March 1960.

13. Feilden, G. B. R., J. D. Thorn, and M. J. Kemper: A Standard Gas Turbine to Burn a Variety of Fuels. Institution of Mechanical Engineers Proceedings, Vol. 170, 1956.
14. Lloyd, P., and R. P. Probert: The Problem of Burning Residual Oils in Gas Turbines. Institution of Mechanical Engineers, Vol. 163, 1950.
15. Larson, V. R., and S. V. Gunn: Helium Heater Design for the Helium Direct Cycle Component Test Facility. AIAA Paper No. 75-1962, presented in Anaheim, California, September 1975.
16. Rackley, R. A.: Marine Closed Gas Turbine and LNG Refrigeration System Study, Part 1 - Closed Gas Turbine Marine Power Systems, Rep. No. MA-RD-920-75003, June 1974.
17. Tillequin, J. F.: Compact Heat Exchanger for Fluid at High Temperature and Pressure. Conference on Recent Developments in Compact High Duty Heat Exchangers, The Institution of Mechanical Engineers, October 12, 1972.
18. LeHaye, P. G.: High Temp Heat Exchanger for Closed-Cycle Coal-Fired Gas Turbine, Gas Turbine, March-April 1967.
19. Kuo, S. C.: Recent Development of Closed-Cycle Gas Turbines and Gas-Cool Nuclear Reactors in West Germany and Switzerland, UTRC Report R76-952566-2, October 1976.
20. Kuo, S. C. et al: Lightweight Propulsion Systems for Advanced Naval Ship Applications, Part I - System Studies. UTRC Report R77-952566-5, May 1977.
21. Kuo, S. C. and H. T. Shu: Alternative Closed-Cycle Gas Turbine System Design Considerations for Ship Propulsion Applications. ASME 78-GT-18, April 1968.
22. Telephone conversation with LTCMDR W. R. Seng, August 30, 1977.
23. Robson, F. L., W. A. Blecher and C. B. Colton: Fuel Gas Environmental Impact, Appendix A, EPA-600/2-76-153, June 1976.
24. Bullock, Jr., H. O.: Consultation on Lightweight Propulsion System Layout and Integration. J. J. Henry Report No. 6654 to UTRC, July 1978.

TABLE 1.1

FOSSIL HEAT SOURCE CYCLE CONFIGURATION SELECTION
CRITERIA AND GENERAL REQUIREMENTS

- Integrable with helium CCGT ship propulsion system and naval ships
- Overall heater efficiency greater than 85 percent
- Compact and low specific weight
- High reliability and good maintainability
- Use of Marine Diesel Fuel
- Maximum hot spot metal temperature less than 985°C (1805°F)
- Maximum utilization of existing component technology

TABLE 1.2

FOSSIL HEATER SYSTEM PERFORMANCE PARAMETERS AND RANGES

<u>Parameters</u>	<u>Ranges</u>
Helium Inlet Temperature	453 C (848 F)
Helium Inlet Pressure	45.96 bars (66.6 psi)
Helium Outlet Temperature	815.55 C (1500 F)
Helium Outlet Pressure	44.82 bars (650 psi)
Helium Mass Flow Rate	75.22 kg/sec (165.82 lb/sec)
Compression Ratio	3:1 to 5:1
Cycle Pressure Loss	0.276 ~ 0.689 bars (4 ~ 10 psi or 8 ~ 20%)
Air Preheater Effectiveness	20 ~ 90%
Hot Gas Inlet/Helium Exit Temperature Difference	55.5 ~ 277.7 C (100 ~ 500 F)
Hot Gas Exit/Helium Inlet Temperature Difference	27.8 ~ 138.9 C (50 ~ 250 F)
Combustion Gas Temperature	1204.4 ~ 2204.4 C (2200 ~ 4000 F)

TABLE 1.3

FUEL SPECIFICATION AND COMBUSTION GAS
CHARACTERISTICS FOR REFERENCE DESIGN

A. Fuel: Marine Diesel Fuel

Low Heating Value	=	18300 Btu/lb (42567 kJ/kg)
Hydrogen Weight Percentage	=	12.7%
Carbon Weight Percentage	=	86.8%
Sulfur Weight Percentage	=	0.5%
Potassium Hydroxide	=	.3 ppm

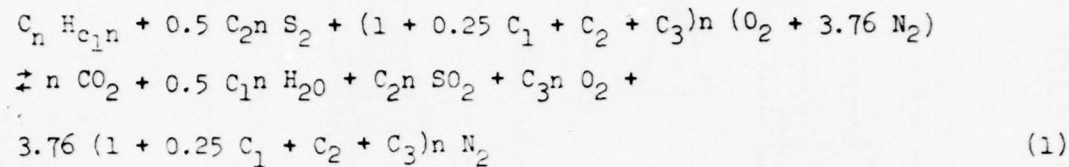
B. Combustion Product Mixture for Fuel Air Ratio of .057755

<u>Species</u>	<u>Mole Fraction</u>
CO ₂	.114640
H ₂ O	.099936
SO ₂	.000247
O ₂	.034728
N ₂	.750450
KOH	.015738 ppm

TABLE 1.4

SIMPLIFIED CHEMICAL REACTING FLOW MODEL BASED
ON MARINE DIESEL FUEL

A. Chemical Equation



where

$$\left. \begin{aligned}
 c_1 &= 1.74342 \\
 c_2 &= 0.00216 \\
 c_3 &= 0.10055 \div (\text{fuel air ratio}) - 1.43801
 \end{aligned} \right\} \tag{2}$$

B. Excess Air (EXA), Total Number of Moles (TNM), and Mole Fraction (MF)

$$EXA = 1.0 + .6954 c_3 \tag{3}$$

$$TNM = 4.76 + 1.44 c_1 + 4.76 c_2 + 4.76 c_3 \tag{4}$$

$$MF \text{ of } CO_2 = 1/TNM \tag{5}$$

$$MF \text{ of } H_2O = 0.5 C_1 TNM \tag{6}$$

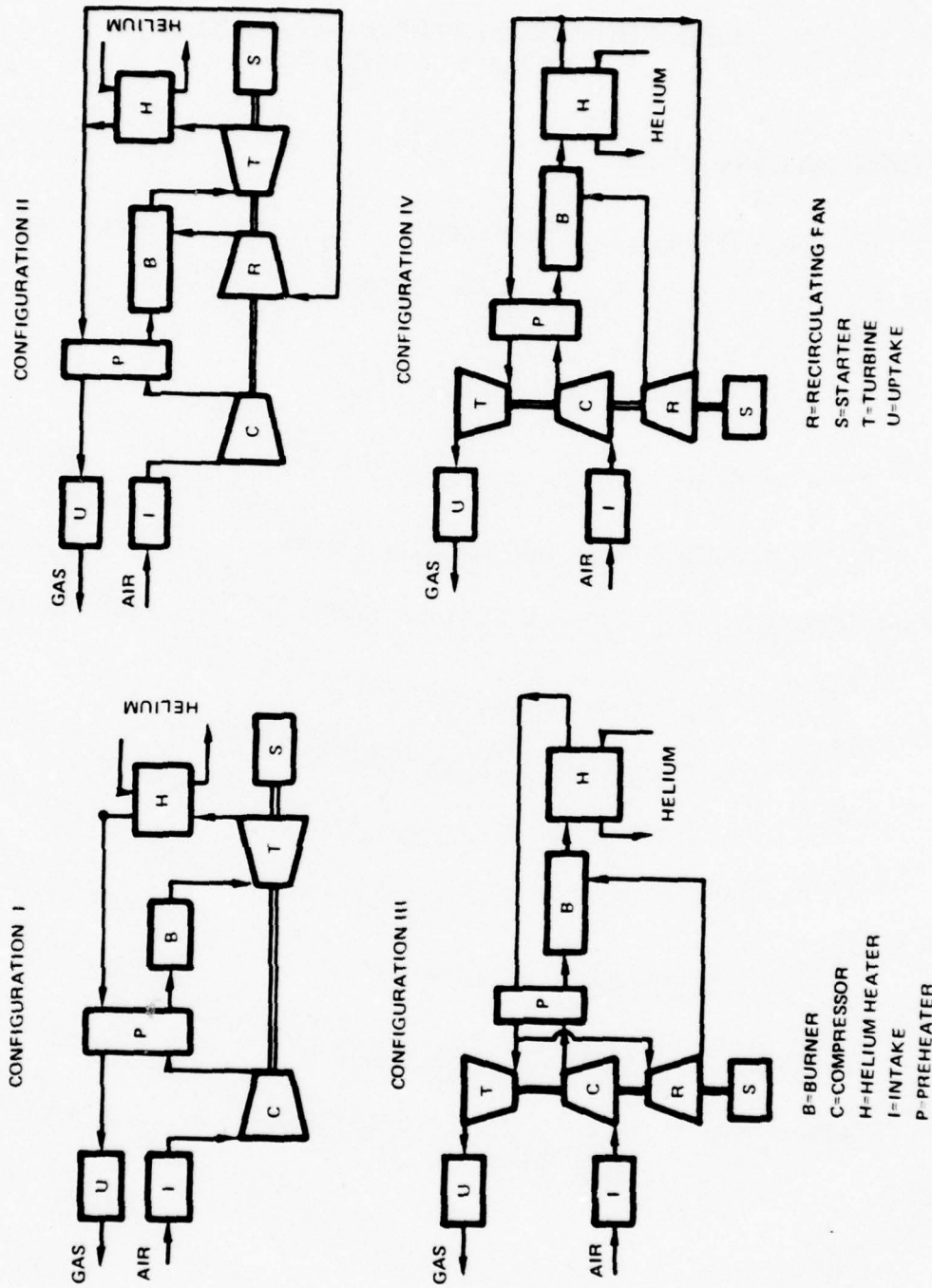
$$MF \text{ of } SO_2 = C_2 / TNM \tag{7}$$

$$MF \text{ of } O_2 = C_3 / TNM \tag{8}$$

$$MF \text{ of } N_2 = (3.76 + 0.94 C_1 + 3.76 C_2 + 3.76 C_3) / TNM \tag{9}$$

$$ppm \text{ of KOH} = (3.6 + 3 C_1 + 4.8 C_2) / (96.64 + 22.16 C_1 + 116.64 C_2 + 84 C_3) \tag{10}$$

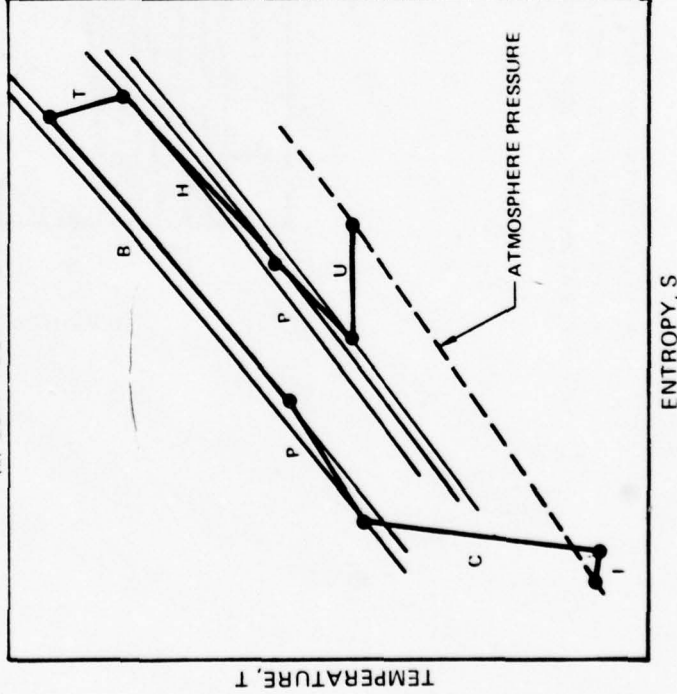
SCHEMATIC DIAGRAMS OF ALTERNATIVE FOSSIL-FIRED HEATER SYSTEMS



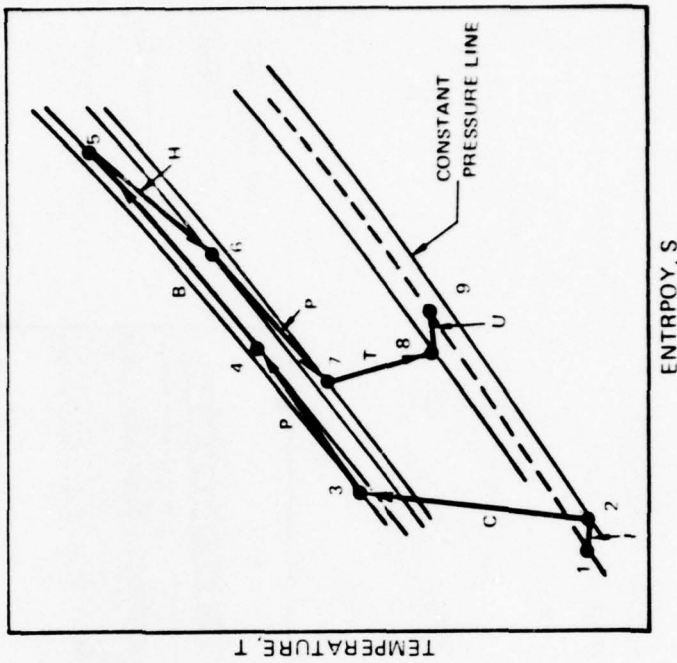
LWSP FOSSIL HEATER T-S DIAGRAM

PROPELLION POWER = 59.7 MW (80000 SHP)
 MAX HEATER METAL TEMP = 950°C
 COMPRESSION RATIO = 4.0
 THE NUMBERS ON T-S DIA REPRESENT THE STATE POINTS SHOWN IN FIG. 1

(a) CONFIGURATION I AND II

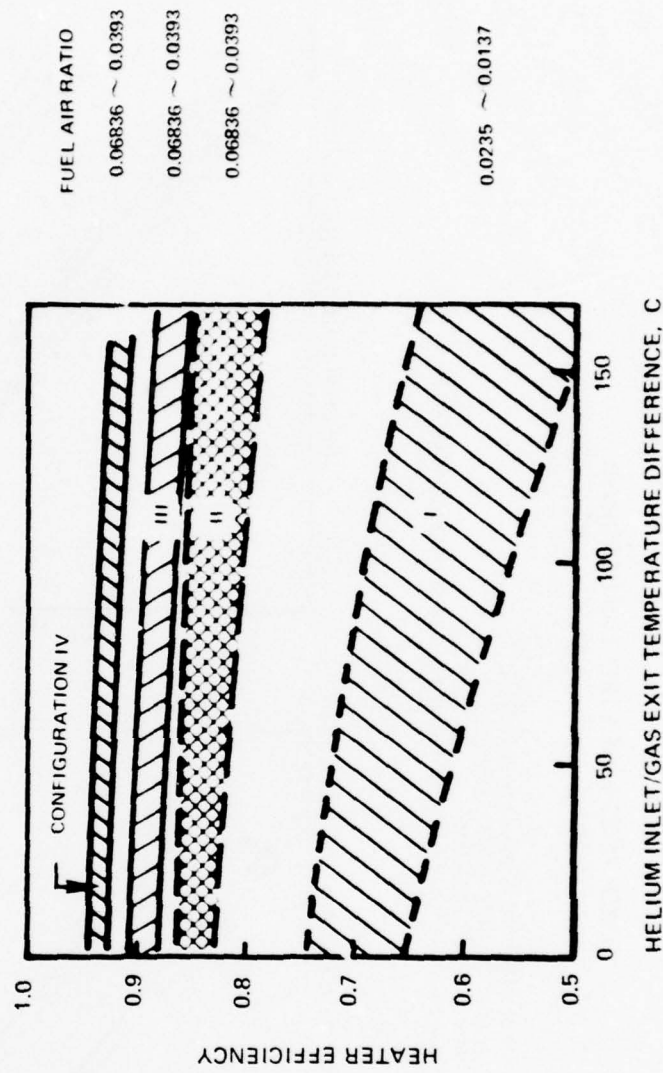


(b) CONFIGURATION III AND IV



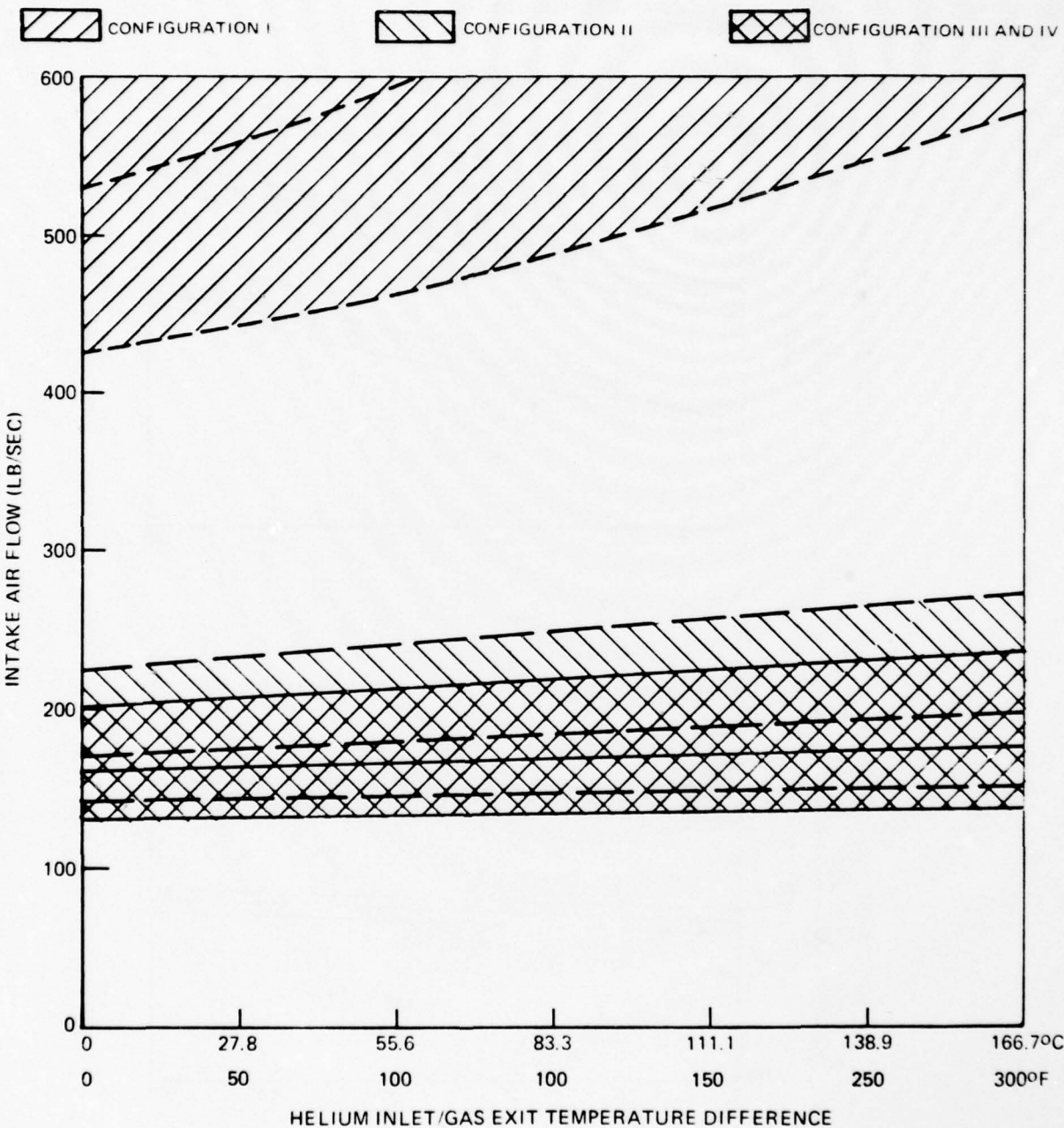
**COMPARISON OF FOSSIL HEATER THERMAL EFFICIENCY FOR VARIOUS
CONFIGURATIONS AND OPERATING CONDITIONS**

- HELIUM OUTLET/GAS INLET TEMPERATURE DIFFERENCE = 166 C
- HEATER SYSTEM PRESSURE LOSS 10% (4.5 psi)
- MAXIMUM METAL TEMP. 925 C



COMPARISON OF INTAKE AIR FLOW FOR VARIOUS FOSSIL HEAT SOURCE CONFIGURATIONS AND OPERATING CONDITIONS

HEATER TEMPERATURE DIFFERENCE = 166°C (300°F)
 CYCLE PRESSURE LOSS = 10% (4.5 PSI)



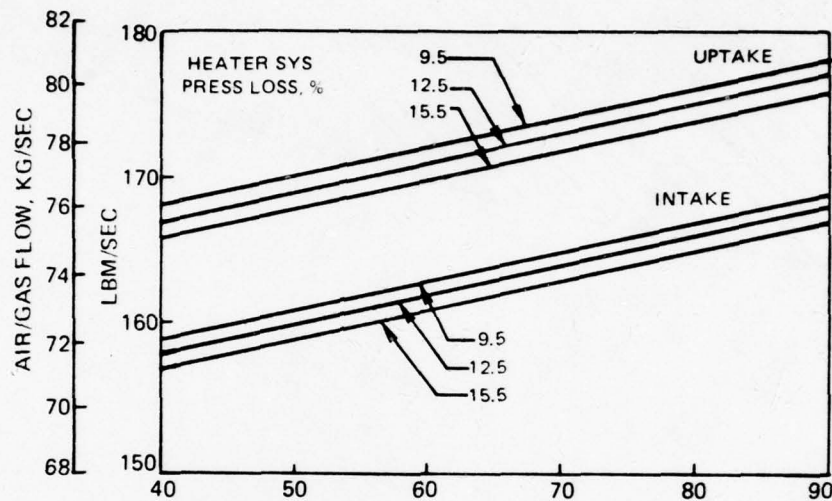
**EFFECT OF PRESSURE DROP AND AIR PREHEATER EFFECTIVENESS
ON LWSP FOSSIL HEATER PERFORMANCE**

PROPELLION POWER = 59680 kW (80000 SHP)

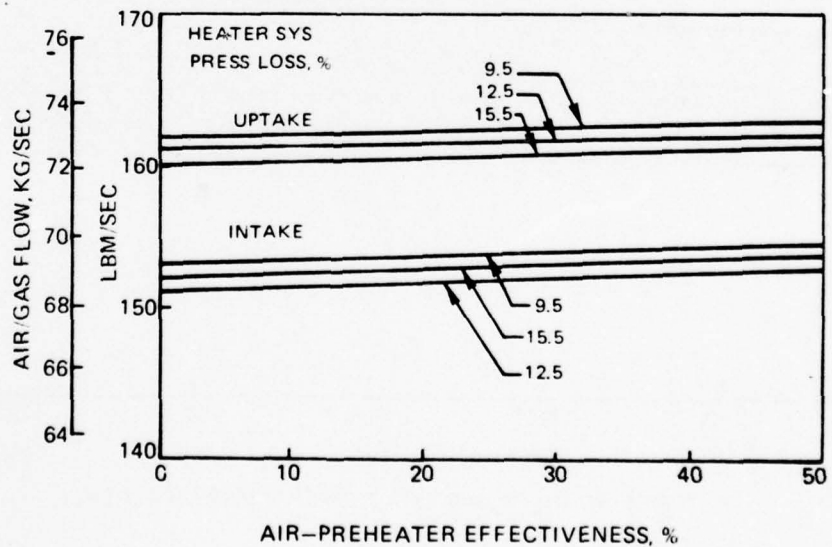
MAX HEATER METAL TEMP = 950°C

COMPRESSION RATIO = 4.0

(a) CONFIGURATION III

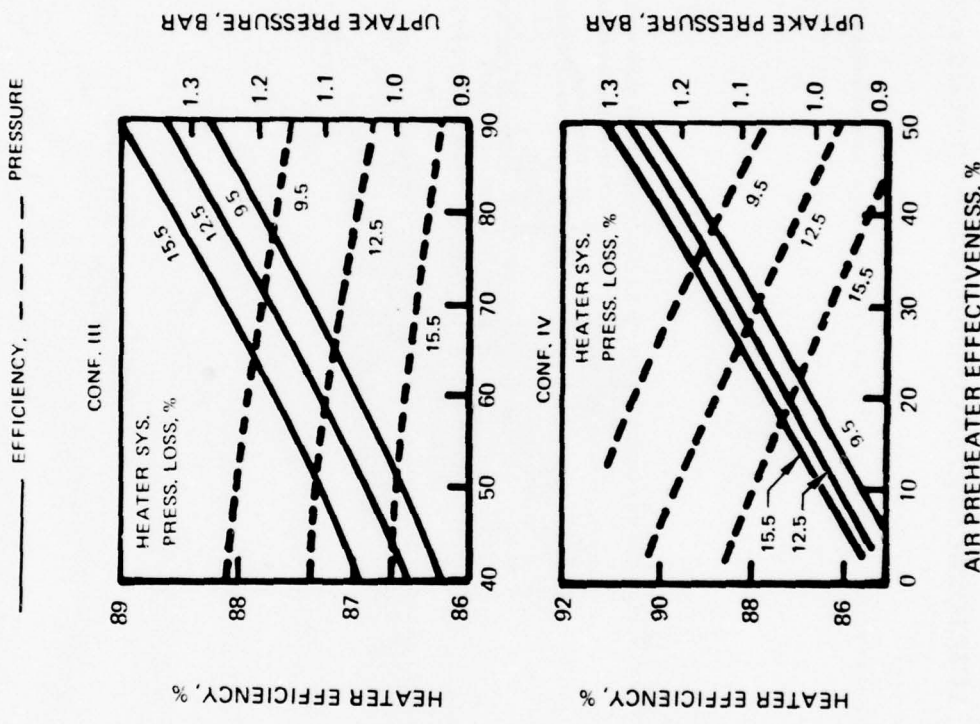


(b) CONFIGURATION IV

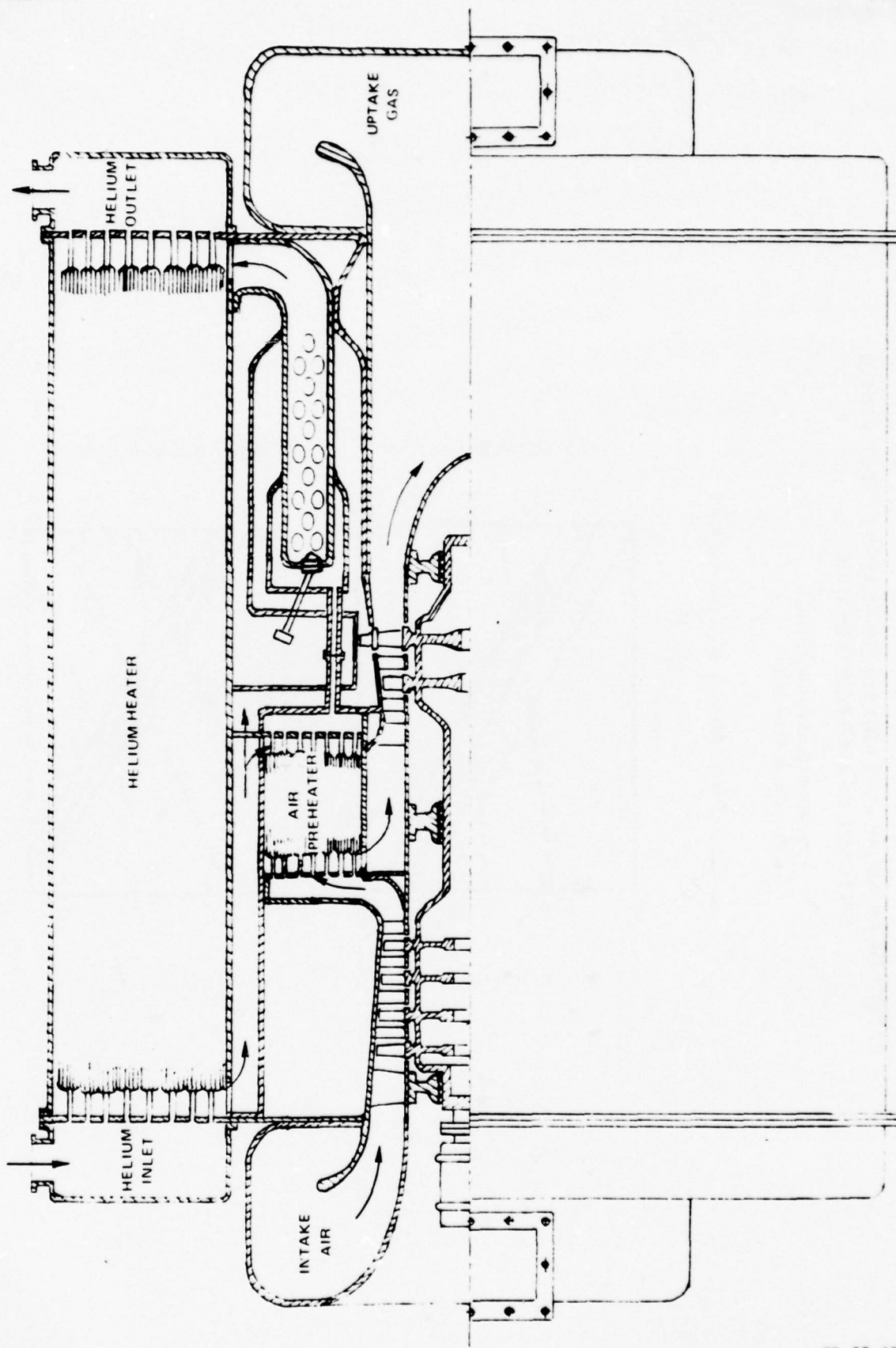


**EFFECT OF PRESSURE LOSS AND AIR PREHEATER EFFECTIVENESS
ON FOSSIL HEATER PERFORMANCE**

- PROPULSION POWER = 80,000 shp
- MAX. METAL TEMP. 925 C

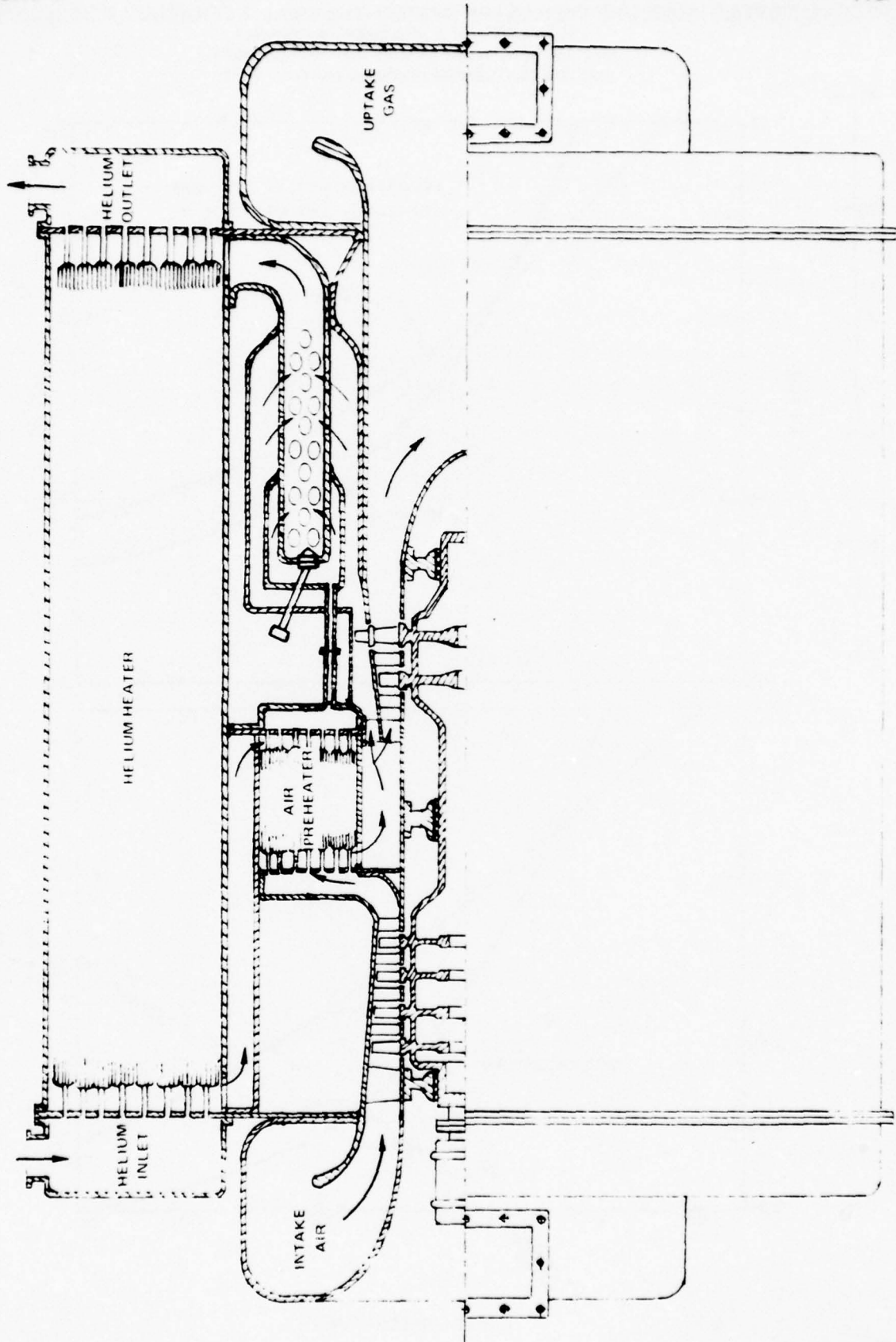


LWSP FOSSIL HEATER CONFIGURATION III DESIGN CONCEPT



78-03-122-01

LWSP FOSSIL HEATER CONFIGURATION IV DESIGN CONCEPT



78-03-122-02

R78-952979-4

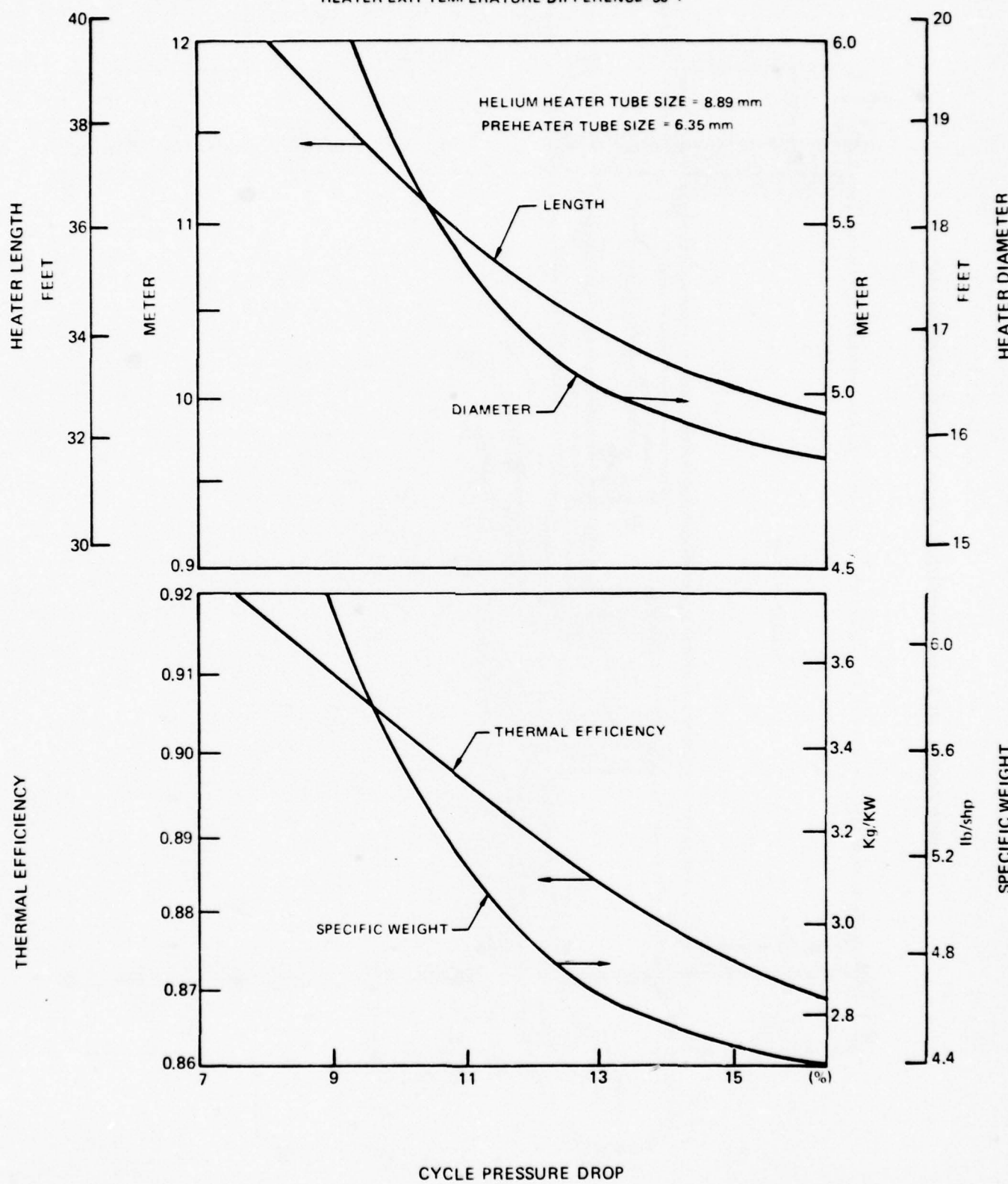
FIG. 1.9

EFFECT OF CYCLE PRESSURE ON HEATER SYSTEM THERMAL EFFICIENCY, SIZE, AND WEIGHT

CONFIGURATION IV FOR 80,000 SHP SYSTEM

HEATER INLET TEMPERATURE DIFFERENCE = 500°F

HEATER EXIT TEMPERATURE DIFFERENCE = 50°F



CYCLE PRESSURE DROP

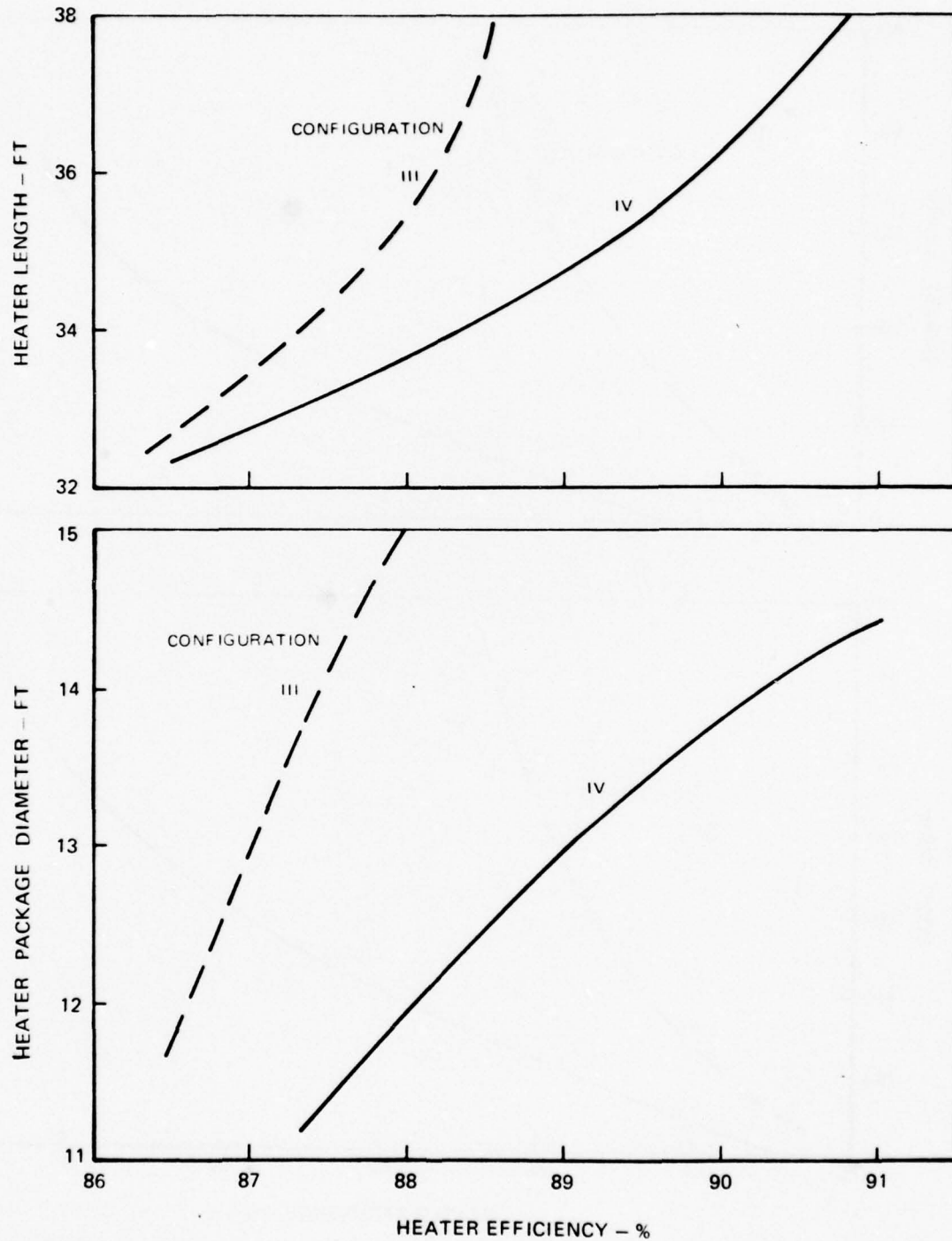
77-10-284-2

R78-952979-4

FIG. 1.10

LWSP FOSSIL HEATER SYSTEM SIZE CHARACTERISTICS

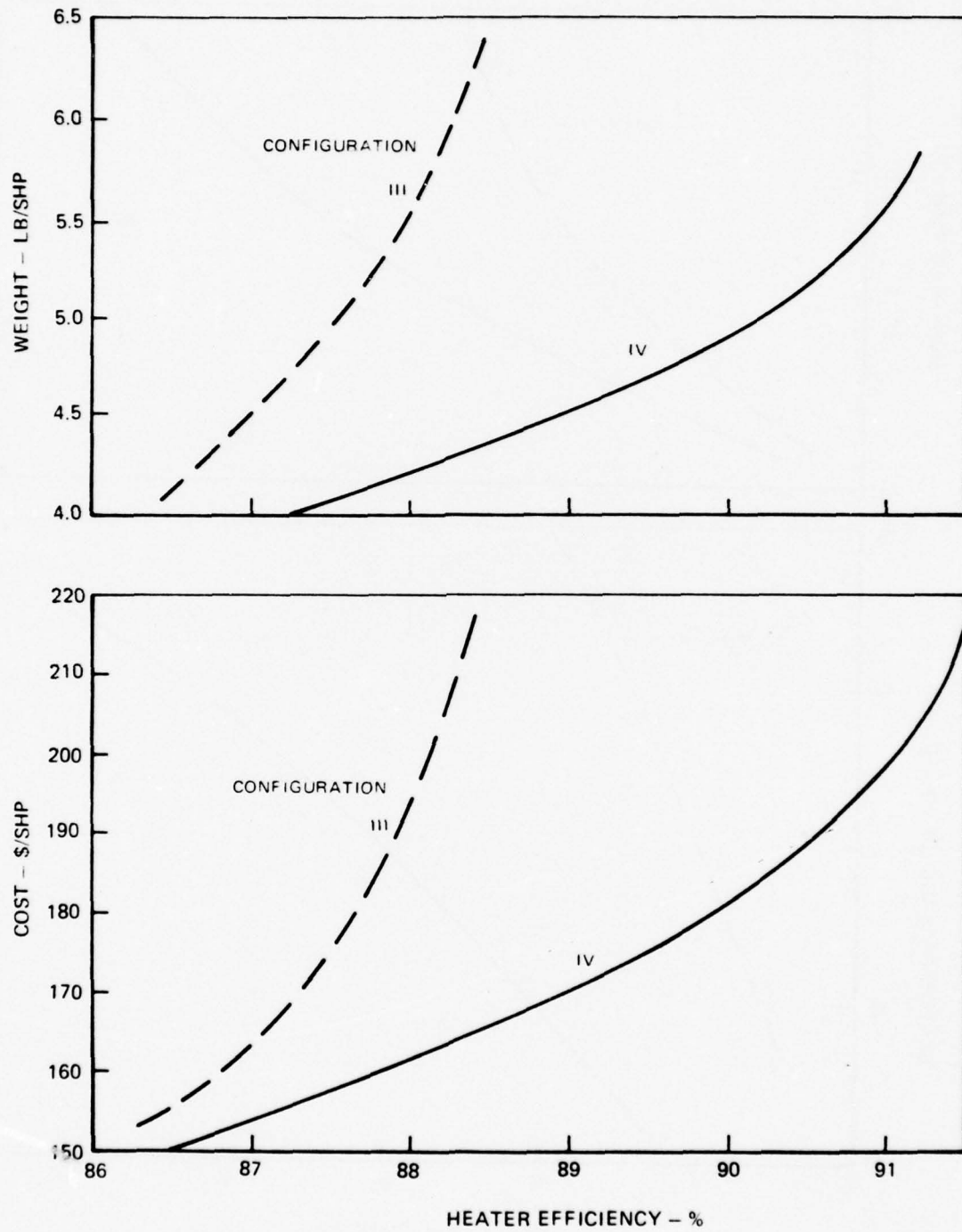
- PROPULSION POWER = 59680 kW (80000 SHP)
- MAXIMUM METAL TEMP = 950°C
- COMPRESSION RATIO = 4.0
- TOTAL PRESSURE DROP = 117.6 TO 212.5 IN. H₂O



78-02-235-4

LWSP FOSSIL HEATER SYSTEM WEIGHT AND COST CHARACTERISTICS

- PROPULSION POWER = 59680 kW (80,000 SHP)
- COMPRESSION RATIO = 4.0
- MAXIMUM METAL TEMP = 950°C
- TOTAL PRESSURE DROP = 117.6 TO 212.5 IN. H₂O

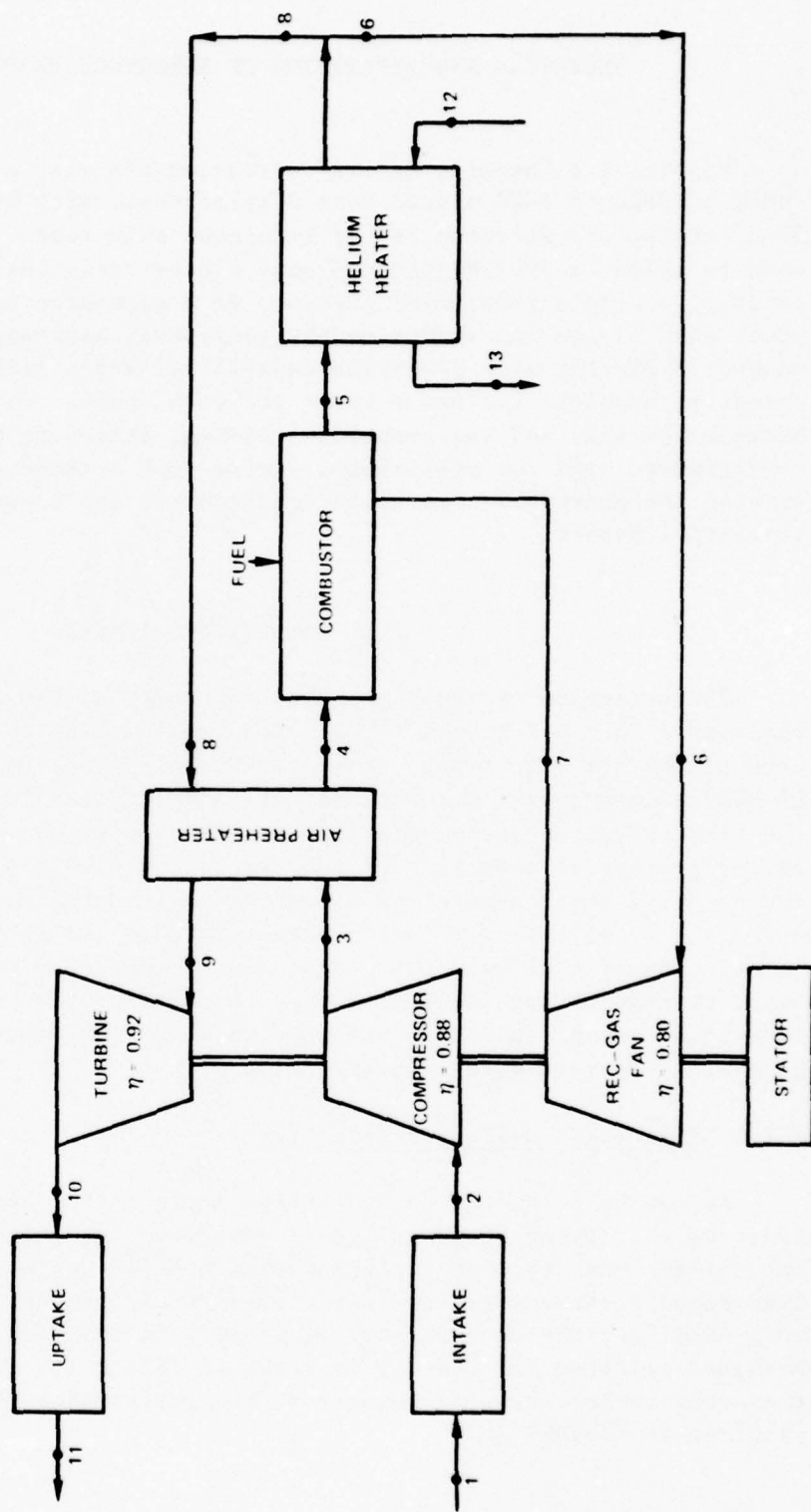


78-02-235-5

CYCLE DEFINITIONS OF PREFERRED FOSSIL-HEATER SYSTEM

- CCHT PROPULSION POWER 59.7 MW
- OVERALL HEATER THERMAL EFFICIENCY = 87.5 %

STATION	AIR			COMBUSTION GAS			HELIUM						
	1	2	3	4	5	6	7	8	9	10	11	12	13
FLOW RATE	kg/sec	68.88		194.64	121.79		72.85						
TEMPERATURE	C	26.7	26.7	191.1	249.0	481.0	500.0	481	430	252	247	453	816
PRESSURE	atm	1.00	0.97	3.88	3.78	3.76	3.48	3.76	3.48	3.39	1.02	1.01	45.36
													44.23



PHASE II-2

SELECTION AND DEFINITION OF REFERENCE PROPULSION SYSTEM

Utilizing a "Benefit Matrix" screening process, a high-speed destroyer (HSD) of 3500 to 4000 metric tons displacement, with maximum/cruise speed of 50/20 knots, was selected as the reference ship type. A similar matrix was used to select a 59.7 MW (80,000 shp) closed-cycle helium turbine (CCGT) incorporating a single free power turbine, as a candidate power conversion system to power each of the two shafts on the conceptual high-speed destroyer. An epicyclic gearbox with reversing capability, and a fixed pitch supercavitating thruster, complete the power train for each shaft. Integration problems between the ship and the propulsion system, including the heater system, were investigated, and the preliminary engine room arrangements were identified to provide the general installation requirements and constraints for component conceptual design.

2.1 Ship Type Selection

The selection of the high-speed destroyer as the reference ship type was based on a "Benefit Matrix" (Table 2.1) which ranks the potential benefit that each of the six ship types considered might accrue, in each of several categories of LWSP program goals (or requirements and constraints) which are imposed on the light-weight closed-cycle gas turbine propulsion system (Ref. II.1). The rating process is comprised of two parts: (1) a weighting factor which indicates the relative importance of each requirement/constraint in the systems evaluation; and (2) a benefit factor (which varies from one to five) to indicate the relative benefit of each LWSP constraint to the ship types considered. The total ratings of each ship type were calculated by summing the products of each individual rating and the corresponding weighting factor, thereby providing a guideline for reference ship selection.

2.1.1 High Speed Destroyer Selection

As can be seen, the total ratings shown in the bottom line of Table 2.1 indicate that among the ship types considered, the high-speed destroyer would benefit the most through implementation of lightweight propulsion systems. The high-speed destroyer rating is followed by the ratings of the surface effect ship (SES) and the conventional destroyer, in that order. The duty-cycle (or mission) selected for the HSD is shown in Fig. 2.1. This is the same duty-cycle presented in Ref. 2.1. A summary of the performance goals for the selected HSD is given in Table 2.2.

The factors which cause the HSD to have a higher rating than the SES are: (1) the need of the HSD for multiple fuel capability, (2) low cost being more important to an HSD, and (3) a long life power conversion system being more important to an HSD. The one LWSP program goal which is more applicable to a SES- than an HSD is the desire to provide low specific weight. Obviously the SES must utilize an extremely lightweight power conversion system, but as can be seen by the ratings for the other ship types, the need for a lightweight propulsion system is also high in an HSD.

In all other program goal categories, the HSD and SES are rated equal. This is reasonable since: (1) both ships require higher power levels than any current ship, (2) both must have good fuel economy to perform their mission, (3) both have an extremely limited volume for housing the required large propulsion power, and (4) both require technology which is advanced beyond the current state-of-the-art.

In two other program goal categories, the HSD and SES are also rated equal, yet other ship types would find still more benefit from these LWSP goals. Both the HSD and SES might be able to accept a power conversion system of lower reliability and shorter life than a cruiser or aircraft carrier, and both SES and HSD may not be the most attractive ships on which to spend high priority naval funds for 1990 mission requirements

After the screening process was completed, the results were reviewed with representatives of the naval architect firm, J. J. Henry, Inc. (JJH) (Ref. 2.2). JJH agreed that the HSD is a better choice as a reference ship type than the SES, if both types are to be powered by the LWSP system. Recent congressional and naval assessments have confirmed the validity of this judgement, as witnessed by the reduction of expenditures and effort on the SES program, and the Presidential desire to build a larger number of displacement ships of a small size, rather than a few large ships. Certainly, if a ship could possess the performance characteristics presented in Table 2.2, a significant naval need could be satisfied.

The JJH representatives feel that the most significant problem associated with the selected HSD would be the design and development of a thruster system which will accept 59.7 MW (80,000 shp) per shaft at the 25.7 m/sec (50 knots) speed desired. In their opinion, both the supercavitating thruster and associated thrust bearings required are well beyond the current state-of-the-art and possibly beyond the 1985 state-of-the-art. Even the shaft may require a new design approach to transmit the thrust load required at the high rotational speeds and small diameters expected. The thruster and gearbox requirements are discussed in more detail in later sections.

2.2 Propulsion System Size and Installation Limitations

For a displacement ship such as an HSD to achieve 50 knots top speed, a slender hull form is required. As a result, payload volumes are at a premium, making the placement of the high powered propulsion system critical to the ultimate ship utilization. The preliminary limitations on this space were estimated after consultations with J. J. Henry Inc. (Ref. 2.2) which identified typical ship hull form, payload and other space requirements as discussed in the section which follows.

2.2.1 Potential High-Speed Destroyer Volume Limitations

The slender destroyer hull form illustrated in Fig. 2.2 represents a logical choice for a vessel capable of speeds on the order of 50 knots. Submarine design has advanced to the point of underwater speeds being comparable to today's surface ships. It is appropriate to assume that in the future, operating speeds for subchasers will increase further, to perhaps 50 knots. However, development of high speed surface ships other than small patrol craft has been hampered by power plant/transmission capability rather than hull form. The general characteristics of high speed hulls have been known for some time, but their fine lines restrict engine room sizes and volumes.

The optimum form for achieving a high ratio of sustained speed to calm water speed, for a high degree of dryness, for reducing oscillatory motions, and for good wavegoing behavior in general, should have the following dimensionless proportions and shape characteristics (Ref. 2.3):

- Have the greatest length possible for the immersed volume; this means a low value of the ratio:

$$\frac{\text{Displacement Volume (ft}^3\text{)}}{(0.1 \times \text{Length (ft}}^3\text{)})}$$

- The displacement/length ratio should be adjusted by manipulating the draft of the vessel rather than the beam. That is, a narrow deep ship is preferred to a wide shallow vessel.
- Have the highest practical freeboard and the lowest practical forefoot; this requirement means the deck should be high above the water's surface and the ship's bow should be as deep in the water as possible.
- Keep section coefficients as small as possible throughout the length, consistent with other requirements which may exist. Small section coefficients insure a high degree of pitch damping.

- . Provide a reasonably high beam to draft ratio on the order of 3.0 and high length to beam ratio on the order of 8.0 so waterline slopes are held to small values.
- . Provide a high degree of inherent roll damping if required by ship's operations. This characteristic is related directly to hull form and arrangements.
- . Forebody sections should be of a V form with moderate or small flare from the ship's baseline to deck.
- . Waterline slopes in the bow should be very small to allow for uniform fluid flow.

The tentative hull form indicated in Fig. 2.2 possesses many of these characteristics; however a number of points deserve discussion in more detail. For comparison, a table of characteristic coefficients was prepared as shown in Table 2.3 for other high speed hull forms. The hull form coefficients of the HSD should compare favorably with the other fast ships given. When definitive hull form information is available, in the form of a lines plan, a more thorough evaluation can be accomplished. The value of the displacement/length ratio may have to be lower, providing an even finer hull form. The value of 1.54 was obtained for Fig. 2.2 by using an estimated draft of 6.1 m (20 feet). However, a more realistic draft for this could be less than 6.1 m, which would tend to reduce the displacement/length ratio below 1.54. With this figure in mind, achieving a displacement of 3500 tons or more with this hull will require careful design, incorporating engine room size requirements compatible with the propulsion system components layout.

The hull form, to assure good hydrodynamic performance, will require very careful design, analysis and model testing. The fine hull form will cut through waves rather than follow them. Undesirable pitching moments can be minimized by design of the hull sections as described previously. The forefoot, or area at the intersection of the stem and baseline, should be relatively square for sea-keeping considerations rather than rounded or raised as shown in this preliminary ships profile. Maneuvering the ship will require a larger rudder area to assure positive response since greater turning moments will be required than for an equivalent slower vessel.

The after sections of the hull require special care in design to assure relatively uniform fluid flow into the propellers. At the operating speeds indicated, separation resulting from poor hull contours would have a detrimental effect on the propulsion efficiency. When a more definitive hull form is obtained, the relative locations of the propellers and control surfaces must be carefully examined. The SCP's have large cavities aft of the propeller, the

length of which are on the order of the propeller diameter. Hence, the rudders should not be placed directly in the propeller race as on a conventional ship. A possible suggestion is a single rudder between the propellers, but this will require careful study.

To comment meaningfully on the stability or structural considerations, a lines plan is required. However, neither of these factors are believed to provide insurmountable problems if the arrangements are about as shown in Figure 2.2. Therefore the engine room dimensions, configurations, and installation requirements which can be scaled from this figure were used in the conceptual design presented in Section II-3 to provide guidelines for component sizing and arrangements. These arrangements, hull forms, and engine room sizing were refined in Section II-4 after completion of the conceptual design.

2.3 Baseline Propulsion System Selection

To provide a basis for further CCGT conceptual design studies, a baseline propulsion system was selected, also using the "Benefit Matrix" approach. The selected system is a closed-cycle helium turbine producing 59.7 MW (80,000 shp) on a single output shaft. Other systems with high value, but not selected as the baseline system, include an open-cycle gas turbine producing 29.8 MW (40,000 shp) and another closed-cycle system producing 89.5 MW (120,000 shp) on a single shaft. The factors considered in this selection are discussed in the sections which follow.

2.3.1 Selection of Propulsion System Size and Configuration

The most attractive propulsion system among those investigated is a closed-cycle helium turbine (CCGT) system rated at 59.7 MW (80,000 shp) with a single free power turbine. The second most attractive closed-cycle system is the 89.5 MW (120,000 shp) system.

The selection of these systems from the many other sizes and configurations considered, resulted from evaluation of the factors shown in Table 2.4 as represented by the ratings shown in Table 2.5. The most important factor among those considered is the compatibility of the propulsion system with the selected ship type. This compatibility factor includes the displacement, speed, installed power, duty cycle/performance, dynamics, and transmission systems. Also included in the general requirements and goals are such incontrovertible items as low specific weight, low specific volume, and cost, a wide fuel-use flexibility, low fuel consumption, high reliability, and maintainability. Simplicity and future naval requirements were also included since operating and maintaining

manpower requirements, as well as quantities of units manufactured, may also have a significant impact on cost and mission. A simpler system, and one which can be put into mass production, would be expected to minimize such requirements.

As can be seen in Table 2.5 an open-cycle power conversion system of 29.8 MW (40,000 shp) unit capacity was rated nearly as high as the selected CCGT system. The following factors represent the most significant reasons for these differences:

- 1) The projected ability of the CCGT to better utilize alternate and/or degraded fuel types in the 1990's,
- 2) The potential for the CCGT to provide a better overall duty-cycle fuel use rate through utilization of the "inventory control" concept,
- 3) The potential of the CCGT to provide more reliable duty-cycle performance and lower life-cycle costs, as a result of a multiplicity of operating arrangements and reconfigurations; and due to the isolation of expensive turbomachine components from the harsh environment experienced in the OCGT.

The selection of the 59.7 MW CCGT system over the 89.5 MW CCGT system was made primarily because of two reasons: first, the realization that the former system is more compatible with the HSD; and second, the expectation that a power conversion system which produces 59.7 MW (80,000 shp) per shaft will have many more applications in future Navy ships than one which produces 89.5 MW.

It was also considered that the use of two units of the 59.7 MW propulsion system would provide better survivability characteristics when compared with the single propulsion system possible with an 89.5 MW CCGT.

Other ship applications which are possible for the 59.7 MW baseline system include such ships as an aircraft carrier, cruiser, large destroyer, and even the FFG-7 and DD963. Indeed, many of these installations would not require extensive technological improvements in the remaining components of the propulsion system, such as the gearbox and thruster.

Although the 89.5 MW CCGT system was not selected as the baseline, it still might exhibit attractive qualities in the areas of lower capital cost per unit power, lower specific weight and volume, simplicity, and better maintainability. Furthermore, the 89.5 MW CCGT system which utilizes two power turbines might be more applicable to current ship and propulsion system requirements due to the reduced output per shaft (44.7 MW). The penalties of this system would include increased specific weight and volume as well as unknown operating

- characteristics associated with the dual turbine configuration. Considerations such as these cause the rating for this system to be lower than either the single turbine 89.5 MW design or the selected 59.7 MW design.

The operating requirements for the selected 59.7 MW CCGT are assumed to be represented by the duty-cycle shown in Figure 2.1. A summary of these requirements and critical design life requirements are presented in Table 2.6.

2.3.2 Thruster and Gearbox Selection

The selection of the thruster and gearbox required for the HSD was based upon both the estimates made in Part I Systems Study and upon consultations with J. J. Henry, Inc. The thruster selected for integration with the HSD and the 59.7 MW CCGT is of the supercavitating fixed pitch type, rotating at 580 rpm. The gearbox considered for integration with the CCGT and the thruster is a two-stage epicyclic design with a reversing capability.

Supercavitating Propeller Characteristics

A supercavitating propeller was chosen for the HSD due to the 50 knot top speed requirement. While it might be possible to design a non-cavitating propeller which could be proven in the laboratory, such a design would have a high probability of encountering partial or complete cavitation under some of the actual HSD operating conditions. With this undesirable possibility in mind, our consultations with J. J. Henry, Inc. indicated that the selection of a supercavitating propeller (SCP) was the most reasonable. Unfortunately, there has been no known operation of an SCP with this high level of power absorption. Furthermore, the efficiency which the SCP has demonstrated to date has been lower than non-cavitating types. Therefore, both the size and efficiency goals established for the SCP of this conceptual design might require additional development to make the selected HSD a feasible design.

The use of a fixed pitch, supercavitating propeller to absorb 59.7 MW (80,000 shp) is probably feasible when based on projected 1990 technology. According to Ref. 2.4, efficient propellers could be designed to absorb up to 373 MW (500,000 shp) or more. A check of later sources brought forth nothing to alter this statement. The primary difficulties in supercavitating propeller applications have been the lack of an adequate design procedure, systematic model tests and limited operating experience. The design of conventional marine propellers has been developed to a high state through systematic studies, tests and many years of ship operating experience. Reference 2.5 presents a comparison of design procedures presently in use, although these encompass propellers on the order of 4 to 5 feet in diameter. Systematic series of model

tests have recently been run for a group of nine propellers and operating experience is expanding rapidly; therefore the practical application of supercavitating propellers will become more widespread. Thus, although the design of supercavitating propellers is more complicated due to the large number of parameters, the interaction of these many factors is becoming better understood and might be resolved by the late 1980's.

Figure 2.3 (Ref. 2.4) was used by JJH to provide additional guidance in selecting a reasonable propeller size for absorbing the required horsepower. Initial estimates by JJH indicated that the "clean hull" thrust requirements for a 3500 metric ton HSD would be approximately 0.890 Mega Newtons (MN) or 200,000 lbf, therefore an SCP with efficiency of 0.70, turning at approximately 300 rpm with a 4.88 mi (16 ft) diameter would be sufficient. However, later hull refinements (presented in Phase II-4 of this report) indicated that the SCP should produce 1.157 MN (260,000 lbf) and rotate at approximately 580 rpm with a diameter of 3.05 M (10 ft). This latter SCP design is intended for a 3800 metric ton HSD design which provides sufficient engine room space for the 59.7 MW CCGT.

As might be noted from the latter thrust requirements, the shaft input power required is approximately 49.6 MW if the SCP efficiency is 0.60. This fact allows the additional power provided by the 59.7 MW CCGT system to be used for a design margin of 20 percent. Such a margin is typical of the relationship found in the Part I report (Ref. 2.1), where installed power is often 120 percent greater than the estimated "clean-hull" power requirements. As stated in the Part I report, this margin is often absorbed in hull appendages as well as used to compensate for barnacle or other degraded hull-surface conditions, and other auxiliary power requirements.

Material selection for supercavitating propellers can be difficult. The properties required include a high fatigue strength when the material is immersed in salt water. Reference 2.4 and 2.5 consider wrought titanium and Inconel as the best materials for SCPs. For either of these materials, the weight of each HSD propeller was estimated by J. J. Henry to be approximately 4 metric tons.

One of the major difficulties limiting the use of supercavitating propellers has been the relatively unpredictable performance at off design conditions. Naval ships spend most of their operating life at less than maximum speed and power; therefore the major operating ranges of the propellers will require careful definition. From an operational/installation standpoint, the primary difficulties would be the possibility of mutual interference of the cavities, or the susceptibility to damage during operations or drydocking. The problems of mutual interference can be controlled by careful stern location. The propellers extending well below the baseline are susceptible to damage from

navigational hazards and would require a special pit or exceptionally high keel blocks for drydocking. These difficulties can be controlled through proper ship handling.

Epicyclic Gearbox Characteristics

Several gearbox types and configurations were considered in the Part I (Ref. 2.1) parametric systems studies. For the 59.7 MW (80,000 shp) propulsion system being designed here, both epicyclic and offset gearboxes were considered. Both of these types were assumed to include two stages of reduction and a reversing capability. These requirements are imposed by the selected supercavitating thruster since it is of the fixed pitch variety operating at 580 rpm, and driven by a power turbine rotating at 4800 rpm in only one direction.

The epicyclic type gearbox was selected for the reference propulsion system since the estimated specific weight of this type (0.45 lb/shp) allows a savings in weight (approximately 0.2 lbs/shp) as compared to a single input offset type, and will be more compact as well. One disadvantage of the epicyclic gearbox is that it requires the power turbine shaft to be aligned with the gearbox centerline. This requirement limits the number of possible arrangements in the engine room. This in turn has an effect on the system layout, as discussed in Phase II-4 of this report. The estimated size of this gearbox is also shown in that Section. In summary, the resulting epicyclic gearbox will require an extension of the technology now being developed (Ref. 2.6) but should not present any unsolvable new problems.

2.4 Requirements for Baseline Propulsion System

Integration of the selected propulsion system components yields the schematic flow diagram shown in Fig. 2.4. Each of the two supercavitating propellers and epicyclic gearboxes required on the HSD are driven by a single output shaft from the CCGT power conversion system (two needed). This output shaft is mounted on a power turbine which is not mechanically connected to the compressor drive shaft. The compressor drive turbine receives helium gas heated to 816 C (1500 F) by the fossil-fired heater and pressurized to 4.14 MegaPascals (MPa), 600 psia, by the two axial compressors. Intercooling is included between the two compressors to reduce the size of the high-pressure compressor and to increase the cycle thermal efficiency. Finally a precooler is used to reject waste heat and maintain compressor inlet temperature at 37.8 C (100 F).

The critical conceptual design requirements for the CCGT power conversion system are then a combination of the parametric study results presented in

Ref. 2.1 and the requirements of the HSD. These requirements, as summarized in Tables 2.6 and 2.7, were utilized in the sections which follow to establish a preliminary conceptual design for a closed-cycle gas turbine power conversion system which produces 59.7 MW (80,000 shp) on a single output shaft.

REFERENCES

- 2.1 Kuo, S. C., T. L. O. Horton, and H. T. Shu: Lightweight Propulsion Systems for Advanced Ship Applications, Part I - System Studies. UTRC Report R77-952566-5, May 1977.
- 2.2 Consultations with J. J. Henry, Inc., January, March, June, and July 1978.
- 2.3 Saunders, H. E.: Hydrodynamics in Ship Design, Vol. III, Society of Naval Architects and Marine Engineers, 1965.
- 2.4 Barr, R. A.: Supercavitating and Superventilating Propellers, Transactions of Society of Naval Architects and Marine Engineers, Vol. 78, 1970.
- 2.5 Hecker, R., and R. Altman: High Performance Marine Propellers - An Overview, Winter Annual Meeting 1976, American Society of Mechanical Engineers.
- 2.6 Folenta, D. J., et al.: Design and Development of High Horsepower Marine Planetary Gears, ASME Paper No. 76-GT-28, March 21, 1976.

TABLE 2.1
SHIP TYPE SELECTION MATRIX

LWSP-CCGT Program Goal	Weighting Factor	Ship Benefit Factor					
		SES*	High Speed Destroyer*	Cruiser	Carrier	Destroyer	Auxiliary
Low Specific Weight	4	5	4	2	1	3	1
High Power Installed	4	5	5	3	5	2	1
Low Specific Volume	3	5	5	3	1	4	2
Low Specific Fuel Consumption	4	5	5	3	1	4	5
Versatile Fuel Capability	3	4	5	5	3	5	5
Low Cost	5	4	5	5	3	5	5
High Reliability	4	3	3	5	4	3	2
High System Lifetime	3	2	3	4	5	4	4
Advanced Technology	3	5	5	3	1	4	1
Projected Naval Mission Requirement by 1990	4	3	3	3	1	5	3
Total Rating		152	159	134	98	144	109

* Approximately 2000 tons displacement for SES and 4000 tons displacement for HSD

TABLE 2.2

High Speed Destroyer Performance Goals

Speed, max	25.7 m/sec (50 knots)
cruise	10.3 m/sec (20 knots)
Installed power	119.3 MW (160,000 shp)
number of propellers	2
Endurance, time	100 hrs
duty cycle range	5560 km (3000 nautical miles)
Duty Cycle	shown in Fig. 2.1
Displacement	3500-4000 metric tons

TABLE 2.3
Comparison of Destroyer Hull Form

Parameter	Displacement (Long Tons)	Horsepower	Vol. Displacement (.1 x Length) ³	Length Draft	Length Beam	Approx Max. Speed
DD 963	7800	80,000	1.84	18.24	9.62	30+
DD931	4050	70,000	1.94	20.92	9.29	33
FFG	3500	40,000	1.39	18.16	9.88	28+
DE 1052	4100	35,000	1.71	17.69	9.37	27+
H.S. Destroyer	3500	160,000	1.54*	21.5**	10.75	50

* Based on a 3500 ton displacement

** Based on assumed draft of 20 feet

TABLE 2.4

GOALS FOR POWER CONVERSION SYSTEM DESIGN

1. Compatibility with selected ship type (High Speed Destroyer)
2. Meets projected Naval Mission requirement by 1990
3. Low initial and operating cost
4. Low specific weight and volume (including fuel)
5. Versatile fuel capability
6. High reliability, minimum vulnerability, and good maintainability
7. System lifetime greater than 30,000 hours

TABLE 2.5
SELECTION MATRIX FOR POWER CONVERSION
SYSTEM OUTPUT AND CONFIGURATION

Power Conversion System Goal or Requirement		Rating* of Relative Compatibility of Power Conversion Systems																	
		Weighting Factor (1 → 5)		Open		Open		Closed		Open		Closed*		Closed		Closed*		Closed	
Configuration, Open or Closed Cycle	-	14.9	22.4	29.8	29.8	29.8**	29.8**	37.3	44.7	44.7*	44.7*	59.7	59.7**	89.5	89.5*	119.3	119.3	119.3**	119.3**
Power Output, MW (1000's ship)	-	(20)	(30)	(40)	(40)	(40)***	(40)***	(50)	(60)	(60)	(60)	(80)	(80)***	(120)	(120)***	(160)	(160)***	(160)	(160)***
Compatibility with Selected Ship Type (high-speed destroyer)																			
Installation	5	3	9	9	8	6	7	7	5	8	6	7	7	9	6	6	6	6	9
Dynamic Performance	4	9	9	10	8	9	10	7	8	7	8	6	7	6	7	6	7	6	7
Duty Cycle Performance	4	8	7	6	9	10	5	8	9	8	9	7	8	8	6	6	7	6	7
Transmission/Thruster	3	8	9	10	10	8	10	10	9	10	9	9	10	9	10	8	10	8	10
Fulfill Naval Need, large number of units	5	8	9	10	10	9	10	10	9	10	10	7	8	4	6	6	6	6	9
Low Cost	5	5	6	7	9	8	6	9	8	10	9	10	9	10	9	10	9	10	9
Life Cycle Capital Development	5	8	8	9	6	5	10	7	6	7	6	8	7	8	7	8	7	8	7
Low Specific Weight, including fuel	5	10	9	9	6	5	8	6	5	5	5	4	5	4	4	4	4	4	3
Low Specific Volume, including fuel	4	7	8	9	7	6	10	8	7	9	7	10	8	10	8	10	8	10	8
Low Fuel Consumption Rate, overall	4	7	7	7	8	7	9	10	9	10	9	10	8	9	8	9	8	9	9
Fuel Flexibility in the future	3	5	5	5	10	10	5	10	10	10	10	10	10	10	10	10	10	10	10
Simplicity	2	8	9	10	8	6	10	8	6	9	7	10	8	10	8	10	8	10	8
Reliability	3	5	4	5	8	6	5	7	6	8	6	7	6	7	6	7	6	7	5
Maintainability	2	5	6	7	5	4	8	6	5	7	6	9	8	9	8	9	8	9	8
Total Weighted Rating	-	402	445	478	457	418	469	459	435	484	440	460	455	433	433	433	433	433	433

* Bat Images are 1-10

** Two power turbines driven by one main turbine

TABLE 2.6

HELIUM CCGT PROPULSION SYSTEM LIFE AND DUTY CYCLE REQUIREMENTS

Life Requirements

- . Total life expectancy \geq 30,000 hrs
- . Time between removals (major overhauls) \approx 15,000 hrs
- . Time between minor overhauls (on board repair or module change) \approx 5,000 hrs
- . Scheduled maintenance (borescoping, inspection, adjustments, etc.) \approx 1,000 hrs

Duty Cycle Requirements

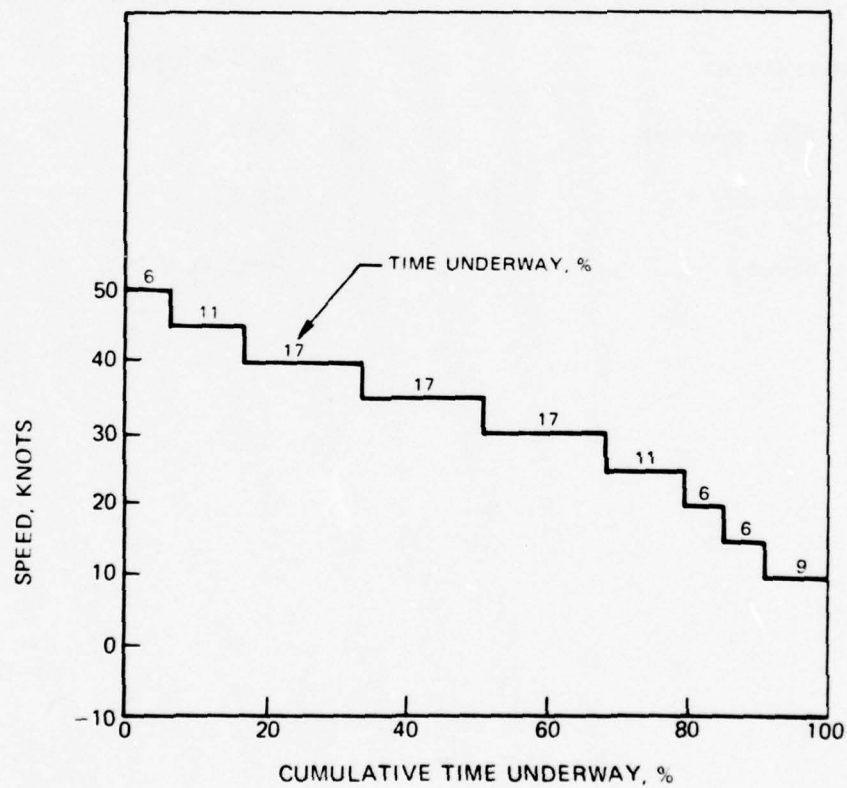
Power output (% max)	Operating mode	Duration (hrs or % time underway)	Comments
0	shutdown	2000 hrs/yr	in port
0 to 20%	bypass, thermal & inventory control	9%	maneuvering- rapid power changes required constantly
20 to 30%	inventory control (& thermal if required)	6%	tanker escort cruise
30 to 40%	inventory control	6%	cargo escort cruise
40 to 50%	inventory control	11%	fleet escort cruise
50 to 60%	inventory, thermal & bypass control	17%	anti-sub attack
60 to 70%	inventory control	17%	shipping lane clearing
70 to 80%	inventory control	17%	scouting
80 to 90%	inventory control	11%	dash or chase
90 to 100%	inventory control	6%	emergency dash or chase

TABLE 2.7

CCGT Power Conversion System Design Requirements

Output Power	59.7 MW (80,000 shp)
Turbine Inlet, temperature pressure	816 C (1500 F) 4.14 MPa (600 psia)
Compression Ratio	3.0 (Intercooled)
Compressor Inlet Temperature (both low and high compressor)	37.8 C (100 F)
Ambient air temperature	37.8C (100 F)
Seawater temperature	26.7 C (80 F)
Regenerator effectiveness	0.90
Cycle pressure loss, %	11.5%
Output shaft speed	4200 rpm

HIGH-SPEED DESTROYER DUTY CYCLE

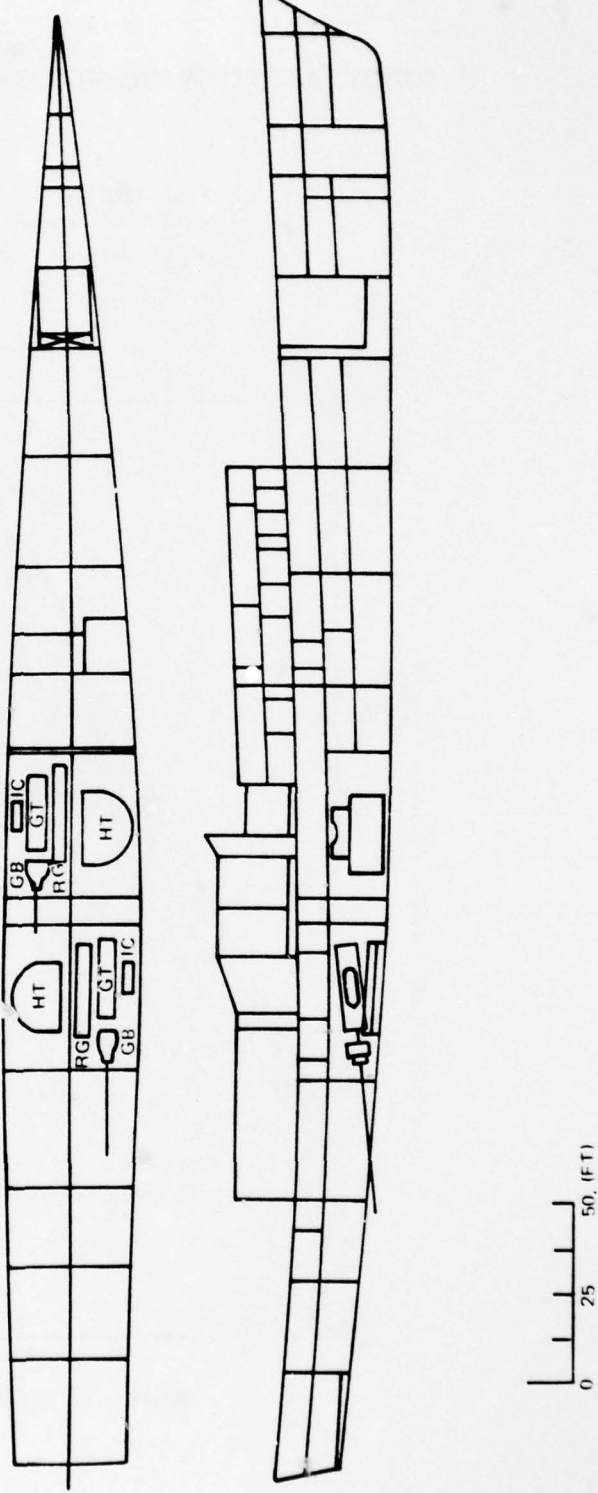


POTENTIAL HIGH SPEED DESTROYER LAYOUT

DISPLACEMENT = 3500 TO 4000 TONS

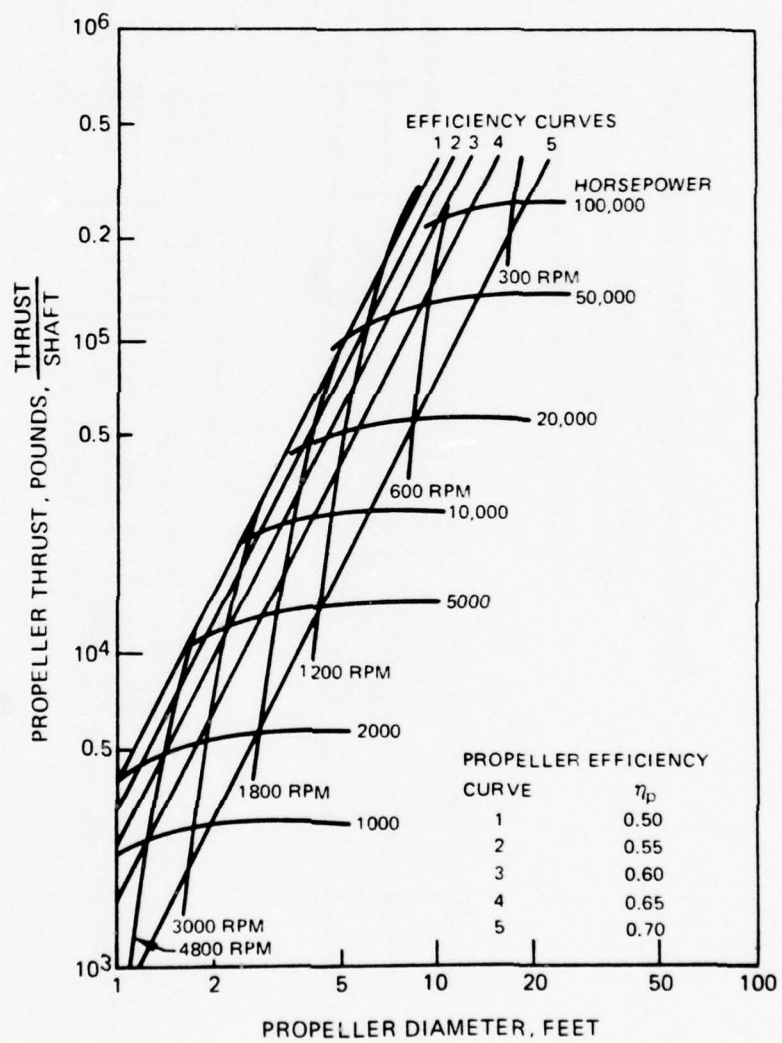
MAX SPEED = 45 TO 50 KNOTS

TOTAL INSTALLED POWER = 119.4 MW (160,000 SHP)



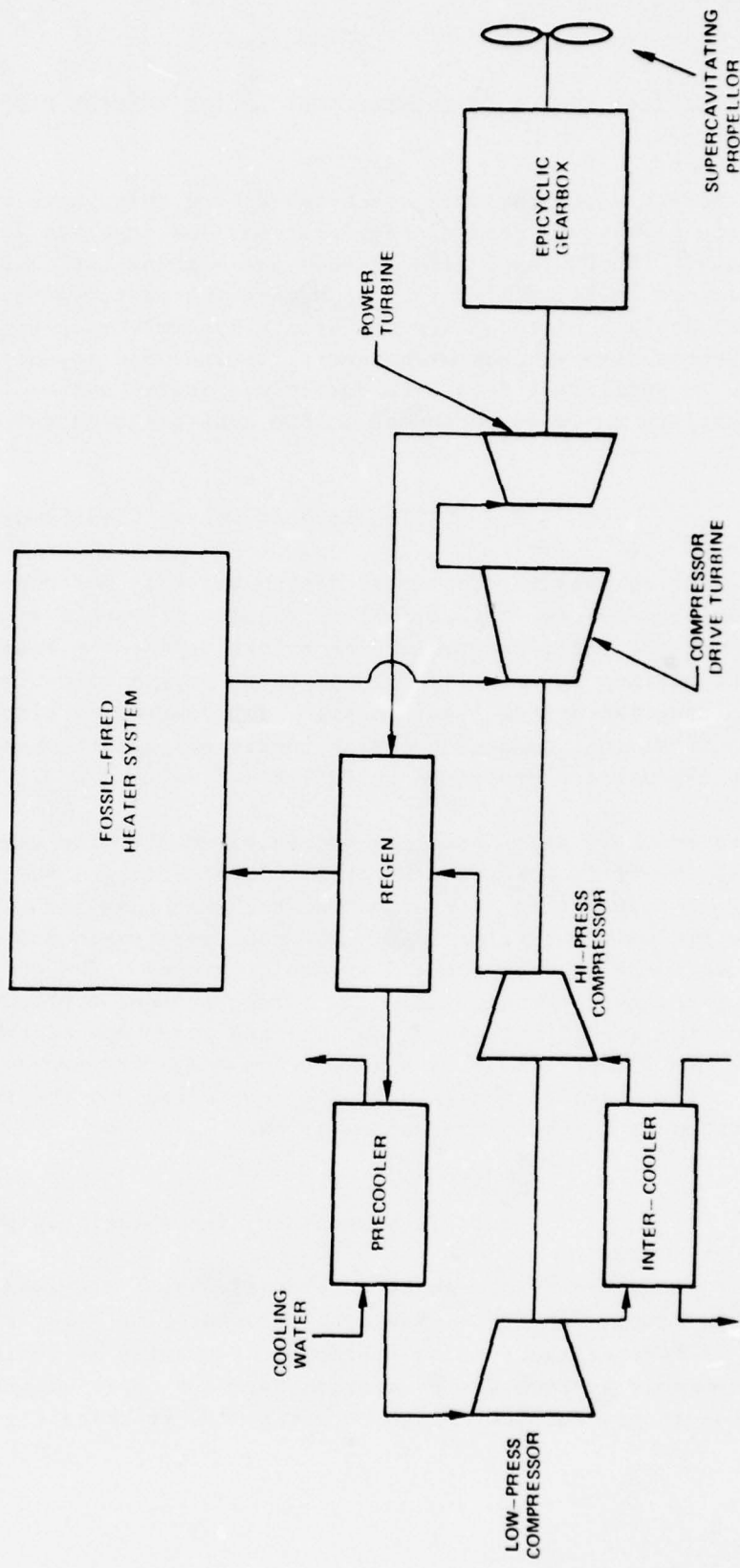
SUPERCAVITATING PROPELLOR PERFORMANCE CURVES

- 80 KNOTS
- 4 BLADED PROP.
- 25,000 PSI DESIGN STRESS



SCHEMATIC DIAGRAM OF FOSSIL-FIRED HELIUM CCGT HELIUM TURBINE PROPULSION SYSTEM

- 59.7 MW (80,000 shp) SHAFT OUTPUT
- HIGH SPEED DESTROYER APPLICATION



PHASE II-3

CONCEPTUAL DESIGN OF CLOSED-CYCLE HELIUM TURBINE PROPULSION SYSTEM

The objective of the work conducted during this phase was to prepare preliminary conceptual design specifications and drawings for the reference 59.7 megawatt (80,000-shp) closed-cycle gas turbine (CCGT) propulsion system defined in Phase II-2 for the high-speed destroyer applications. The conceptual designs of the power conversion system components, including the helium turbomachinery, heat exchangers, ducting, and inventory tanks were performed in sufficient detail to enable meaningful system layout studies and reliability analysis performed in the subsequent phases of this study.

3.1 CCGT Component Design Conditions

In order to prepare conceptual design drawings for the selected 59.7-MW CCGT propulsion system, the parametric results of Part I System Study were reviewed and the reference propulsion system defined in Phase II-2 of this report was refined to identify the component design conditions based on the overall propulsion system requirements. The results obtained for the cycle specification, component design conditions, and turbomachinery installation requirements are presented in Tables 3.1, 3.2, and 3.3, respectively.

Based on these specifications and requirements, the engine design section at the Pratt & Whitney Aircraft (P&WA) Group, a subsidiary of United Technologies Corporation, performed the turbomachinery conceptual design, including the material selections, component aerodynamic and mechanical designs, engineering drawing, and weight estimates. The conceptual design of the heat exchangers needed, including a recuperator, a precooler, an intercooler and the specifications of ducting and inventory control systems were performed by UTRC utilizing extensively the computer programs developed in the past. The detailed design approach considered and the results obtained are described in the sections which follow.

3.2 Turbomachinery Conceptual Design

The turbomachinery design point specifications provided by the Light-weight Ship Propulsion System Research Group at UTRC were reviewed and verified by P&WA design section. Some minor changes in design specifications were recommended by P&WA design section based on their expertise and vast experiences in gas-turbine design to assure the practicality of the turbomachine

designed. The results of this design study presented here include: (1) component material selections, (2) compressor aerodynamic selection, (3) turbine aerodynamic selection, (4) mechanical arrangement thrust balancing, and conceptual design drawing, and (5) weight estimates.

3.2.1 Material Selections

Technological advances in designing and manufacturing turbomachinery components have reached a relatively high level in the past 30 years due to the extensive research and development on high-temperature turbine blade materials and cooling technologies. The design of present lightweight closed-cycle gas turbine propulsion system has incorporated significantly these technologies. Since the maximum turbine inlet temperature was selected to be 815.6 C (1500 F), turbine blades cooling is not necessary. The paragraphs which follow review the status of pertinent material technologies and then select the candidate materials for the major turbomachinery components.

Turbine Material

Part of the possible improvement in specific horsepower (hp/lb-sec of engine airflow) and thermal efficiency for a simple-cycle gas turbine can be attributed to the high turbine inlet temperature that can be achieved whereas the increase in turbine inlet gas temperature will require development of improved turbine materials. The gains in turbine material technology have been most significant for the nickel-base alloys, allowing an improvement of more than 165 C (297 F) in temperature capability over the past decade. Presently nickel-base cast blade alloys, such as B-1900 and International Nickel Company's IN-100, have, in some propulsion systems, replaced forged Udiment 700 (U-700) for high-temperature applications, offering a reduced thermal-fatigue failure rate by a factor of five. Wrought Udiment 500, heat-treated for long-life, offers high-strength capabilities for use in many high-performance industrial designs, while cast Udiment 500 and Udiment 700 hollow blades are being exploited for utilization in the more advanced gas turbine designs.

The predicted long-time creep-strength characteristics (1 percent creep in 100,000 hr) for three generations of advanced turbine-blade materials are shown in Fig. 3.1. The first- and second-generation alloy creep strength properties were estimated by applying Larson-Miller type extrapolations to the short-time properties of the respective materials. The creep-strength properties estimated for the third-generation material reflect a 20 F/yr rate of improvement in temperature capabilities. As previously mentioned, modified heat treatment cycles would have to be developed for these short-time, high-strength alloys to provide them with 100,000 hr creep-strength properties

depicted in Fig. 3.1. Also shown in Fig. 3.1 for comparative purposes are estimated creep strength properties for two cobalt-base alloys (SM 302 and AMS 5382) that have frequently been used in aircraft gas turbine designs.

Creep strength improvements for vane alloys have not been as great as they have for blade alloys; and WI-52, a cast cobalt-base alloy, has been a primary vane alloy since 1958. Nickel-base alloys have been used for vanes in some power plants to take advantage of their relatively high strength and improved thermal-fatigue resistance characteristics, but generally they have shown relatively poor oxidation-corrosion resistance by comparison with cobalt-base alloys, and they require relatively difficult weld repair procedures.

Coatings have been developed which provide adequate corrosion resistance for the blades and vanes. The two most successful coatings, both aluminum base, have been Type UC (developed by Chromalloy Corporation) for WI-52 and "Jo-Coat" for nickel-base alloys. Although blade and vane coating lives in aircraft propulsion system designs are measured in terms of a few thousand hours, considerably longer coating lives could be attained in industrial designs through the application of coatings with thicknesses greater than those used in the aircraft versions (Ref. 3.1).

Turbine disks in current industrial power plants that operate at gas temperatures between 870 and 925 C are maintained at metal temperatures on the order of 315 to 340 C (Ref. 3.2) through forced cooling by the air extracted from the compressor. Because of these moderate disk temperatures, fairly inexpensive materials such as austenitic iron-base alloys have been used in the stationary gas turbine designs. Industrial gas turbine manufacturers often utilize CR-MO-V (a low-alloy steel) alloy in their intermediate- and large-size (greater than 36 in. dia) turbine disks; this material is the same as that used in their large steam turbine rotors (Ref. 3.3). When the turbine inlet gas temperature is increased to a level on the order of 1090 C or above, disk materials similar to those used in aircraft propulsion systems capable of withstanding metal temperatures as high as 650 to 760 C will have to be utilized. Typical materials are IN-100 for operation up to 760 C and Incoloy 901 (austenitic iron-nickel alloy) for operation at temperatures from 480 to 705 C.

Compressor Materials

In aircraft gas turbine propulsion systems where light weight is a primary design criterion, titanium alloy, such as Ti-6Al-4V (AMS 4928), is used

extensively for compressor vanes, blades, and disks subjected to temperatures not exceeding 400 C. Incoloy 901 is commonly used in the high-pressure stages of relatively high-pressure-ratio compressor designs where rim temperatures might exceed 400 C. Industrial gas turbines, which normally experience compressor rim temperatures below 425 C, commonly utilize a martensitic corrosion resistant steel (AISI Type 410) for blade and vane materials, and a low alloy steel such as AISI 4340 for disks. It would appear that large-capacity base-load gas turbine designs will continue to use AISI 4340 and Incoloy 901 alloys, respectively for the low-pressure-ratio and high-pressure-ratio turbine disks (as determined by the aforementioned temperature limits). In order that desirable blade stiffness can be maintained in the first few stages of a low-pressure compressor of large unit capacity without having to reduce blade aspect ratio below approximately 3.0 and/or revert to the use of blade stiffeners (thus compromising efficiency), it might be desirable to substitute AMS 4928 for AISI Type 410 as blade and vane material in appropriate stages; Incoloy 901 alloy would be used in the relatively high (greater than about 400 C) temperature region stages.

Major changes in the selection of compressor materials for lightweight propulsion system could be stimulated by efforts to fabricate lightweight and stiff blades, a feature that would permit blade designs with aspect ratios greater than 3.0 (thus reducing mass and, hence, cost of both blade and supporting disk) without having to compromise performance through the use of stiffening rods. Among the most important materials offering these features are the fiber-reinforced composite materials. The two most promising fibers at the present time appear to be silicon carbide-coated boron fiber and carbon fiber. Carbon/epoxy (for temperatures less than 115 C), carbon/polyimide (for temperatures of 120 to 315 C) and Borsic/Ti (for temperatures greater than 315 C) composites are currently being developed for compressor components in aircraft engines and should be economically feasible for future industrial units designed for LWSP system applications.

Casing Materials

The inlet and casings of a typical industrial-designs compressor are fabricated from cast iron, whereas the turbine shell is usually fabricated from nodular iron (Ref. 3.4). These types of materials should also suffice in the high-temperature, high-pressure-ratio advanced gas turbine designs, provided external cooling (more likely with water) of the turbine casing is employed.

Selection of LWSP Turbomachinery Materials

Materials selected for the conceptual turbomachinery design are based on the life and duty cycle requirements specified in Table 2.6 as well as the

requirements for low weight and low cost, plus ease of weld repair and reoperation without stress relief.

Since the gas working fluid used is helium, internal corrosion problems are not anticipated. For the most part, external surfaces are expected to be sufficiently cool that the only necessary protection from the salt air environment would be a high temperature paint. A thermal blanket surrounding the external cases aft of the thrust mount might be desirable to prevent excessive heat radiation in the engine room and accidental burning of personnel.

The forward end of the turbomachinery unit consists of AISI 403 or 401 stainless steel bearing units, supports, and rotor drums, with cast Greek Ascoloy blades. Stators are cast 17-4 PH and outer cases are AM 363 coated on the outside for corrosion resistance. The low pressure compressor exit scroll material is INCO 718. The material in the outer case aft of the compressors is Waspaloy, while the bearings and their supports are produced from AISI 410. Compressor drive turbine (CDT) disks are machined from Astroloy; the turbine blades and vanes are produced from INCO 713, with the exception of the first stage nozzle vane, which is produced from IN100. Hubs and tiebolts are made of AMS 6304, and the high temperature scrolls are fabricated from Haynes 188 or INCO 625. In the power turbine, the material in the disks is Waspaloy, that in the blades is AMS 5382, that in the stators is IN713, while that in the hubs is AMS 6304. The exit scroll is manufactured from IN 718.

3.2.2 Compressor Aerodynamic Selection

This task was oriented toward substantiating the performance numbers derived by UTRC (Table 3.4) and to evaluate possible improvements in the configurations assumed by UTRC. The results of this task indicated that the performance values were reasonable, depending upon the assumed running clearances, and that the assumed configurations would provide adequate loading capability. However, it was estimated that inlet preswirl, achieved through the addition of inlet guide vanes, would be required to optimize efficiency and to provide the best possible surge line efficiency at off-design conditions.

It was thought that a reduction in the number of stages in the design configurations developed by UTRC could be achieved with little performance penalty, if an increase in rotational speed could be affected. However, because a speed change would necessitate changes to the turbine and other components, this possible change was not investigated further. The consideration of increasing the through-flow Mach numbers (axial velocities) to reduce the number of stages was also investigated, but this approach was found to affect efficiency adversely at approximately the same surge margin.

The number of stages in the low pressure compressor can be reduced from 12 to 8 if the flow coefficient, V_x/U_m , is increased from 0.60 to 0.83. However, the adiabatic efficiency will drop approximately 2.3 percent in this case.

The predicted efficiencies and exit temperatures for the low pressure compressors at two values of design inlet swirls, two values of exit swirls, and two values of clearances are shown in Table 3.5. Inlet swirl would require the use of inlet guide vanes, which would provide a better surge-line/efficiency match at off-design operation. On the other hand, exit swirl would likely increase the outlet temperature drop to an unacceptable degree and therefore was not considered in this preliminary conceptual design. The 0.40 percent clearance-to-height (blade) ratio would correspond to an average running clearance of 0.01 in., which is quite tight for a compressor of this type; whereas, a 1.0 percent clearance-to-height (blade) ratio, while tight, is probably more reasonable for this type of configuration and was therefore selected. Comparison of the predicted low pressure compressor exit temperature for conditions of 1.0 percent clearance-to-height (blade), a 62 degree inlet swirl, and an axial exit swirl, with the temperature values presented in Table 3.4 shows that the former temperature is estimated to be about 0.83°C (1.5°F) cooler.

The predicted efficiencies and exit temperatures for the high pressure compressors at two values of design inlet swirls, two values of exit swirls, two values of exit swirls, and two values of clearances are also presented in Table 3.5. As is the case with the low pressure compressor, the inlet swirl would require an inlet guide vane, while exit swirl would likely be unacceptable because of increased loss downstream of the high pressure compressor. As before, an inlet guide vane would also provide a better surge-line/efficiency match at off-design operation. The initially assumed 0.72 percent clearance-to-height (blade) ratio would correspond to an average running clearance of 0.01 in.; whereas, a 1.7 percent clearance-to-height (blade), while tight, is probably more reasonable for this configuration and was selected. Comparison of the predicted high pressure compressor exit temperature for conditions of 1.7 percent clearance-to-height (blade), a 62 degree inlet swirl, and an axial swirl configuration with the temperature values presented in Table 3.4 shows that the former temperature is estimated to be approximately 5.6°F hotter.

Accordingly, the combination of typical running clearances for both the low, and high pressure, compressors, a 62 degree inlet swirl angle, and an axial exit swirl, with approximately a 53 percent reaction is predicted to produce a slightly higher temperature rise (approximately 4.0°F) than that presented for the system described in Table 3.4 which was used in the optimization studies.

The results of low- and high-compressor stage design details are presented in Tables 3.6 and 3.7, respectively.

Both the low- and high-pressure compressors in the configurations selected by UTRC should have low exit Mach numbers (approximately 0.20 axial with blockage) and therefore should not require the use of a diffuser downstream of the compressors.

3.2.3 Turbine Aerodynamic Selection

A three-stage compressor drive turbine (CDT) and a five-stage power turbine were selected as a result of the preliminary design study; a performance summary is presented in Table 3.8 for each turbine. Both turbines are predicted to produce the required horsepower at the operating conditions of flow, pressure ratio, speed, and temperature specified by UTRC.

A modification of CDT design philosophy was made by P&WA-GPD. Representatives of P&WA-GPD selected a three-stage CDT at a mean diameter of 102.6 cm compared with the UTRC design which incorporates six stages with a mean diameter of 76.30 cm. The use of six stages with a lower pressure ratio per stage represents a bigger performance risk than does the use of a three-stage design with a higher pressure ratio per stage since higher pressure ratio per stage enhances each row airfoil design. This change should meet required performance at reduced weight, cost, and risk.

The predicted effect on overall efficiency of changing the mean diameter and number of stages of the CDT is presented in Fig. 3.2. Also shown is the effect on efficiency created by changing the exit annulus area of the selected three-stage configuration. The optimum exit annulus area defined by maximum efficiency was selected for the preliminary design.

The power turbine elevation selected by UTRC was used by P&WA-GPD personnel in their conceptual design. The five-stage turbine has a mean diameter of 130.35 cm; a value which was based on consideration of weight down and the desire to maintain the external envelope of the UTRC baseline system. A five-stage design is predicted to meet the desired UTRC operating pressure ratio, but there will be a performance risk associated with this selection because of the low pressure ratio per stage. A reduction in the number of stages from five to three at the selected diameter would increase the overall power turbine pressure ratio from 1.674 to 1.712, thereby increasing the stage pressure ratio to a level consistent with the CDT. This may be favorable from the aerodynamics standpoint, but it may not be desirable when the performance and size limitations are considered. Therefore, the five-stage power turbine configuration was used in conceptual design drawings.

The predicted effect of power turbine mean diameter and number of stages on overall efficiency is shown in Fig. 3.3. Also shown is the effect on overall efficiency as influenced by the choice of exit annulus area for the selected five-stage configuration. As was the case in the CDT design, the optimum exit annulus area for maximum efficiency was selected.

Based on the results of turbine aerodynamic analyses, the blade and vanes elevations for CDT and power turbine are shown in Fig. 3.4 to indicate their relative dimensions and number of blades and vanes for each stage.

3.2.4 Mechanical Arrangement and Conceptual Design Drawing

The turbomachinery package consists of a low pressure compressor (LPC), a high pressure compressor (HPC), a compressor drive turbine (CDT), and a power turbine together with support cases for bearings and seals and appropriately oriented scrolls at the intake and exhaust. A detailed conceptual design drawing is presented in Fig. 3.5.

The intake and exhaust scrolls, with the exception of that at the exit of the power turbine are all located with openings on the horizontal centerline. This allows a total of four scrolls at the No. 2 and 3 bearing locations to be combined in two structural cases which thereby serve a multiple purpose. Each case forms two scrolls, acts as a bearing and seal support, and serves as a mount point for the unit.

The power turbine and LPC exit scrolls may be oriented in any convenient direction simply by indexing bolt holes at the attachment flanges. It is assumed, however, that the precooler will be located to the right of the turbomachinery (as viewed from the rear), and the intercooler to the left. The regenerator will be located above the precooler, and the heater will be located above the intercoolers. This arrangement will minimize the lengths of communicating piping between units. This is especially important for the ductwork between the compressor discharge and turbine inlet ports because of the high pressure/high temperature environment.

The turbine inlet scrolls are isolated and thermally insulated from the structural case members to minimize thermal growths throughout the length of the turbomachinery unit as well as to minimize distortion in the major cases. In order to assemble the hot scrolls in the No. 3 and No. 4 bearing locations, the outer cases must be split. In the No. 3 position, the left-hand aft portion of the case is segmented; in the No. 4 position the case is split circumferentially. The outer cases of both the LPC and HPC are longitudinally split to facilitate assembly of case halves over the drum rotor. All other cases are cylindrical.

Provisions are made to bleed up to 30 percent of total flow at each of two axial positions in each compressor. Two ports in each plane, located 15 degrees above the horizontal centerline, are manifolded together to satisfy this bleed requirement. A similar system is used to manifold two ports located 20 degrees

above the same centerline in the interturbine case thereby allowing up to 100 percent of total turbine flow to be bled for fast response to propulsive power requirements. Since this is a closed-cycle system, all gas bled at these points would be reinjected into the system downstream of the turbomachinery unit. It is believed that all other cross-bleed requirements for propulsive control can be met through interconnections between the various pipes.

Mounting planes are provided at each of the bearing locations in order to minimize the possible effect structural deformation created by distortions in the ship's hull. A mount point at each bearing location would minimize rotor-case rubbing by allowing any deflections created to be transmitted to the turbomachinery unit at those points least likely to affect the rotor-stator operation.

For study purposes, the bedplate considered is comprised of a parallel I-beam structure which could be a part of the ship's hull structure. The additional four mount points allow vertical and side loads to be transmitted to the bedplate, but do not restrain axial movement created by thermal growth in the system. All thrust loads are transmitted through turbomachinery outer cases to a single point located on the interturbine case. From here these thrust loads are transmitted through shock mounts to the bedplate.

The shaft extending from the rear of the turbomachinery unit allows this unit to be a flexibly coupled attachment to the reduction gearbox. An accessories drive pad is provided at the forward end of the unit, and it is from this location that the oil pressure and scavenge pumps are driven. If the final bearing design indicates that start-up oil pressure is necessary, an auxiliary oil system will be required.

Tilting pad journal bearings are used throughout the unit because of the size of the machinery and the requirements for long operational lifetime of the unit. Each individual pad is supplied with oil under pressure to maintain a constant film of oil between the shaft journals and pads. The journals were designed to maintain surface running velocities of less than 300 ft/sec at all locations. All bearing compartment seals are buffeted with intermediate pressure helium so that no helium-to-air leaks are possible.

Instrumentation in the form of pressure and temperature probes at the front and rear of each component is provided in six circumferential locations. Two vibration pickups at each bearing location as well as oil pressure and temperature readouts can also be provided.

Inspection and minor repair work to external system components can be performed onboard ship, but in the case of a need for major repairs, it would seem more expeditious to remove the entire turbomachinery unit to a repair depot. Borescope ports would be provided in six circumferential locations in

each of 21 planes located throughout the length of the compressors and turbines. By utilizing the design proposed it should be possible to remove a compressor or turbine component by sliding the unaffected units longitudinally on the bedplate to disengage bearings and splines and then remove the affected unit vertically. A new component could be lowered into position on the bedplate and assembled with the unaffected units in a reverse order to that of disassembly.

The LPC and HPC units are oriented to each other so that they share a common inlet case containing two scrolls and a support bearing. Accordingly the LPC exit and HPC inlet are located convenient to the intercooler on the left-hand side of the unit, and the LPC inlet is adjacent to the precooler on the right-hand side of the unit.

Both compressors are comprised of 12 stages. A drum rotor is provided with circumferential slots for blade attachments, while longitudinally split cases support cantilevered stators and variable inlet guide vanes are provided for the first three stators. This rotor configuration should be stiffer and lighter in weight than a built-up rotor. The one-piece rotor will also minimize unbalance problems by eliminating the possibility of "snap diameter jumping" and tiebolt stretching.

From a mechanical design standpoint, the compressor drive turbine acts as the transition duct from the compressor discharge to the inlet of the power turbine. This also saves a few inches in transition duct length because of the shallower duct angle. For this reason, the need to keep the overall weight and diameter of the package down, the mean diameter recommended by UTRC for the power turbine was retained by the designers at P&WA-GPD.

The rotor thrusts of the two compressors are directly opposed to each other, rather than being additive as is the case in a conventional turbine engine. This is accomplished by orienting the inlets and outlets in the manner shown to accommodate the other systems components in the total power package. However, coupling the compressors to the CDT creates a resultant rearward loading of the rotor. Thrust balancing directed toward reducing the bearing loading may be undertaken in the cavities forward of either the No. 2 or the No. 4 bearing supports, or forward of both, if desired. Thrust balancing may be undertaken in the power turbine rotor by introducing high-pressure gas into the cavity forward of the No. 6 bearing support.

3.2.5 Turbomachinery Weight Estimates

The base weight for the 59.7-MW (80,000-shp) gas turbine engine is 9,533 kg (21,015 lb or 0.26 lb/shp), including a contingency allowance of 436 kg (960 lb). Not included are the weights for the engine controls, pipes, valves, gearboxes, oil coolers, and electrical components. The weights presented for the configuration shown are based on past engine experience in part thickness, size, and material selections.

A weight breakdown for steel- and nickel-base materials for the base configuration is shown in Table 3.9, Item (A). It is believed that lighter weight configurations could be achieved by using titanium in the compressors. Item (b) of Table 3.9 shows a weight breakdown for: (1) titanium compressor rotors and steel stators and cases; and (2) steel- and nickel-base rotors with titanium stators and cases. The use of titanium for fabricating the compressor rotors, stators and cases would have to be investigated further because of the potential fire hazard associated with their use. Further weight saving could be achieved by the judicious use of aluminum components, but this possibility was not investigated.

3.3 Conceptual Design of Heat Exchangers

Heat exchangers are used throughout every power station and chemical process plant to transfer heat from one fluid (liquid or gas) to another fluid. The closed-cycle gas turbine power conversion system being investigated in this study (Fig. 2.4) requires four major heat exchangers; helium heater, recuperator, precooler, and intercooler. The helium heater is needed to transfer heat from a heat source (fossil or nuclear) to the cycle working fluid (helium). In view of the high temperature and high pressure requirements and the complex heat transfer phenomena between the combustion gas (fossil-fueled) and the working fluid inside the tubes, the helium heater was singled out for detailed discussion in Phase II-1. The recuperator is used to improve the cycle thermal efficiency by reducing the amount of waste heat rejection. The precooler is needed to reject waste heat while the intercooler is needed to allow a higher cycle pressure ratio (with two compressors in series) without severe penalty on the compressor efficiencies through intermediate cooling of the working fluid. Preliminary conceptual designs of the recuperator, the precooler, and the intercooler were made in the present task for the selected baseline (80,000-shp) lightweight ship propulsion system. The design point requirements, the selection of heat exchanger types and materials, and the design approach used in this study are discussed in the sections which follow.

3.3.1 Design Point Specifications

The thermodynamic specifications for the three heat exchanger designs are included in Tables 3.1 and 3.2. It must be mentioned that weight and volume are the two most important design considerations for the lightweight ship propulsion system. In this respect, the preliminary analyses carried out in the Part I study indicated that the heat exchanger tube diameters should be as small as possible in order to achieve these goals. However, in order to assure the structural integrity and reliable operation, all heat exchangers must be designed in

accordance with the Standards established by the Tubular Exchanger Manufacturer's Association (Ref. 3.5) and the American Society of Mechanical Engineers (Ref. 3.6). Additionally, compliance with the marine regulatory body code requirements, such as those of Lloyds (Ref. 3.7), of U.S. Coast Guard (Ref. 3.8), and of the American Bureau of Shipping (Ref. 3.9), must be observed.

Based on the cycle definitions, the dimensions of turbomachinery conceptual design drawing (Fig. 3.5), and the drawings for the selected reference high-speed destroyer (Fig. 3.6), the maximum effective tube length was estimated to be not more than approximately 5.5 meters (18 ft) for recuperator, and 1.4 meters (4.6 ft) for both precooler and intercooler. This tube length requirement would provide a reasonable integration of the three heat exchangers with the turbomachinery without requiring excessive ductings, thereby minimizing the number of bends and the total pressure loss throughout the piping systems.

To design a heat exchanger that is compact and lightweight, yet offering low pumping power (low pressure drop) and free from excessive thermal and pressure stress is truly a difficult task which requires extensive compromise. Therefore, a computer-aided design approach was used to obtain a desirable geometry which would significantly enhance the internal heat transfer characteristics, thus reduce the exchanger size and weight. Furthermore, by adopting modular design concept with tube bundle construction, the heat exchanger components can be shop-fabricated to assure high degree of integrity, and reasonably quick and easy assembly. Considerations were also given to the possibility of reducing the manufacturing cost and achieving a high reliability.

3.3.2 Selection of Heat Exchanger Types

The selection of heat exchanger types depends on many factors; in addition to the lightweight and compactness mentioned earlier, initial cost, component integrity, service lifetime, and ease of maintenance should also be given proper attention. Three heat exchanger types, namely, flat plate, finned tube in shell, and bare tube in shell were considered and the bare-tube-in-shell type was selected for further design studies.

Flat plate heat exchangers offer the advantage of utilizing less expensive sheet stock rather than tubing per unit heat transfer surface area. Furthermore, flat sheets construction offers many alternative flow passage designs with excellent fluid flow characteristics to minimize pressure loss in the heat exchanger. Fluid passages can be formed by corrugating or stamping the sheets and then soldering, brazing, or welding them together. However, units of this construction have the disadvantage of stress concentrations at the seam-soldered joints which can cause cracks if large pressure differentials exist. Previous system performance analysis indicated that the pressure differentials for precooler, intercooler and recuperator are approximately 100, 200, and 400 psia respectively. In addition to these large pressure

differentials, the long-life design requirements ($\geq 30,000$ hrs) and the expected internal temperature and pressure change resulting from frequent load variations responding to the ship duty cycle operation would rule out the suitability of flat plate heat exchangers for lightweight ship propulsion system applications.

Finned-tube-in-shell type is known to be a good choice for liquid to gas (or vice versa) heat exchangers. By introducing finned surfaces to increase the heat transfer area on the gas side (to compensate for its lower heat transfer coefficient as compared to that of the liquid side), the heat exchanger size can be reduced significantly compared with that utilizing bare tubes. However the use of finned-tube could result in structural complexity which is undesirable from the reliability and maintainability viewpoint. It was estimated that the size of the heat exchanger can be maintained reasonably compact if smaller bare tubes are used and that this type heat exchanger could be cheaper to manufacture and more reliable to operate because of its simplicity as compared with the finned tube heat exchanger. Therefore, the bare-small-tube-in-shell exchanger type was selected for the conceptual design of all three heat exchangers.

3.3.3 Selection of Heat Exchanger Materials

Since the working fluid selected for the reference power conversion system is purified helium and the highest temperature encountered by the heat exchanger (i.e. recuperator) would be lower than 538 C (1000 F), hot-corrosion and oxidation problems as experienced in the fired heaters do not exist here. The material selections for all exchangers were based on the creep strength requirements at the design pressures and temperatures, the requirements for lightweight, low capital cost, good fabricability, compatibility with brazing filler metals, and metallurgical stability unaffected by the temperature variations caused by the operating duty cycles.

Most of the existing recuperator designs have utilized low alloy steel (AMS 6300 series) with brazed and welded types of construction (Ref. 3.10). Low alloy steel offers low cost, good fabricability, and good weldability and brazability but is poor in oxidation corrosion resistance. It forms a thin, adherent oxide film in dry air particularly at temperatures above approximately 370 C (800 F); scaling becomes appreciable above 538 C (1000 F). The next class of recuperator material is AISI 400 series materials. These alloys have excellent oxidation resistance, low thermal expansion, and can be easily brazed. These two types of materials have the same magnitude of creep strength applicable to the present operating condition (temperature and pressure). The selection between AMS 6300 and AISI 400 series, therefore, would depend on the cost factor considered. Based on the past experiences (Ref. 3.11), the cost of heat exchanger using AISI 400 series is about 2 to 3 times higher than that using AMS 6300 series. In view of the fact that the cost of the recuperator is approximately one-third that of the total power

conversion system cost, it was concluded that AMS 6300 series material would be more desirable. Therefore, this material was used in the design of the recuperator for the lightweight ship propulsion system. The oxidation resistance against the marine environmental conditions for this recuperator material can be strengthened by painting the outside surface of the recuperator with high-temperature paint.

Compared to the recuperator, the lower operating temperatures and pressures in the precooler and intercooler would mean less severe material selections in these components. With maximum metal temperatures not exceeding 100 C (212 F), creep considerations are not the dominant design criteria here. The most important requirement would be the need for water treatment and purification system to keep the metal corrosion rate within the allowable limit. Since the combined capital cost for both precooler and intercooler is only a small fraction of the overall power conversion system cost, Monel, which is known to have excellent resistance to corrosion in both natural water and salt water, was considered as an ideal choice for the intercooler and precooler tube material; AMS 6323 was chosen for the shell material as in the case of recuperator design.

3.3.4 Heat Exchanger Design Approach

Based on the design criteria and requirements discussed heretofore, the existing UTRC computer programs for heat exchanger designs were used to estimate the design details needed for preparing the conceptual design drawings.

The computer program would first compute the two percent yielding stress based on the averaged material temperature for the tube and shell materials specified. The calculated two percent yielding stress for tubes was then divided by the tube design safety factor to obtain design stress data for estimating the tube wall thickness for selected tube outside diameters. To minimize the capital cost, the wall thickness determined from the above analytical calculation was compared with commercial tubing data. A standard commercial tube with the same tube O.D. and same tube thickness or thicker than the analytical result was used in the conceptual design.

The physical properties of the working fluid, such as the flow density, viscosity, thermal conductivity, specific heat, and Prandtl numbers, etc., were determined based on the averaged bulk temperature on each side of the exchanger. Because the equations used in computing the overall heat transfer coefficient and the pressure loss are coupled and highly nonlinear, a special iteration process was required in the heat exchanger design. The iteration process would identify the exchanger geometry such that the flow conditions in the heat exchanger would conform with the thermodynamic cycle specifications. It should be mentioned that the iteration procedures used in designing the recuperator, precooler and intercooler are different. In the recuperator design, all the flow conditions (mass flow rate, inlet and outlet

temperature and pressure) were specified from the cycle performance analysis. It required only one more input parameter, i.e., tube size, to determine the unique design for the given exchanger type. Flow rate, temperature and pressure at both inlet and outlet of the tube and shell sides were already specified in the cycle definition. The surface geometry of a recuperator is therefore determined once the tube size is selected. In other words, there exists only one mechanical design (i.e., number of tubes, tube pitch, effective tube length and flow velocities on both tube and shell sides) which would satisfy the design-point thermodynamic conditions (mass flow rate, inlet and outlet temperatures and pressures of the working fluid, helium) selected from the cycle performance analyses. The results of this computer design for the recuperator are presented in Table 3.10.

In designing of the precooler and intercooler, the parameters specified in Table 3.1 are not sufficient. Five more input parameters on the cooling water side are needed. These are: (a) cooling water inlet temperature, (b) temperature rise (c) inlet pressure, (d) tube size, and (e) water velocity inside the tube. Based on these 10 input parameters, the heat exchanger design program would perform iterative calculations between these inputs and the required surface geometry until the unique design is obtained. If the design appears unreasonable, e.g., if the tube pitch is incorrect, modifications of the tube size or water velocity input would be necessary. Tables 3.11 and 3.12, respectively, present the results of preliminary conceptual designs for the precooler and the intercooler.

3.3.5 Mechanical Arrangement and Conceptual Design Drawing

A representative conceptual design drawing for the three exchangers investigated is shown in Fig. 3.7 and its dimensional nomenclature and numerical values are presented in Fig. 3.8 and Table 3.14, respectively.

Due to the use of unusually small tubes (6.4 mm O.D.) with close tube spacing (less than 2 mm) to yield compact heat exchanger designs, modular construction concept as shown in Fig. 3.9 was necessary in all three exchangers. The close tube spacing can be maintained by a wire-wrap spacer (1.70 mm dia for the regenerator and 1.91 mm dia for the precooler and intercooler) at a wrapping axial pitch of about 30 cm. There are 300 active tubes and one no-flow (idle) tube per module; this no-flow tube is placed on the centerline of the tube bundle to provide the required flow velocity in the shell at the design condition. As shown in the module assembly drawing of Fig. 3.9, all 300 active tubes are brazed to a 108 mm O.D. module header tube, but the no-flow tube is not joined to the header tube because of the stress level limitation. The cone-shaped module header provides a stronger joint between the exchanger tubes and the module header tube because the ligament in the tube sheet is thicker. As compared to the hemispherical and flat-plate header for the same header thickness, the cone-shaped header would yield a safety factor approximately 1.5 times greater than that for the other two types. Therefore, the cone-shaped header concept was selected for the conceptual design.

Each module assembly is wrapped with a module sleeve which not only guides the flow direction on the shell side but also provides better modular rigidity for support. The modules are evenly supported by several module support plates, and the maximum tube length between support plates were limited to 914.4 mm (36 in.). Detailed data for the module assemblies are contained in Tables 3.10 to 3.12 for the three heat exchanger designed.

Each module header tube will be belled and welded to a one-inch thick double packed floating tube sheet as shown in Fig. 3.10. The floating tube sheet design was used to eliminate some of the thermal expansion problems which might be encountered during the normal duty cycle and emergency ship operation. The design results shown in Fig. 3.10 are based on the Standards of Tubular Exchanger Manufacturers Association (Ref. 3.5).

The pressure loss characteristics due to the flow contraction at the core entrance, core friction inside the bundle, the flow expansion at the core exit, and the flow acceleration between the core entrance and exit for three exchangers designed are presented in Table 3.14. These pressure loss characteristics combined with the pressure losses in the piping (ducting) system were fed back to the computer program to correct for the overall cycle efficiency of the propulsion system.

3.3.6 Overall Weight and Size

The estimated exchanger weights and their major dimensions are presented in Table 3.14. The total weight of the three exchangers without supporting structure and bedplate is approximately 0.93 kg/kW (1.53 lb/shp) which is quite agreeable with the results obtained in Part I of this study. This result was used in the system layout study which is discussed in Phase II-4 of this report.

3.4 Power System Component Integration

Based on the results of turbomachinery and heat exchanger conceptual designs presented above, a preliminary power conversion system layout was prepared and the result was used in designing the ducting system required to connect the power conversion system components. As an integral part of the power conversion system, the inventory control tank required was also estimated. The method used and the results obtained for these studies are presented in the following sections.

3.4.1 Ducting System

In estimating the size (length, ID and OD) of ducting needed for various segments, pressure losses associated with the wall friction, flow velocity, expansion, contraction, turns, and elbows within each line were considered. In order to identify the allowable working stress for each section, preliminary selections of ducting materials were made. AISI 410 series were

selected for the high pressure and/or high temperature segment while standard ASTM 106 carbon steel was selected for the low temperature and/or low pressure ducting.

The results of ducting systems design are summarized in Table 3.15. The largest diameter of the ducts selected is 38.1 cm for use in the section between the heater and the high turbine and also the section between the power turbine and the recuperator. Many of the ducting sections are less than one meter long, indicating that the problem of thermal expansion in the ducting system will not be severe. Overall pressure drop of the working fluid (helium) in the entire ducting system was estimated to be approximately 2.0 percent which is consistent with the cycle definition shown in Table 3.1. The ducting system without insulation and structural support would weigh approximately 730 kg.

3.4.2 Inventory Control Tank Size

It was assumed that up to 90 percent of the helium gas in the power conversion system can be readily removed by inventory control to provide various output horsepower required of the ship operation. For example, a conceptual high speed destroyer would require approximately 7 percent of the maximum design power for cruise, but the mass inventory at this power level is approximately 10 percent of the inventory required for full power. This nonlinearity between the helium inventory and the power output is mainly attributed to the degraded turbomachinery efficiency at the low inventory (commonly recognized as Reynolds number effect).

In order to estimate the size of the inventory control tank, helium inventories for both full- and 10-percent load were estimated (Table 3.16). The difference of these two estimates is 83 kg which is the total mass of helium to be stored in the inventory tank. It was assumed that this 83 kg helium would be stored at 32 C and 41.38 bar (600 psi). Therefore, six units of cylindrical tank with 0.67 meters in diameter and 6.61 meters in length (see Item B of Table 3.16), would be needed. The total weight for the inventory tank without insulation and structural supports is approximately 6300 kg.

3.4.3 Overall System Integration

While the detailed system integration layout is discussed in Phase II-4 of this report, the size and weight estimated for the major power conversion system components needed for the 80,000-shp fossil-fired helium CCGT propulsion system are summarized in Table 3.17. These results would indicate that no severe integration problems are to be expected for this propulsion engine aboard a conceptual high-speed destroyer shown in Fig. 3.6.

REFERENCES

- 3.1 Biancardi, F. R. and G. T. Peters: Status Report on the Utilization of Low-Cost Fuels in Gas-Turbines, UARL Report F-110278-23, October 1967.
- 3.2 Schloesser, V. V.: A Large Peaking Gas Turbine, Westinghouse Report, April 1969.
- 3.3 Gas Turbine Reference Library, Gas Turbine Materials, General Electric Company Report GER-218213, 1968.
- 3.4 Ludwig, G. A.: Marinization of Industrial Heavy-Duty Gas Turbines, General Electric Gas Turbine Marine Conference, September 1969.
- 3.5 Standards of Tubular Exchanger Manufacturer Association, Tubular Exchanger Manufacturers Association Inc., 1959.
- 3.6 ASME Boiler and Pressure Vessel Code, Division I, Section VIII, American Society of Mechanical Engineers, 1974 ED.
- 3.7 Rules and Regulations for the Construction and Classification of Steel Ships, Lloyd's Register of Shipping.
- 3.8 Code of Federal Regulation, Title 46 - Shipping, Chapter I - Coast Guard, Department of Transportation, Subchapter F - Marine Engineering, published of Office of the Federal Register.
- 3.9 Rules for Building and Classing Steel Vessel, American Bureau of Shipping, 1967.
- 3.10 Kind, R. W. and R. Ruhe: Tubular Gas Turbine Recuperator, ASME 77-WA-HT-8, Winter Annual Meeting, Atlanta, Georgia, November 27 - Dec. 2, 1977.
- 3.11 Kuo, S. C., et al.: Solar Power Conversion Systems Utilizing Closed-Cycle Air Turbines, UTRE Report R78-954142-1, October 1978.

TABLE 3.1

CYCLE DEFINITIONS OF HELIUM CCGT PROPULSION SYSTEM

Intercooled Recuperator Cycle

Turbine Inlet Temperature, C	815.56
Compressor Inlet Temperature, C	37.78
Turbine Inlet Pressure, bar	44.83
Compression Ratio	3.0
Recuperator Effectiveness, %	90.0
Cycle Pressure Loss, %	13.5
Heater, %	3.0
Recuperator, %	4.0
Intercooler, %	1.5
Precooler, %	3.0
Ducting, %	2.0
Output power, MW	59.7 (80,000 shp)

TABLE 3.2

59.7-MW FOSSIL-FIRED HELIUM CCGT PROPULSION SYSTEM
COMPONENT DESIGN CONDITIONS

	Mass Flow Rate kg per sec	Temperature, C in/out	Pressure, bar in/out
I. Heater System			
Compressor	69.582	26.7/191.1	1.0/4.01
Preheater (T)	69.582	191.1/292.8	4.01/3.94
(S)	73.392	481.1/391.7	3.70/3.63
Combustor	73.392	292.8/1926.7	3.94/3.92
Heater (T)	76.250	453.3/815.6	46.16/44.83
(S)	194.685	1093.3/481.1	3.92/3.70
Turbine	73.392	391.7/220.6	3.63/1.06
Recirculation fan	121.338	481.1/495.0	3.70/3.92
II. Power Conversion System			
Low Compressor	76.25	37.8/123.7	15.51/26.87
High Compressor	76.25	37.8/125.1	26.47/46.54
High Turbine	76.25	815.6/640.0	44.83/27.48
Power Turbine	76.25	640.0/490.0	27.48/16.70
Recuperator (T)	76.25	123.9/453.3	46.39/46.16
(S)	76.25	490.0/160.6	16.66/16.08
Precooler (S)	76.25	160.6/37.8	16.01/15.53
Intercooler (S)	76.25	126.7/37.8	27.26/26.85

TABLE 3.3
TURBOMACHINERY INSTALLATION REQUIREMENTS

Envelope:

All turbomachinery and related attached hardware (oil pumps, bleed lines, linkages, etc.) should fit inside a cylindrical envelope with dimensions of 7 feet diameter and 30 feet length.

Bleed Provisions:

1. Up to 30% of total flow for each compressor
2. Allowance for interstage bleeds for each compressor to accommodate development problems
3. Up to 100% of total flow for both compressor drive turbine and power turbine

Instrumentation:

1. Pressure and temperature rakes at 6 circumferential positions at the front and rear of each component
2. Vibration pickups at the two circumferential locations at the front and rear of each component
3. Pressure level or delta across the helium to air sealing surfaces
4. Normal engine instrumentation (oil pressure & temperature, etc.)

Borescope Ports:

At six circumferential locations in planes located at front and rear of each component subassembly and after each succeeding two stages of each component.

Mounting Requirements:

The turbomachinery may be assumed to be supported from below or/and above, whichever is more convenient. Mounting structure should be consistent with naval shock loading requirements.

TABLE 3.4

HELIUM CCGT COMPRESSOR AERODYNAMIC SPECIFICATION

Rating: 59.7-MW (80,000-shp)

	<u>Low Pressure Compressor</u>	<u>High Pressure Compressor</u>
Number of Stages	12	12
Rotational Speed, rpm	8200	8200
Mean Blade Velocity, U_m , mps	320	328
Work Coefficient, $2C_p \Delta t / U_m$	0.73	0.71
Flow Coefficient, V_x / U_m	0.55	0.55
Reaction	0.50	0.50
Mass Flow Rate, kg/sec	74.12	74.12
Corrected Mass Flow Rate, kg/sec	11.089	6.50
Inlet Temperature, °C	37.78	37.78
Outlet Temperature, °C	123.67	125.07
Inlet Pressure, bar	15.51	26.47
Outlet Pressure, bar	26.87	46.54

TABLE 3.5

PREDICTED HELIUM CGGT COMPRESSOR EFFICIENCIES AND OUTLET TEMPERATURES

This Table was provided by the
Government Products Division of Pratt & Whitney Aircraft Group

Configuration	Low Pressure Configuration				High Pressure Configuration			
	1	2	3	4	1	2	3	4
Inlet Swirl, Degrees	62	90	62	90	62	90	62	90
Exit Swirl, Degrees	62	90	90	90	62	90	90	90
Avg. Reaction, %	50	70.4	53	70.4	50	72	53	72
Avg. Clearance/Height, %	0.4	0.4	1.0	1.0	0.72	0.72	1.7	1.7
Adiabatic Eff., %	90.5	89.5	89.5	89.5	89.2	88.3	87.5	86.8
Outlet Temp, C (F)	121.9 (251.4)	122.8 (253.0)	123.7 (254.7)	125.7 (258.2)	126.9 (260.4)	128.2 (262.7)	128.6 (263.5)	

TABLE 3.6

59.7-MW HELIUM CCGT LOW PRESSURE COMPRESSOR STAGE DESIGN DETAILS

Stages	1	2	3	4	5	6
	B	V	B	V	B	V
Blades & Vanes	89	74	89	74	97	76
No. of Blades or Vanes	41.021	41.021	41.021	41.021	41.021	41.021
Tip Radius, cm	41.021	41.021	41.021	41.021	41.021	41.021
Blade Height, mm	74.22	73.15	72.11	71.12	69.19	68.25
Pitch, mm	26.37	34.21	26.37	34.21	24.18	30.86
Actual Chord, mm	35.13	42.27	35.13	42.27	41.15	32.23
Thickness, mm	4.39	5.28	4.39	5.28	4.04	5.16

Stages	7	8	9	10	11	12
	B	V	B	V	B	V
Blades & Vanes	97	76	97	76	97	78
No. of Blades or Vanes	41.02	41.02	41.02	41.02	41.02	41.02
Tip Radius, cm	41.02	41.02	41.02	41.02	41.02	41.02
Blade Height, mm	63.09	62.31	61.54	60.81	60.07	59.33
Pitch, mm	24.18	30.86	24.18	30.86	24.18	30.07
Actual Chord, mm	32.23	41.15	32.23	41.15	32.23	40.11
Thickness, mm	4.04	5.16	4.04	5.16	4.04	5.00

TABLE 3.7

59.7-MW HELIUM HIGH PRESSURE COMPRESSOR STAGE DESIGN DETAILS

Stages	Blades & Vanes	1		2		3		4		5		6	
		B	V	B	V	B	V	B	V	B	V	B	V
No. of Blades or Vanes		113	88	113	88	113	90	113	90	113	90	113	92
Tip Radius, cm		40.26	40.26	40.26	40.26	40.26	40.26	40.26	40.26	40.26	40.26	40.26	40.26
Blade Height, mm	41.53	41.05	40.23	39.67	39.14	38.61	38.10	37.59	37.11	36.63	36.17	35.71	
Pitch, mm	21.29	27.33	21.29	27.33	21.29	26.72	21.29	26.72	21.29	26.72	21.29	26.14	
Actual Chord, mm	28.37	36.42	29.37	36.42	28.37	35.64	28.37	35.64	28.37	35.64	28.37	34.85	
Thickness, mm	3.56	4.55	3.56	4.55	3.56	4.45	3.56	4.45	3.56	4.45	3.56	4.37	

Stages	Blades & Vanes	7		8		9		10		11		12	
		B	V	B	V	B	V	B	V	B	V	B	V
No. of Blades or Vanes		113	92	113	92	113	94	127	94	127	94	127	94
Tip Radius, cm		40.26	40.26	40.26	40.26	40.26	40.26	40.26	40.26	40.26	40.26	40.26	40.26
Blade Height, mm	35.28	34.82	34.42	34.01	33.60	33.20	32.82	32.44	32.05	31.70	31.37	31.12	
Pitch, mm	21.29	26.14	21.29	26.14	21.29	25.58	18.92	25.58	18.92	25.58	18.92	25.58	
Actual Chord, mm	28.37	34.85	28.37	34.85	28.37	34.11	25.25	34.11	25.25	34.11	25.25	34.11	
Thickness, mm	3.56	4.37	3.56	4.37	3.56	4.27	3.15	4.27	3.15	4.27	3.15	4.27	

TABLE 3.8

HELIUM CCGT TURBINE AERODYNAMIC SPECIFICATIONS

Rating: 59.7-MW (80,000 shp)

	<u>Compressor Drive Turbine</u>	<u>Power Turbine</u>
No. of Stages	3	5
Loading Parameter, $\Delta H_o/T_o$	0.200	0.210
Inlet Flow Parameter, $W \cdot T_o/P_o$	11.13	16.61
Inlet Speed Parameter, N/T_o	185.2	118.3
Inlet Flow Angle	90	65.6
Efficiency, %	0.904	0.906
Pressure Ratio, %	1.628	1.674
Rotor Speed, rpm	8200.	4800.
Exit Flow Parameter, $W \cdot T_o/P_o$	16.61	25.35
Exit Flow Coef, V_x/U_m	0.610	0.674
Exit Mach Number	0.167	0.146
Exit Swirl Angle, degree	64.9	69.60
Inlet Pressure, bar	44.83	27.48
Inlet Temperature, K	1088.9	914.7
Mass Flow Rate, kg/sec	74.12	74.12
Mean Velocity Ratio, V_x/U_m	0.566	0.577
Mean Wheel Speed, mps	440.	327.7
Horse Power	90370	80000

AD-A062 746

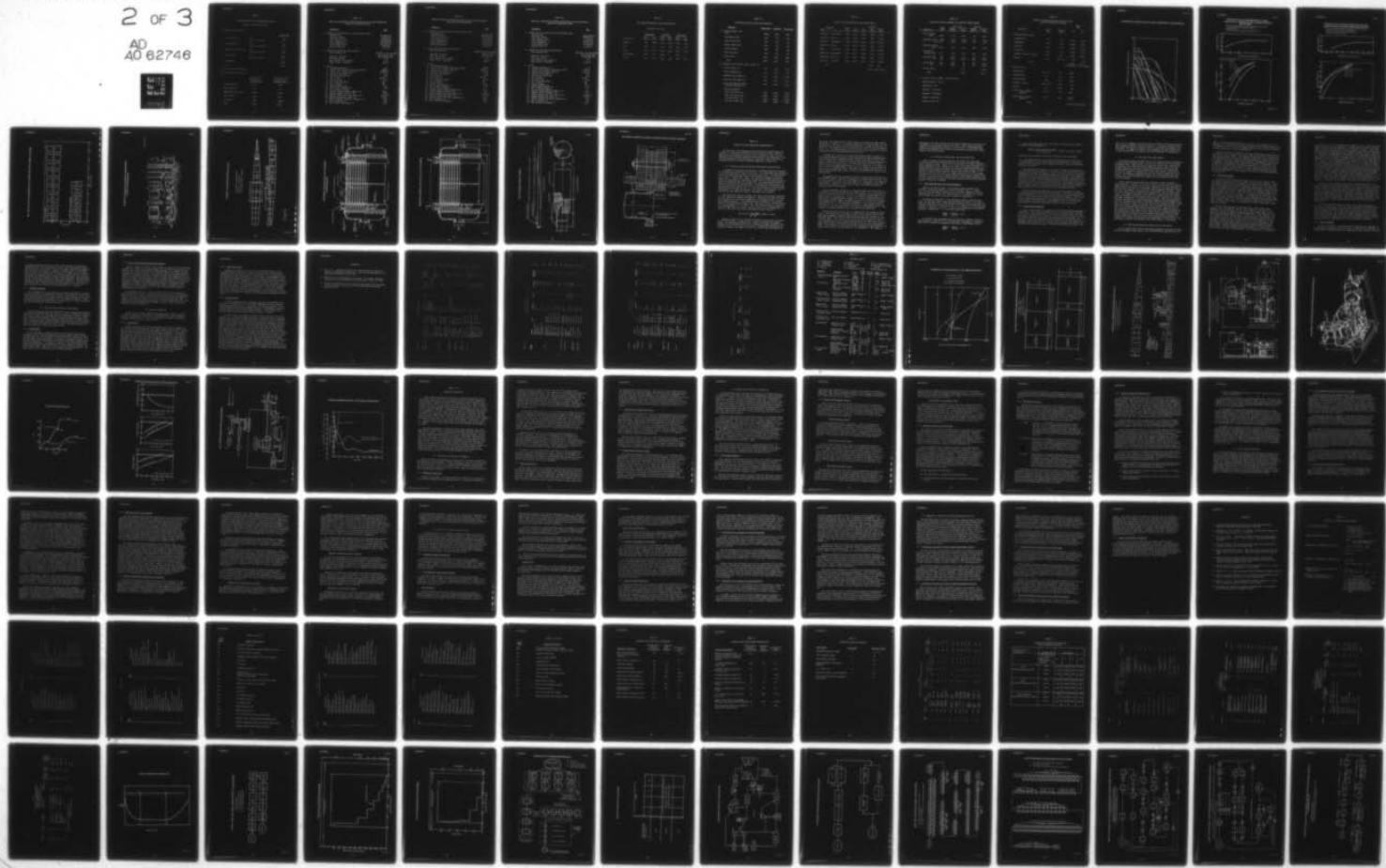
UNITED TECHNOLOGIES RESEARCH CENTER EAST HARTFORD CONN F/G 13/10
LIGHTWEIGHT PROPULSION SYSTEMS FOR ADVANCED NAVAL SHIP APPLICAT--ETC(U)
NOV 78 S C KUO, T L HORTON, H SHU, C W DEANE N00014-77-C-0735

UNCLASSIFIED

2 OF 3
AD
AO 62746

UTRC/R78-952979-4

NL



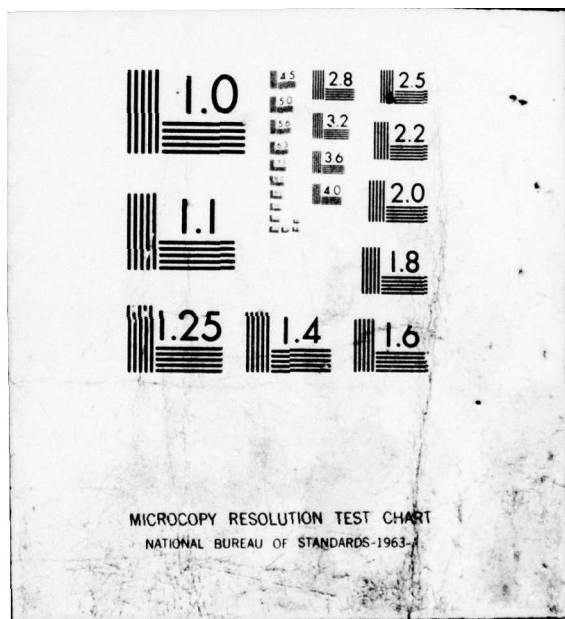


TABLE 3.9

ESTIMATED HELIUM CCGT TURBOMACHINERY WEIGHT

Rating: 59.7-MW (80,000 shp)

(a) Reference Design Case

		<u>Weight (kg)</u>
Front Compressor	Rotor	610
	Stators and Cases*	1,012
Rear Compressor	Rotor	587
	Stators and Cases*	797
Compressor Drive Turbine	Rotor	642
	Stators and Cases*	1,642
Power Turbine	Rotor	1,537
	Stators and Cases*	2,271
Contingency		<u>436</u>
Total		<u>9,533</u>

* Includes bearings and hardware

(b) Using Alternate Materials

	<u>Titanium Rotor, Steel Stators and Cases (kg)</u>	<u>Steel/Nickel Rotor, Titanium Stators and Cases (kg)</u>
Front Compressor	1,337	1,300
Rear Compressor	1,110	1,176
Compressor Drive Turbine	2,283	2,283
Power Turbine	3,808	3,808
Contingency	<u>436</u>	<u>436</u>
Total	<u>8,974</u>	<u>9,003</u>

TABLE 3.10

**RESULTS OF RECUPERATOR CONCEPTUAL DESIGN FOR A 59.8-MW (80,000-shp)
HELIUM CCGT PROPULSION SYSTEM**

<u>Parameters</u>	<u>Data</u>
A. Design Point Flow Conditions, Tube side/shell side:	
. working fluid	helium/helium
. flow rate, kg/sec	76.23/76.23
. flow velocity, m/sec	19.80/50.80
. inlet temperature, C	123.78/489.81
. outlet temperature, C	453.20/160.43
. inlet pressure, bar	46.39/16.66
. pressure drop, bar	.232/.583
B. Design Point Mechanical Specifications	
. heat exchanger type	tube-shell type in single pass counter flow
. materials, tube/shell	AMS 6323/AMS 6323
. tube size, OD, mm	6.35
. max. effective tube length, m	<u>< 5.5</u>
. safety factor, tube/shell	6.0/4.0
C. Results	
1. log-mean-temperature, C	18.85
2. overall heat transfer coefficient, W/m ² -C	888.84
3. overall heat transfer area, m ²	45,359.70
4. effective tube length, m	5.31
5. tube wall thickness, mm	0.56
6. No. of tubes	48,300
7. tube pitch, mm	8.50
8. No. of tube per module	300
9. No. of modules	161
10. modular diameter, cm	15.30
11. space between modules, cm	1.27
12. No. of modular supports	7
13. distance between modular support, cm	88.40
14. modular support thickness, cm	1.91
15. modular heading tube size, OD/ID in cm	10.8/10.16
16. modular heading tube pitch, cm	16.51
17. modular heading tube sheet thickness, cm	2.54
18. shell thickness, cm	2.54
19. heat transfer area margin, %	5.0

TABLE 3.11

**RESULTS OF PRECOOLER CONCEPTUAL DESIGN FOR A 59.7-MW (80,000-shp)
HELIUM CCGT PROPULSION SYSTEM**

<u>Parameters</u>	<u>Data</u>
A. Design Point Flow Conditions, Tube side/shell side:	
. working fluid	water/helium
. flow rate, kg/sec	880.00/76.23
. flow velocity, m/sec	2.44/88.68
. inlet temperature, C	29.44/160.43
. outlet temperature, C	42.64/37.78
. inlet pressure, bar	13.79/16.00
. pressure drop, bar	0.20/0.48
B. Design Point Mechanical Specifications	
. heat exchanger type	tube-shell type and single counter flow
. materials, tube/shell	monel/AMS 6323
. tube size, OD, mm	6.35
. max. effective tube length, m	≤ 1.4
. safety factor, tube/shell	110/5.0
C. Results	
1. log-mean-temperature, C	23.55
2. overall heat transfer coefficient, W/m ² -C	3,086.21
3. overall heat transfer area, m ²	4,521.00
4. effective tube length, m	1.35
5. tube wall thickness, mm	0.56
6. No. of tubes	18,300
7. tube pitch, mm	8.26
8. No. of tube per module	300
9. No. of modules	61
10. modular diameter, cm	16.32
11. space between modules, cm	1.27
12. No. of modular supports	3
13. distance between modular support, cm	67.67
14. modular support thickness, cm	1.91
15. modular heading tube size, OD/ID in cm	10.8/10.16
16. modular heading tube pitch, cm	17.59
17. modular heading tube sheet thickness, cm	2.54
18. shell thickness, cm	0.95
19. heat transfer area margin, %	7.0

TABLE 3.12

**RESULTS OF INTERCOOLER CONCEPTUAL DESIGN FOR A 59.7-MW (80,000-shp)
HELIUM CCGT PROPULSION SYSTEM**

<u>Parameters</u>	<u>Data</u>
A. Design Point Flow Conditions, Tube side/shell side:	
. working fluid	water/helium
. flow rate, kg/sec	702.00/76.23
. flow velocity, m/sec	2.44/62.72
. inlet temperature, C	29.44/126.73
. outlet temperature, C	41.46/37.78
. inlet pressure, bar	13.79/27.26
. pressure drop, bar	0.21/0.41
B. Design Point Mechanical Specifications	
. heat exchanger type	tube-shell type and single pass counter flow
. materials, tube/shell	monel/AMS 6323
. tube size, OD, mm	6.35
. max. effective tube length, m	\leq 1.4
. safety factor, tube/shell	40.0/4.5
C. Results	
1. log-mean-temperature, C	15.31
2. overall heat transfer coefficient, W/m ² -C	3,495.68
3. overall heat transfer area, m ²	2,718.00
4. effective tube length, m	1.35
5. tube wall thickness, mm	0.56
6. No. of tubes	15,000
7. tube pitch, mm	8.26
8. No. of tube per module	300
9. No. of modules	50
10. modular diameter, cm	16.32
11. space between modules, cm	1.27
12. No. of modular supports	3
13. distance between modular support, cm	67.97
14. modular support thickness, cm	1.9
15. modular heading tube size, OD/ID in cm	10.8/10.16
16. modular heading tube pitch, cm	17.59
17. modular heading tube sheet thickness, cm	2.54
18. shell thickness, cm	1.27
19. heat transfer area margin, %	10.0

TABLE 3.13

HEAT EXCHANGER PRESSURE LOSS CHARACTERISTICS

pressure loss in psi

Working Fluid	Regenerator		Precooler		Intercooler	
	Shell Helium	Tube Helium	Shell Helium	Tube Water	Shell Helium	Tube Water
Entrance	0.81	0.088	2.46	0.49	2.04	0.52
Core	8.46	3.36	6.97	2.91	6.97	2.99
Exit	0.15	-0.09	-0.09	-0.25	-0.18	-0.26
Acceleration	-0.26	0.13	-0.78	0	-0.59	0
Total	9.16	3.49	8.56	3.15	8.24	3.25

TABLE 3.14

ESTIMATED EXCHANGER WEIGHTS AND DIMENSIONS

<u>Component</u>	<u>Regenerator</u>	<u>Precooler</u>	<u>Intercooler</u>
A. Exchanger Weight, (kg)			
Tube	203900	2480	2040
Wrap spacing wire	2090	370	310
Module wrap sleeve	2820	290	340
Module heading tube	1230	470	380
Module supports	1340	320	230
Tube head sheets	1110	570	450
Shell weight	14550	1520	1680
Total	44040	6020	5430
B. Exchanger Size in Meters, (Ref. to Fig. 3.8)			
Overall length, L_1	7.62	3.16	3.16
Overall diameter, D_1	2.36	1.60	1.43
Exchanger core length, L_2	6.53	2.26	2.26
Effective tube length, L_3	5.31	1.35	1.35
Shell side inlet and outlet connector distance, L_4	5.92	1.60	1.60
Connector Diameters:			
Shell side inlet, D_{si}	0.381	0.305	0.305
Shell side outlet, D_{so}	0.305	0.305	0.305
Tube side inlet, D_{ti}	0.305	0.610	0.610
Tube side outlet, D_{to}	0.305	0.610	0.610

TABLE 3.15

RESULTS OF POWER CONVERSION SYSTEM PIPING DESIGN

<u>From</u>	<u>Components</u>	<u>To</u>	<u>Length</u> (m)	<u>O.D.</u> (cm)	<u>I.D.</u> (cm)	<u>Pressure</u>	<u>Weight</u> (kg)
Low-Comp.	Intercooler		.6904	30.48	28.63	.0382	47.628
Intercooler	Hi-Comp.		.6331	30.48	28.63	.0268	43.546
Hi-Comp.	Regenerator		2.1604	30.48	28.63	.0697	148.781
Regenerator	Heater		1.0692	30.48	28.63	.0692	73.483
Heater	Hi-Turbine		3.1251	38.10	36.20	.1079	278.057
Power Turb.	Regenerator		.5432	38.10	36.20	.0334	48.535
Regenerator	Precooler		.6242	30.48	28.63	.0643	43.092
Precooler	Low-Comp.		.6355	30.48	28.63	.0466	43.999
Total						0.456	730.
(2.0%) (0.0122 kg/kW)							

TABLE 3.16
ESTIMATES OF HELIUM INVENTORY AND INVENTORY CONTROL VESSEL

A. Components	Volume (m ³)	Full Load		10% Load	
		Density (kg/m ³)	Inventory (kg)	Density (kg/m ³)	Inventory (kg)
Heater (Helium Side)	16.810	2.315	38.92	.304	5.103
Regenerator (HP)	7.500	3.897	29.26	.531	3.970
(LP)	11.433	1.336	15.29	.173	1.973
Precooler (Helium Side)	1.129	2.129	2.40	.260	0.293
Intercooler (Helium Side)	.914	3.785	3.45	.462	0.422
Compressor (HP)	.430	2.872	1.24	.350	0.150
(LP)	.368	4.954	1.82	.604	0.223
Turbine (HP)	.359	1.695	.61	.204	0.075
(LP)	.354	1.208	.43	.148	0.052
Ducting (Total)	-	-	2.17		0.285
Total			95.58		12.55

B. Inventory Control Vessel - Low Alloy Steel

Maximum Capacity = 83. kg

Temperature = 32 C

Pressure = 41.379 bar

Diameter = .6706 meter

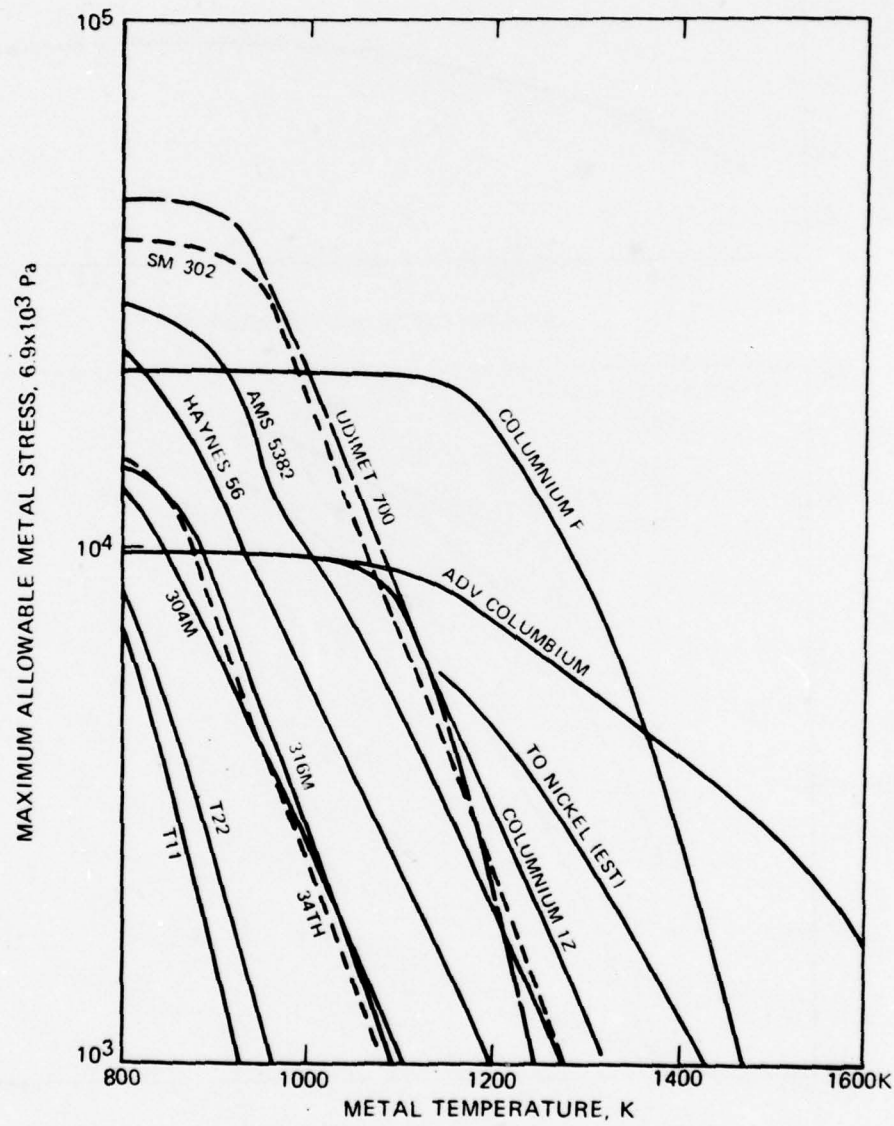
Length = 6.614 meter

Number of Units = 6

TABLE 3.17
SUMMARY OF LIGHTWEIGHT POWER CONVERSION SYSTEM
COMPONENT DIMENSIONS AND WEIGHT

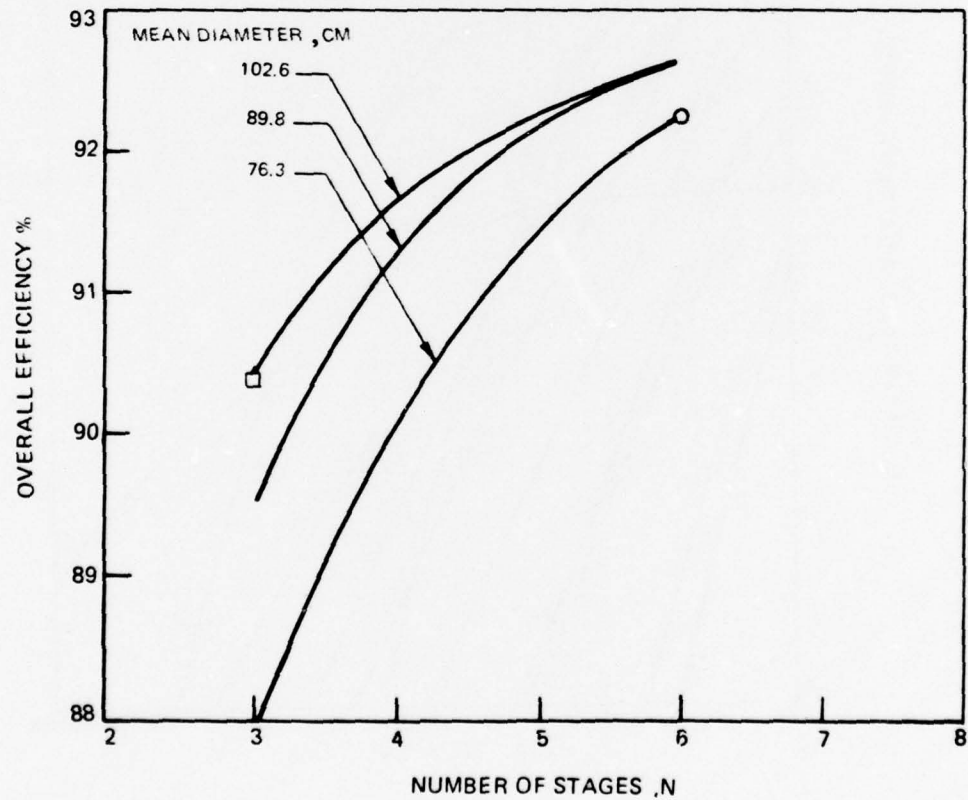
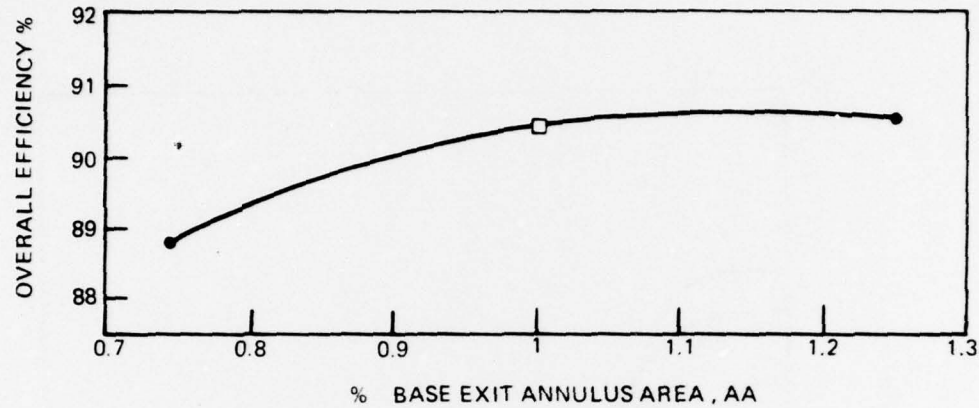
Components	Length (m)	Diameter (m)	Dry	Weight (kg)
				Wet
A. Power Conversion System				
Turbomachinery	6.70	1.52	9,545	9,559
Regenerator	7.62	2.36	44,040	44,128
Precooler	3.16	1.60	6,020	9,366
Intercooler	3.16	1.43	5,430	7,897
Inventory Vessels (6 Units)	6.60	0.67	6,294	6,294
Ducting	9.45	30 ~ 0.4	729	731
Total			72,058 (=1.98 lb/shp)	77,975 (=2.14 lb/shp)
B. Heater Systems				
Helium Heater	6.55 x 5.33	2.74	40,130	
Turbomachinery	1.22	1.22	3,022	
Air Recuperator	1.98	1.37	2,596	
Combustor & Mixer	1.98 x 1.52	0.76	682	
Ducting	6.10	3.66	435	
Intake (duct, silencer & demister)	12.20	3.66	18,727	
Uptake (duct, silencer & educator)	12.20	3.05	48,636	
Total			114,464 (=3.15 lb/shp)	

ADVANCED GAS TURBINE MATERIAL STRESS-TEMPERATURE CHARACTERISTICS



**PREDICTED EFFECT OF COMPRESSOR DRIVE TURBINE
ANNULUS AREA , NUMBER OF STAGES , AND MEAN DIAMETER
ON EFFICIENCY**

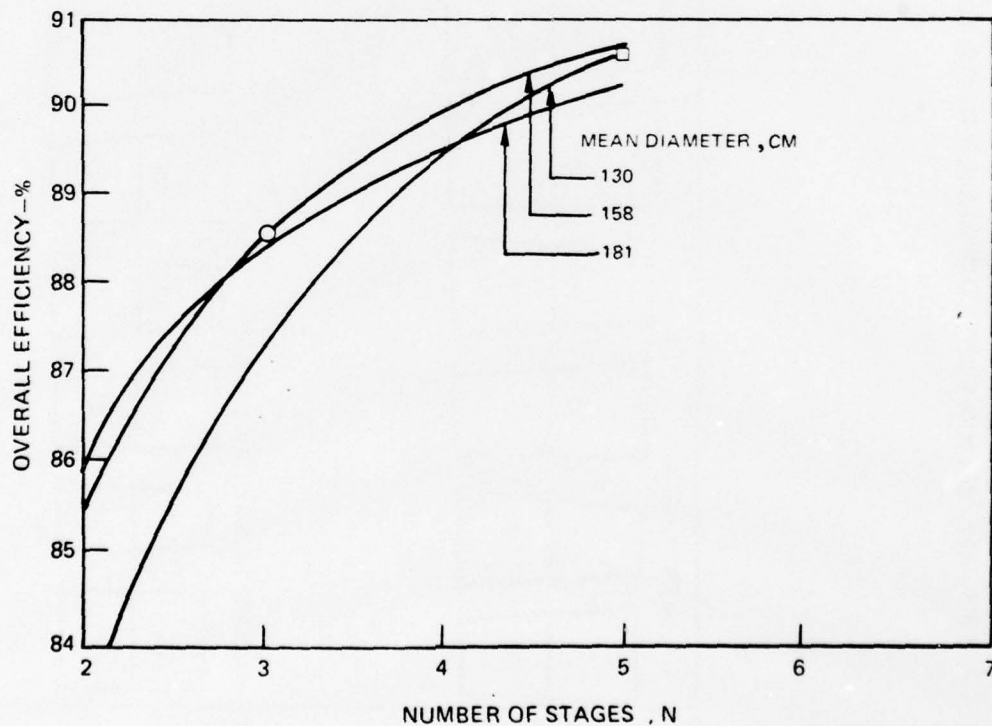
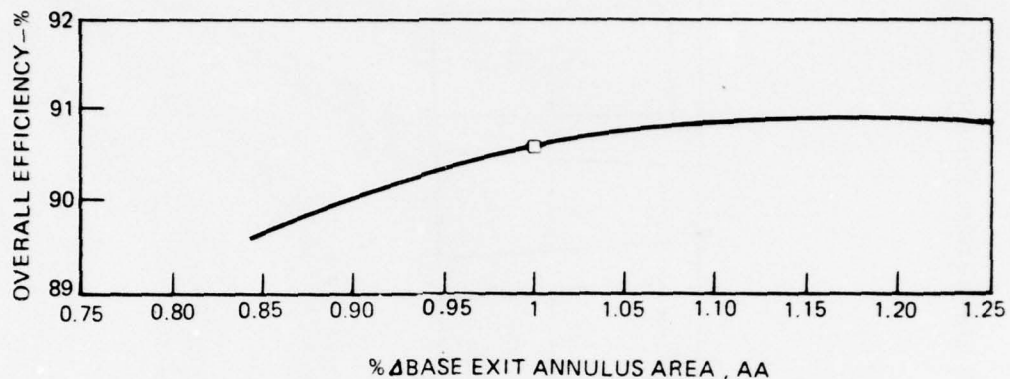
- THIS FIGURE IS PROVIDED BY THE GOVERNMENT PRODUCTS DIVISION
OF PRATT & WHITNEY AIRCRAFT GROUP (P&WA)
- P&WA'S SELECTION
- UNITED TECHNOLOGIES RESEARCH CENTER'S SELECTION



78-02-235-10

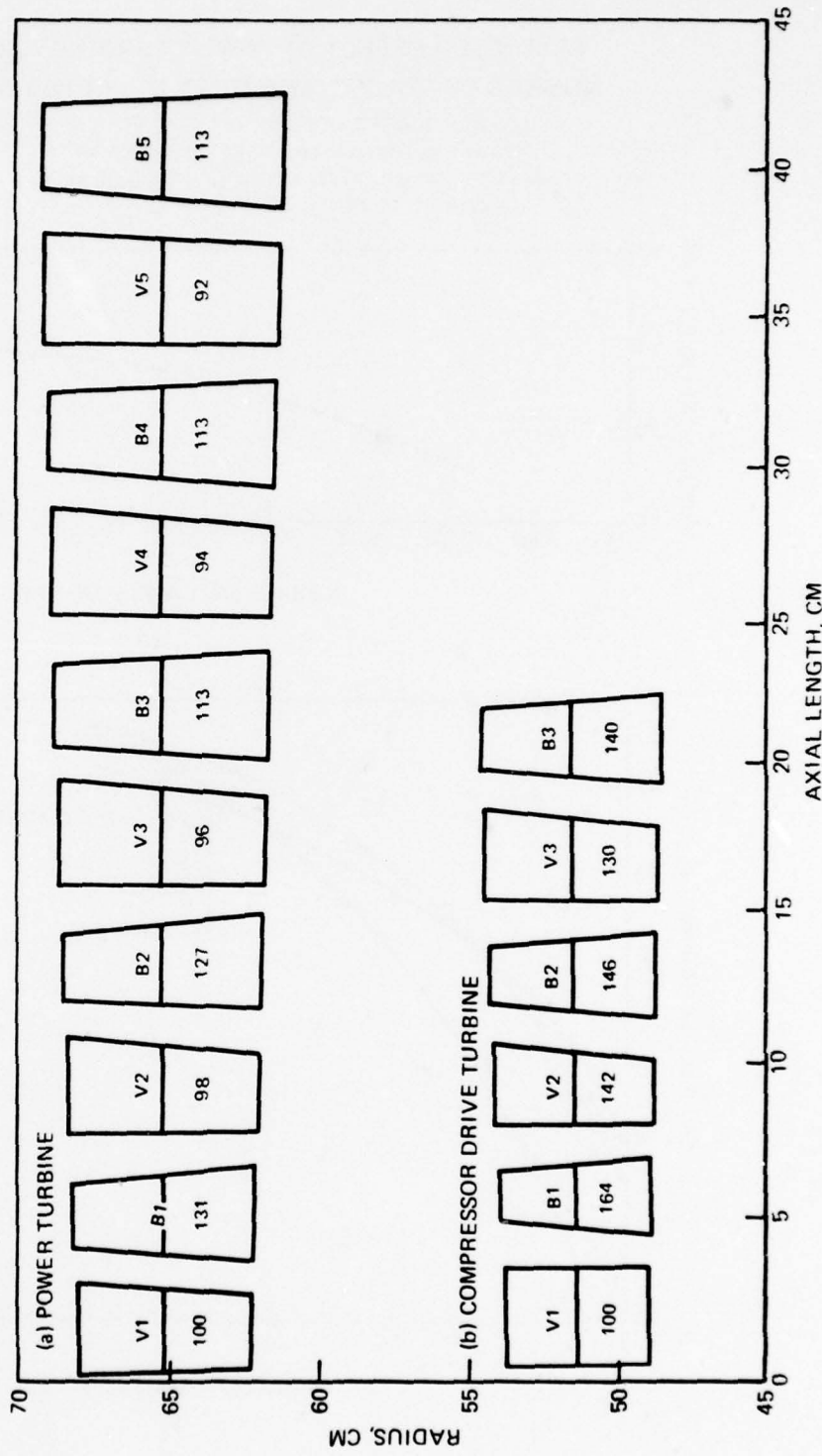
**PREDICTED EFFECT OF POWER TURBINE ANNULUS AREA,
NUMBER OF STAGES, AND MEAN DIAMETER ON EFFICIENCY**

- THIS FIGURE IS PROVIDED BY THE GOVERNMENT PRODUCTS DIVISION
OF PRATT & WHITNEY AIRCRAFT GROUP (P&WA)
- REFERENCE DESIGN SELECTED BY UTRC AND P&WA
- POTENTIAL ALTERNATIVE DESIGN



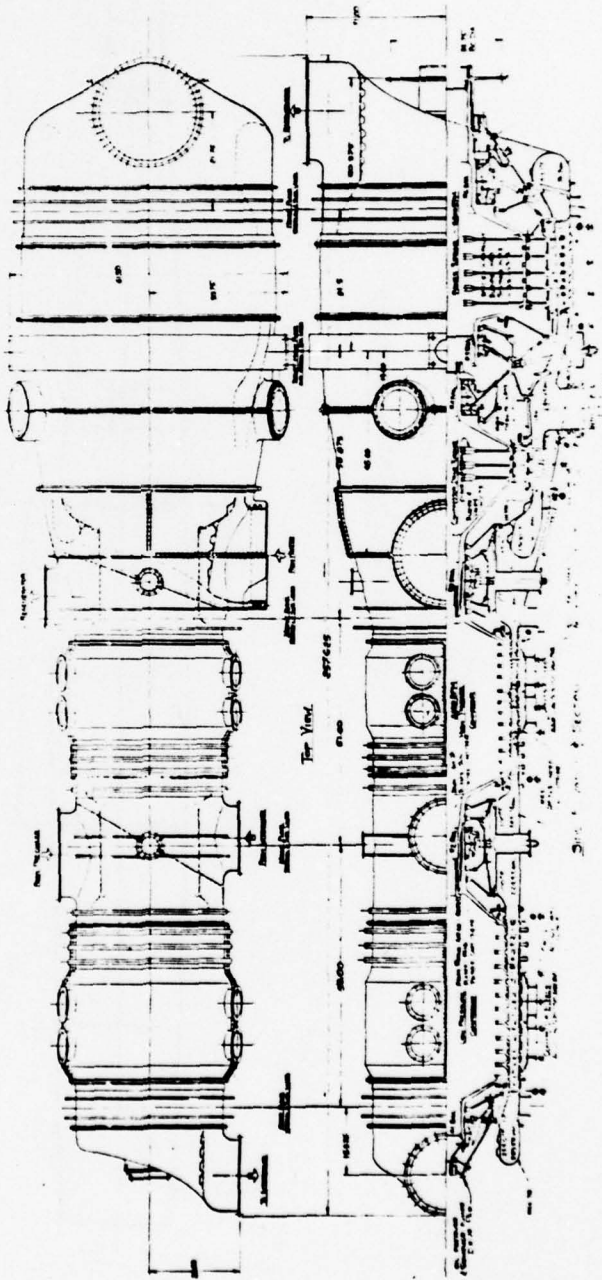
78-02-235-11

59.7-MW HELIUM CCGT COMPRESSOR DRIVE TURBINE AND POWER TURBINE ELEVATIONS



CONCEPTUAL DESIGN OF HELIUM CCGT TURBOMACHINERY
• RATING=59.7 MW (80,000 shp)

Pratt & Whitney Aircraft Group

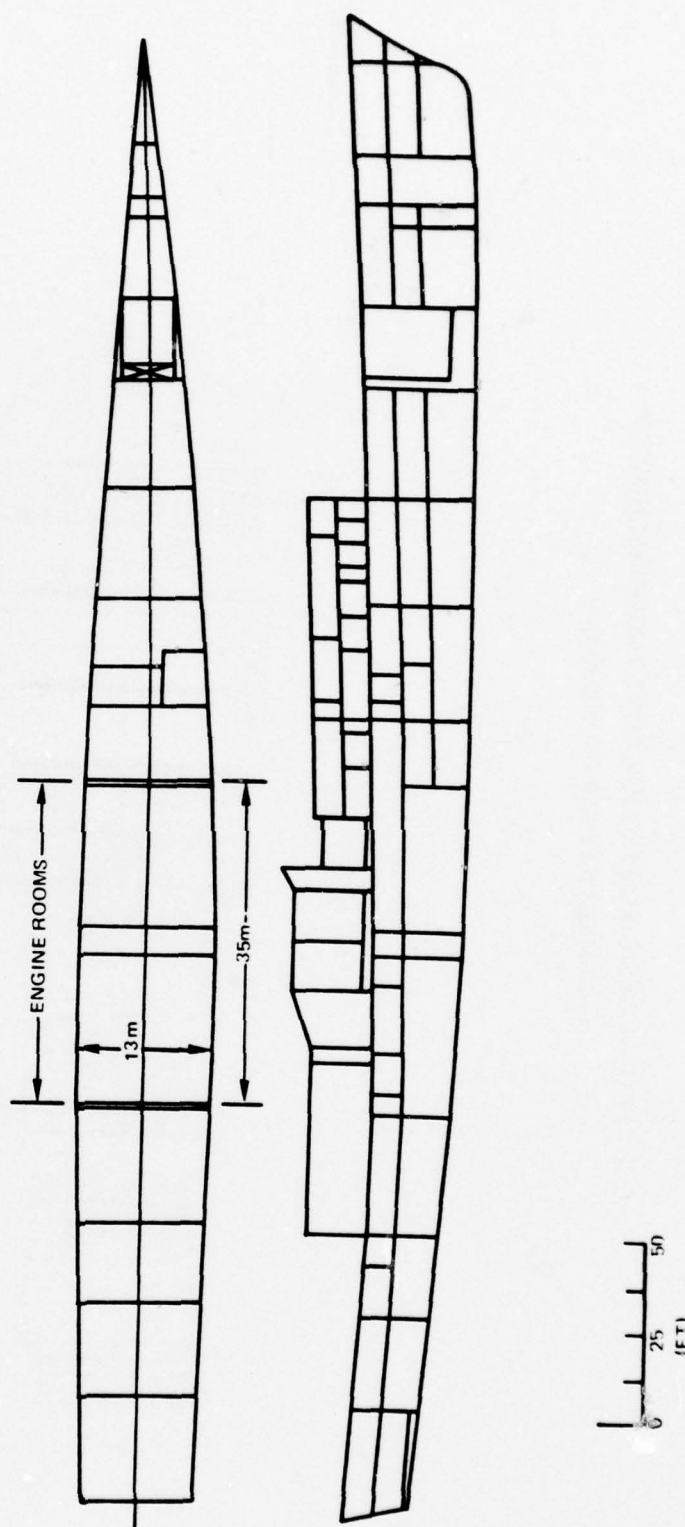


POTENTIAL HIGH SPEED DESTROYER LAYOUT

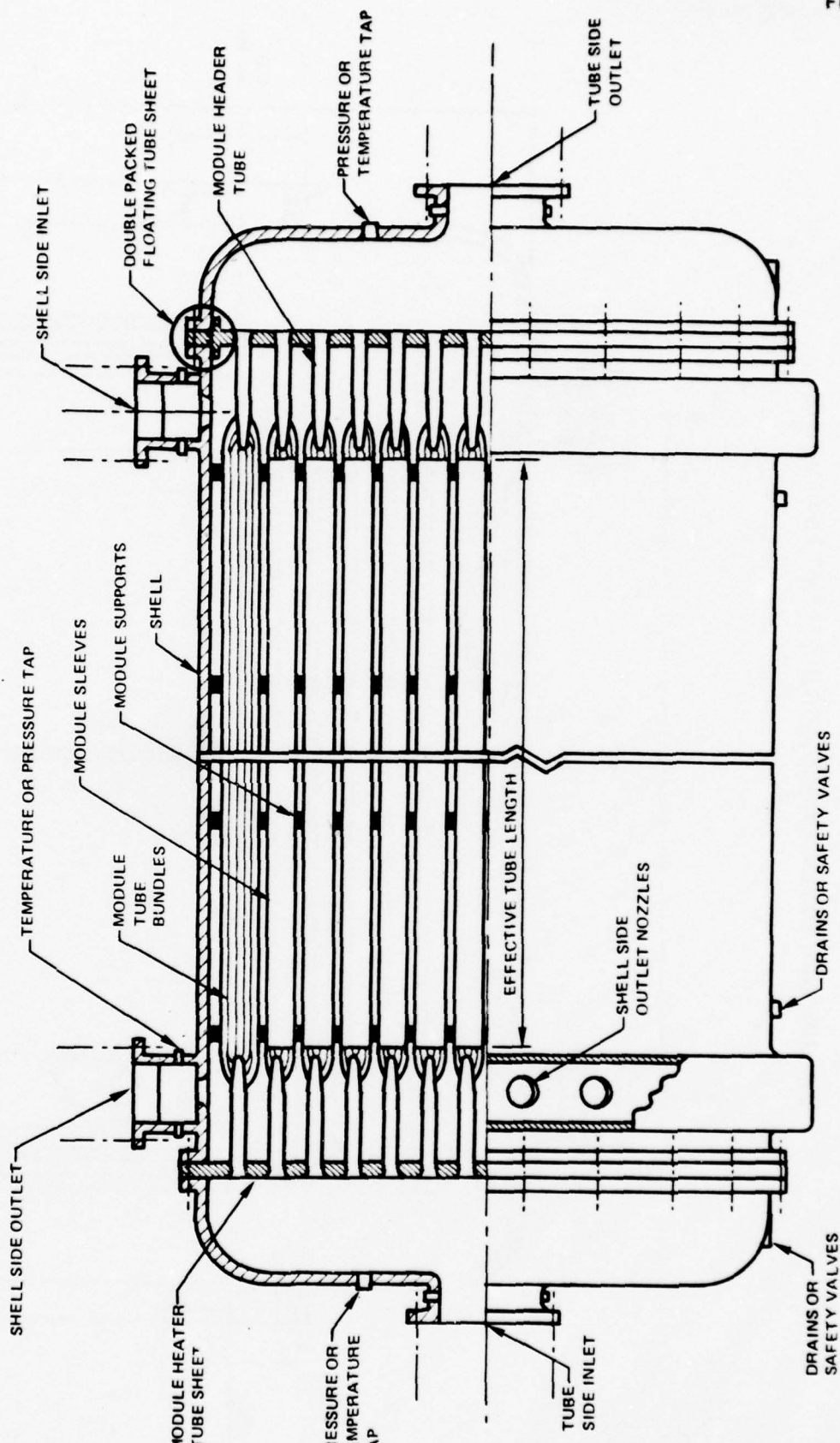
DISPLACEMENT = 3500 TO 4000 TONS

MAX SPEED = 45 TO 50 KNOTS

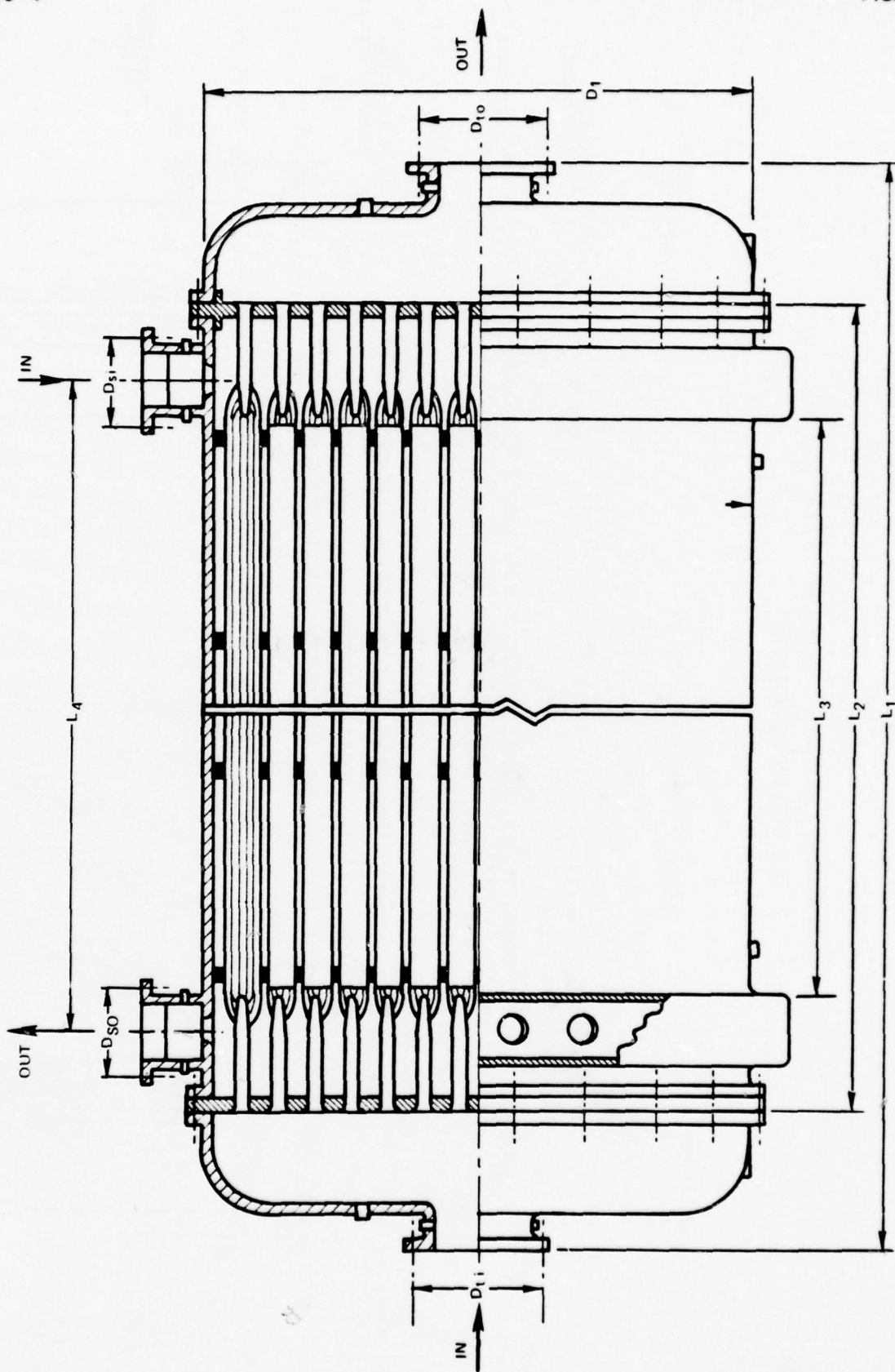
TOTAL INSTALLED POWER = 160,000 SHP



PRELIMINARY DESIGN OF CCGT HEAT EXCHANGERS
• 59.8 MW (80,000 SHP)

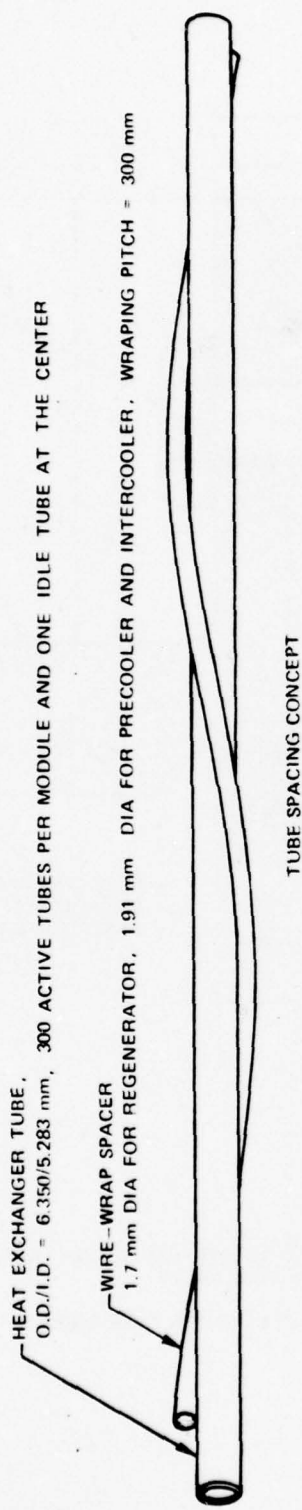


DIMENSIONAL NOMENCLATURE FOR CCGT HEAT EXCHANGERS

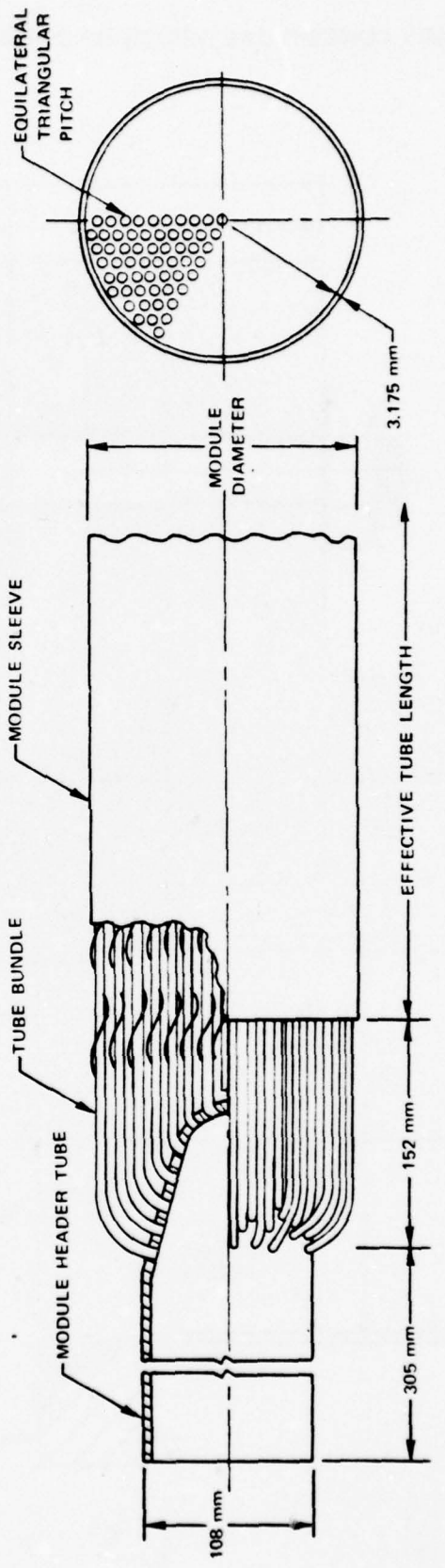


78-06-57-4

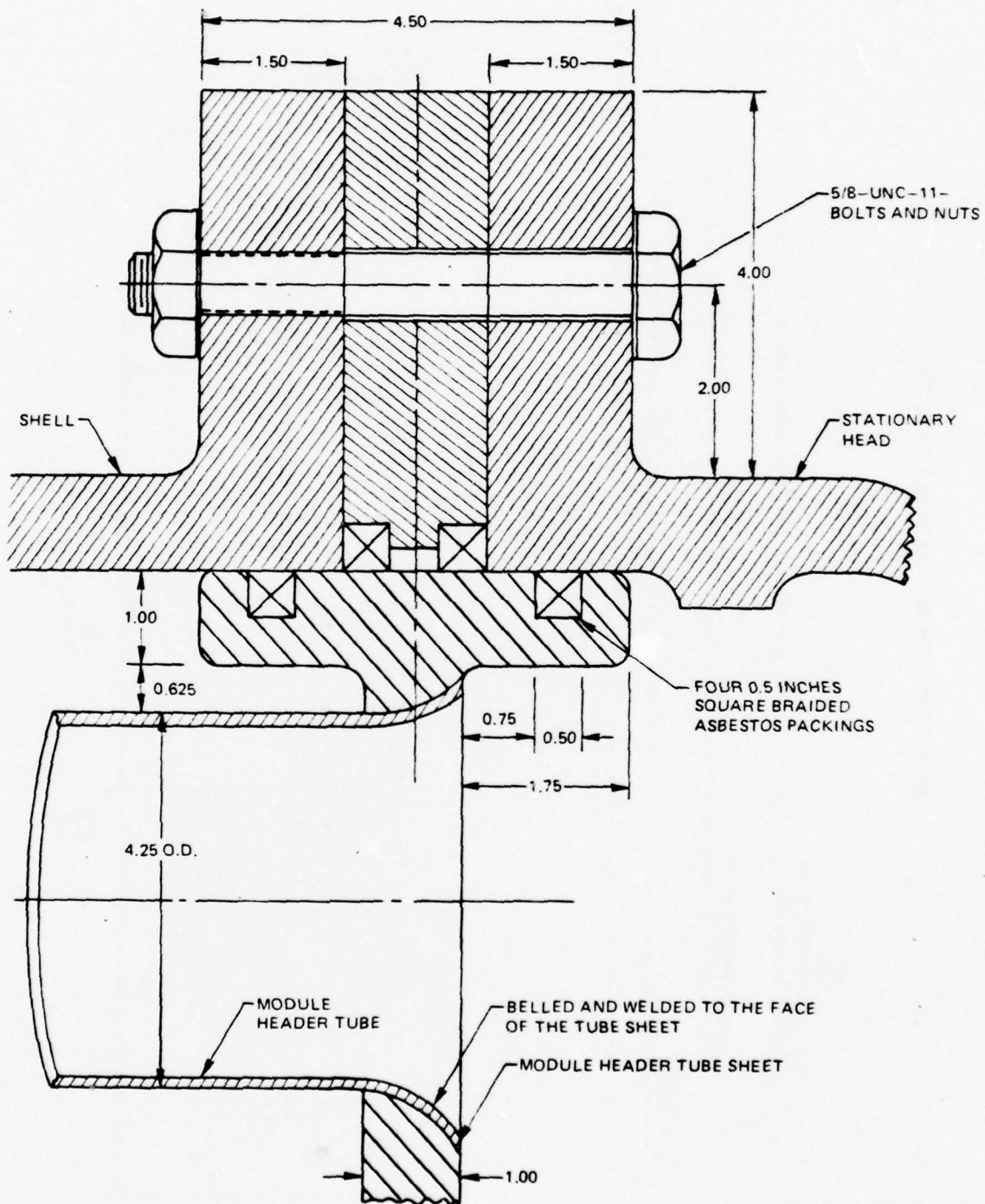
HEAT EXCHANGER MODULE CONCEPT



TUBE SPACING CONCEPT



PRELIMINARY CONCEPTUAL DESIGN OF DOUBLE PACKED FLOATING TUBE SHEET



PHASE II-4

SYSTEM LAYOUT AND OPERATIONAL CHARACTERISTICS

In this phase of the program a practical propulsion system layout plan suitable for integrating the baseline closed-cycle gas turbine propulsion system into the reference ship type selected in Phase II-2 (Ref. 4.1), was developed and the potential operating characteristics were investigated. The baseline propulsion system characteristics are based on the results of the conceptual design of the major components summarized in Phase II-3.

4.1 Propulsion System Installation Requirements and Constraints

To prepare the propulsion system layout, the maximum dimensions available for the machinery platform must be identified. The requirements and constraints can be best appreciated in terms of an engine room layout. A refined version of this layout was developed from the one presented in Phase II-2 based on input from J. J. Henry, Inc., (JJH). The following paragraphs discuss the effect of the refined hull dimensional characteristics on the ship's stability and on the available space for the machinery. The representatives from JJH provided a series of hull form analyses. The dimensional characteristics of various hulls plotted against the thruster shaft power for the selected high-speed destroyer are shown in Fig. 4.1. The results indicate that for a given displacement, the longer and narrower ships require less horsepower. In choosing the hull dimensions, however, compromises are necessary.

Hull dimensions, especially length, are chosen as the minimum compatible with the required displacement and powering. The longer and finer hull forms are desirable from a resistance standpoint, but necessary stability requirements impose limitations. The standard measure of stability is a numerical quantity called metacentric height or GM. The typical value of GM for destroyers is approximately 1.2 m (4 feet). This value provides adequate stability, and at the same time not so short a period of roll as to be uncomfortable to the crew. The roll period can be approximated using the equation:

$$\text{Roll Period} = \frac{0.4 \times \text{Beam}}{\sqrt{\text{GM}}} \quad (\text{numbers in feet})$$

Assuming a beam of 12.2 m (40 feet) and GM of 1.2 m (4 feet), the period of roll is 8 seconds. A value of 8 sec is about the minimum; for smaller values, the ship becomes uncomfortable. Assuming the center of gravity to be between 0.3 m (1 ft) and 0.6 m (2 ft) above the Design Waterline and the displacement constant, the longer the vessel for a given beam, the greater will

be the GM. The longer the GM, the more rapidly the vessel will right itself, resulting in a "snap roll." To assure adequate but not excessive GM, the ideal proportion for the type of vessel being considered is a beam to draft ratio of about 3.0. The proportions are indicated by cross curves for each displacement in Fig. 4.1. The maximum beam for a given length of ship should not be greater than 110 percent of the beam defined by these curves.

Although some variation can be permitted depending upon the final hull form, the maximum beam obtained, as described above, provides reasonable space for propulsion plant installation; hence, larger widths should not be considered. In addition, it should be noted that the values obtained represent the maximum width of the ship's hull; to define usable space inside the engine room, a reduction of approximately 0.6 m (2 ft) is necessary. This allows for 0.3 m (1 ft) of nonusable space on each side of the engine room into which the ship structural members will fall. Therefore, the maximum beam length for the engine rooms would be about 12.6 m (41.5 ft) to 13.5 m (44.4 ft) for the ship type selected.

The maximum length of the machinery space is derived from an estimation of the floodable length. The basic requirement for a combat vessel over 91 m (300 ft) long is that it is able to sustain damage over 15 percent of its length and remain afloat. Therefore, a ship 122 m (400 ft) in length must remain afloat if the hull is ruptured for 18.3 m (60 ft) and a 152 m (500 ft) ship must survive a 22.8 m (75 ft) rupture.

Based on available information, the maximum length of the 122 m (400 ft) vessel which can be flooded and the ship remain afloat is 35 m (115 ft) and for the 152 m (500 ft) vessel, 43.6 m (143 ft). Two engine room arrangements, as shown in Fig. 4.2 are possible. For the 122 m (400 ft) configuration, if the engine rooms are adjoining and we assume a 7.6 m (25 ft) auxiliary machinery room, we get a maximum length of engine rooms of 13.7 m (45 ft) each, as shown in Arrangement No. 1. The alternative arrangement is to separate the engine rooms with a 3.4 m (11 ft) cofferdam resulting in a longer overall length of 15.9 m (52 ft) for each engine room as illustrated in Arrangement No. 2. This information provides a guideline for propulsion system layout plan.

Additional limitations also must be considered for the propulsion system layout. The centerline of the propeller shaft, thrust bearing location and size, and arrangement of gearbox input/output can also have an effect on the CCGT-LWSP layout. The propeller shaft and thrust bearing locations were identified as shown in Fig. 4.3, and as discussed earlier in Phase II-3, an epicyclic gearbox with reversing capabilities was selected. This latter selection means that the shaft of the power turbine must be in line with the propeller shaft. This constraint in turn positions the turbomachinery and establishes the length of the hot duct from the heater to the turbomachine. This length is

much greater than that possible with an off-set gearbox which could allow the turbomachine to be mounted closer to the heater. Thus, should an off-set gearbox be considered more desirable at a future date, the CCGT-LWSP might achieve some advantages which could be traded against the potentially higher weight of the off-set gearbox.

4.2 Propulsion System Layout and Installation Plan

After the engine room sizes have been identified, the preliminary propulsion system layout was made based on the sizes of the major components of the propulsion system. Figure 4.4 is a plan view of the system and Fig. 4.5 shows a perspective view. Based on this layout, the propulsion system, including the power conversion system, the inventory control system, the heater system, and the transmission gearbox, would occupy a space of about 11.4 m (37.5 ft) in width, 12.8 m (42 ft) in length, and 5.3 m (17.5 ft) in height. Combining this result with the engine room size characteristics shown in Figs. 4.2 and 4.3, one can see that the installation of the present lightweight propulsion system into the selected high speed destroyer ship would not encounter any major installation problems.

4.2.1 High Speed Destroyer Hull Form Refinements

Based on the above results, a more detailed layout drawing of the propulsion system was prepared by the naval architect firm, J. J. Henry, Inc. The size and weight characteristics of the major components that were summarized earlier in Table 3.17 were provided to J. J. Henry, Inc., as input for weight distribution and center of gravity computations.

To arrange the machinery, it was necessary to select a specific hull form; thus the beam, draft, length and displacement are fixed. To provide a vessel of sufficient width for the machinery plant and hull structure with the U-shaped helium heater illustrated in Fig. 4.4, a beam of 13.1 m (43 feet) was selected. A draft of 4.3 m (14.0 ft) was derived considering the approximate proportion of Beam/Draft = 3.0, the actual value being:

$$\frac{\text{beam}}{\text{draft}} = \frac{43.0 \text{ ft}}{14.0 \text{ ft}} = 3.07$$

A relatively high length/beam ratio was selected to maintain as thin a form as possible compatible with the displacement requirements. A length of 128 m (420 ft) between the perpendiculars provides a length/beam ratio of:

$$\frac{\text{length}}{\text{beam}} = \frac{420 \text{ ft}}{43 \text{ ft}} = 9.77$$

Assuming a block coefficient of 0.53 which is consistent with modern destroyers, the displacement is:

$$\frac{420 \text{ ft} \times 43 \text{ ft} \times 14.00 \text{ ft} \times 0.53}{35 \text{ ft}^3/\text{ton s.w.}} = 3830 \text{ L Tons } (3.89 \times 10^6 \text{ kg})$$

which meets the requirement of having a relatively high displacement.

An estimate was made of the stability characteristics of the hull; the GM is approximately 1.5 m (5 feet) and the roll period 8 sec. Both these quantities can be adjusted to more favorable values as the hull form characteristics are refined.

The supercavitating propeller, 3 m (10 ft) in diameter and rotating at about 580 revolutions per minute, is of sufficient size to absorb the required horsepower and develop the necessary thrust, the thrust required being in the neighborhood of 1.157×10^6 newtons (260,000 lbf) per shaft. This judgement is based on the preliminary information currently available regarding the hull form to be utilized. A more detailed analysis can be made later when the hull and propeller designs are more accurately defined. The propeller structural strength becomes a critical issue when the screw of this relatively small diameter is heavily loaded. This can be resolved only through a total propeller design analysis which was not possible in this preliminary analysis.

Propeller shaft angles and propeller locations were chosen to provide a reasonable propeller tip clearance from the hull. In order to avoid vibrational problems in the stern, the propeller blade tip should be between 0.2 D and 0.4 D away from the hull, where D is the propeller diameter. In the case of the supercavitating propeller, this clearance should be as generous as possible and on the present ship is approximately 1.5 to 1.8 m (5 to 6 ft). Both propeller shafts have been angled outboard to aid the situation.

4.2.2 Engine Room Arrangement

Figure 4.3 illustrates the engine room locations and possible arrangement of machinery. Engine rooms approximately 14.6 m (48 ft) long were inserted into the vessel and separated by a 4.9 m (16 ft) cofferdam. Thus, the floodable length requirements are satisfied. For this preliminary design, any space not directly affected by the engine room insertion was not modified or rearranged. To fit all elements of the power plant into the ship and maintain a reasonable shaft alignment, the inventory tanks were moved from under the turbine and placed lower in the ship. It should be noted that this ship is very

space critical; probably, more space should be allowed for additional machinery such as pumps, generators, valves and controls. To develop a realistic ship, these additional machinery components should be specified and integrated into the design. In summary, the engine room arrangements and sizes shown in Fig. 4.3 are consistent with the required size and displacement of the HSD ship.

4.3 Ship Operational Requirements

The system response time from loiter to full speed, as well as capabilities for maneuvering and reverse power, are crucial to the mission of future high-performance ships. OCGT systems can respond much quicker than steam systems. In comparison, the closed-cycle gas turbine may encounter some of the same thermal response restrictions as steam systems; CCGT are still expected to provide better operation characteristics than steam systems. This would be particularly apparent if computerized total ship control systems were incorporated. The following paragraph discusses the anticipated HSD operational requirements and the relevant power system operational characteristics and control techniques.

Power conversion systems (PCS) for an HSD must be able to respond to rapid transients. Further, for the ship to attain its full potential response characteristics, the overall ship control system should not only supervise the PCS but should also match the interrelated capabilities and operating requirements for the remainder of the propulsion system components including: propeller speed, shaft torque, hydraulic system requirements, and clutching, among others. For example, very rapid power response is required when operating in rough seas because the propeller can unload in as short a time as 0.1 seconds and remain unloaded for 1.5 seconds during broaching. OCGT controls presently available can meet this situation and prevent dangerous turbine overspeeds on existing high-speed ships (such as hydrofoils) where the most stringent requirements, of all vessel types studied, are placed on the propulsion system. Thus rapid PCS response, high-power-to-weight ratio, and small PCS sizes are all vital to the successful functioning of high-speed ships. Rapid start-up is also important to these vessels since a long start-up period would negate much of the advantage of high speed on short dash missions. Automated and computerized control systems may also be a necessary requirement to provide these vehicle capabilities. Thus, the overall ship system controls necessary to integrate the propulsion system with vessel requirements, characteristics, and constraints can affect the feasibility and effectiveness of a new system.

4.4 Power System Operational Characteristics and Control

As can be appreciated from the operational strategies discussed previously, the rate of change of power output of the CCGT-LWSP may be required to be very

rapid. For the design presented here, this rate is not limited by the turbo-machinery. It is primarily a selected limitation of 222 C (400 F) per hour, on the temperature rise of the heat exchanger materials, which dictate the gradual increase or decrease in operating temperature.

For the selected ship operation, the required PCS response characteristics are generally less stringent than those already available with aircraft-derivative, open-cycle gas turbines. For example, sophisticated control systems have been developed which allow aircraft propulsion engines to transit from idle to full power in less than 5 seconds while avoiding or accommodating engine dynamic problems. For a marine OCGT to accelerate from idle to full power in 30 seconds is not unreasonable, although more impressive is the fact that only 90 seconds is typically required to go from an inoperative "cold iron" condition to full power as shown in Fig. 4.6. While the CCGT-LWSP might not match this latter performance, it might approach the former by utilizing appropriate control methods.

4.4.1 Rapid Power Changes

The type of control system and primary heat source will directly affect the response of the closed-cycle gas turbine to power change commands. Studies conducted of response rate for the HTGR gas turbine (Ref. 4.2) indicated that for a nuclear heat source with slow temperature change rates (0 to 100 percent power in 20 minutes), the ability to make rapid power changes required the heat source to be maintained at full temperature while a gas bypass around the core and recuperator was utilized. Such a system was still believed capable of full power changes in less than five seconds. Instantaneous drop loads were also handled with only 10 percent overspeed. The determining factor in these cases was maximum bypass valve slew rate and maximum allowable system pressure change rate. Pressure change rates of 300 psi/sec were estimated with valve slew rates of 90°/sec (Fig. 4.7) when incorporated into large, single-shaft, direct-drive gas turbines.

For the 57.9 MW (80,000-shp) CCGT-LWSP system, many of these same characteristics are expected. Bypass control similar to that used in the HTGR (Ref. 4.2) can be expected to provide any rapid power changes, once the system has attained the normal operating temperatures. These response rates should then equal OCGT characteristics. As can be seen in the potential control schematic of Fig. 4.8, the heater would be protected from the high rates of change in pressure since these will occur only in the bypass duct. And should the revised power level be desired for a period of time greater than a few minutes, a more gradual change of inventory and/or temperature would then be made. The most stringent operational characteristics of the CCGT-LWSP required to provide satisfactory HSD performance is the time required to proceed from "cold iron" to maximum power. This characteristic is restricted

by the limit placed on the maximum rate of temperature (222 C, 400 F per hour) change allowed in the heat exchangers. A change from "cold iron" to maximum power could take over two hours if no other measures are taken. These other measures should include maintaining the regenerator and heater heat exchangers at a temperature of approximately 200 C (392 F) and 400 C (752 F), respectively. This would allow 80 percent of maximum speed (at approximately 40 percent rated power) to be attained within eight minutes by increasing the helium working gas to the rated inventory (pressure) but at a lower TIT of approximately 565 C (1050 F). At this degraded TIT, the temperature of hot helium entering the recuperator would be approximately 800 F, or only 50 F above the warm recuperator temperature maintained. Further reduction in the 80 percent-speed start time is possible with overpressurization of the system for up to 20 percent (through inventory control) but requiring appropriate system design modifications. Pressure changes can generally be made more rapidly than temperature changes. For example, a period of two minutes would be an acceptable time-span to allow for transition from minimum to maximum pressurization. This means that rapid power output changes could also be made through the use of inventory control processes, although not as rapidly as through bypass configurations. A schematic for the control requirements is shown in Fig. 4.8.

Keeping the heat exchangers warm could be accomplished by the use of electric heaters or by "firing" the heater at a low fuel flow rate. Of course, thermal insulation would be used to keep the outer surface of the insulation below 66 C (150 F) so that there would be no hot surfaces for personnel injuries; this insulation would also cut the amount of electric power required to keep the equipment warm. The final insulation requirements would have to be determined in the detailed design. Additionally, the heater design will also have to be examined to determine if any other restrictions attributable to the heater exist (e.g., thermal stresses) which might limit propulsion system start-up time.

A 57.9 MW (80,000 HP) design utilizing a free turbine would tend to accelerate at a much higher rate in the event of propeller broaching than the single shaft nuclear design. However, actual experience with the FT4 free turbine in marine service indicates that a control system can handle these events satisfactorily. The closed-cycle bypass system is expected to be as fast acting as the FT4 open-cycle fuel control; consequently, it is expected that even small free turbine units should be controllable. Figure 4.9 illustrates the response time expected for total instantaneous load losses.

4.4.2 Thrust Reversing

To reverse the thrust, the response time is expected to be comparable or better than a steam system, but not as fast as an OCGT system. This might be accomplished by combined procedures of bypassing the power turbine, declutching

the gearbox, braking the propeller shaft, shifting gears to reverse mode, reconnecting the clutch, decoupling the brake, and increasing power output before zero output is obtained. The use of a bypass around the turbomachine power turbine is projected to be capable of reducing power to zero output within 1 minute (at a maximum rate of reduction in power output of 2 percent per second), by opening a valve in this turbine bypass loop. This process removes the driving energy from the power turbine and thus allows the generator and turbine drag to rapidly slow down these components. The declutching, braking, and shifting gears would be performed concurrently. When the short acceleration time is included, the total time required to convert from full power forward to full reverse should be approximately 1 1/2 minutes.

4.4.3 Emergency Shutdown

For an emergency, the high compressor discharge helium could, of course, be directly vented to the atmosphere. However, the consequences of the rapid thermal gradient which occur in the recuperator, along with the limitations for time periods required for recharging, must be carefully considered. A more desirable emergency shutdown would utilize bypass modes to reduce output shaft speed and then gradually reduce heater output.

4.5 Propulsion System Operating Requirements

Operating procedures for the CCGT-LWSP will not be significantly different from existing land-based CCGT power conversion systems. Even without computerized control systems, the CCGT-LWSP should be considerably simpler to operate than a steam turbine propulsion system, although not nearly as simple as an OCGT. In order to meet the HSD performance, defined earlier, without exceeding the CCGT operational capabilities and limitations discussed in the previous section, certain requirements will have to be met. The most significant of these are discussed in the sections which follow.

4.5.1 Standby Power

For the CCGT-LWSP, the amount of power required to maintain the heat exchangers at their operating temperatures during standby is about 100 kWe, including power for a small blower to circulate the helium through the system at a low rate to minimize temperature differences. Keeping the system at its operating temperatures would permit fast starts without severe thermal gradients in the regenerator. This amount of heating is calculated from the heat losses from the regenerator covered with 12.7 cm (5 inches) of rock-wool insulation with thermal conductivity of 0.07 watts/m-C (0.04 Btu/hr-ft-F). The power required could be supplied by the auxiliary generator.

4.5.2 Control Monitoring and Sensing Requirements

The use of modern electronic control systems is expected for the CCGT-LWSP installation. This will allow many parameters to be monitored effectively and used for both control and protection of the CCGT-LWSP. For example, the main ducting control valves will have to be carefully controlled to avoid potential resonances or unstable conditions; in addition, many other parameters given in Table 4.1 should be monitored by the control system. These parameters are used not only to control the performance (P) of the system, but also to check on the health (H) of many critical components and notify the operators of any serious degradation or dangerous operating conditions present. Furthermore, many parameters will indicate when a shutdown (S) should be performed, either immediately, or within a short period of time. These shutdown signals are listed separately in Table 4.2.

The maintenance of such a control system is thus crucial to assure its proper operation. Therefore, a procedure to maintain this control system at a high level of accuracy and confidence should be established for the CCGT-LWSP system. Of course, the same type of control system procedures have been proposed for the steam turbine systems, but the reduced complexity of the CCGT should allow such automated control systems to be more easily serviced and maintained to function properly.

4.6 Auxiliary Components

In addition to the major components discussed above, there are a number of auxiliary components required by the CCGT-LWSP system. These components include a starting motor, a cooler for the lubrication system, a helium-oil separator, and an electronic control system.

4.6.1 Starter Motor

Various startup alternatives were considered, and an electric motor was selected for its simple operation. Both diesel engine and gas turbine starters were considered, but they were rejected primarily because of the fact that an onboard electrical power generating system would be available. A "blowdown" start procedure similar to that utilized for the UTC FT50 (Ref. 4.3) was also considered since the inventory tanks could provide a source of high pressure helium which could be injected into the compressor inlet to initiate compressor shaft rotation. This system was also rejected because the tank volume is limited and would be exhausted after more than three start attempts in a period of one day. Converting this system to one capable of meeting repeated starting requirements not only would require a much larger charging system but also would result in the rejection of turbine exhaust helium to the atmosphere during starting to avoid excessive back-pressure in the turbine.

4.6.2 Lubrication System

Turbomachinery required to produce the 57.9 MW (80,000 shp) of this conceptual design, and using the journal bearing concept, would encounter significant frictional power losses in the bearings. It is estimated that the CCGT-LWSP design will experience friction losses of approximately 0.5 MW at design point conditions, and much of this energy must be removed through the lubrication system. Therefore, a lubricant cooler which utilizes a standard shell and tube heat exchanger was provided to reject this energy into an external water source. The exit temperature of this water should be approximately 40.9 C (105 F) at a mass flow of 11 kg/sec. An oil filter system is specified to handle the 189 liters (50 gallons) of oil which are contained within the closed-loop oil system and a degasser is also specified to recover the helium which leaves the closed-cycle loop through the scavenge and breather lines.

4.6.3 Control System

A control system must also be provided to operate the CCGT-LWSP system and also to provide protection for the LWSP components should any unusual operating circumstances occur. Furthermore, this control system will allow a semi-automatic starting and shutdown procedure to be performed, as well as provide monitoring of the critical LWSP components. The parameters which would be monitored were presented earlier in Tables 4.1 and 4.2.

An electric motor is provided to provide initial rotation of the turbomachinery up to a self-sustaining speed where the thermal input is sufficient to accelerate the CCGT to a stable idle point. This motor, rated at 600 kWe (800 hp), would require power from an auxiliary electric generator on the ship. A motor of this power should be sufficiently powerful to accelerate the compressor shaft from zero rpm to a starting rotational speed of 1500 rpm within three to five minutes. At this point, thermal energy from the heater would allow additional acceleration to a stable idle condition of 538.1 C (1000 F) at a compressor speed of 3010 rpm and power turbine speed of 3600 rpm. Efforts during the subsequent phase of this program should be directed toward identifying the characteristics of the required control schemes and the potential for using bypass paths. Computerized control systems for closed-cycle systems similar to those proposed for automated steam plants would have to be developed to allow for rapid transients and simple component efficiency matching. It should be understood that the control requirements and system responses of a closed-cycle gas turbine power generating system presently are not well defined due to the limited experience available. This is probably the least known area in closed-cycle gas turbine systems.

REFERENCES

- 4.1 Kuo, S. C.: Closed-Cycle Gas Turbine Heater Analysis and Conceptual Design of a 80,000-shp Turbomachinery. Quarterly Program Report, No. 2., UTRC Report R78-952979-2, March 1978.
- 4.2 HTGR Direct Cycle Turbomachinery Technology. Final Report PSD-R-106, Prepared under Contract SC546734 to General Atomic, October 15, 1976.
- 4.3 Technical Specification for the FT50 Power Pak, Prepared by Turbo-Power and Marine Systems, Subsidiary of United Technologies Corporation, August 20, 1975.

TABLE 5.1
MONITORING PARAMETER MONITORS

Component	Parameter	Source	Signal Type	# Sensors	Destination	Frequency of Measurement	Use
Turbine - Compressor Drive	Temperature - Inlet	Inlet annulus	Thermocouple (TC)	3	Multiples (8)	Continuous (C)	P,H,S
	Pressure - Inlet	Inlet annulus	Transducer (TD) or Strain gauge (SG)	3	M	C	P,H
RPM	Front compressor case		Pulse pickup (PP)	2	M & Hard wired (HW)	C	P,H,S
	Temperature - Exit	Exit annulus	Thermocouple	3	M	Intervals of 1 sec	P,H
	Pressure - exit	Exit annulus	TD or SG	3	M	(1-1)	P,H
	Bearing oil Pressure				1-1		H,S
Turbine - Power	Temperature - Inlet	Inlet annulus	TC	3	M	C	P,H,S
	Pressure - Inlet	Inlet annulus	TD or SG	3	M	C	P,H
	RPM	exit case or generator	PP	2	M & HW	C	P,H,S
	Temperature - Exit	Exit annulus	TC	3	M	1-1	P,H
	Pressure - Exit	Exit annulus	TD or SG	3	M	1-1	P,H
	Bearing oil Pressure				1-1 or C		H,S
Bypass Valve - Power turbine	Position Feedback	Valve shaft	Analog (A) or Digital (D)	2	M	C	P,S,H
	Valve drive	Valve actuator	Analog or digital	2	M	C	P,S
	Duct Temperature	Valve case	TC	2	M	1-1	H,S
	Pressure - Exit	Duct exit	TD or SG	2	M	1-1	P,H,S
Throttling valve - turbine	Position Feedback	Valve shaft	A or D	2	M	C	P,S,H
	Valve drive	Valve actuator	A or D	2	M	C	P,S
	buct temperature	Valve case	TC	2	M	1-1	H,S
Bypass Valve - total turbine	Position Feedback	Valve shaft	A or D	2	M	C	P,S,H
	Valve drive	Valve actuator	A or D	2	M	C	P,S
	buct temperature	Valve case	TC	2	M	1-1	H,S
regenerator	Temperature - Inlet (Hot)	Inlet duct (Hot)	TC	2	M	Intervals of 2 sec	H
	Pressure - Inlet (hot)	Inlet duct (Hot)	TD or SG	2	M	(1-2)	H,S
	Temperature - Shell, Inlet (Hot)	Shell	TC	2	M & HW	1-2	H,S
	Temperature - outlet (Hot)	outlet duct (Hot)	TC	2	M & HW	1-2	P,H
	Pressure - outlet (Hot)	outlet duct (Hot)	TD or SG	2	M & HW	C	H,S
	Temperature - Shell, outlet (Hot)	Shell	TC	2	M & HW	1-2	H
	Temperature - inlet (cold)		TC	2	M & HW	1-2	H

TABLE 4.1 (Cont'd)
POSITIONING PARAMETER MEASUREMENTS

<u>Component</u>	<u>Parameter</u>	<u>Source</u>	<u>Signal Type</u>	<u># Sensors</u>	<u>Destination</u>	<u>Frequency of Measurement</u>	<u>Use</u>
Precooler	Pressure - Inlet (Cold)	TB or SG	TC	2	M 6 HW	C	H
	Temperature, Shell (Cold) Inlet	TC	TC	2	M 6 HW	1-2	H
	Temperature, Outlet (Cold)	TC	TC	2	M 6 HW	1-2	H
	Pressure, Outlet (Cold)	TB or SG	TC	2	M 6 HW	C	H,S
	Temperature, Shell, Outlet (Cold)	TC	TC	2	M 6 HW	1-2	H,S
	Temperature - Exit	Inlet Duct	TC	2	M 6 HW	1-2	P,H
	Pressure - Exit	Inlet duct	TB or SG	2	M	C	P,H,S
	Temperature - Water, Inlet	Water pipe, Inlet	TC	2	M 6 HW	1-2	P,H
	Temperature - Water, Exit	Water pipe, exit	TC	2	M	1-2	H,S
	Pressure - Water Inlet	Water pipe, Inlet	TB or SG	2	M	C	P,H,S
	Pressure - Water exit	Water pipe, exit	TB or SG	2	M	1-1	H
	Flow rate - Water Inlet (AP)	Water pipe, Inlet	TB or SG	4	M 6 HW	1-1	P,H,S
Precooler Water Valve	Position Feedback	Valve shaft	A or D	2	M	C	P,H,S
	Valve Drive	Valve actuator	A or D	2	M	C	P,S
Inventory System	Temperature of storage	Storage tanks	TC	1 per tank	M 6 HW	1-1	P,H
	Pressure of storage	Storage tanks	TB or SG	1 per tank	M 6 HW	C	P,H,S
	Volume of Storage	Storage tanks	A or D	1 per tank	M 6 HW	1-2	P,S
Inventory Valve, Comp. Inlet	Position Feedback	Valve shaft	A or D	2	M	C	P,H,S
	Valve Drive	Valve actuator	A or D	2	M	C	P,S
Inventory Valve, Comp. Exit	Position Feedback	Valve shaft	A or D	2	M	C	P,H,S
	Valve Drive	Valve actuator	A or D	2	M	C	P,S

TABLE 5.1 (Cont'd.)
CONTINUED: PARAMETER PRIORITIES

Component	Parameter	Source	Signal Type	# Sensors	Destination	Frequency of Measurement	Use
Inventory Valve, Bleed/Charge	Position Feedback	Valve shaft	A or D	2	H	C	P,H,S
	Valve Drive	Valve actuator	A or D	2	H	C	P,S
Low Compressor	Temperature, Inlet	Inlet annulus	TC	3	H	C	P,H,S
	Temperature, Exit	Exit annulus	TC	3	H	C	P,H,S
	Pressure, Inlet	Inlet annulus	TD or SG	3	H	C	P,H,S
	Pressure, Exit	Exit annulus	TD or SG	3	H	C	P,H,S
	Surge Detector	Compressor case	SG	1	H	C	P,H,S
	Temperature, Exit	Inlet Duct	TC	2	H 6 HW	I-1	P,H
	Pressure, Exit	Inlet Duct	TD or SG	2	H	C	P,H,S
	Temperature, Water	Water pipe, Inlet	TC	2	H 6 HW	C	P,H,S
	Temperature, Water	Water pipe, exit	TC	2	H	I-1	H,S
	Pressure, Water Inlet	Water pipe, inlet	TD or SG	2	H	C	P,H,S
Intercooler and Precooler	Pressure, Water exit	Water pipe, exit	TD or SG	2	H	C	P,H,S
	Flow rate, water	Water pipe, inlet	TD or SG	4	H 6 HW	I-2	H
	inlet (AP)					I-1	P,H,S
	Temperature, Water	Water pipe, exit	TC	2	H	I-1	H,S
	Pressure, Water	Water pipe, inlet	TD or SG	2	H	C	P,H,S
	Flow rate, water	Water pipe, inlet	TD or SG	4	H 6 HW	I-1	P,H,S
	Surge Detector	Compressor case	SG	1	H		
Intercooler Water Valve	Position Feedback	Valve shaft	A or D	2	H	C	P,H,S
	Valve drive	Valve actuator	A or D	2	H	C	P,S
High Compressor	Temperature, Inlet	Inlet Annulus	TC	3	H	C	P,H,S
	Temperature, Exit	Exit annulus	TC	3	H	C	P,H,S
	Pressure, Inlet	Inlet Annulus	TD or SG	3	H	C	P,H,S
	Pressure, Exit	Exit annulus	TD or SG	3	H	C	P,H,S
	Surge Detector	Compressor case	SG	1	H	C	P,H,S
	Pressure, Main pump	Oil line	TP	1	H 6 HW	C	H,S
Oil System	Oil level, low limit	Oil tank	Switch	1	H 6 HW	I-1	H
	Oil temperature	Oil return line	TC	1	H	I-1	H
	Oil Metal Chip detector	Oil return line	Switch	1	H	C	H
	Pressure, oil filter	Oil filter	Switch or TD	1	H	I-1	H,S
	Breather pressure	Breather line	TD or SG	1	H	I-1	H,S
					H		

TABLE 4.1
MONITORING PARAMETER REQUIREMENTS

<u>Component</u>	<u>Parameter</u>	<u>Source</u>	<u>Signal Type</u>	<u># Sensors</u>	<u>Destination</u>	<u>Frequency of Measurement</u>	<u>Use</u>
Hydraulic System	Bearings	Vibration	Case	Proximity pickup	4	M	I-I
	Pressure	Main pump	Oil line	TD	1	M 6, HW	C
	Fluid level, low limit	Reserve tank	Switch	1	M 6, HW	I-S	
	Fluid temperature	Pressure line	TC	1	M	I-I	
	Chip detector	Return line	Switch	1	M	I-I	
	Fluid filter, /P	Filter	TD or switch	1	M	C	

TABLE 4.2

Shutdown Signals

TC = Thermocouple
 TD = Transducer
 SG = Strain Gage
 A = Analog

D = Digital
 PP = Pulse Pickup
 C = Continuous
 I-# = Intervals of # Sec

TBD = To be determined
 ①=Also rate of increase limited
 ②=Also signal loss

<u>Component</u>	<u>Parameter</u>	<u>Limit</u>	<u>Signal Type</u>	<u>No. of Sensors</u>	<u>Freq. Sample</u>	<u>Action</u>
Turbine-Compressor Drive	Temperature-Inlet	1800°F	TC	3	I-1	Bypass Turbines
	RPM	110%②	PP	2	C	" "
	Bearing Oil Pressure	Min TBD	TD	1	I-30	Reduce RPM
Turbine-Power	Vibration	Max TBD	PP	2	I-1	Reduce RPM
	Temperature-Inlet	1600°F	TC	3	I-1	Bypass Power Tu
	RPM	110%②	PP	2	C	" "
Bypass Valve Power Turbine	Bearing Oil Pressure	10 psig min	TD	1	I-30	Reduce RPM
	Vibration	Max TBD	PP	2	I-1	Reduce RPM
	Position Feedback	Signal loss A or D		2	C	Bypass Turbines
Throttling Valve Power Turbine	Temperature, Case	TBD	TC	2	I-5	" "
	Position Feedback	Signal loss A or D		2	C	Bypass Turbines
	Temperature, Case	TBD	TC	2	I-5	" "
Bypass Valve - All Turbines	Position Feedback	Signal loss A or D		2	C	Emerg. Turbine
	Temperature, Case	TBD	TC	2	I-5	" Bypass "
	Position Feedback	Signal loss A or D		2	C	Close valve
Inventory Valve - Compressor Inlet	Temperature, Case	TBD	TC	2	C	Close valve
	Position Feedback	Signal loss A or D		2	C	Close valve
	Position Feedback	Signal loss A or D		2	C	Close valve
Low Compressor	Temperature Inlet	TBD, ②	TC	3+5	C	Bypass Turbines
	Pressure Inlet	Signal loss	TD or SG	3+5	C	" "
	" "	TBD	TD or SG	3+5	C	" "
	Surge Detector	TBD ²	TD or SG	2	C	" "
	Bearing Oil Pressure	Min TBD	TD	1	I-30	Reduce RPM
	Vibration	Max TBD	PP	2	I-1	Reduce RPM
High Compressor	Temperature Inlet	TBD, ②	TC	3+5	C	Bypass Turbine
	Pressure Inlet	Signal loss	TD or SG	3+5	C	" "
	" "	TBD	TD or SG	3+5	C	" "
	Surge detector	TBD ²	TD or SG	2	C	" "
	Bearing Oil Pressure	Min TBD	TD	1	I-30	Reduce RPM
	Vibration	Max TBD	PP	2	I-1	" "
Oil & Hydraulic System	Pressure Main Pump	Min TBD	TD	1	I-30	" " or Bypa
	Temperature	Max 200°F	TC	2	I-30	Turbine
	Oil Level	Min TBD	A or D	2	I-30	" " "

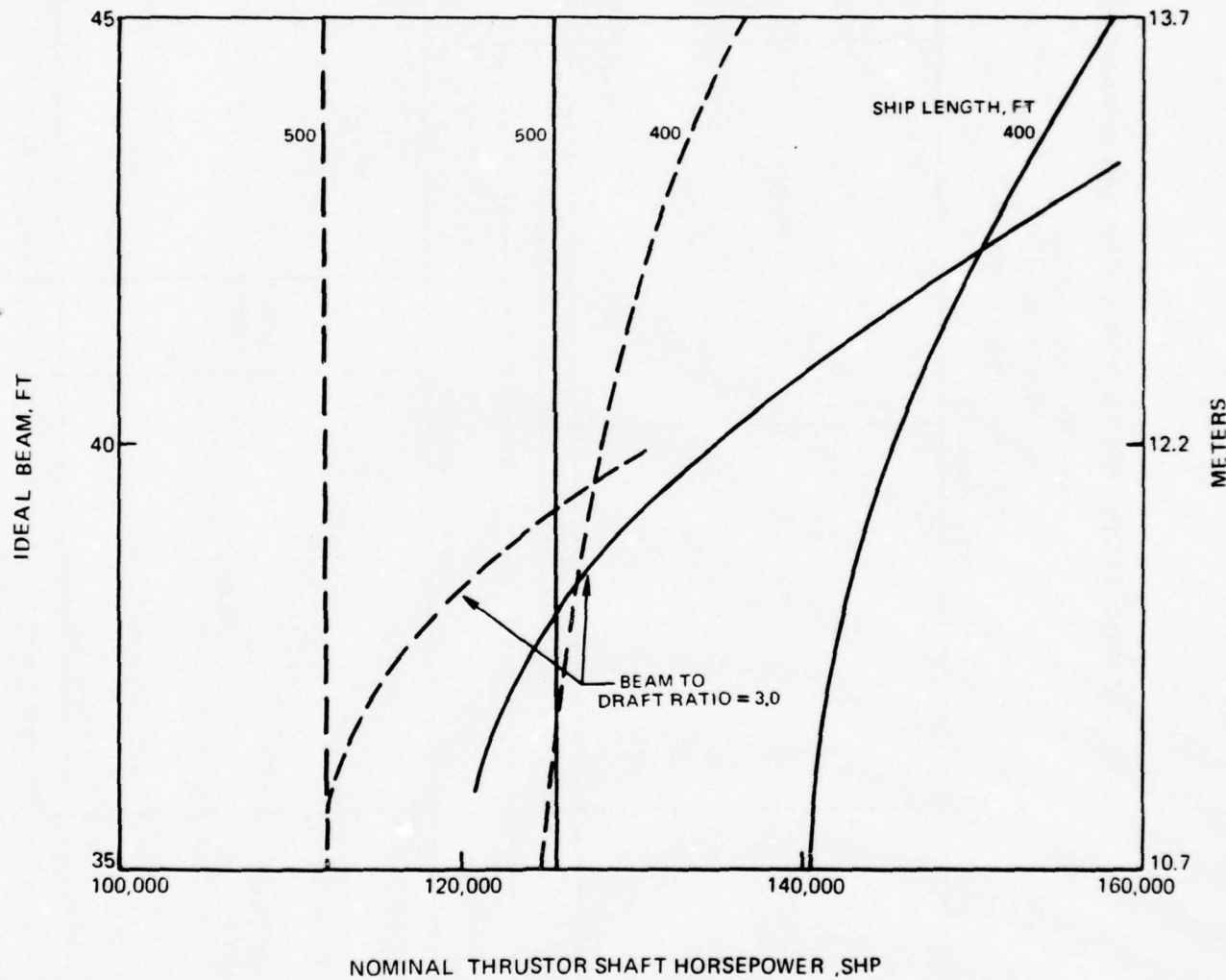
DIMENSIONAL CHARACTERISTICS OF HIGH-SPEED DESTROYERS

MAXIMUM SPEED = 50 KNOTS

BLOCK COEFFICIENT = 0.59

— 3500 TONS DISPLACEMENT

— 4000 TONS DISPLACEMENT

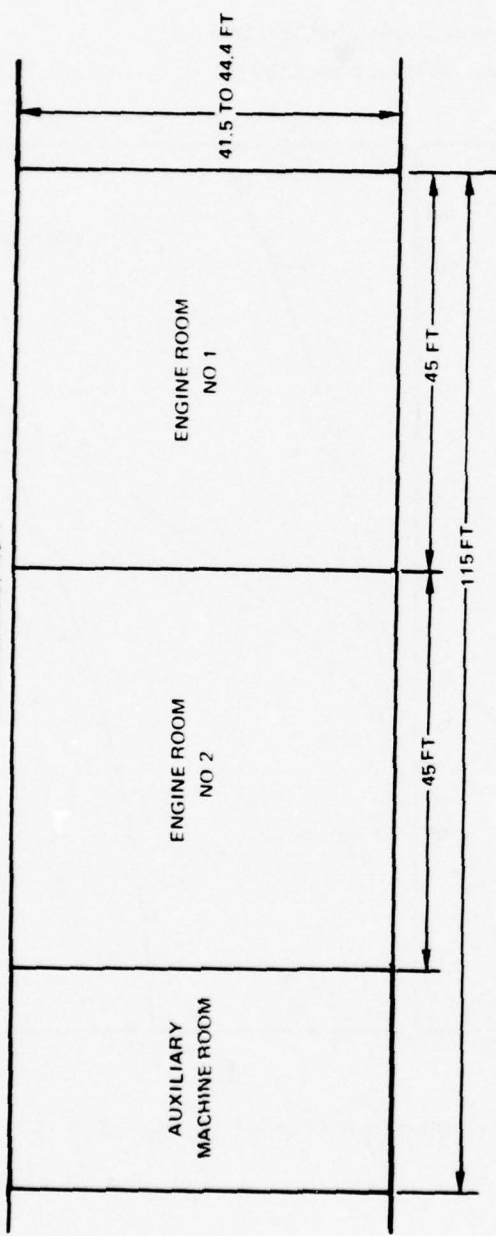


PRELIMINARY ENGINE ROOMS DIMENSIONS AND ARRANGEMENTS

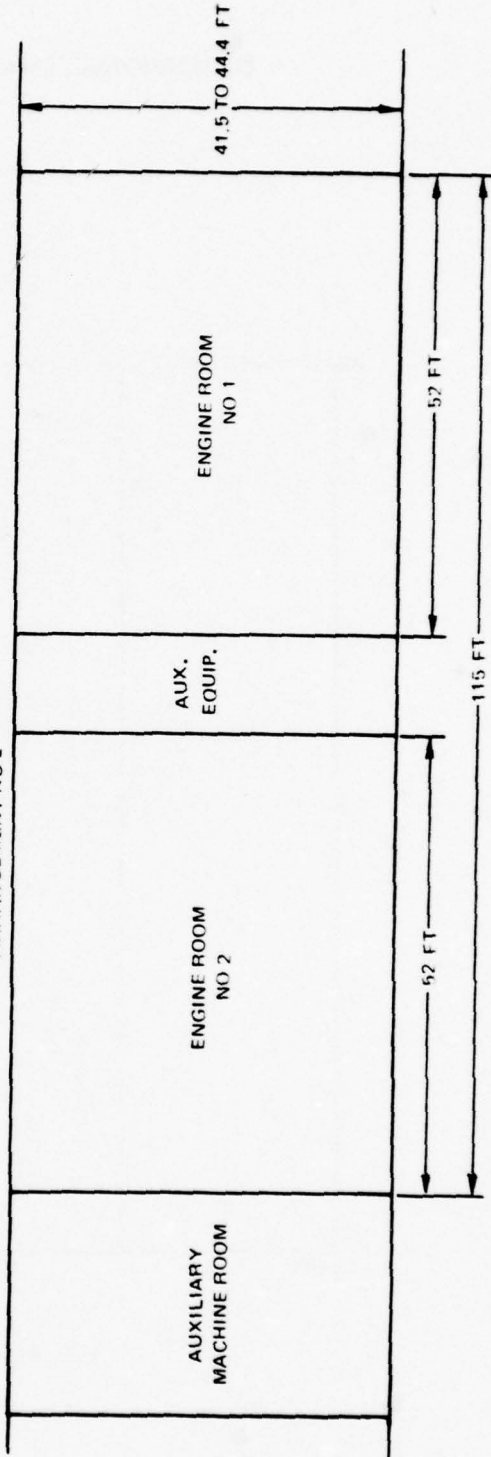
DISPLACEMENT = 4000 TONS
 SHIP LENGTH = 400 FT

THRUSTOR POWER > 150,000 SHP

ARRANGEMENT NO 1

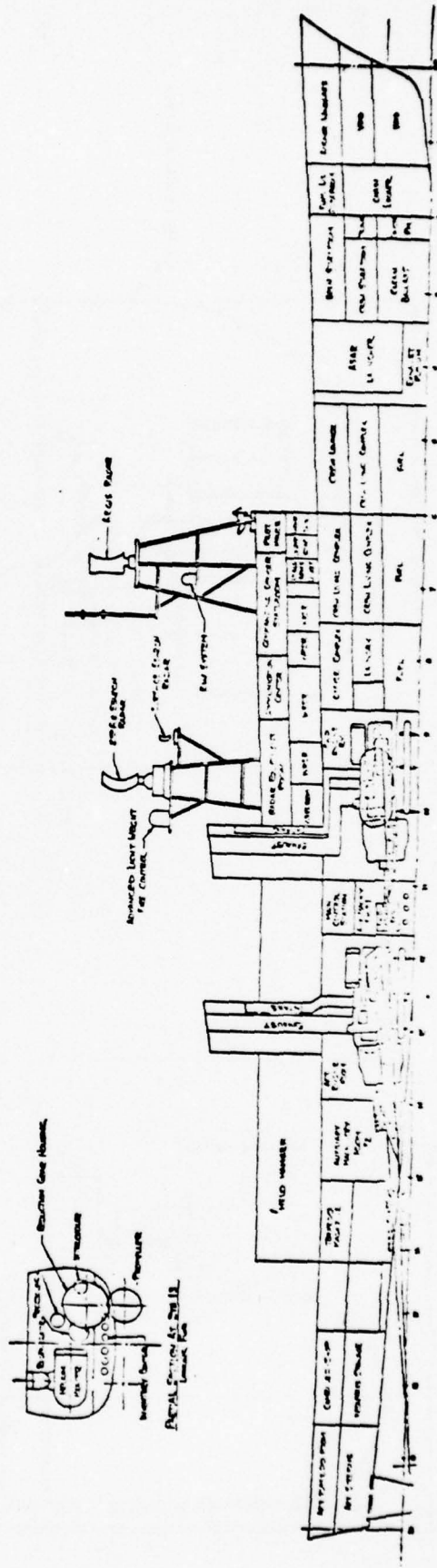
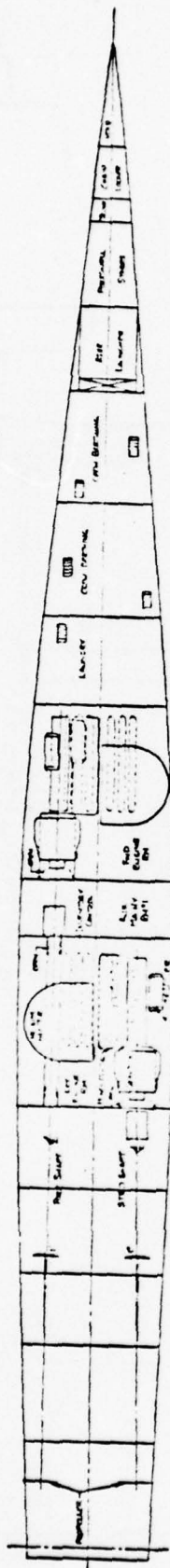


ARRANGEMENT NO 2



CONCEPTUAL LIGHTWEIGHT PROPULSION SYSTEM LAYOUT

- 3500 TO 4000 TONS HIGH-SPEED DESTROYER
- 45 TO 50 KNOTS MAXIMUM SPEED
- 2 X 80,000 shp CLOSED CYCLE GAS TURBINES



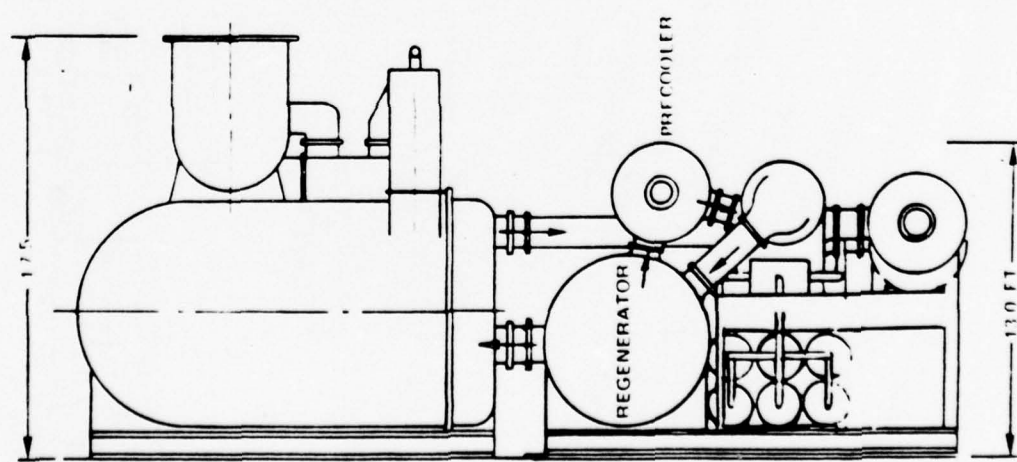
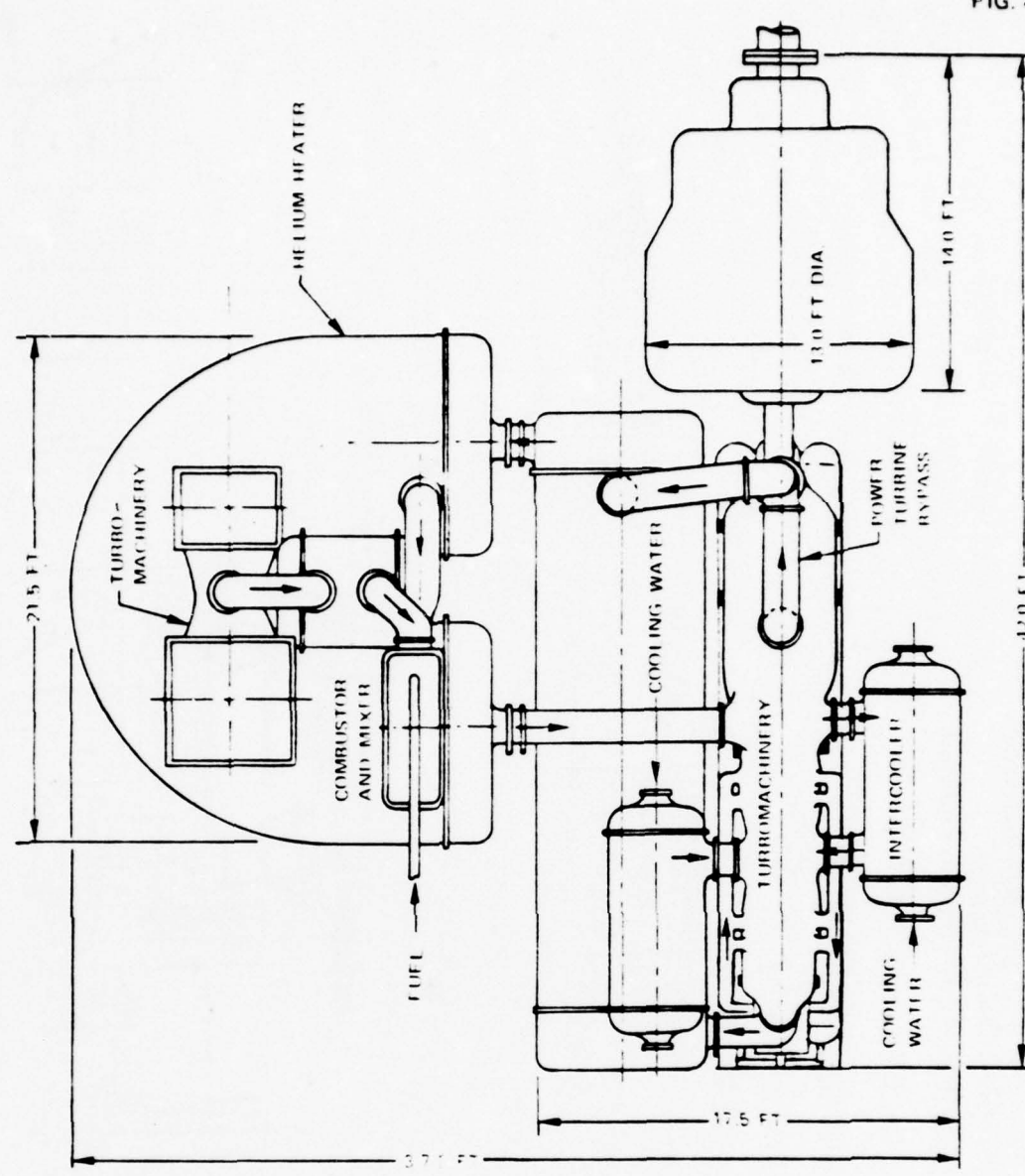
PRELIMINARY HIGH-SPEED DESTROYER PROPULSION SYSTEM LAYOUT

DISPLACEMENT 1,600 TO 4,000 TONS

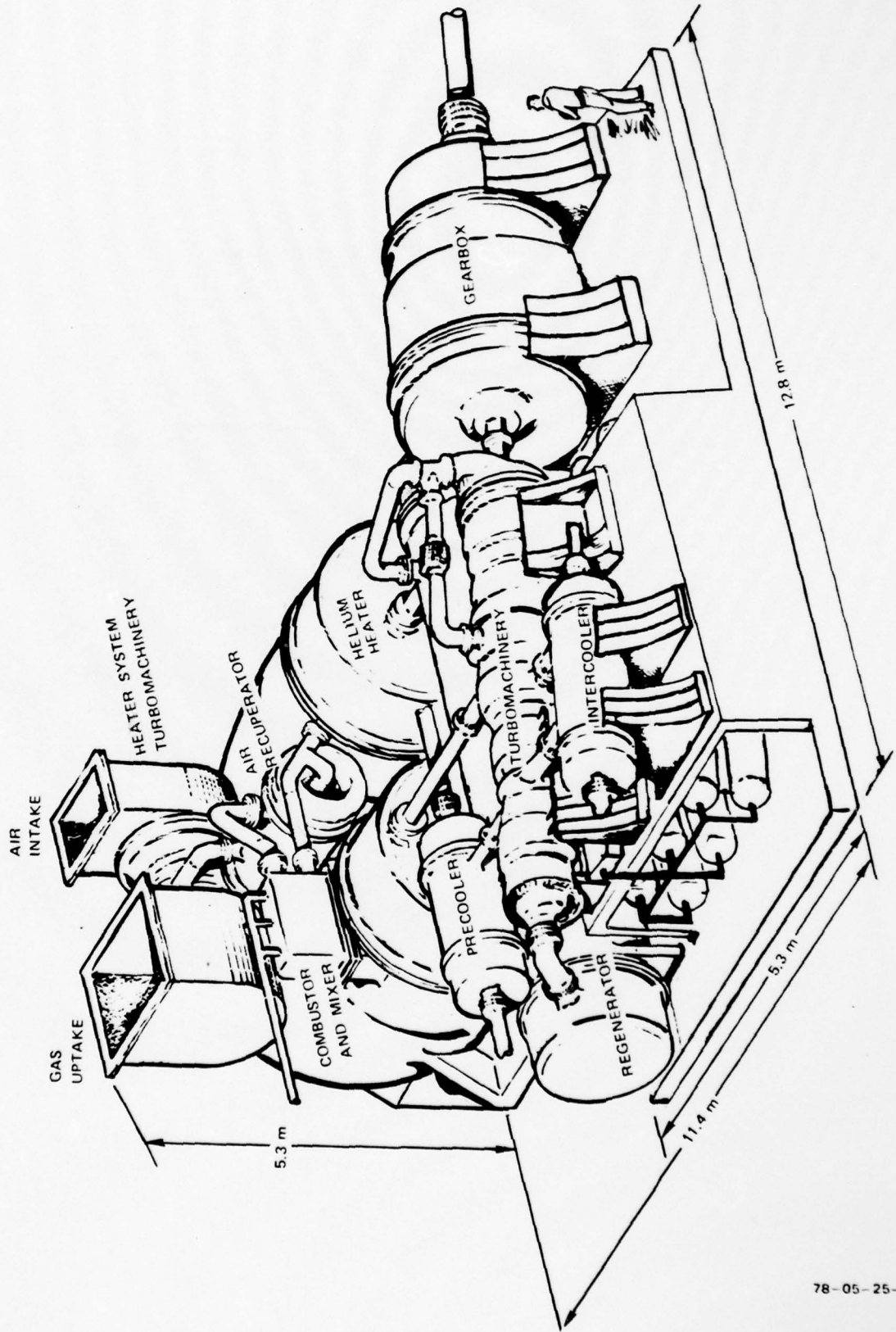
MAX SPEED 45 TO 50 KNOTS

TOTAL INSTALLED POWER 160,000 SHP

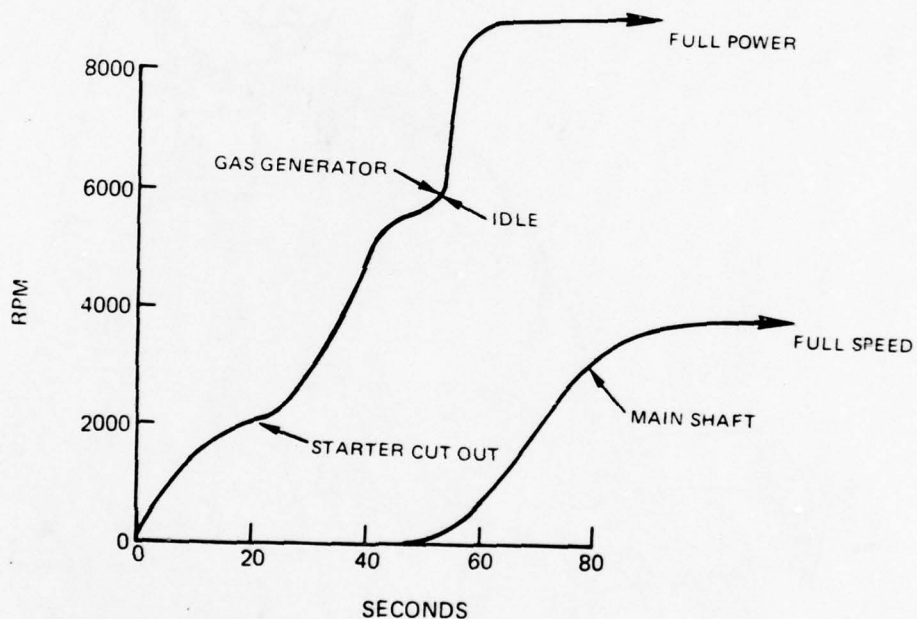
PROPELLION SYSTEM UNIT POWER 30,000 SHP



PRELIMINARY HIGH SPEED DESTROYER PROPULSION SYSTEM PERSPECTIVE

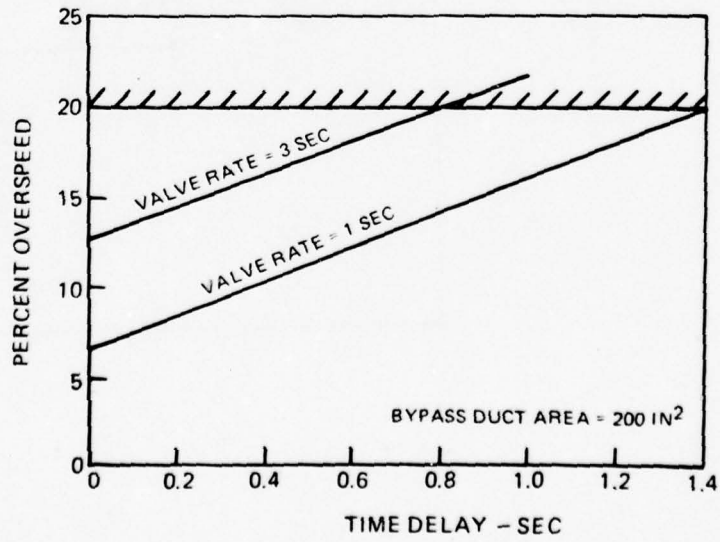
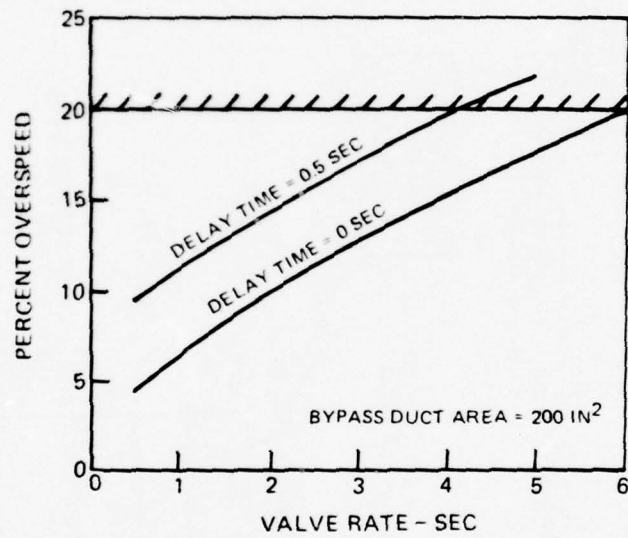
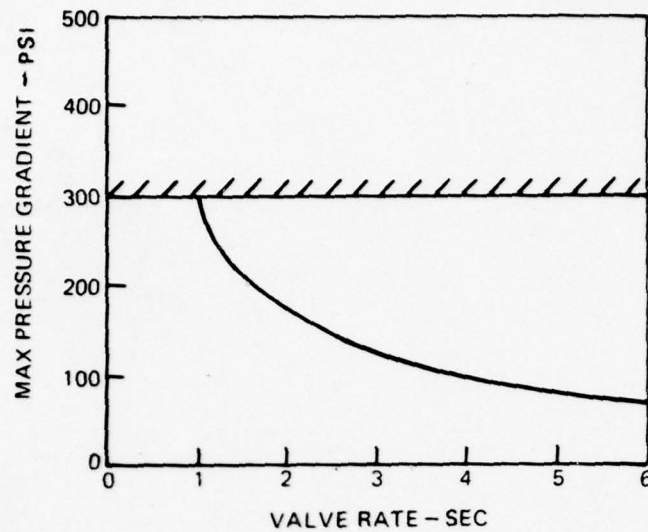


TYPICAL OCGT STARTING TIME



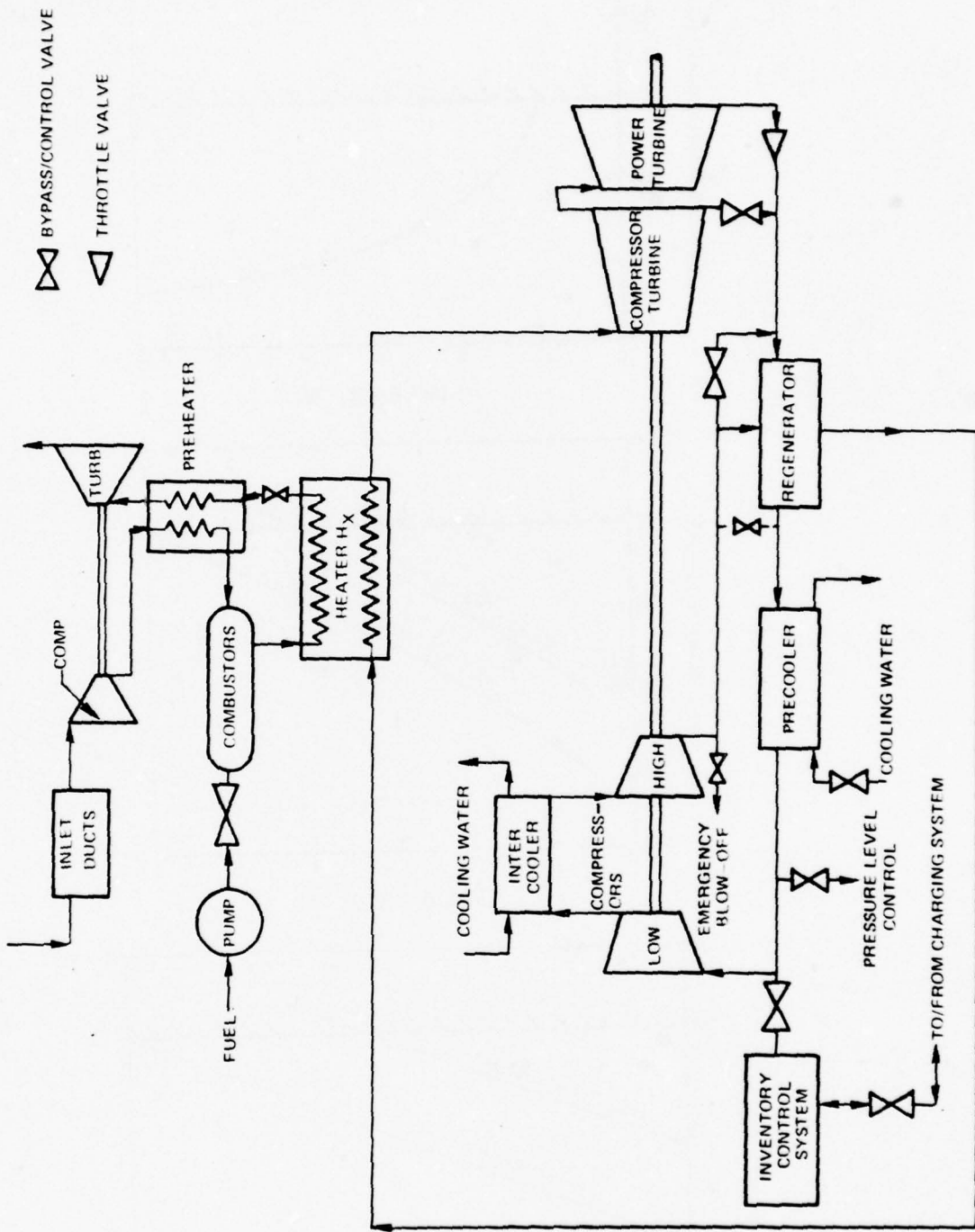
77-04-222-20

CONTROL ANALYSIS FOR CCGT (HTGR) BYPASS VALVE

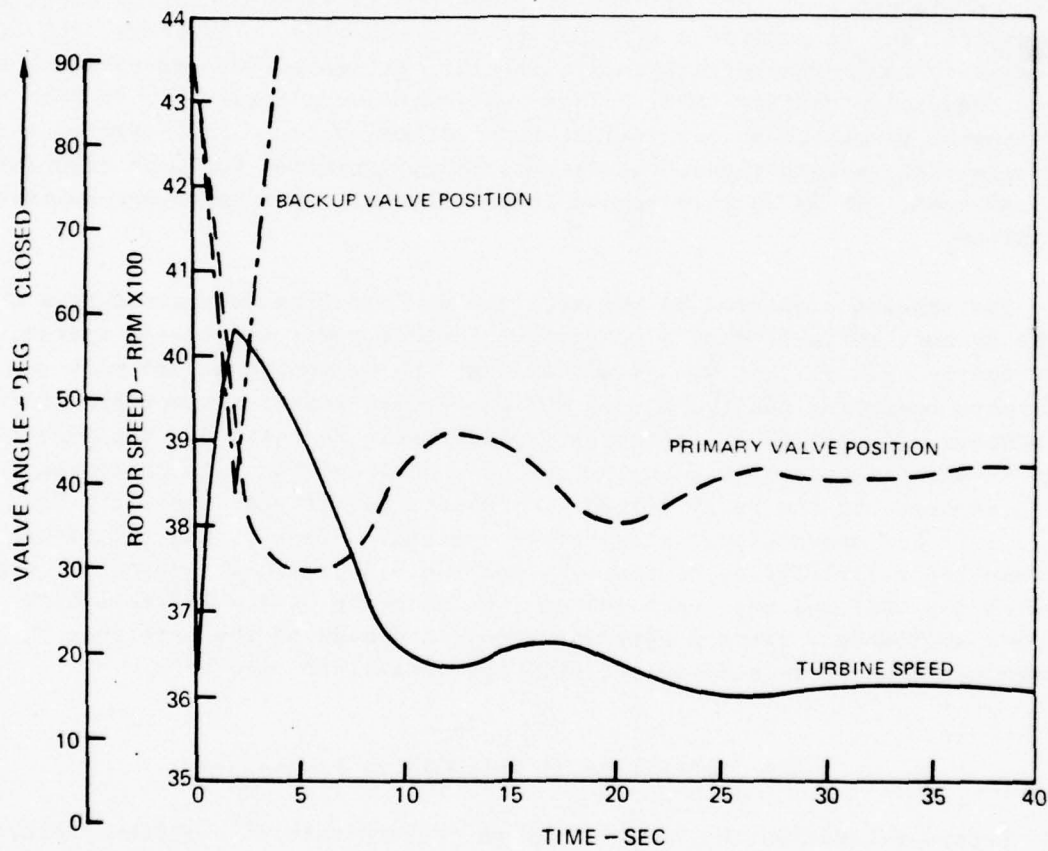


77-04-222-19

CCGT-LWSP PRELIMINARY CONTROL REQUIREMENTS



ESTIMATED RESPONSE FOR CCGT (HTGR) DROP LOAD CONDITION



PHASE II-5

RELIABILITY EVALUATION

It has long been recognized that one of the major advantages of closed-cycle gas turbines (CCGT) is their outstanding reliability when compared with that of more conventional power generating equipment, such as open-cycle gas turbines (OCGT). However, as seen in the previous sections, a power conversion system using the CCGT is more complex than one using an OCGT. Thus it would be valuable to estimate whether the projected CCGT advantages are lost as a result of this increased complexity. Unfortunately, a direct comparison with existing OCGT turbomachinery is not prudent since the OCGT system operating experience is insufficient to provide a firm basis for comparison. Therefore, the CCGT reliability was compared with the reliability estimated for conventional steam power conversion systems (SPS). These estimates were consistent in both operating/maintenance practices and in failure rate methodologies. Furthermore, a range of reliability values rather than single point estimates could be calculated and compared. It is in this regard that the results presented are believed to be unique.

The results presented in the sections which follow indicate that a CCGT might be more reliable than a conventional steam power conversion system; more importantly, however, it was estimated that the conventional SPS must use many alternate operating configurations and in-service repair/replacement practices to achieve high levels of reliability predicted. Furthermore, the methodology used in this assessment also helps one to understand the high component failure rates reported in the Naval Reliability/Maintainability/Availability Data Bank (Ref. 5.1) for conventional steam power systems. Finally, the relationship between the reliabilities of the CCGT and the SPS provides a means of comparison between the CCGT and any other system (including an OCGT when these data becomes available), since a separate comparison made to the reference steam system can then be related to the CCGT/SPS comparison made here.

5.1 Definition of Reliability Parameters

Before estimating the reliability or failure rate of a system, several key definitions must be established. The most important of these are the definitions of "reliability" and of "failure". Careful consideration must also be given to the term "mission," as well as to the data sources of reference failure rates, and to the adjustment factors which must be used to make this data representative of the system being considered.

5.1.1 Reliability Definition

As used in this report, the term reliability is defined as the probability of a successful completion of an identified mission. The letter designation, R,

is used to identify reliability and the term, $R = e^{-\lambda_m t}$, has been used to calculate the system reliability. This exponential relationship is a mathematical term based on probability theory. The term λ_m is the mission failure rate, or the number of failures per mission. This relationship is normally used when failures occur in a random fashion and is based on the assumption that the system is "mature" having proceeded to the point in its useful life where "initial infant mortality" (such as initial design or assembly problems) has been overcome, but not to the point where the required hardware has reached its "wearout" age. This period of time is indicated on the familiar "bathtub" curve shown in Fig. 5.1.

In assessing system reliability as it is used in this program, the assumption that the operating period would lie between infancy and system wearout was checked by comparing the mean time between failure (MTBF) for each component against the mission time. It was found that the MTBF sufficiently exceeded the mission time, and thus this assumption could be held valid. Had this not been the case, a more complex Weibull distribution analysis would have been required in order to account for increases in failure rate as the wearout age is approached (Ref. 5.2). The equations needed to estimate reliability in the Weibull method are presented in Table 5.1 along with other critical equations used in this analysis.

The mission failure rate, λ_m , is the most critical parameter in a reliability estimate. The value of this parameter can be estimated from a "block diagram" approach (see Fig. 5.2) representing the interaction of significant components needed to produce the desired output. This diagram most frequently presents these components in either a series or a parallel arrangement. When components are arranged in series, as shown in Fig. 5.2, a failure of any one will result in total system failure. When components are in parallel, a failure of one will not necessarily lead to a system failure.

In Table 5.1, Eq. (3) indicates the reliability of a series of components as the product of the component reliabilities. However, when components are arranged in parallel, the reliability is expressed by Eq. (4) in Table 5.1. Thus when estimating the reliability of any system, these mathematical relationships can be used when the individual component failure rate, λ_c , and the overall mission failure rate, λ_m , are available.

5.1.2 Failure Definition

In this study, a "failure" is identified as any event which could prevent the ship from completing its entire mission. However, when mission reliability calculations are based on this simple definition, complications arise because of mission requirements, component capabilities, and operational and maintenance practices. For example, if mission operational requirements specify that the system must have the capability to attain 100 percent of installed power at all times, then any failure which causes a partial reduction in power output would

be responsible for a mission failure. By contrast, if this 100 percent output were required only at specified times, then a failure which causes a reduction in output still may allow many segments of the mission to be completed. To avoid this confusion, mission requirements were separated into several individual power block segments, and a failure rate was estimated for each of these selected partial power conditions. Clarification of the definition of failure is important to understand the implications of the missions selected in a later section, as well as to comprehend the reliability methodology used in this program.

5.1.3 LWSP High-Speed Destroyer Mission

The HSD mission profile shown in Fig. 5.3 was developed from the duty-cycle presented in Fig. I-4 of Ref. 5.1. The total elapsed mission time of 292 hours is comprised of a 100-hour operational period and a 192-hour shut-down period between missions. The 100-hour operational period allows the HSD to travel more than 5560 km (3000 nautical miles) when operated in accordance with the duty cycle profile shown in Fig. 5.3. The amount of fuel needed for this mission is such that almost 20 percent of displacement still can be allocated to payload. The number of hours selected for each duty-cycle mission allows a total of thirty missions to be undertaken annually, and this number is consistent with information obtained in consultation with J. J. Henry, Inc. regarding typical destroyer operational characteristics.

The duty cycle profile in Fig. 5.3 would indicate that the HSD is operated at power requirements below 40 percent of full installed power during 73 percent of the operational period. This fact would further mean that careful consideration must be given to any failure which causes a reduction of maximum capacity, since the degraded output may still be able to provide power needed for segments of the mission requirements.

5.1.4 Conventional Destroyer Mission

The steam system aboard a conventional destroyer is the reference power system against which the LWSP of the HSD would be compared. This selection was made because it was believed that of all available ship types, the conventional destroyer would experience environmental and operational conditions most similar to those of the HSD. The conventional destroyer was assumed to follow the mission profile shown in Fig. 5.4. This figure was derived from the information in Fig. 1.3 of Ref. 5.1 by assuming an operational duty-cycle period of 200 hours. Although the speed of a conventional destroyer is less than that of the HSD selected, this time period would allow distance of 3320 nautical miles which is comparable to the distance covered during the HSD mission. A total yearly operation of 3000 hours was also assumed for the conventional destroyer even though this resulted in half the number of missions assumed for the HSD.

5.2 Methodology for Reliability Evaluation

The methodologies used to evaluate the reliability of a LWSP system and of a steam power system (SPS) are based on the mathematical equations presented in Table 5.1. However, due to the complexity of the overall system several methods are available to estimate the mission failure rate. The simplest of these is to consider the propulsion system as a single package and then find an existing power system with similar characteristics and operating requirements. The failure rate and/or reliability of the new system would then be estimated through careful adjustments to the reference system which accommodate the operating conditions and requirements of the new system. Unfortunately, in the case of the LWSP system, there is no closely related existing power system to which adjustments could be made.

Because a similar propulsion system does not exist, the LWSP power system was divided into subsystems and components which could be related more closely to existing hardware. The failure rates and/or reliability data for this existing hardware were then adjusted by using engineering judgement to estimate the value of multiplicative correction factors in four separate areas: (1) design difficulty considerations - f_1 ; (2) duty cycle considerations - f_2 ; (3) environmental considerations - f_3 ; and (4) state-of-the-art considerations - f_4 . As shown in Fig. 5.5 these adjusted component failure rates were then combined to estimate a failure rate for each subsystem, and the subsystem failure rates were then combined to estimate a failure rate for each mission power level. Estimations of these failure rates required the creation of appropriate reliability block diagrams to show the interdependency of these components at each of the mission power levels.

The failure rate at each power level, λ_p , was then multiplied by the time spent at that power level to provide a submission failure rate, $\lambda_p t_p$. The total mission failure rate (λ_m) was then found by summing all the individual power level failures. Reliability was then calculated by using the reliability formula based on random failures discussed previously.

5.2.1 Block Diagram Approach

The reliability block diagrams form the base of any reliability assessment since they represent the true interdependency (such as series or parallel arrangements) of all critical system components. The complexity of both the CCGT and SPS required that numerous block diagrams be generated for each power level. Not only did these block diagrams represent alternate system configurations, but they also represent variances in maintenance practices which affect the interdependency of specific component blocks.

Baseline block diagrams created for both the CCGT and SPS systems identified the relationship of over 100 critical components which are required to produce full output power. These baseline diagrams were then altered by eliminating or

rearranging some components blocks to represent their modified relationships under the "repair and/or replacement practices" and "alternative configurations" considered. These variations and the resultant block diagrams are discussed in the following sections and in Appendix A-1.

5.2.2 Failure Rate Adjustment Factors

Failure rates for reference hardware were adjusted for the differences between the reference application and the future application. Factors in four areas of consideration were: (1) design severity; (2) duty cycle requirements; (3) environmental condition; and (4) state-of-the-art technology. The overall adjustment of reference failure rates was accomplished by multiplying the failure rate of the reference system by a factor which was itself the product of the four separate factors identified.

Design Adjustment Factor

The design adjustment factor is intended to take into consideration differences between the reference component design and the design of the selected Navy ship application. For example, if the reference failure rate data were for a component designed for stationary use, the design adjustment factor must allow for the uncertainties related to adaptation of this design to shipboard conditions where rapid power changes and sudden shock loadings are prevalent. The correction factor for this example would be approximately 1.2.

Duty Cycle Adjustment Factor

The duty cycle adjustment factor takes into consideration differences between the severity of the operating schedule (or mission duty cycle) of the reference component application relative to the mission of the selected Navy ship. For example, a stationary steam powerplant would normally be operated at constant power output for months while a power plant aboard ship might be required to cycle from zero to maximum power and back to zero many times within a period of 100 hours. Such cycling might significantly increase the failure rate of components which were not originally intended to be operated in this manner. In this example, the correction factor would have to be near a value of 1.5.

Environment Adjustment Factor

The environment adjustment factor takes into consideration the differences in operating environment of the new power system and that of the reference system. Not only are salt air and water significant, but shock loading as well as well as crew characteristics and maintenance limitations are important. For example, failure rates for land-based stationary power plants required environmental factors up to 2.0 or larger when operating in a seagoing environment.

Failure rates for components derived from mobile land or air applications generally required lower environmental adjustments, however. In practically no case was the environmental adjustment factor judged to be less than 1.0 based on the reference system data available.

State-Of-The-Art Adjustment Factor

The state-of-the-art adjustment factor takes into consideration failure rate differences due to component utilization in a future time period. For example, a component which will be used in the same future application as it is in the current reference system, e.g., a steam turbine, might be able to achieve a slightly lower failure rate due to further improvements. In contrast, a component which has not yet been put into destroyer service, e.g., a closed-cycle air charging compressor, would be expected to experience greater rates of failure in the early years following system installation. In the former case, the magnitude of the correction factor was selected near 0.9 while in the latter it was selected near 1.1.

5.2.3 Spectrum of Reliability Evaluations

The reliability evaluations performed during this program result from two sets of hardware characteristics and limitations: "repair and replacement maintenance practices" and "alternate operating configurations". The first relates to the possibilities for prolonging the effective MTBF of critical components. The second considers methods to minimize the chances of failing to produce the required power, through the rearrangement or reconfiguration of propulsion system components. Such reconfigurations would allow partial power output to be achieved should a portion of these components fail.

These two approaches were considered in detail by dividing each into categories to represent varying levels of effort and complexity. Then, by combining these various categories, several different conditions were created for which the reliability could be estimated. The combinations considered in this study are shown in the matrix of Fig. 5.6. The reliability estimate for each of these matrix blocks was calculated by: generating a representative block diagram to depict the interrelationship of all components for each category; determining an estimated component failure rate for each of the blocks; and finally; using the mathematical relationships shown in Table 5.1 and methodology shown in Fig. 5.5, to calculate reliability. The applications for each of three such matrices were:

- (1) LWSP operating on the HSD mission
- (2) LWSP operating on a conventional destroyer mission
- (3) A steam propulsion system operating on a conventional destroyer mission.

A total of 36 system reliability assessments were created in this manner. The details considered in establishing these categories and the philosophies used to generate the required block diagram are included in the sections which follow.

5.2.4 Maintenance Practices

Onboard ships, maintenance practices are dictated by many factors, the most significant of which is whether the ship is in-service or in dry-dock. When the ship is in-service, certain maintenance operations can be performed. Preventive maintenance (such as oiling, changing filters, etc.) can be performed at almost any time, and was assumed to be undertaken in accordance with present maintenance practices. In contrast, timely repair and/or replacement of failed components has a significant effect on operation of the ship. Accordingly, three categories of repair/replacement practices were established:

- (1) None - No repair or replacement is allowed during the entire mission. Thus, if a component malfunctions or fails when the ship is in-service, the ship must be taken out of service to perform the necessary repair. Besides being classified as a mission failure, it could also jeopardize the completion of 30 mission cycles per year (Ref. Figs. 5.3 and 5.4).
- (2) Routine - Repair and/or replacement is to be performed onboard a ship while it is in-service (at sea or in port) such that the mission (including time between operating periods) is not affected. Thus, if a component fails, it will be repaired during the shutdown periods of the mission (or possibly while the ship is in operation if the repair is small).
- (3) Major - Repair and/or replacement maintenance practices performed while the ship is in-service are beyond the scope of what is presently routine. New design concepts, such as the use of modular heat exchangers and other advanced methods of reducing repair time and difficulty, must be instituted before operations placed in this category could be performed without interfering with the mission requirements.

Consideration of these three practices creates a variety of reliability assessments rather than a single approach which may not represent the real possibilities onboard a Navy ship. These three categories also serve to indicate the amount and quality of manpower required to keep the power system operating effectively. As allowances for increased amounts of in-service repair are made, additional expenses might be incurred by the Navy to station moderately skilled labor properly throughout the world.

5.2.5 Alternate Operating Configurations

To complete the spectrum of reliability evaluations, a second set of hardware characteristics and limitations, "alternate operating configurations", was considered. These alternatives can drastically improve the probability of mission success. Included in this category are reconfigurations of component arrangements which allow a ship to continue operating when a single component in the propulsion system fails. When such a failure and reconfiguration occur, the power conversion system is often capable of producing only a portion of its installed output capacity. This capability is still important since, as noted, a large portion of the mission is spent at power levels considerably below the maximum rating (see Figs. 5.3 and 5.4), and thus a system capable of achieving partial output power still could perform a major part of its mission.

The applicability of these reconfiguration to the mission requirements will depend on the time it takes to make the necessary changeover. Certain failures will require negligible time for changeover (such as a reduction in heater or condenser capacity due to a partially plugged heat exchanger).

Indeed, some component failures would not require immediate corrective action, and the system could continue to operate under reduced output. However, when all major components are accessible, as in the LWSP and SPS systems considered in this analysis, many other alternate configurations exist which will provide partial power output. For example, the possibility exists to bypass the failed components and still achieve a substantial fraction of installed power capacity. Some of these bypasses can be made quickly, merely by opening and closing valves, while others will require one hour or more for changeover (such as establishing a cross-connection between heater rooms). In this report, any of these actions are called a system alternate configuration.

A critical consideration for these reconfigurations is the time required to bypass the failed component. Therefore, to evaluate the reliability of the power system, four classifications of alternate configurations which could provide reduced system output were established. Reliability calculations were made for each of the alternate configurations which:

- (a) require negligible time to convert from the original maximum capacity configuration to the degraded partial capacity configuration (for example, in-service heat exchanger tube blockage)
- (b) require approximately 5 minutes to convert from the full to reduced capacity configuration
- (c) require approximately 60 minutes to convert from the full to reduced output configuration

(d) require approximately three hours to convert from the full to reduced output configuration.

It is important to note that it has been assumed that: the mission power requirements occur in the order presented in Figs. 5.3 and 5.4; only a system capable of full output will begin a mission; and maximum power will be required only at the start of each mission operating period and not again until the start of the next operating period.

In consideration of the repair-reconfiguration philosophy discussed, a matrix of parametric studies was generated as shown in Fig. 5.6. From this, a set of twelve reliability calculations were undertaken for each mission/pro-pulsion system combination. However, the reliability calculations for a LWSP system operated on a high-speed destroyer (HSD) were considered meaningful only if they could be compared with similar values for established system. Furthermore, the reliabilities of both systems should be calculated concurrently, by the same organization, to assure consistency in the comparison.

Accordingly, the reliability was also estimated for a steam propulsion system thought to be representative of that which may be used on conventional destroyers in 1990. The same matrix of 12 conditions was considered, but to avoid handicapping the conventional system, its mission was that of the conventional destroyer duty-cycle, shown in Fig. 5.4, rather than the HSD duty-cycle. Finally, for the purpose of making the comparison between the LWSP and steam system even more consistent, further calculations were undertaken to estimate the LWSP reliability as if it was operating in accordance with a conventional destroyer duty cycle.

5.3 Block Diagram Allocations

As stated previously, the key aspect of any reliability assessment is the ability to specify appropriate block diagrams which accurately represent the dependency between components and subsystems for a specified level of output. In this study, block diagrams were specified for both the LWSP and steam power generation systems for each of the twelve categories represented in the matrices of Fig. 5.6. These block diagrams represented the interrelationship among significant components needed to perform the functions indicated on the duty-cycle diagrams shown in Fig. 2.4 for the CCGT-LWSP and in Fig. 5.7 for the steam system. When it was felt that typical Navy practice or potential future design recommendations warranted, both series and parallel component arrangements are included in the block diagrams representing these cycles.

5.3.1 Basic LWSP and Steam Power System Block Diagrams

The preliminary basic block diagrams shown in Fig. 5.2 and 5.8 present the critical subsystems interdependency for the CCGT-LWSP and steam systems, respectively. These systems were further subdivided into more than 100 critical components as illustrated for these two systems in Figs. 5.9 and 5.10. The identification of the function for each block number in these latter figures is given in Tables 5.2 and 5.3. It can be noted that for both systems, parallel subsystems and components are provided for the electro-hydro-mechanical controls as well as for the boiler required in the steam power system. Further, it was assumed that each boiler would be designed to provide 100 percent of the energy needed at full installed power operation.

Associated with each of the components represented by the blocks in this diagram is an MTBF, and hence a component failure rate (λ_c) which was used to calculate the reliability of each component. After the reliability of each component was calculated, the overall reliability of components arranged in series and in parallel was calculated using the expressions presented in Table 5.1.

The system reliabilities calculated by using the baseline block diagrams in Figs. 5.9 and 5.10, represent the probabilities of achieving 100 percent output power on a continuous basis prior to taking into consideration the operating requirements and repair/replacement practices discussed earlier. A significantly different reliability would result if many of the less reliable parts, such as components in the electro-hydro-mechanical control system, were periodically replaced before failure occurred. Therefore, the reliabilities calculated for the systems represented by the block diagrams in Figs. 5.9 and 5.10 are those which allow neither repair/replacement, nor potential reconfigurations to be considered.

When routine or major repair and/or replacement maintenance practices are included in the specification of reliability block diagrams, many of the components become extremely reliable, and for the purpose of this study, they have been assigned a 100 percent reliability. These highly reliable components then could be grouped into larger blocks which replaced the original detailed breakdown.

5.3.2 Routine Repair Replacement Practices

The groupings of components for the LWSP and the steam system shown in Figs. 5.11 and 5.12, respectively, were prepared using the groundrule that routine maintenance would be allowed. In these figures, the large blocks represent groups of components which are assumed to be replaceable or

repairable with routine procedures. However, for the components represented by the small blocks, it was assumed that routine repair and/or replacement (either while the ship is in-service at sea or in port) could not be performed. Accordingly, these are components which would contribute to the overall system failure rate.

The logic used for selecting those components which could be maintained onboard the ship in a routine manner, was primarily based upon component accessibility, repair time (i.e., this time must be less than that time between operational periods), and the acceptability of working in an uncontrolled environment (such as during at-sea conditions). For example, the typical plug-in/plug-out concepts used for many current electronic control systems led to the assumption that the entire control system (electronics, transducers, actuators, etc.) for both the LWSP and conventional power systems could be maintained while the ship is in-service. By contrast, large components, such as the main heat exchangers, recuperator, precooler, condenser, and boilers, were assumed to require more than routine repair/replacement practices, or have associated with them difficult working environments, and hence the latter components could not be classified as being in the routine repair and/or replacement category.

In addition to such straightforward items as plug-in/plug-out electronics, it was assumed that certain other more complicated repairs or replacements could be routinely performed. For the LWSP system, some of the select components which could be classified in this category are: tanks and valves of the inventory control system; valves and pumps for the precooler and intercooler; air blowers, combustors, and fuel supply equipment for the heater; cases and stators and external accessories for the turbomachinery. This last equipment category is included because the aircraft gas turbine design allows modular disassembly of the turbomachinery for repair/replacement of cases, stators, and accessories. These procedures should allow the complete repair/replacement to be completed during the mission down times.

For the steam system, components which were assumed to be routinely repairable or replaceable at sea or in port (but which would not require the use of a dry dock), included the pressurizing water pumps and their drive turbines and valves. The main heat exchangers and large power turbines were assumed to require more than routine repair and/or replacement practices.

All of the routinely maintainable components were then grouped by subassembly type into blocks with which there was associated an extremely high reliability. The ducts which connect these components were also placed in this high-reliability grouping. Finally, as a simplifying assumption, all of the components in these highly reliable groups were assumed to have a 100 percent reliability. This allowed the reliability effects of the remaining critical components to be more closely evaluated.

5.3.3 Major Maintenance Block Diagrams

The block diagram used to represent components subject to routine maintenance practices can be further simplified, as shown in Figs. 5.13 and 5.14 for the LWSP and steam systems, if major repair/replacement practices are allowed. The additional components which can be placed in this classification were then grouped together as represented by the large blocks shown in these figures. These components, which include heat exchangers, are those which might be maintained while the ship is in-service by using unusual repair practices, which will not delay the start of the next mission operating period. While it is felt that these repair/replacement practices are not realistic when using today's repair techniques and designs, it may be possible that future designs will incorporate features which would allow easier repair of major components. One such design approach might be a modular heat exchanger concept which would allow the failed portion of a heat exchanger to be removed quickly.

The rotating turbomachinery components (rotors, bearings, seals, etc.) were not considered to be repairable/replaceable even under the "major" category since their service would require a quality and time of repair not believed possible under "in-service" conditions. This assumption is based on the fact that the highly-pressurized closed cycle machine contains many critical sealing surfaces for helium retention, and because many ducts would have to be moved to allow for removal of the rotor. In fact, if a rotating component were to fail, it might be easier to remove the entire gas turbine rather than to perform an on-board repair. Removing the CCGT is not anticipated to be as easy a job as removing an open-cycle gas turbine, primarily because of the added complexity of duct connections and also the unit size. However, the fact that the CCGT is of aircraft derivative design should make this removal process less troublesome than that of removing a steam turbine. For these reasons, the rotating components (the rotors and bearings for both CCGT-LWSP and steam systems) become the only components which are not assumed to have 100 percent reliability under the groundrule of allowing major repair and/or replacement practices.

5.3.4 Alternate Configuration Component Block Diagrams

Because HSD and conventional destroyers spend a large percentage of time at low power levels during their respective missions, it is possible that some system components could fail, yet the required level of power would still be available. It is also possible that portions of some components could malfunction, (such as would occur with a partial heater or boiler blockage) and the mission could still be completed. In consideration of these particular situations, additional reliability block diagrams had to be created.

It becomes apparent that a large number of alternate configurations is possible in the basic system block diagram (Figs. 5.9 and 5.10) are examined. Even when the routine and major maintenance block diagrams cases (Figs. 5.11 through 5.14) are examined, it can be seen that a large number of combinations of failed subcomponents still is possible. Therefore, in the analyses, it was assumed only one component would fail in each reconfigured block diagram. Further it was assumed that the degraded operating conditions considered would be limited to those shown in Tables 5.4 and 5.5, for the LWSP and steam systems respectively. These limitations still allow individual failures or degradations of each major component to be considered as shown by the dashed lines in the block diagrams of Figs. 5.11 for the CCGT-LWSP and in Fig. 5.12 for steam systems.

While some of these reconfigurations cannot be undertaken in a simple manner aboard a ship, others may take very little effort or time. Therefore, for each of the identified reconfigurations it was decided to categorize reliability for each in terms of the time it would take to complete the configuration changeover.

Four categories of these changeover times were established as follows: (a) configurations for which there is no alternative configuration; (b) reconfigurations which would take approximately five minutes for adjustment (such as converting from dual-shaft to single-shaft propellor operation, (c) reconfigurations which would take approximately 60 minutes for conversion and adjustment (such as to install or remove a blank-off plate for intercooler bypass); (d) reconfigurations which would take approximately 180 minutes for conversion and adjustment (such as to establish a cross connection between turbomachinery engine rooms).

The discussions which follow explain the effect that some of these reconfigurations could have on the routine maintenance block diagrams. It should be realized, however, that diagrams were considered in this study under the "no repair/replacement" and "major" repair/replacement criteria; further explanations of the block diagrams for each of these alternate configurations are presented in Appendix A.

Degraded heat exchanger block diagrams

The failure of components such as the recuperator, preheater, or intercooler was handled by assuming that a bypass loop was available. The amount of power that can still be produced under these conditions was calculated, and these calculated estimates are shown in Tables 5.4 and 5.5.

A partial degradation of critical heat exchangers was also considered. For the LWSP, heater systems with reductions in total capacity of 20, 40, and 60 percent were considered. The block diagrams for these configurations are shown schematically by the dashed lines in Fig. 5.11 which pass through the blocks labeled H.2, H.4, H.6, respectively. For the conventional steam system, reductions in total condenser capacities of 20, 40, and 60 percent are illustrated by the dashed lines in Fig. 5.12 which pass through blocks 29.2, 29.4, and 29.6 respectively. Furthermore, it was assumed that two boilers are installed to provide energy for each shaft in the steam system, and that either could supply all of the energy required to produce 100 percent of installed power. Block diagrams for all of these noted systems are shown in Appendix A.

In the CCGT-LWSP system, bypassing each of the other major heat exchangers (precooler, intercooler, and recuperator) was also considered, and these arrangements are shown by dashed lines in Fig. 5.11. A cross connection with the other shaft heater was also considered for the CCGT-LWSP system, as shown in Fig. 5.11, similar to the cross-connection with the other shaft boiler rooms considered in the steam system. Separate block diagrams for each of these configurations are presented in Appendix A.

Degraded turbomachinery block diagrams

A failure of the compressor in one of the turbomachines was handled by assuming a cross connection could be made between the other engine on board the ship, and the power turbine of the failed engine. This practice was assumed to restrict the power attainable to a level of only 40 percent of total installed power (both shafts). Again Fig. 5.11 illustrates this configuration with a dashed line through Block No. 111, while Appendix A provides a separate block diagram in Fig. A-14.

Steam turbine systems were also assumed to be capable of producing at least a fraction of their total rating even if one of the three steam turbines (cruise, low-pressure, or high-pressure) fails. The power output attainable with the remaining, unbypassed turbines was assumed equal to those levels shown in Table 5.5. The block diagram for these configurations are shown in Figs. A-15, 16, and 17, in Appendix A, and by the dashed lines in Fig. 5.12 which pass through blocks numbered 118, 123, and 126.

Failure of an entire power system

A different situation occurs if an entire power train were to fail and only one propellor could drive the ship. In this case, it was assumed that a maximum speed of only 20 knots could be achieved. This speed requires four percent of the installed power for the HSD and 14 percent of installed power.

for the conventional destroyer. Therefore, only mission power requirements at or below these levels could be considered in this configuration. Typical block diagrams for the CCGT-LWSP and steam systems operating according to these configurations are shown by the dashed lines which pass through blocks numbered 112 and 125 of Figs. 5.11 and 5.12, respectively, and also in Fig. A-18 of Appendix A.

5.4 Estimation of Component Failure Rates

As explained earlier, all reliability estimations depend on the failure rates estimated for each of the components identified. Since there has been no experience to establish reference failure rates for closed-cycle gas turbine system installed onboard ships, these rates had to be estimated by adjusting the failure rates of components designed and operated similarly. As discussed earlier, the adjustment procedure used in this analysis involved the multiplication of four factors in series where each of the factors accounted for the difference in a specific characteristic of the reference system compared to that of the new CCGT design. The logic and data sources used in estimating these factors are discussed in the sections which follow.

5.4.1 Reference Failure Rate Sources

Several sources were used to obtain the failure rate of components similar to those in the CCGT-LWSP and in the steam power system (SPS). A list of code numbers assigned to these sources is presented in Table 5.6. Whenever possible, source 1 (Ref. 5.1) and other Navy data sources were used so Naval destroyer environment and operating conditions would be applied directly to the reference component.

5.4.2 LWSP Component Failure Rate Estimates

The failure rate estimates for each of CCGT-LWSP components shown schematically in Fig. 5.9 were calculated from the values shown in Table A-1 of Appendix A; a portion of Table A-1 is reproduced in Table 5.7. Several of the adjustments for critical components deserve particular attention, and these are specifically discussed here.

Heat Exchangers

The most difficult estimation of failure rate occurred for the CCGT heater since no component of this type has been operated onboard ships for sufficient lengths of time to generate useable failure rate data. Therefore, it was decided to use the failure rate data for the superheater section of

Navy destroyer boilers as the reference design data source. J. J. Henry, Inc. supplied this data which indicates that the MTBF for superheaters is approximately 10,000 hours; this corresponds to a failure rate of 0.100 per 1,000 hours. After the four adjustment factors presented in Table 5.7 are applied to this base failure rate value, the newly estimated failure rate for the heater section in the CCGT becomes 0.103 per 1,000 hours.

For this component, the design adjustment factor was judged to be slightly greater than 1.0 since the temperature of the helium gas is higher than that normally encountered in a steam system. This indicates that more stringent design stress considerations would be required.

The duty-cycle factor is judged to be slightly less than 1.0 since the CCGT would operate for a lower percentage of time at high power (for either HSD or conventional destroyer missions) than do steam systems.

The environment adjustment factor was also estimated to be less than 1.0 since the heat exchanger tube cores are expected to be damaged less by the clean helium than by the steam normally used in superheaters, all other environmental considerations remaining essentially the same.

Finally, the state-of-the-art factor was estimated to be greater than 1.0 since CCGT heater designs may encounter more problems than would well-developed steam superheaters.

Turbomachinery

In the case of turbomachinery, the reference failure rate data was based on Pratt & Whitney Aircraft commercial aircraft experience (Ref. 5.5 and 5.6). To illustrate, the adjustments of the compressor drive turbine design are discussed below.

The design adjustment factor for the reference compressor drive turbine rotor data (block number 95) was estimated to be less than 1.0 since such design considerations as operating temperature, and stress are significantly less severe in the CCGT-LWSP design than in commercial aircraft service. Furthermore, the weight requirements are not as critical. The duty-cycle adjustment factor was also estimated to be less than 1.0 since that experienced by short-haul aircraft (for which the reference engine type generally is used) requires this engine to be operated through many more daily cycles from idle to 100 percent power than would be expected during destroyer missions. The typical duty cycle presented for this engine in Fig. 5.15 may be compared with the assumed destroyer duty cycles presented previously.

An environment adjustment factor of less than 1.0 was selected since the CCGT turbine will not be exposed to products of combustion and to salt in the air as is typical in aircraft operation. Finally, the state-of-the-art factor was estimated to be greater than 1.0 since helium turbomachinery characteristics are not as well understood as the air turbines used in aircraft.

Other CCGT-LWPS Components

The heat exchanger and turbomachinery components serve as examples of the approach used in selecting and adjusting the adjustment factors and calculating the reliability factors for the CCGT-LWPS. Other system component reliability characteristics were calculated and adjusted in a similar manner.

5.4.3 Steam System Component Failure Rate

The steam system with which the CCGT-LWSP was compared, was assumed to be one that had advanced from current technology and would be available for fleet deployment in 1990. Consequently, even when a reference failure rate was based on current destroyer operation, it was often assumed that state-of-the-art improvements could be made to reduce this failure rate. The reference failure rates and adjustments made to these values are shown in Table A-2 of Appendix A.

It has already been noted that whenever possible, the reference data were based on destroyer applications. However, it was discovered that failure rates for many Naval ship propulsion components were neither carefully tabulated nor widely distributed, and consequently, data were not always available. In these cases, other references were used, and the adjustment factors often diverged significantly from a value of 1.0. It should be emphasized that the low reliability estimated for the SPS without reconfiguration is a result of the high failure rate data obtained from Refs. 5.1 and 5.4, and the fact that adjustment factors on this data were seldom far from a value of 1.0 for the steam system components.

5.4.4 Baseline System Reliability

When the reliabilities of the baseline configurations represented by the block diagrams in Fig. 5.9 and 5.10 were calculated, the results were surprisingly low. These results, classified as "no repair and/or replacement allowed," and "no alternate configurations allowed," are presented in Table 5.8. They indicate that for the LWSP system studied, the probability the high-speed destroyer would complete its mission is only slightly more than 40 percent ($R = 41.8$ percent). The corresponding calculation for a conventional steam propulsion system, operated under a conventional destroyer duty-cycle yields a reliability of slightly under 10 percent (9.4 percent). These values reflect the fact

that if even one small component, such as a valve transducer, blower, or accessory steam turbine, (for which redundancy was not provided) were to fail, the entire power system would be incapable of providing output power. This is obviously unrealistic, since normal maintenance procedures are used to check, adjust, service, or replace a component prior to its failure (Ref. 5.10). Thus, many of these components could be prevented from failing by the institution of appropriate repair and/or replacement practices. The estimates for reliability under such conditions are discussed in the sections which follow.

5.4.5 Reliability with Allowance for Repair/Replacement

As might be expected, the two procedures, "routine-replacement", and "major-maintenance", each of which would be allowed while the ship is in-service, were found to have a significant effect on mission reliability. When routine replacement maintenance is allowed, the only components which were considered to affect reliability were those shown in the small, numbered blocks shown in Figs. 5.11 and 5.12.

When the estimated failure rates for these components (see Tables 5.7, A-1 and A-2) were computed in accordance with the mathematical relationships in Table 5.1, the reliabilities for the CCGT-LWSP and the steam propulsion system become 0.7414 and 0.3157, respectively. These values are markedly improved over the reliabilities estimated under a "no repair and/or replacement" ground rule.

If major repair and replacement practices are allowed aboard a ship which is in-service, configuration corresponds to the reliability block diagram shown in Figs. 5.13 and 5.14. The respective CCGT-LWSP and steam propulsion system reliabilities under these conditions become 0.8502 and 0.6977, respectively. The difference between those two values is due primarily to the higher failure rate expected for the steam turbines when compared with that estimated for the helium turbomachinery. In fact, this is one of the major advantages expected of the CCGT-LWSP.

5.4.6 Reliability with Allowance for Reconfigurations

The flexibility of both the CCGT-LWSP and the steam propulsion systems for component reconfigurations or rearrangements allows a limited number of the failed components to be bypassed or accommodated as discussed earlier. This flexibility of operation has a significant effect on mission reliability.

To estimate reliability when alternate configurations are allowed, the block diagrams presented earlier for the three repair and/or replacement practices had to be reexamined so the effect these reconfigurations had on the component interrelationships could be taken into account. Therefore, each of

the block diagrams presented in Figs. 5.9 through 5.14 was redrawn for the reconfigurations which require 5, 60 or 180 minutes for changeover. The redrawn block diagrams were then used to estimate the reliabilities under each of the reconfigurations presented in Tables 5.9 and 5.10. The reliability at each power level was calculated for only those (block diagram) configurations capable of achieving that power (see Tables 5.4 and 5.5). The equations and configurations shown in Table 5.11 for the CCGT-LWSP in the HSD and in Table 5.12 for the steam system in a conventional destroyer, were then used to calculate overall mission reliability. It should be noted that these tables only apply to the "routine" repair and/or replacement practices and that two additional sets of tables were used to calculate reliabilities using alternate configurations when repair and/or replacement was assumed to be "none" or "major". These later calculations are shown in Tables A-3 through A-10 in Appendix A.

It should be noted that estimates were also made for the reliability of the CCGT-LWSP power system if the HSD were operated in accordance with the conventional destroyer mission (Fig. 5.4). For this purpose, another set of tables similar to Tables 5.9 through 5.12 and A-3 through A-10 was prepared.

The results obtained from all these calculations indicate that major improvements can be made in mission reliability when alternate configurations are allowed. As can be seen from the results in Table 5.8, the CCGT-LWSP power system reliability becomes 0.9383 for reconfigurations which require five minutes or less for conversion and no in-service repair/replacement is allowed. When routine or major repair/replacements are allowed the calculated reliability increased to 0.9804 or 0.9844, respectively.

Additional small improvements in reliability are possible when 60 or 180 minutes are allowed for configuration changeover. The reliability under routine repair and/or replacement practices increases from .7414 at negligible change over time allowance; to 0.9802 at 5 minutes changeover time; and then to 0.9830 and 0.9874, respectively, at 60 and 180 minutes changeover times. Correspondingly, the "major repair/replacement" practice increases reliability from 0.8502 to 0.9844 and 0.9885 at 10-, 60-, and 180-minutes changeover times, respectively. The calculations for some of these projections are shown in Tables 5.9 through 5.12 and in Appendix A, Tables A-3 through A-10.

For a steam system, and for the CCGT-LWSP installed in an HSD operating according to the conventional destroyer mission, 24 additional reliability calculations were undertaken. These results are also summarized in the matrices shown in Table 5.8. The differences between the results for the steam and CCGT-LWSP systems, as well as the significance of these differences, are

5.5 Comparison of LWSP System and Steam System Reliabilities

The CCGT-LWSP system is projected to provide a higher mission reliability than a typical steam power conversion system. When estimates allowing routine repair/replacement practices are considered, the results indicate that the CCGT-LWSP could be as little as 5.7 percentage points better than a steam system (0.989 vs 0.932 when alternate configurations are allowed to take 180 minutes for changeover) to as much as 42 percentage points better (0.741 vs 0.316 when alternative configurations are severely limited). While the absolute values for these reliabilities should not be considered sacrosanct, the relative values can be considered consistent and indicative of a reduction in complexity and an increase in reliability with a CCGT-LWSP. A more detailed discussion presented in the following sections considers separately the reliabilities projected for the three categories of repair/replacement practices: "major", "routine," and "none."

5.5.1 Reliability with Major In-Service Repair/Replacement Practice

When the reliability calculations, for the matrix of conditions presented in Fig. 5.6, were completed, the results presented in Table 5.8 were obtained. When these results are plotted (see Fig. 5.16), the envelope of values for the LWSP generally represents a higher set of reliability values than does the envelope of values estimated for the steam system. When major repair/replacement practices are included, the margin between the LWSP and CCGT reliability is small, generally covering a spread of from 2.3 to 15.3 percentage points.

As noted, both systems are projected to be highly reliable when allowances are made for using alternate configurations which require up to 180 minutes for adjustment or changeover. However, this margin becomes much larger as shorter time allowances are imposed for the changeover. If an instantaneous need for full output capacity were required, only those configurations which require negligible time for changeover could respond. In this case the differences between the LWSP and SPS, shown on the left-hand side of Fig. 5.16, indicate a margin of approximately 15 percentage points (0.850 for CCGT, 0.697 for SPS).

5.5.2 Reliability with Routing In-Service Repair/Replacement Practices

When "routine" repair and/or replacement practices are included in the reliability calculations, the CCGT-LWSP is estimated to be 5.7 to 43.5 percentage points more reliable than the steam system. The smallest differential is again found when alternate configurations are included which require up to 180 minutes for changeover. The largest differential occurs under the assumption that the only alternate configurations allowed are those which require negligible time for changeovers. Under these latter conditions, the steam power conversion

system exhibits a reliability of less than 40 percent while that of the LWSP is greater than 70 percent (see Table 5.8). This difference highlights important features of the two systems. The steam system is much more complex and appears to rely on the many alternate operating configurations provided by this complexity to achieve high reliability. However, it is this same complexity that causes a higher probability that a component will fail, and thus require the system to shift to an alternate operating configuration.

The reliability estimates which should be considered the most representative of actual operating practices, are those calculated for routine repair/replacement when alternate configurations which require approximately 5 minutes for changeover are allowed. This period of time is short enough to allow these changeovers to occur at any time during the mission without causing a significant impact. Thus, the effective mission reliability of the CCGT should be near 98.0 percent, and the effective SPC mission reliability appears to be near 85.5 percent.

5.5.3 Reliability with No In-Service Repair/Replacement

When the restriction of no in-service repair/replacement is applied, the margin by which the CCGT exceeds the SPS reliability increases, the CCGT system reliability becoming 18.6 to 37.8 percentage points higher. Under the assumption that alternate configurations are allowed which take up to 180 minutes for changeover, the CCGT might exhibit a reliability of 0.956 while the SPS would be approximately 0.770.

When the fewest alternate configurations are allowed, the reliabilities of both systems become quite low. That of the CCGT system would be near 47 percent while that of the SPS would be near 10 percent. Again, the latter set of values are evidence of system complexities. Since both the CCGT and steam systems rely on numerous components, both systems will not fare well if repair/replacement cannot be performed during the shutdown periods between mission operating periods.

Although it is unrealistic not to allow repair/replacement, the reliabilities projected for the CCGT are respectable when alternate configurations are allowed which require only 5 minutes for changeover. Under these conditions, the CCGT reliability becomes approximately 93 percent while that for the SPS system is approximately 73 percent. Thus, the CCGT might offer the convenience of a power conversion system which can provide many of the advantages of alternate operating configurations without the limitations of a steam system.

5.5.4 CCGT-LWSP Reliability when Operated on Conventional Mission

As discussed previously, the LWSP system reliability was also calculated when the system is operated in accordance with a conventional destroyer mission

profile. The results presented in Table 5.9 indicated that the reliability associated with this revision is very little different from that calculated for the HSD mission. The reason for this can be appreciated by realizing that although the conventional destroyer mission requires more operating hours per mission, the 59.7 MW CCGT power conversion system will be operating at only a fraction of its rated output most of this time. These factors appear to trade with each other in terms of making the operating requirements more severe in time and less severe in power level. Furthermore, this result indicates that an HSD which utilizes a CCGT-LWSP might effectively perform a conventional destroyer mission as well.

5.5.5 Impact of Reliability Estimations

In conclusion, the use of CCGT-LWSP power systems should provide a higher mission reliability than a steam power system (SPS). In addition, many of the advantages associated with open-cycle gas turbines should be available for use in CCGT operation and maintenance practices, while the flexibility of operating with alternate operating configurations and alternate fuels (typical of a steam system) would also be possible. More detailed designs and evaluations of CCGT systems are therefore in the interest of the Navy since both future operational flexibility, and life cycle cost, should be improved.

REFERENCES

- 5.1 Reliability/Maintainability/Availability Design Data Bank Report, Revision A, Naval Ship Engineering Center, June 1975.
- 5.2 Yurkowsky, W., D. F. Cottrel, T. R. Gagnier: Non-Electronic Reliability Notebook, Hughes Aircraft Co., January 1975.
- 5.3 Kuo, S. C., et al.: Lightweight Propulsion Systems for Advanced Naval Ship Applications -- Part I - System Studies. UTRC Report R77-952566-5, May 1977.
- 5.4 Telcons with Reliability/Maintainability/Availability Design Data Bank personnel, NAVSEC, June, July, August 1978.
- 5.5 Engine Unplanned Removal Report, JT8D, January 1977 through December 1977, Pratt and Whitney Aircraft Group, Commercial Products Division, January 1978.
- 5.6 Commercial Engines, Engine Inflight Shutdown Report, JT8D and JT3D, October 1976 through September 1977, Pratt and Whitney Aircraft Group, Commercial Products Division, October 1977.
- 5.7 Telcons, meetings and correspondence with representatives of J. J. Henry, Inc., Crystal City, Washington, D. C., April 1978.
- 5.8 Rothbart, H. A.: Mechanical Design and systems Handbook, McGraw-Hill Book Co.
- 5.9 Report on Equipment Availability for the Ten Year Period 1966-1975, Edison Electric Institute, Publication No. 76-85, December 1976.
- 5.10 Lang, C. J., et al.: Quality Assurance-Reliability Handbook, U. S. Army Material Command, October 1968, Report No. AD 702936.
- 5.11 Guide Manual for Reliability Measurement Program, Dept. of Navy Special Projects Office, Report No. NAVWEPS OD 29304.

TABLE 5.1
RELIABILITY MATHEMATICAL RELATIONSHIPS

Basic Reliability Equation

$$R = \exp(-\lambda t) = \exp(-\lambda_m)$$

λ = failure rate
 t = mission duration

λ_m = number of mission failures

Weibull Reliability Equation

$$R = \exp \left[-\frac{(t-\gamma)^{\beta}}{\alpha} \right]$$

where: α , γ , β are shape, scale, (2)
and location parameters

Reliability of Components in Series (R_s)

$$R_s = (R_1)(R_2)(R_3) \dots (R_i)$$

$$R_1, R_2, \dots, R_i = e^{-\lambda_i}$$

$$R_s = e^{-\sum \lambda_i}$$

Reliability of Components in Parallel (R_p)

$$R_p = 1 - Q_p$$

$$R_p = 1 - (1 - R_1)(1 - R_2) \dots (1 - R_i)$$

Probability of failure of Components in Parallel (Q_p)

$$Q = 1 - R$$

$$Q_p = (Q_1)(Q_2)(Q_3) \dots (Q_i)$$

Estimation of failure rate for a new component design/application

$$\lambda_c = \lambda_r (f_1)(f_2)(f_3)(f_4)$$

λ_c = new component failure rate

λ_r = reference component failure rate

f_1 = design adjustment factor

f_2 = duty-cycle adjustment factor

f_3 = environment adjustment factor

f_4 = state-of-the-art adjustment factor

Table 1

LSSP CONTROL BLOCK IDENTIFICATION

Block Number	Component Description
1	Setting lever, cables and connectors
2	Parallel setting system
3	Fuel flow signal
4	Parallel fuel flow signal
5	Power turbine control valve signal #1
6	Parallel power turbine control signal
7	Power turbine control valve signal #2
8	Parallel power turbine control signal #2
9	Final turbine control signal
10	Parallel turbine control signal
11	Water cooling valve signals
12	Parallel cooling water signals
13	Inventory control valve signals
14	Parallel inventory signals
15	Overtemperature sensors
16	Parallel overttemperature sensors
17	Overspeed sensors
18	Parallel overspeed sensors
19	Overpressure sensors
20	Parallel overpressure sensors
21	Oil and fuel system sensors
22	Fuel, oil and fuel sensors
23	Vibration sensor
24	Parallel vibration sensor
25	Low pressure storage tank & receiver
26	Control system computer
27	Parallel (back-up) computer
28	Control power supply
29	Routing from power turbine & compressor, b. to/from regenerator
30	Should side heat exchanger (regenerator hot-side)
31	Bypassing and switching components to bypass regenerator hot-side
32	Water pump & ducts
33	Parallel pump & ducts
34	Switching system for parallel pumps
35	Water valve & ducts
36	Parallel valve & ducts
37	Switching system for parallel valves
38	Precooler heat exchanger
39	Water/water heat exchanger
40	Switching system & ducts to bypass precooler
41	Low pressure valves and ducts for inventory
42	Medium pressure valves and ducts for inventory
43	High pressure valves and ducts for inventory
44	Low pressure storage tank & receiver
45	Medium pressure storage tank & receiver to top tank system
46	Top tank system

TABLE 5.2 (Cont'd)

<u>Block Number</u>	<u>Component Description</u>	<u>Block Number</u>	<u>Component Description</u>
47	Switching system for parallel tanks	70	High compressor stators
48	High pressure tanks and accessories	71	High compressor bearings, seals
49	Backup tank system		
50	Switching system for parallel tanks	72	High compressor rotors
51	Charging compressor ducts and accessories	73	Ducting to regenerator cold-side
52	Backup compressor system	74	Regenerator heat exchanger cold-side (tubes)
53	Switching system for parallel charging system	75	Ducting from regenerator to heater
54	Emergency valve & ducts	76	Switching system and ducts to bypass regenerator cold-side (tubes)
55	Low compressor cases	77	Fuel pump
56	Low compressor stators	78	Fuel valve & accessories
57	Low compressor bearings (2) & oil system	79	Backup valve & accessories & switching system
58	Accessory gearbox and starter	80	Combustor #1
59	Low compressor rotors, shafts, etc.	81	Combustor #2
60	Water pump and ducts	82	Combustor #3
61	Backup water pump & ducts	83	Combustor #4
62	Switching system for parallel pumps	84	Heat exchanger & mixer ducts
63	Water valve and ducts	85	Preheater hot-side
64	Backup valve	86	Bypass system (preheater hot side)
65	Switching system for parallel valves	87	Turbine
66	Intercooler heat exchanger	88	Control
67	Water/water heat exchanger	89	Compressor
68	Switching system & ducts to bypass intercooler		
69	High compressor cases		

TABLE 5.2 (Cont'd)

<u>Block Number</u>	<u>Component Description</u>
90	Preheater cold-side
91	Switching and bypass system (preheater cold-side)
92	Duct from heater to turbine
93	Compressor drive turbine (CD) cases & supports
94	CD stators
95	CD rotors
96	CD bearings, seals, etc
97	Control valve
98	Alternate control valve & accessories
99	Control valve ducting
100	Alterante control valve switch and duct system
101	Power turbine (PT) case & supports
102	PT stators
103	PT rotors
104	PT bearings, seals, etc
105	PT exhaust ducting
106	PT control valve
107	Backup valve ducting
108	Backup control valve
109	Alt. control valve switch & duct system
110	Parallel heater system (from other heater room)
111	Parallel compressor system (from other engine room)
112	Parallel power system (from other shaft)

TABLE 5.3
STEAM SYSTEM COMPONENT BLOCK IDENTIFICATION

<u>Block Number</u>	<u>Component Description</u>	<u>Block Number</u>	<u>Component Description</u>
1	Setting lever cables and connectors	27	Control power supply
2	Parallel setting system	28	Parallel power supply
3	Fuel flow signal	29	Main condenser
4	Parallel fuel flow signal	30	Ducting to/from condenser
5	Cruise turbine control valve signals	31	Cooling water supply lines
6	Parallel control valve signals	32	Cooling water pumps
7	High pressure turbine control valve signals	33	Cooling water rejection heat exchanger
8	Parallel control valve signals	34	Main condensate feed pump
9	Low pressure turbine control valve signals	35	Water supply lines
10	Parallel control valve signals	36	Turbine to drive condenser feed pump
11	Feed pump signals	37	Ducts and valves to/from above turbine
12	Parallel feed pump signals	38	Air ejector
13	Boiler pressure signals	39	Gland exhaust condenser
14	Parallel boiler pressure signals	40	Ducts and valves to/from ejector
15	Overtemperature protection signals	41	Gland condenser pump
16	Parallel overttemperature signals	42	Ducts to/from deaerator
17	Overspeed sensors	43	Deaerating feedwater heater
18	Parallel overspeed sensors	44	Main boiler booster feed pump
19	Overpressure sensors	45	Parallel boiler booster feed pump
20	Parallel overpressure sensors	46	Lines to/from boiler booster pump
21	Oil and fuel system sensors	47	Parallel boiler booster pump lines
22	Parallel oil and fuel system sensors	48	Turbine to drive main feed booster pump
23	Vibration sensors	49	Parallel boiler turbine to drive above pump
24	Parallel vibration sensors	50	Lines and ducts to/from main feed pump
25	Control system computer	51	Parallel boiler lines and ducts for feed pump
26	Parallel computer	52	Main feed valve
		53	Parallel boiler main feed valve

TABLE 5.3 (Cont'd)

Block Number	Component Description	Block Number	Component Description
54	Boiler main feed pump	82	Steam drum
55	Parallel boiler main feed pump	83	Parallel boiler steam drum
56	Lines and valves for main feed pump	84	Ducts from superheater
57	Parallel boiler lines and valves	85	Parallel boiler ducts from superheater
58	Turbine to drive main feed pump	86	Valve, main steam stop
59	Parallel boiler turbine feed pump drive	87	Parallel boiler steam stop valve
60	Ducts to/from drive turbine for feed pump	88	Regulator for steam supply
61	Parallel boiler ducts for drive turbine	89	Parallel boiler regulator
62	Valves for drive turbine for feed pump	90	Fuel-oil heater
63	Parallel boiler valves for feed pump drive turbine	91	Parallel boiler fuel-oil heater
64	Feedwater check valve	92	Pump for fuel-oil heater
65	Parallel boiler feedwater check valve	93	Parallel boiler pump for fuel-oil heater
66	Ducts and lines to feedwater valve	94	Turbine to drive the fuel-oil heater pump
67	Parallel boiler ducts and lines	95	Parallel boiler fuel-oil pump drive turbine
68	Fuel supply valves	96	Ducts to/from fuel-oil drive turbine
69	Parallel boiler fuel supply valves	97	Parallel boiler ducts to/from turbine
70	Economiser heat exchanger	98	Pump, main lube oil
71	Parallel boiler economiser	99	Parallel boiler main lube pump
72	Main boiler heat exchanger	100	Turbine to drive main lube pump
73	Parallel boiler heat exchanger	101	Parallel boiler main lube pump turbine
74	Air blower	102	Air ejector
75	Parallel boiler air blower	103	Parallel boiler air ejector
76	Turbine to drive air blower	104	Ducts for air ejector
77	Parallel boiler blower drive turbine	105	Parallel boiler air ejector ducts
78	Ducts and valves for blower drive turbine	106	Ducts for auxiliary steam system
79	Parallel boiler ducts and valves	107	Parallel boiler auxiliary steam system ducts
80	Superheater	108	Valves, auxiliary steam unloading
81	Parallel boiler superheater	109	Parallel auxiliary steam valves

TABLE 5.3 (Cont'd)

<u>Block Number</u>	<u>Component Description</u>
110	Valves and ducts, accessory power
111	Parallel valves and ducts, accessory power
112	Strainer, main steam
113	Ducts, to/from strainer
114	Guarding valves
115	Cross-over ducts and valves
116	Cruise turbine control valves
117	Ducts for cruise turbine controls
118	Cruise turbine
119	High pressure turbine
120	Ducts to high pressure turbine
121	Low pressure turbine
122	Ducts to low pressure turbine
123	Bypass system for high pressure turbine

TABLE 5.4
DEGRADED OUTPUT LWSP-CCHT CONFIGURATIONS

<u>Condition Description</u>	<u>Maximum Output Possible % of Installed</u>	<u>Changeover Time, Minutes</u>	<u>Configuration Code</u>
Basic Power System with Routine Repair/Replacement Practices	100	0	III-A
Heater Capacity Reduced 20%	100	5	IV
Precooler Bypassed	60	60	V
Intercooler Bypassed	60	60	VI
Regenerator Cold-Side Bypassed	60	180	VII-A
Regenerator Totally Bypassed	60	180	VII-B
Heater Capacity Degraded by 40%	60	5	VIII
Cross-Connection of Heater Rooms	40	180	IX
Cross-Connection of Compressor Turbomachinery	40	180	X
Heater Capacity Degraded by 60%	40	5	XI
Single Propeller Shaft Operation	40	5	XII

TABLE 5.5
DEGRADED OUTPUT STEAM SYSTEM CONFIGURATIONS

<u>Condition Description</u>	<u>Maximum Output Possible % of Installed</u>	<u>Changeover Time, Minutes</u>	<u>Configuration Code</u>
Baseline Configuration All Subsystems Capable of Installed Capacity Liberal at Sea Repair Allowed	100	0	A
One Boiler Inoperative on Single Shaft	100	60	A-I
Condenser Capacity Reduced 20% (Blockage, Etc.)	60	5	A-II
Condenser Capacity Reduced 40%	60	5	A-III
Condenser Capacity Reduced 60%	40	5	A-IV
Bypass of Inoperative High Pressure Turbine	60	60	A-V
Bypass of Inoperative Low Pressure Turbine	60	60	A-VI
Cross-Connection with Other Shaft Boiler Room	45	180	A-VII
Bypass of Both High & Low Pressure Turbines, Only Cruise Turbine Operating	30	180	A-VIII
Single Propeller Operation, Limited to Speeds of 20 Knots or Less	20	5	A-IX

TABLE 5.6
REFERENCE FAILURE RATE SOURCES

<u>Source Name</u>	<u>Code Number</u>	<u>Reference Number</u>
NAVSEC RMS Design Data Bank	1	5.1, 5.4
P&WA Unplanned Removal	2	5.5
P&WA Inflight Shutdown	3	5.6
Hughes Nonelectric Reliability Notebook	4	5.2
J. J. Henry, Inc.	5	5.7
Mechanical Design & Systems Handbook	6	5.8
Edison Electric Institute Equipment Availability	7	5.9

TABLE 5.7
SAMPLE LMSP COMPONENT FAILURE RATE ESTIMATION CALCULATION SHEET

Block #	Subsystem Name	Component Description	Reference Failure Rate, No./1000 Hrs		Adjustment Factors		State-of-Art	Estimated Failure Rate No./1000 Hrs	Mean Time Between Failures, hrs
			Reference Design	Source	Rate	Design			
New Design	Reference Design	Source	Rate	Design	Buoy Cycle	Environment			
88	Heater	control & fuel subsystem	.010	1.0	0.6	1.1	1.2	.008	125,000
89	Heater	compressor & bearings	.070	0.9	0.7	1.2	1.0	.053	18868
90	Heater	preheater cold side	.001	0.7	0.7	1.6	1.0	.0008	1,250,000
91	Heater	switching & bypass ducts	.001	1.2	1.2	1.5	1.0	.002	500,000
92	Turbine	duct from heater	.001	1.2	1.2	1.5	1.0	0.002	500,000
93	Turbine	CDT cases & supports	.003	0.8	0.6	1.2	1.1	.0019	526316
94	Turbine	CDT stators	.025	0.6	0.6	0.8	1.2	.0086	116779
95	Turbine	CDT rotors	.007	0.7	0.6	0.8	1.2	.0028	357143
96	Turbine	CDT oil system, bearings seals	.010	0.9	0.6	1.0	1.2	.0065	153846
97	Turbine	bypass control valve	.107	0.5	1.0	1.1	1.0	.060	16667
98	Turbine	backup bypass valve	.107	0.5	1.0	1.1	1.0	.060	16667

TABLE 5.8

RELIABILITY ASSESSMENT MATRIX FOR LWSP
AND STEAM PROPULSION SYSTEMS

Propulsion System and Mission	Considerations	Reliability			
		Reconfiguration Time Min.	Repair Replacement Practices		
		0.1		5	60
LWSP Hi-Speed Destroyer Mission	None	0.4718	0.9383	0.9453	0.9561
	Routine	0.7414	0.9802	0.9830	0.9874
	Major	0.8502	0.9844	0.9844	0.9885
LWSP Conventional Destroyer Mission	None	0.4178	0.9211	0.9300	0.9504
	Routine	0.7414	0.9790	0.9831	0.9894
	Major	0.8502	0.9868	0.9868	0.9902
Steam Propulsion Conventional Destroyer Mission	None	0.0940	0.7275	0.7526	0.7700
	Routine	0.3157	0.8546	0.9123	0.9323
	Major	0.6977	0.9585	0.9585	0.9655

TABLE 5.9

UNSP CONFIGURATION RELIABILITY CALCULATIONS
ROUTINE REPAIR/REPLACEMENT PRACTICES

Configuration #	Description	Conversion Time	Maximum Power Attainable, C/O Installed	Reliability Equation $R_{IIA} = \frac{(R_{10})(R_{91})(R_{49})(R_{59})(R_{40})(R_{57})}{(R_{53})(R_{66})(R_{67})(R_{58})(R_{71})(R_{72})(R_{75})(R_{76})(R_{84})(R_{55})(R_{90})(R_{91})(R_{95})(R_{96})(R_{100})(R_{103})(R_{104})}$	Probability of Operation Reliability
III-A	Basic Power System With Routine Repair/Replacement Practices	0	100	$R_{IIIA} = \frac{(R_{10})(R_{91})(R_{49})(R_{59})(R_{40})(R_{57})}{(R_{53})(R_{66})(R_{67})(R_{58})(R_{71})(R_{72})(R_{75})(R_{76})(R_{84})(R_{55})(R_{90})(R_{91})(R_{95})(R_{96})(R_{100})(R_{103})(R_{104})}$	$\approx .7437$
IV	Heater Capacity Reduced 20%	5	100	$R_{IV} = \frac{R_{IIA} [R_{HT-20}] [1 - (R_{90})(R_{85})(R_{84})]}{(R_{90})(R_{85})(R_{84})}$	$\approx .09276$
V	Precooler Bypassed	60	60	$R_{V} = \frac{R_{IIA} [1 - (R_{38})(R_{39})]}{(R_{38})(R_{39})}$	$\approx .02793$
VI	Intercooler Bypassed	60	60	$R_{VI} = \frac{R_{IIA} [1 - (R_{66})(R_{67})]}{(R_{66})(R_{67})}$	$\approx .02793$
VII A	Regenerator Cold-side Bypassed	180	60	$R_{VIIA} = \frac{R_{IIA} [1 - (R_{74})]}{(R_{74})}$	$\approx .03803$
VII B	Regenerator Totally Bypassed	180	60	$R_{VIIB} = \frac{R_{IIA} [1 - (R_{30})]}{(R_{30})}$	$\approx .00373$
VII	Heater Capacity Degraded by 40%	5	60	$R_{VII} = \frac{R_{IIA} [R_{HT-40}] [1 - (R_{90})(R_{85})(R_{84})]}{(R_{90})(R_{85})(R_{84})}$	$\approx .09523$
VIII	Cross-Connection of Heater Pumps	180	40	$R_{VIII} = \frac{R_{IIA} [1 - (R_{85})(R_{87})(R_{90})] (R_{110})}{(R_{90})(R_{85})(R_{84})}$	$\approx .09046$
X	Cross-Connection of Compressor Turbo Machinery	180	40	$R_{X} = \left[\frac{R_{IIA}}{(R_{10})(R_{103})(R_{100})} \right] \left[\frac{(R_{10})(R_{103})}{(R_{100})(R_{111})} \right]$	$\approx .19695$
XI	Heater Capacity Degraded by 60%	5	40	$R_{XI} = \frac{R_{IIIA} [R_{HT-60}]}{(R_{90})(R_{85})(R_{84})} [1 - (R_{90})(R_{85})(R_{84})]$	$\approx .09775$
XII	Single Propeller Shaft Operation	5	40	$R_{XII} = (R_{IIIA})(1 - R_{IIA})$	$\approx .19174$

TABLE 5.10

Configuration #	Description	Conversion Time	Maximum Power Attainable % Installed	Reliability Equation	(Probability Config. Operation) R1	Reliability
A	Baseline Configuration All Subsystems Capable of Installed Capacity Liberal At Sea Repair Allowed	0	100	RA = (RCCF) (RBP) (RTT)		.31572
AI	One Boiler Inoperative On Single Shaft	6.0	100	RAI = (RCCF) (RBI) (RTT) [1-RBI]		.09027
AII	Condenser Capacity Reduced 20% (Blockage, Etc.)	5	100	RAII = (R29.2) (R38) (R39) (RBP) (RTT) [1-(R29)(R33)]		.07851
AIII	Condenser Capacity Reduced 40%	5	60	RAIII = (R29.4) (R38) (R39) (RBP) (RTT) [1-(R29)(R33)]		.08254
AIV	Condenser Capacity Reduced 60%	5	40	RAIV = (R29.6) (R38) (R39) (RBP) (RTT) [1-(R29)(R33)]		.08763
AV	Bypass of Inoperative High Pressure Turbine	60	60	RAV = (RCCF) (RBP) (R121) (R122) (R123) [1-R119]		.06219
AVI	Bypass of Inoperative Low Pressure Turbine	60	60	RAVI = (RCCF) (RBP) (R119) (R126) [1-(R121)(R122)]		.06223
AVII	Cross-Connection With Other Shaft Boiler Room	180	4.5	RAVII = (RCCF) (R124) (RTT) [1-RBP]		.05065
AVIII	Bypass of Both High & Low Pressure Turbines, Only Cruise Turbine operating	180	30	RAVIII = (RCCF) (RBP) (R118) [1-RTT]		.12493
AVIX	Single Propeller Operation Limited To Speeds of 20 Knots Or Less	5	20	RAIX = (RA) (1-RA)		.21604
Note: RCCF = (R29.0(R33)(R38)(R39)) RBI = (R70)(R72)(R80)(R82)(R90) (R102) RBP = 1-(1-RBI) ² RTT = (R119)(R121)(R122)						

TABLE 5.11

MISSION RELIABILITY CALCULATION SHEET

- HI-SPEED DESTROYER MISSION
- ALL CONFIGURATIONS ALLOWED WHICH MIGHT REQUIRE 180 MINUTES OR LESS FOR CONVERSION
- ROUTINE REPAIR/REPLACEMENT PRACTICES

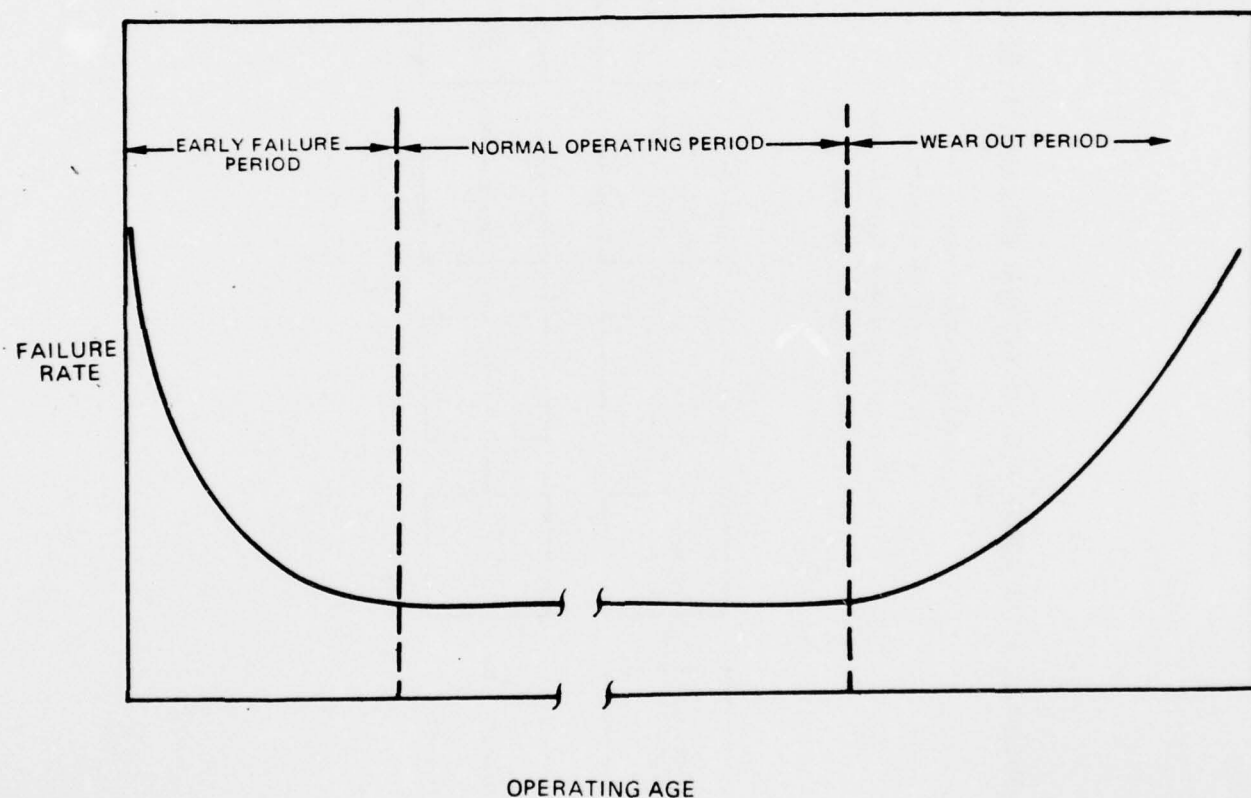
Power Level %Max	Allowable Configurations	Reliability Equation $Q_{li} = 1 - R_{li}$ = unreliability or Probability of Failure	Reliability At Power Level, R_p	Effective Failure Rate λ_p per 1000 hrs $\lambda_p = (\ln R)$	Time At Power Level tp 1000 hrs	$\lambda_p t_p$	MTBF At Constant Power Level Setting, $1/\lambda_p$ 1000 hrs
100	IIIA, IV	$R100\% = 1 - (Q111A)(Q1V)$.7654	.2674	.006	.0016	3,7397
55	IIIA, IV, V, VI, VIIA, VIIB, VIIII	$R55\% = 1 - (Q110Z)(QV)(QV1)(QV1A)(QV1B)$ (QV111)	.8078	.2134	.011	.00235	4,686
38	IIIA, IV, V, VI, VIIA, VIIB, VIIII, IX, X, XI	$R38\% = 1 - (Q55Z)(Q1X)(QX)(QX1) = 1 - Q38Z$.8733	.1355	.017	.0023	7,380
26	Same as 38%	$R26Z = R38Z$.8733	.1355	.017	.0023	7,380
16	Same as 38%	$R16Z = R26Z$.8733	.1355	.017	.0023	7,380
10	Same as 38%	$R10Z = R16Z$.8733	.1355	.011	.00149	7,380
7	All Above Plus XII	$R7Z = 1 - (Q38Z)(Q38Z)$.9839	.0162	.006	.000097	61,728
4	Same As 7%	$R4Z = R7Z$.9839	.0162	.006	.000097	61,728
3	Same as 7%	$R3Z = R4Z$.9839	.0162	.009	.000146	61,728
$R = e^{-\sum \lambda_p t_p}$							$\sum \lambda_p t_p$.9874
Mission As Stated Above $R = e^{-\lambda_m t}$, where $\lambda_m = \sum \lambda_p t_p$							$\sum \lambda_p t_p$.0168

TABLE 5.12

STEAM POWER SYSTEM MISSION RELIABILITY CALCULATIONS
 AII, ALTERNATE, DEGRADED CONFIGURATION
 CONVERSIONS ALLOWED WHICH TAKE UP TO
 180 MINUTES FOR CONVERSION
 ROUTINE AIR-SEA REPAIR/REPLACEMENT PRACTICES

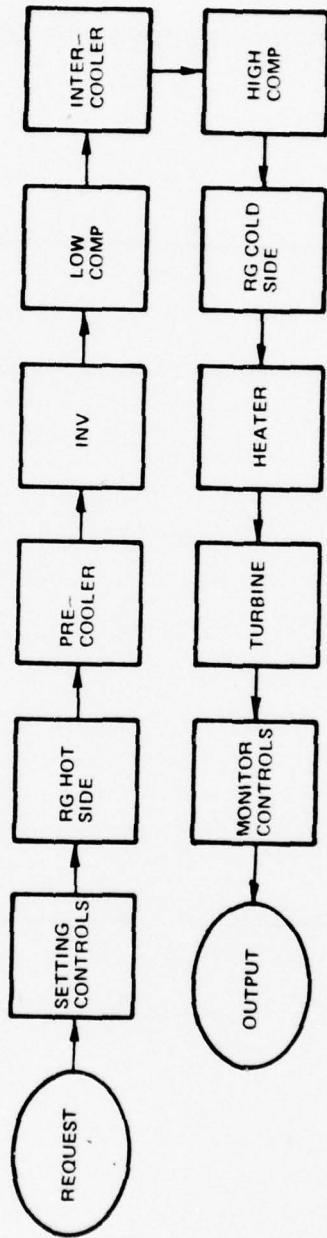
Speed Knots	Power Level % Max	Allowable Configurations	Reliability Equation $Q_1 = 1 - R_1$	Reliability At Power level, R_p hrs $\lambda p^x (1/nR)$	Effective Failure Rate λ_p per 1000 hrs	Time At Power Level t_p 1000 hrs	$\lambda p t_p$	MTBF At Constant Power Level $MTBF = 1/\lambda_p$
35 + 30	100	A, AI, AII	$R_{100\%} = 1 - (Q_A)(Q_{AI})(Q_{AII})$.42636	.85247	.0028	.00239	1.173
30 + 25	58	A, AI, AII, AIII, AV, AVI	$R_{58\%} = 1 - (Q_A)(Q_{AI})(Q_{AII})$ (Q _{AIII})(Q _{AV})(Q _{AVI})	.53516	.62520	.0066	.00413	1.599
25 + 20	30	A, AI, AII, AIII, AIV, AV, AVI, AVII	$R_{30\%} = 1 - (Q_{58\%})(Q_{VI})(Q_{VII})$ (Q _{IV})	.59736	.51524	.0530	.2731	1.941
20 + 15	14	A, AI, AII, AIII, AV, AVI, AVII, AVIII, AVX	$R_{14\%} = 1 - (Q_{30\%})(Q_{VII})$ (Q _{IX})	.72379	.32326	.0640	.02069	3.093
15 + 0	2.0	Same as 14%	$R_{2\%} = R_{14\%}$	= .72379	.32326	.0736	.02379	3.093
Mission As Stated Above:								
$R_m = \text{Mission Reliability}$								
$R_m = e^{-\lambda_m t}$								
$\lambda_m = \sum \lambda p t_p$ = Mission Failure Rate								
.9323								
$\Sigma \lambda p t_p =$								
.07005								

TYPICAL FAILURE RATE DISTRIBUTION



OVERALL LWSP-CCGT POWER SYSTEM RELIABILITY BLOCK DIAGRAM

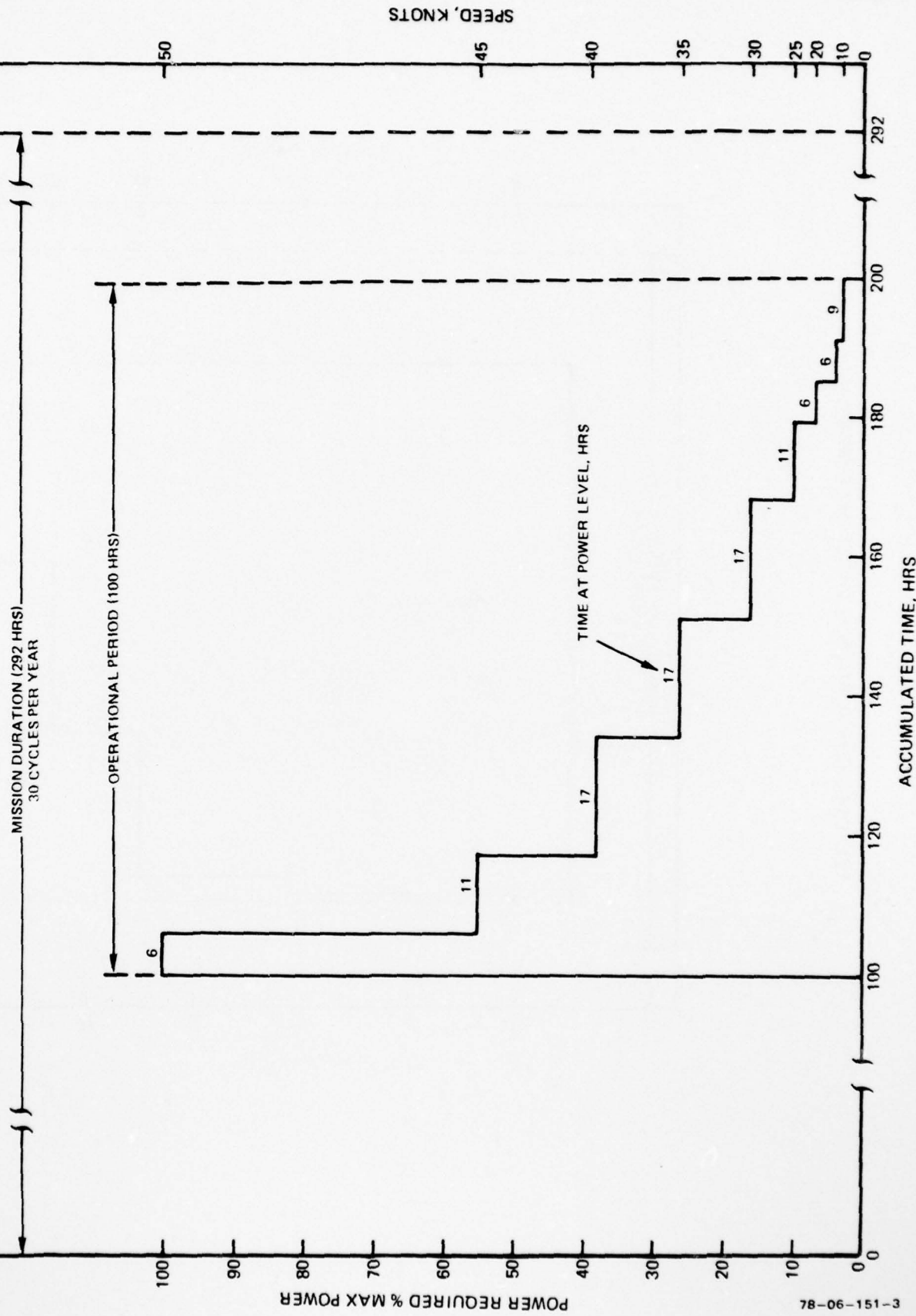
- MAJOR SUBSYSTEMS
- INV = INVENTORY SUBSYSTEM
- RG = REGENERATOR SUBSYSTEM
- COMP = COMPRESSOR SUBSYSTEM



R78-952979-4

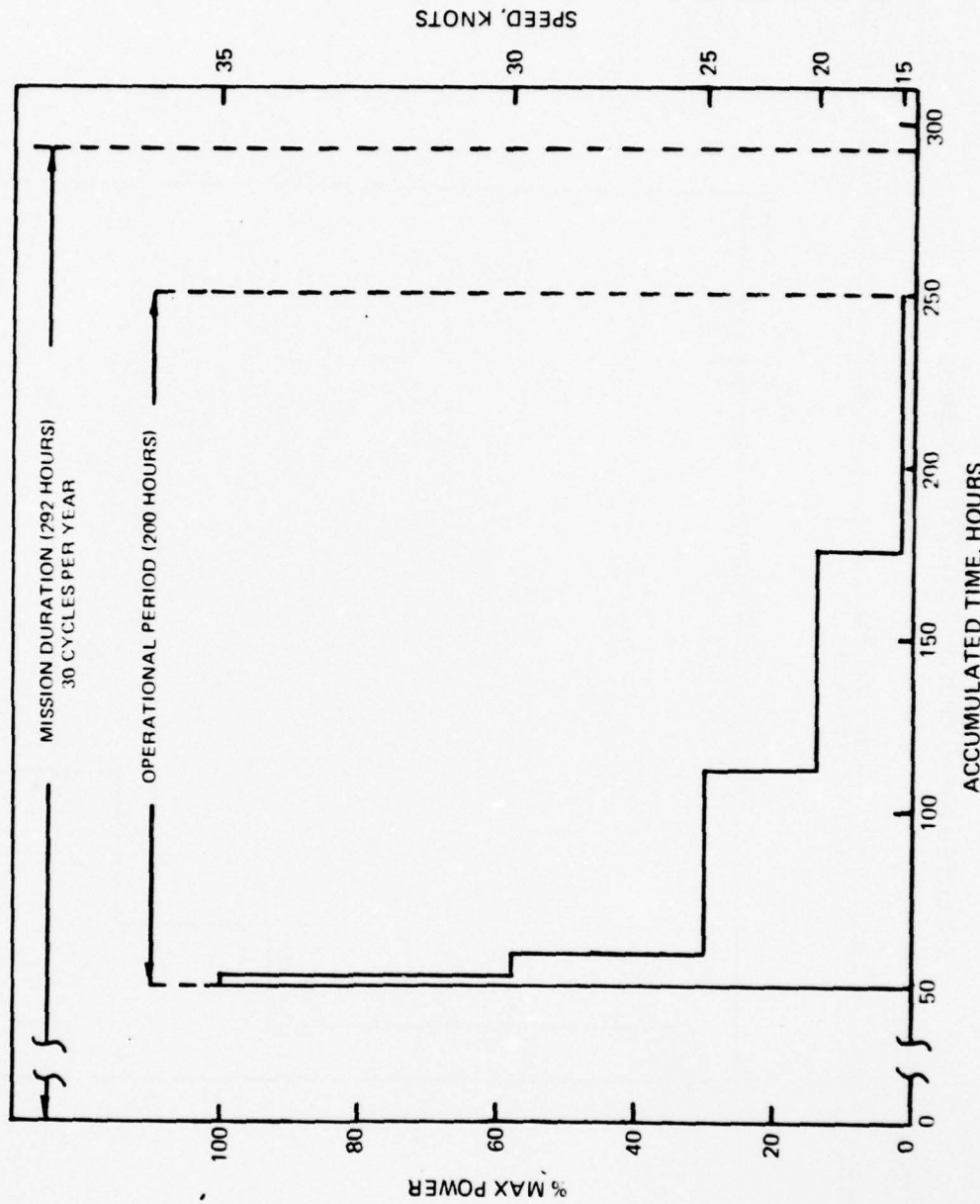
FIG. 5.3

SELECTED HIGH-SPEED DESTROYER MISSION

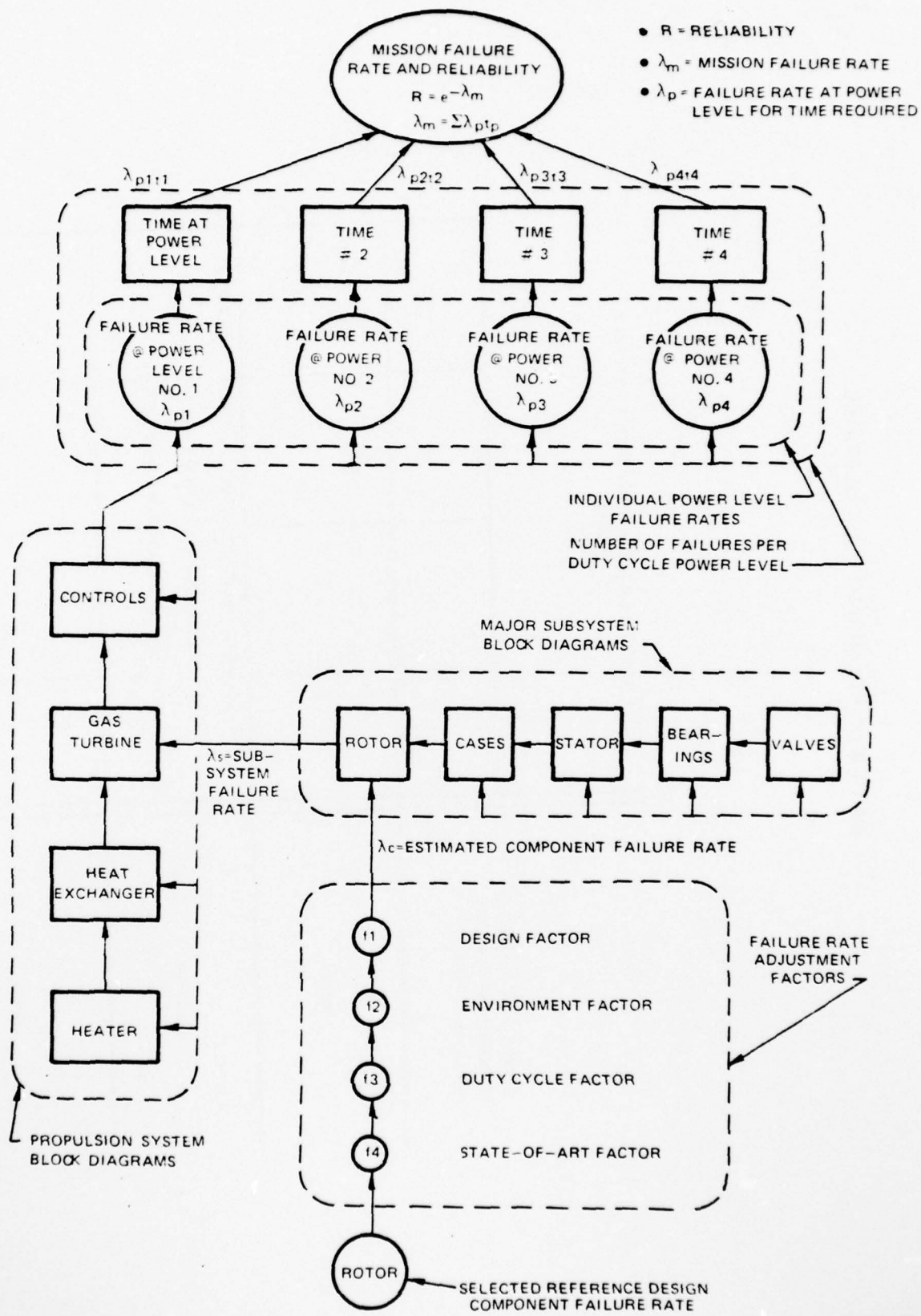


78-06-151-3

SELECTED CONVENTIONAL DESTROYER MISSION



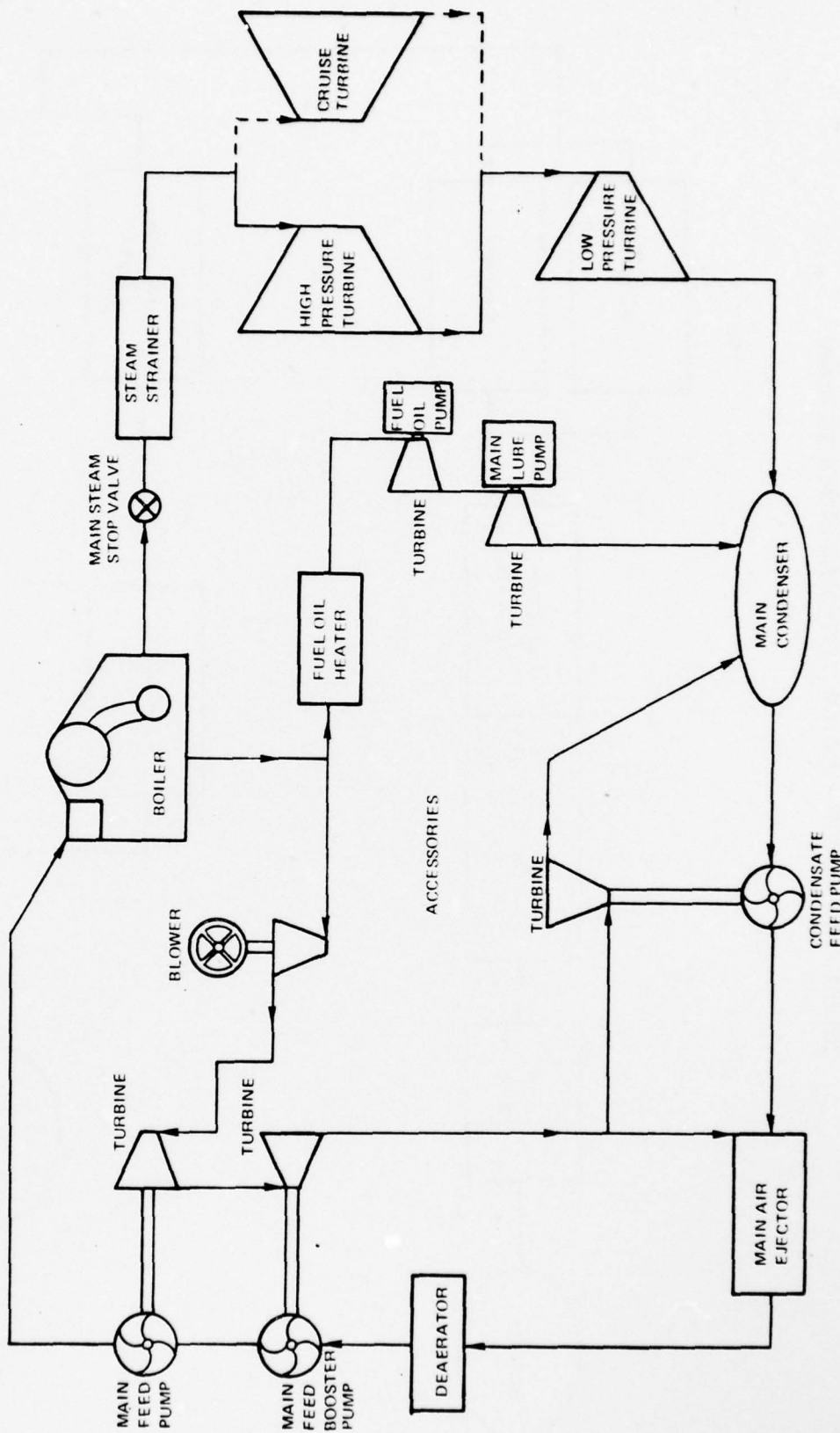
LWSP RELIABILITY ESTIMATION METHODOLOGY



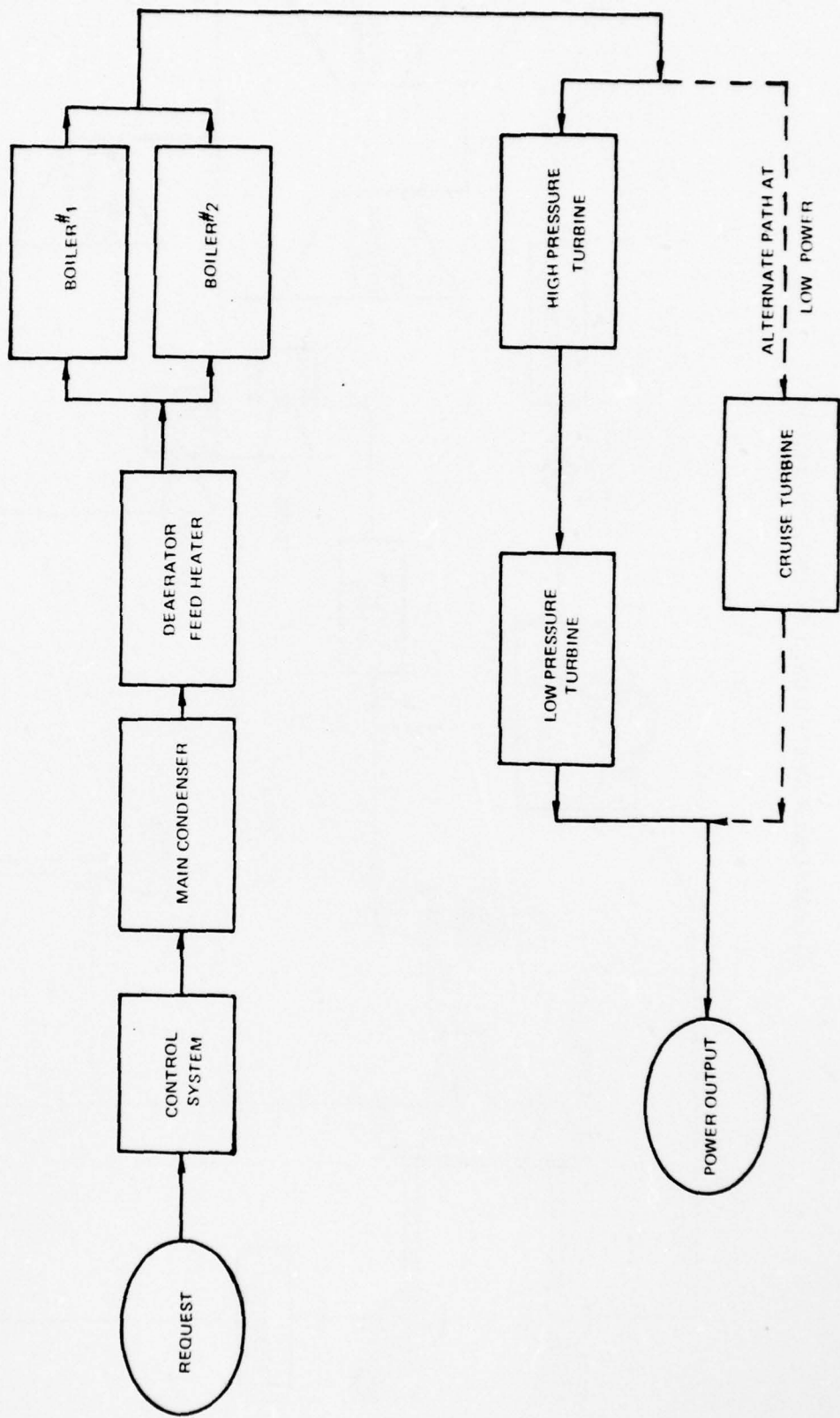
MATRIX OF RELIABILITY CALCULATIONS

		ALTERNATIVE CONFIGURATION CHANGEOVER TIME MINUTES				
		0.1	5	60	180	
REPAIR OR REPLACEMENT MAINTENANCE PRACTICE WHILE IN SERVICE	NONE					VALUES WERE CALCULATED FOR RELIABILITY FOR EACH OF THESE BLOCKS WHICH RESULT FROM ROUTINE COMBINATIONS OF THESE PHILOSOPHIES
	MAJOR					
	MINOR					

STEAM POWER SYSTEM CYCLE CONFIGURATION

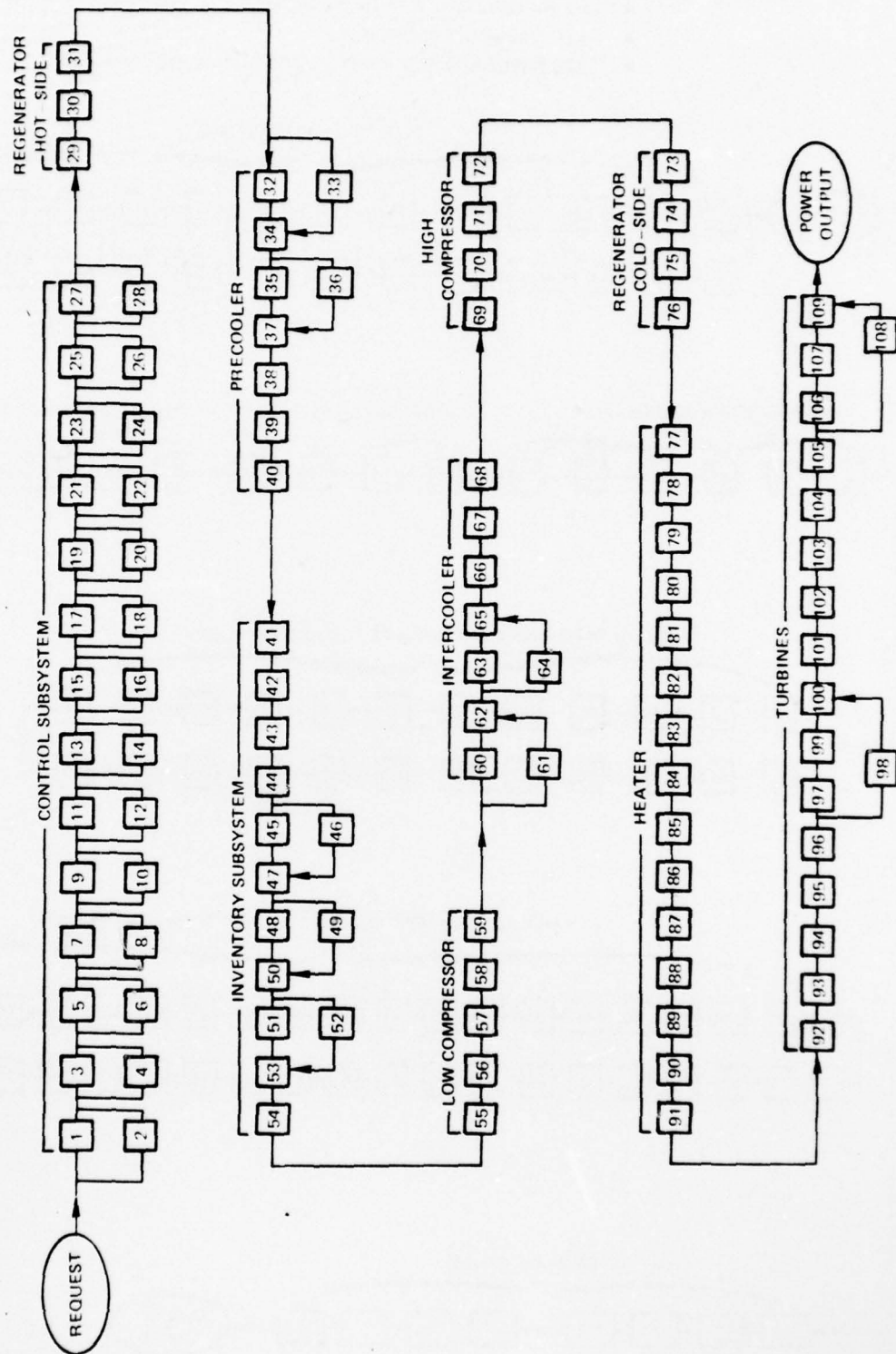


STEAM POWER SYSTEM MAJOR SUBSYSTEM BLOCK DIAGRAM



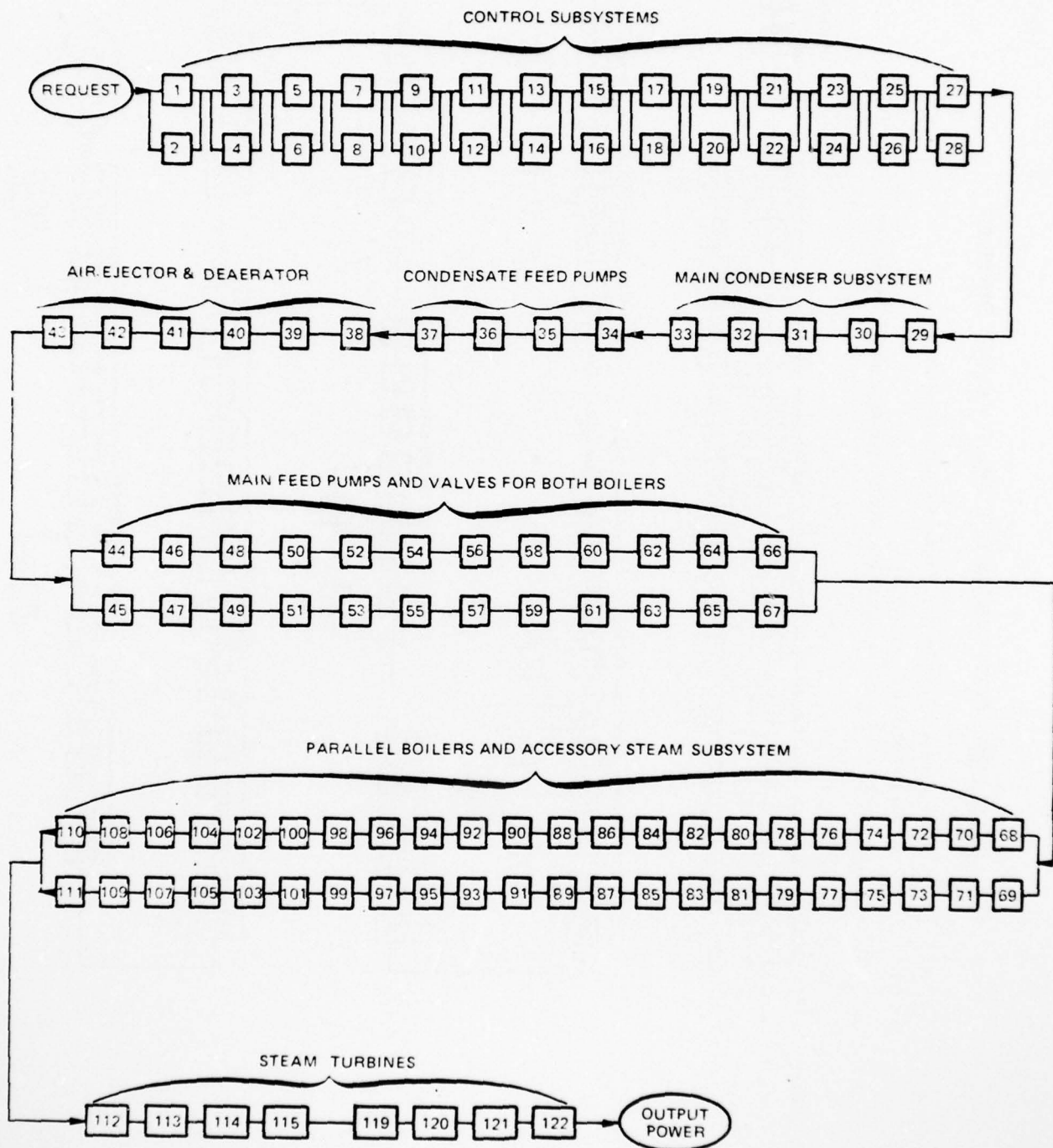
BASIC LWSP-CCGT SYSTEM RELIABILITY BLOCK DIAGRAM

- NO IN SERVICE REPAIR/REPLACEMENT IS ALLOWED
- ALL POWER LEVELS POSSIBLE
- SEE TABLE V-2 FOR IDENTIFICATION OF COMPONENT BLOCK NUMBERS



BASIC STEAM POWER SYSTEM RELIABILITY BLOCK DIAGRAM

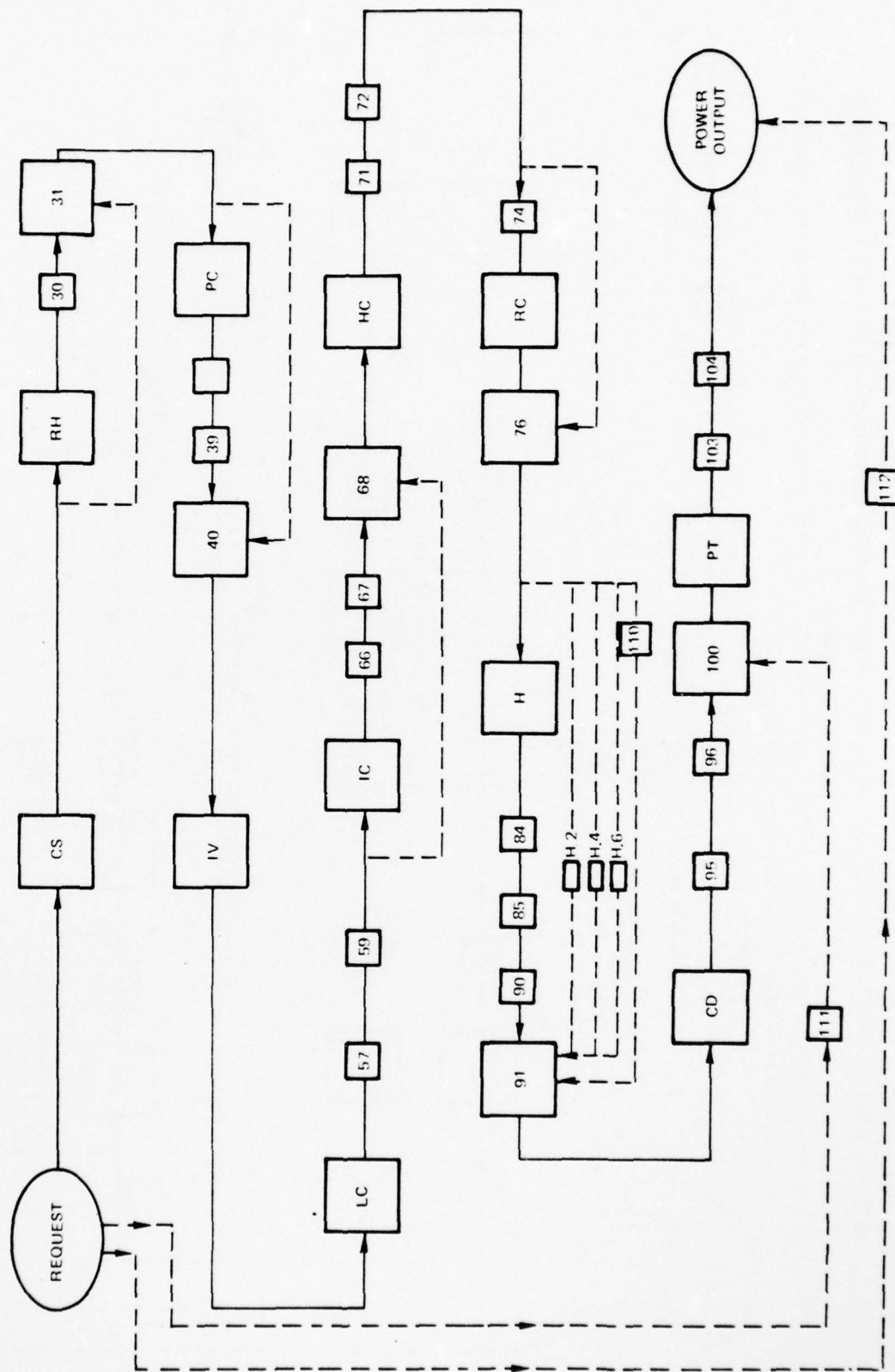
- NO IN-SERVICE REPAIR/REPLACEMENT ALLOWED
- ALL POWER LEVELS POSSIBLE
- SEE TABLE V-3 FOR IDENTIFICATION OF BLOCK NUMBERS



LWSP-CCGT RELIABILITY BLOCK DIAGRAM FOR ROUTINE REPAIR/REPLACEMENT PRACTICES

(CONFIGURATION # IIIB)

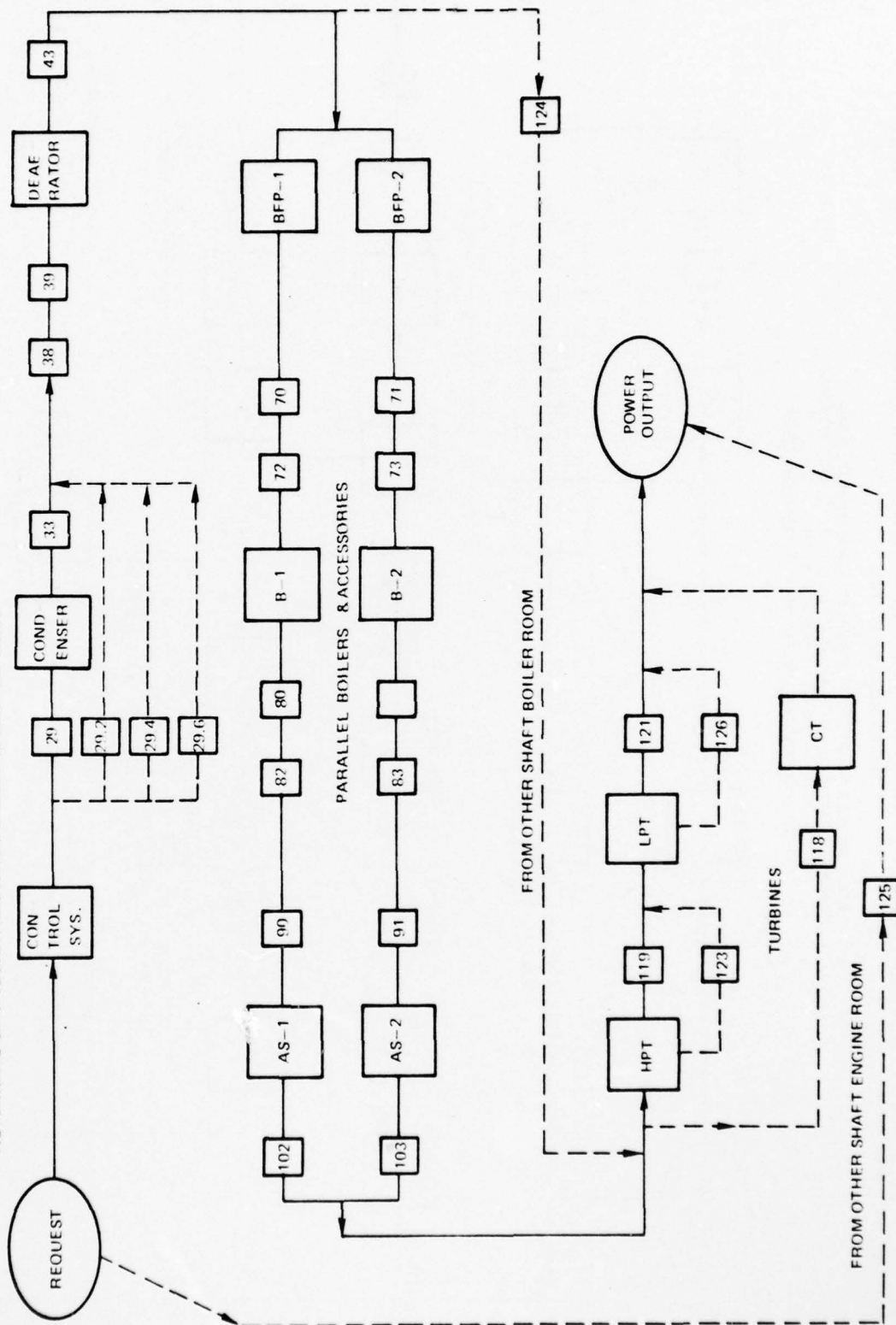
- LARGE BLOCKS REPRESENT GROUPS OF COMPONENTS WHICH CAN BE REPAIRED OR REPLACED WITHOUT AFFECTING MISSION
- ALL POWER LEVELS POSSIBLE ON SOLID PATH
- ALTERNATE CONFIGURATIONS SHOWN WITH DASHED LINES



STEAM SYSTEM RELIABILITY BLOCK DIAGRAM FOR ROUTINE REPAIR/REPLACEMENT PRACTICES

(CONFIGURATION A)

- LARGE BLOCKS REPRESENT GROUPS OF COMPONENTS WHICH CAN BE REPAIRED OR REPLACED WITHOUT AFFECTING MISSION
- ALTERNATE CONFIGURATION PATHS SHOWN AS DASHED LINES



LWSP-CCGT RELIABILITY BLOCK DIAGRAM FOR MAJOR REPAIR/REPLACEMENT PRACTICES
(CONFIGURATION IIIC)

- ALL POWER LEVELS ATTAINABLE
- LARGE BLOCKS REPRESENT GROUPS OF COMPONENTS WHICH CAN BE REPAIRED/REPLACED WITHOUT AFFECTING MISSION

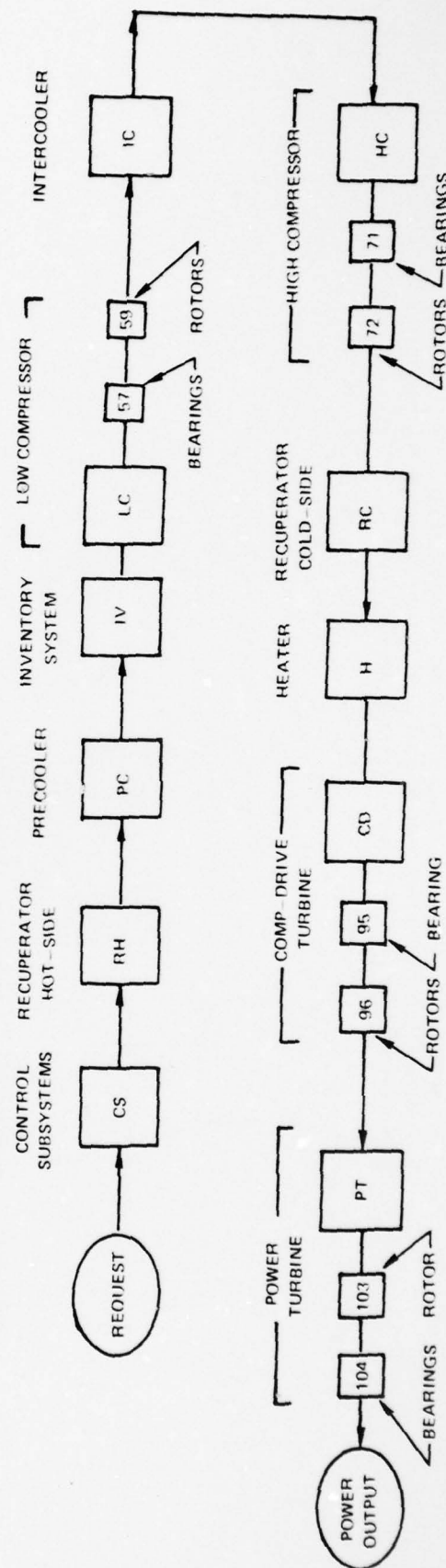


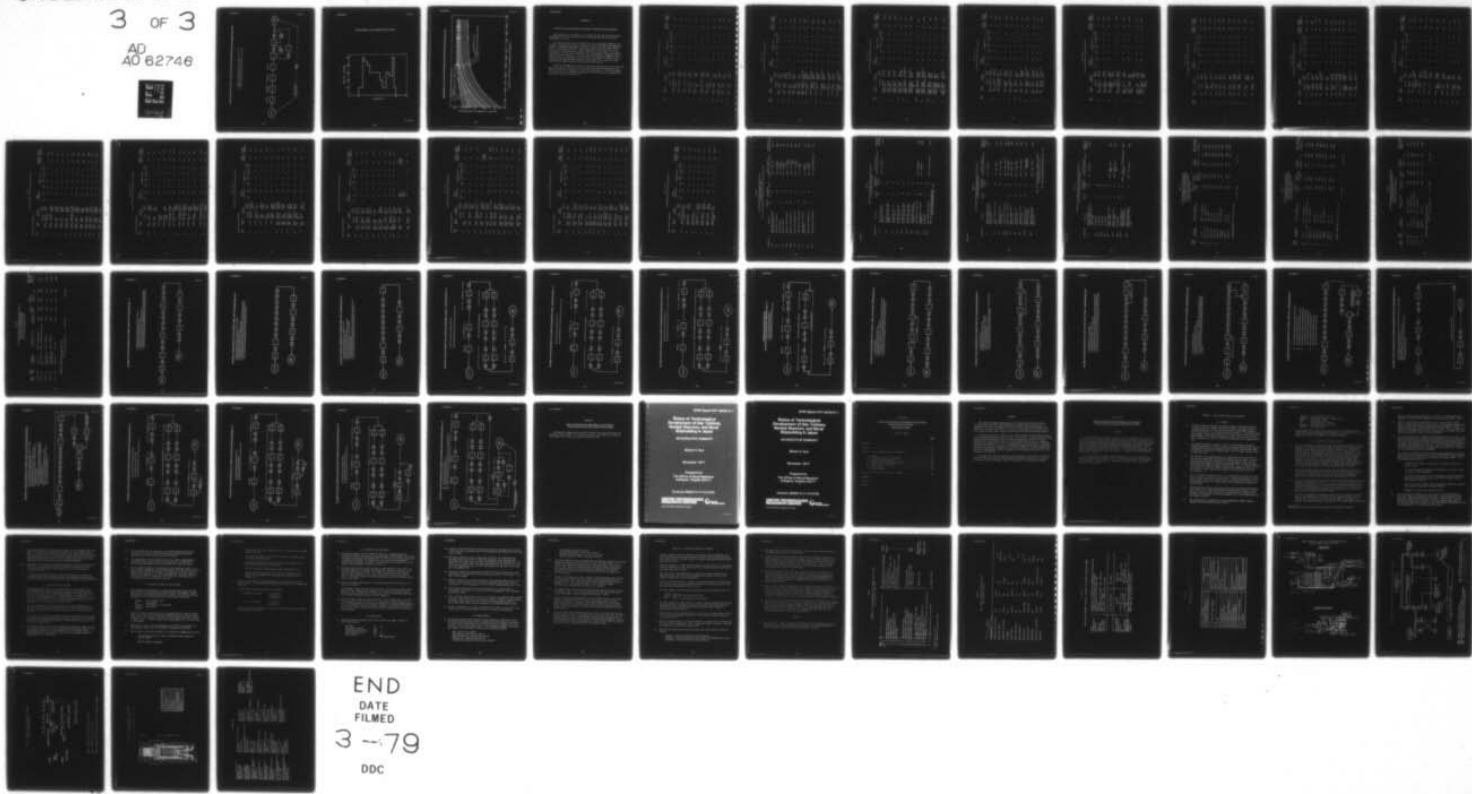
FIG. 5.13

AD-A062 746

UNITED TECHNOLOGIES RESEARCH CENTER EAST HARTFORD CONN F/G 13/10
LIGHTWEIGHT PROPULSION SYSTEMS FOR ADVANCED NAVAL SHIP APPLICAT--ETC(U)
NOV 78 S C KUO, T L HORTON, H SHU, C W DEANE N00014-77-C-0735
UNCLASSIFIED NL
UTRC/R78-952979-4

3 OF 3
AD 82746

REF FILE



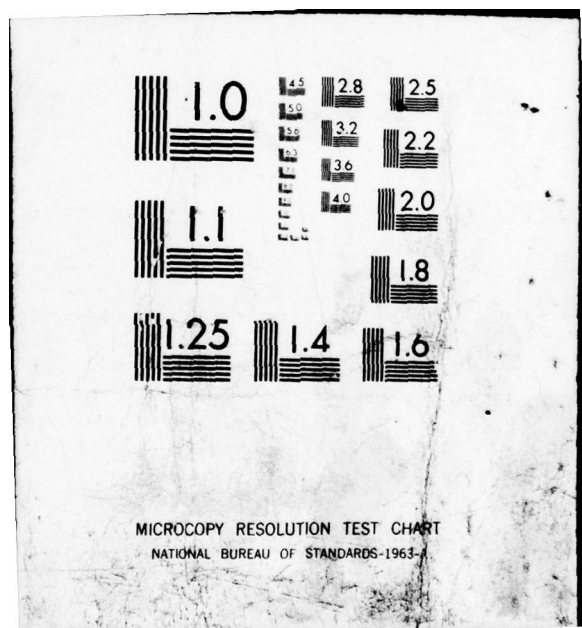
END

DATE

FILMED

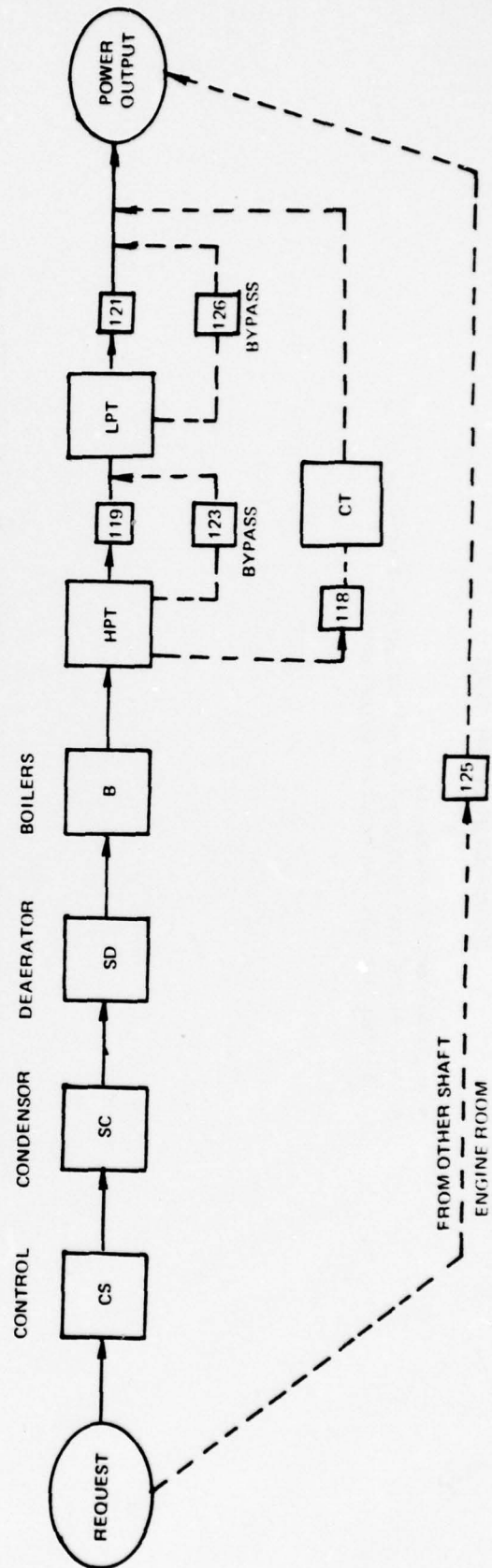
3 - 79

DDC

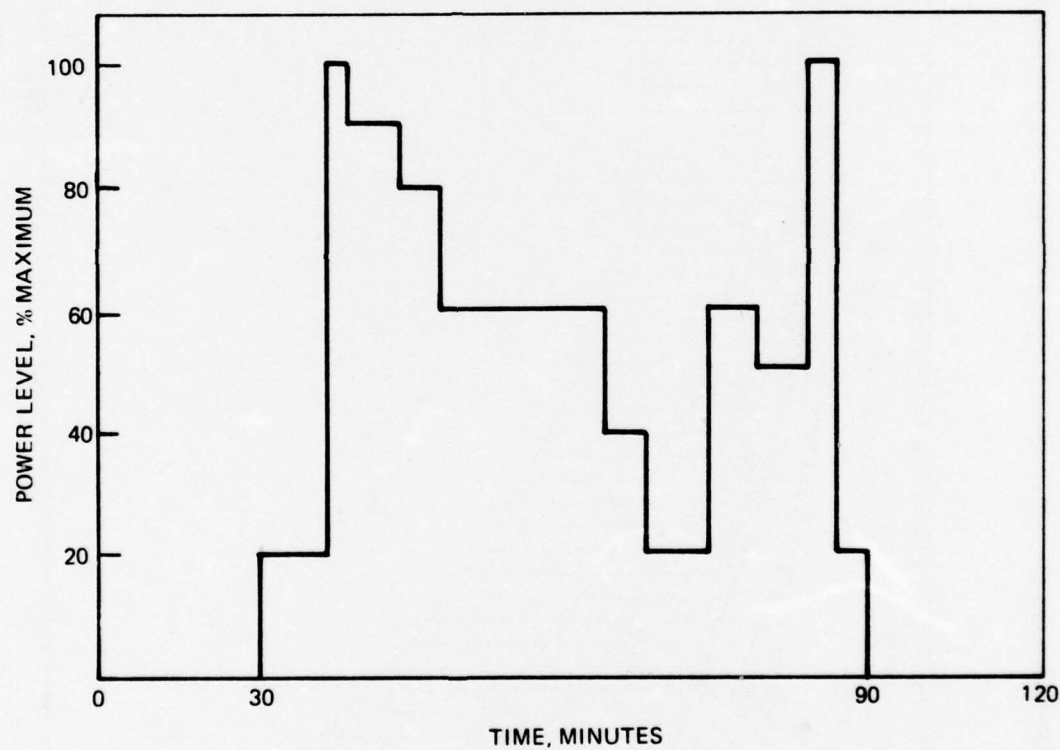


STEAM SYSTEM RELIABILITY BLOCK DIAGRAM FOR MAJOR REPAIR/REPLACEMENT PRACTICES

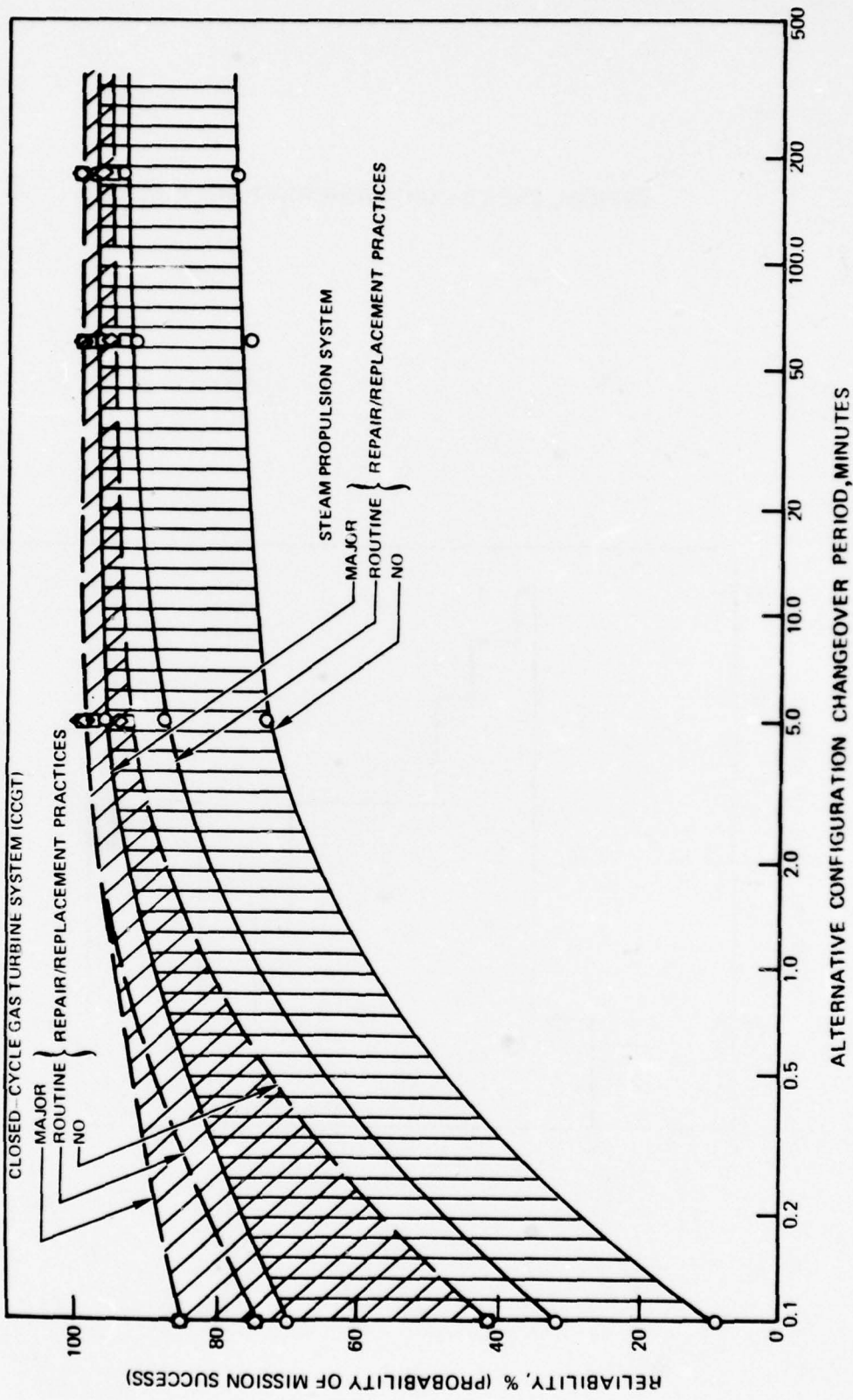
- LARGE BLOCKS REPRESENT GROUPS OF COMPONENTS WHICH ARE ASSUMED TO BE REPAIRABLE OR REPLACEABLE
- ALTERNATE CONFIGURATION PATHS SHOWN AS DASHED LINES



TYPICAL SHORT-HAUL AIRCRAFT DUTY-CYCLE



COMPARISON OF CCGT AND STEAM PROPULSION SYSTEM PROJECTED RELIABILITIES



APPENDIX A

RELIABILITY DATA ADJUSTMENT AND ALTERNATE CONFIGURATION CALCULATIONS

The purpose of this appendix is to present the detailed calculations and adjustments of failure rate data used in estimating the reliability values presented in the text.

The expected failure rates estimated for each of the major components are presented in Tables A-1 and A-2, respectively for the CCGT-LWSP and steam power systems. Adjustments were made to reference failure rate data taken from the sources indicated in Table 5.6. These adjustment factors considered in the following four potential power system differences or variations: (1) design differences; (2) duty cycle differences; (3) environmental differences; and (4) state-of-the-art differences. The mean time between failures (MTBF) for each component was then calculated from the failure rate ($MTBF = 1/\text{failure rate}$) for the purpose of identifying any component which would not be expected to last significantly longer than the mission duration (292 hours).

Tables A-3 through A-10 present the equations used and the results calculated for the estimated reliability of alternative operating configurations and the application of these configurations to mission performance. The block diagrams used to generate the reliability estimates for these alternative configurations are shown in Figs. A1 through A-18.

TABLE A-1
USSP COMPONENT FAILURE RATE ESTIMATION CALCULATION SHEET

Block #	Subsystem Name	Component Description	Reference Failure Rate, No./1000 hrs			Adjustment Factors			Estimated Failure Rate No./1000 hrs	Mean Time Between Failures, hrs
			Source	Rate	Design	Duty Cycle	Environment	State-of-Art		
1, 2	New design	actuators airborne	4	.137	0.5	0.8	1.1	1.2	.072	13889
3, 4	Control (Setting)	setting lever cable & converter								
5, 6	Control (Setting)	fuel signals pump valve	4	.194	0.5	0.8	1.1	1.1	.094	10638
7, 8	Control (Setting)	bypass valve signal	4	.254	0.5	0.8	1.1	1.2	.134	7463
9, 10	Control (Setting)	PI, throttle valve signal	4	.254	0.5	0.8	1.1	1.2	.134	7463
11, 12	Control (Setting)	tot. turb bypass valve signal	4	.254	0.5	0.8	1.1	1.2	.134	7463
13, 14	Control (Setting)	inventory control signals & energ. blow	4	.196	0.5	0.8	1.1	1.3	.054	18519
15, 16	Monitor Control	overtemp sensors	4	.130	0.5	1.0	1.2	1.0	.078	12821
17, 18	Monitor Control	overspeed sensors	4	.002	0.8	1.1	1.2	1.0	.002	500000
19, 20	Monitor Control	overpress sensors	1	.015	0.8	1.1	1.2	1.0	.016	62500
21, 22	Monitor Control	oil & fuel system sensors	4	.250	0.5	1.0	1.2	1.0	.015	66667

TABLE A-1 (Cont'd)
LWSP COMPONENT FAILURE RATE ESTIMATION CALCULATION SHEET

Block <i>#</i>	Subsystem Name	Component Description	Reference Failure Rate, No./1000 Hrs.			Adjustment Factors			Estimated Failure Rate No./1000 Hrs.	Mean Time Between Failures, Hrs.	
			New Design	Reference Design	Source	Rate	Design Environment	Duty Cycle	Environment		
23, 24	Monitor Control	vibration sensors	accelero-meters airborne	4	.229	0.5	1.1	1.2	1.0	.151	6623
25, 26	Monitor Control	control computer	computer components shipboard	4	.200	1.1	1.0	1.0	1.2	.264	3788
27, 28	Monitor Control	power supply	power supply destroyer	1	.177	1.0	1.0	1.0	1.0	.177	5650
29	Monitor Control	ducting	ducting general	1	.0	7.0	1.1	1.1	1.0	.001	100000
30	Monitor Control	shell side ht. exch.	boiler casing	1	.073	0.4	1.0	0.2	1.0	.006	166667
31	Monitor Control	bypass ducts & blank-offs	ducts and blank-off plates, general	6	.001	1.2	1.2	1.5	1.0	.002	500000
32, 33	Precooler	water pump 6 duct	centrifugal pump, destroyer	1	.057	1.0	1.0	1.0	1.0	.057	17544
34	precooler	switching system for water pumps	Ducts and blank-off plates, general	6	.001	1.2	1.2	1.5	1.0	.002	500000
35, 36	precooler	water valve & duct	control valve & manifolds airborne	4	.107	0.5	0.8	1.2	1.0	.051	19608
37	precooler	switching system for parallel valves	ducts and blank-off plates, general	6	.001	1.2	1.2	1.5	1.0	.002	500000
38	precooler	prime heat exch.	heat exchanger submarine	4	.003	0.8	1.1	1.2	1.0	.003	333333
39	precooler	secondary ht. exch. & duct	cooling coils submarine	1	.028	0.8	1.0	1.2	1.0	.027	37037
40	precooler	switching system for parallel valves	ducts and blank-off plates, general	6	.001	1.2	1.2	1.5	1.0	.002	500,000

TABLE A-1 (Cont'd)
LSSP COMPONENT FAILURE RATE ESTIMATION CALCULATION SHEET

Block <i>#</i>	Sub-system Name	Component Description	Reference Failure Rate, No./1000 Hrs.			Adjustment Factors			Estimated Failure Rate No./1000 Hrs.	Mean Time Between Failures, Hrs.
			Reference Design	Design	Source	Rate	Design	Duty Cycle		
41	Inventory low press. control valves & subsystem ducts	valve, comp bleed JTRD	3	.001		0.8	0.9	1.1	1.0	.001
42	Inventory med press. control valves & subsystem ducts	valve, comp bleed JTRD	3	.001		0.9	0.9	1.1	1.0	.001
43	Inventory high press. control valves & subsystem ducts	valve, comp bleed JTRD	3	.001		1.0	0.9	1.1	1.0	.001
44	Inventory low press. control storage tanks	tanks compressed gas airborne	4	.138		0.5	1.0	1.2	1.0	.083
45, 46	Inventory med press. control storage tanks	tanks compressed gas airborne	4	.138		0.6	1.0	1.2	1.0	.099
47	Inventory switching control system for subsystem parallel tanks	ducts and blank- off plates, general	6	.001		1.2	1.2	1.5	1.0	.002
48, 49	Inventory high press. control storage tanks	tanks com- pressed gas airborne	4	.138		0.7	1.0	1.2	1.0	.116
50	Inventory switching control system for subsystem parallel tanks	ducts and blank- off plates, general	6	.001		1.2	1.2	1.5	1.0	.002
51, 52	Inventory charging control compressor & ducts	compressor 200 psi destroyer	1	.235		1.2	0.5	1.0	1.1	.155
53	Inventory switching control system for subsystem parallel charging systems	ducts & blank-off plates general	6	.001		1.2	1.2	1.5	1.0	.002
54	Inventory emergency control valve & subsystem ducts	main boiler safety valve DIG	1	.005		0.8	1.0	1.0	1.0	.004

TABLE A-1 (Cont'd)
LWSP COMPONENT FAILURE RATE ESTIMATION CALCULATION SHEET

Block <i>#</i>	Subsystem Name	Component Description	Reference			Failure			Adjustment Factors			Estimated Failure Rate No./1000 Hrs	Mean Time Between Failures, Hrs	
			Reference Design	Source	Rate	Design	Cycle	Environment	Design	Cycle	Environment			
						New Design	Rate	Design	Cycle	Environment	Environment	State-of Art		
55	Low	low compressor compressor cases, JT8D	2	.006	0.8	0.6	1.1	1.1	.003	333,333				
56	Low	low compressor compressor stators, JT8D	2	.004	0.8	0.6	1.0	1.2	.002	500,000				
57	Low	low compressor bearings seal, seals oil supply JT8D	2	.008	1.0	0.6	1.0	1.2	.006	166,667				
58	Low	accessory Compressor gearbox & starter JT8D	2	.008	1.0	0.8	1.2	1.0	.008	125,000				
59	Low	low compressor rotors & shafts JT8D	2	.003	0.9	0.6	1.0	1.2	.002	500,000				
60, 61	Inter-cooler	water pump & duct DD service pump 60 psi	1	.038	1.1	1.0	1.0	1.0	.042	23810				
62, 64	Inter-cooler	water valve & duct	4	.107	1.0	0.8	1.0	1.0	.086	11628				
65	Inter-cooler	switching system for parallel valves	6 manifolds	.001	1.2	1.2	1.5	1.0	.002	500,000				
66	Inter-cooler	prime heat exch.	heat exchanger submarine	.003	0.8	1.1	1.2	1.0	.003	333,333				
67	Inter-cooler	secondary heat exch.	cooling coils subm line	.028	0.8	1.0	1.2	1.0	.027	37017				
68	Inter-cooler	intercooler bypass duct & switching	ducts and blank-off plates, general	.001	1.2	1.2	1.5	1.0	.002	500,000				

TABLE A-1 (Cont'd)
LSSP COMPONENT FAILURE RATE ESTIMATION CALCULATION SHEET

Block <i>#</i>	Subsystem Name	Component Description	Reference Failure Rate, No./1000 Hrs		Adjustment Factors		Estimated Failure Rate No./1000 Hrs	Mean Time Between Failures, Hrs
			Reference Design	Source Rate	Design	Cycle	Environment	State-of Art
69	High Compressor compressor cases	compressor cases JT8D	2	.006	0.8	0.6	1.1	1.1
70	High Compressor compressor stators	compressor stators JT8D	2	.004	0.8	0.6	1.0	1.2
71	High Compressor pressure bearings seals oil supply	compressor bearings seals oil supply JT8D	2	.010	1.0	0.6	1.0	1.2
72	High Compressor pressure rotors & shafts	compressor rotors & shafts JT8D	2	.003	0.9	0.6	1.0	1.2
73	Regener- ator from H.C. Cold Side	manifold submarine	1	.015	0.8	1.1	1.1	1.0
74	Regener- ator Cold Side	tube side heat exch.	5	0.100	0.5	0.5	0.4	1.0
75	Regener- ator Cold Side	super- heater steam boiler destroyer	1	.015	0.8	1.1	1.1	1.0
76	Regener- ator Hot Side	manifold submarine ducts & switching system & ducts to bypass regenerator	6	.001	1.2	1.2	1.5	1.0

TABLE A-1 (Cont'd)

LWSP COMPONENT FAILURE RATE ESTIMATION CALCULATION SHEET

Block #	Sub-system Name	Component Description	Reference Failure Rate, No./1000 Hrs		Adjustment Factor ₂	Hot Cycle Environment	State-of Art	Estimated Failure Rate No./1000 Hrs	Mean Time Between Failures, Hrs		
			Reference Design	Source	Rate _c	Design _c					
77	Heater	fuel pump JTRD	fuel pump JTRD	3	.001	1.0	0.6	1.1	1.0	.0007	1,428.571
78	Heater	fuel control valves & lines	fuel control JTRD	3	.001	1.0	0.6	1.1	1.0	.0007	1,428.571
79	Heater	backup fuel control & lines	fuel control JTRD	3	.001	1.0	0.6	1.1	1.0	.0007	1,428.571
80	Heater	combustor #1	combustor JTRD	2	.002	0.9	0.6	1.5	1.1	.0018	555.556
81	Heater	combustor #2	combustor JTRD	2	.002	0.9	0.6	1.5	1.1	.0018	555.556
82	Heater	combustor #3	combustor JTRD	2	.002	0.9	0.6	1.5	1.1	.0018	555.556
83	Heater	combustor #4	combustor JTRD	2	.002	0.9	0.6	1.5	1.1	.0018	555.556
84	Heater	heat exch. & mixer	superheater destroyer boiler	5	0.100	1.1	0.8	0.9	1.3	0.103	9,709
85	Heater	preheater hot side	superheater, destroyer	5	0.100	0.4	0.6	0.9	1.0	.022	45.454
86	Heater	bypass system	ducts & blank-off plates general	6	.001	1.2	1.2	1.5	1.0	.002	500,000
87	Heater	turbine & bearings	turbine JTRD	2	.110	0.7	0.6	1.5	1.0	.069	14493

TABLE A-1 (Cont'd)
LMSP COMPONENT FAILURE RATE ESTIMATION CALCULATION SHEET

Block <i>#</i>	Sub-system Name	Component Description	Reference Failure Rate, No./1000 Hrs			Adjustment Factors			Estimated Failure Rate No./1000 Hrs	Mean Time Between Failures, hrs		
			New Design	Source	Rate	Rev. Len.	Envir.	State-of-Art				
88	Heater	control & fuel subsystem	fuel & control JTBD	3	.010	1.0	0.6	1.1	1.2	.008		
89	Heater	compressor & bearings	compressor JTBD	2	.070	0.9	0.7	1.2	1.0	.053		
90	Heater	preheater cold side	heat exch. airborne	4	.001	0.7	0.7	1.6	1.0	.0008		
91	Heater	switching & bypass ducts	ducts and blank-off plates, general	6	.001	1.2	1.2	1.5	1.0	.002		
92	Turbine	duct from heater	ducts general	6	.001	1.2	1.2	1.5	1.0	.0002		
93	Turbine	CDT cases & supports	high turbine cases JTBD	2	.003	0.8	0.6	1.2	1.1	.0019		
94	Turbine	CDT stators	high turbine stators JTBD	2	.025	0.6	0.6	0.8	1.2	.0086		
95	Turbine	CDT rotors	high turbine rotors JTBD	2	.007	0.7	0.6	0.8	1.2	.0028		
96	Turbine	CDT oil system, bearings seals	high turbine oil system, etc JTBD	2	.010	0.9	0.6	1.0	1.2	.0065		
97	Turbine	bypass control valve	control valves airborne	4	.107	0.5	1.0	1.1	1.0	.060		
98	Turbine	backup bypass valve	control valves airborne	4	.107	0.5	1.0	1.1	1.0	.060		

TABLE A-1 (Cont'd)
LWSP COMPONENT FAILURE RATE ESTIMATION CALCULATION SHEET

Block <u>#</u>	Subsystem <u>Name</u>	Component <u>Description</u>	Reference Failure Rate, No/1000 Hrs				Adjustment Factors			Estim. ed Failure Rate No/1000 Hrs	Mean Time Between Failure, Hrs		
			Reference Design		Source	Rate	Design	Duty Cycle	Environment				
			New Design	Ref. Design									
99	Turbine	bypass duct from CDT	ducts general	6	.001	.001	1.2	1.2	1.5	1.0	.002	500,000	
100	Turbine	alternate control valve switching & ducting	ducts & blank-off plates general	6	.002	.002	1.2	1.2	1.5	1.0	.004	250,000	
101	Turbine	PT case & supports	low turbine case & supports JT8D	2	.003	.003	0.8	0.6	1.2	1.1	.0019	526316	
102	Turbine	PT stators	low turbine case & supports JT8D	2	.013	.013	0.6	0.6	0.8	1.2	.0045	222,222	
103	Turbine	PT rotors	low turbine rotors JT8D	2	.003	.003	0.7	0.6	0.8	1.2	.0012	833,333	
104	Turbine	PT oil system, bearings seals	low turbine oil system, etc JT8D	2	.010	.010	0.9	0.6	1.0	1.2	.0065	153,846	
105	Turbine	PT exh. duct	low turbine exh. case JT8D	2	.005	.005	0.8	0.6	1.2	1.1	.0032	312500	
106	Turbine	PT throttle valve	control valve airborne	4	.107	.107	0.5	1.1	1.1	1.0	.065	15385	
107	Turbine	backup control valve duct	ducts general	6	.001	.001	1.2	1.2	1.5	1.0	.002	500,000	
108	Turbine	backup control valve	control valve airborne	4	.107	.107	0.5	1.0	1.1	1.0	.059	16,949	

TABLE A-2
STEAM SYSTEM COMPONENT FAILURE RATE ESTIMATION CALCULATION SHEET

Normal Configuration (Undegraded)

Block #	Subsystem Name	Component Description	Reference Failure Rate, No./1000 Hrs		Adjustment Factors		Estimated Failure Rate No./1000 Hrs	Mean Time Between Failures, Hrs			
			New Design	Source	Design	Duty Cycle					
1, 2	Control (Setting)	lever cable & converter	setting actuators airborne	4	.137	0.5	0.8	1.1	1.2	.072	13889
3, 4	Control (Setting)	pump valve	fuel signals transducer fluid flow airborne	4	.194	0.5	0.8	1.1	1.1	.094	10638
5, 6	Control (Setting)	valve signal	valve motionals airborne	4	.254	0.5	0.8	1.1	1.2	.134	7463
7, 8	Control (Setting)	valve signal	transducer motionals airborne	4	.254	0.5	0.8	1.1	1.2	.134	7463
9, 10	Control (Setting)	valve signal	transducer motionals airborne	4	.254	0.5	0.8	1.1	1.2	.134	7463
11, 12	Control (Setting)	water cooling valve signals	transducer fluid flow airborne	4	.194	0.5	0.8	1.1	1.1	.094	10638
13, 14	Control (Setting)	control signals	transducer pressure airborne	4	.094	0.5	0.8	1.1	1.3	.054	18519
15, 16	Monitor Control	overtemp sensors	thermo-couples airborne	4	.130	0.5	1.0	1.2	1.0	.078	12821
17, 18	Monitor Control	overspeed sensors	tachometer submarine	4	.002	0.8	1.1	1.2	1.0	.002	500000
19, 20	Monitor Control	overpress sensors	press switch submarine	1	.015	0.8	1.1	1.2	1.0	.016	62500
21, 22	Monitor Control	oil & fuel system sensors	switches & transducers airborne	4	.250	0.5	1.0	1.2	1.0	.015	66667
23, 24	Monitor Control	vibration sensor	accelerometers airborne	1	1	1	1	1	1	1	1

TABLE A-2 (Cont'd)
STEAM SYSTEM COMPONENT FAILURE RATE ESTIMATION CALCULATION SHEET

Normal Configuration (Undegraded)								Reference Design	Failure Rate, No/1000 hrs	Duty Cycle	Environment	State-of Art	Mean Time Between Failures, Hrs
Block #	Subsystem Name	Component Description	Source	Rate	Design	Adjustment Factors							
	New Design												
25, 26	Monitor Controls	control computer	computer components shipboard	4	.200	1.1	1.0	1.0	1.0	1.0	.264	.177	5650
27, 28	Monitor Controls	power supply	power supply destroyer	1	.177	1.0	1.0	1.0	1.0	1.0	.264	.3788	
29	Condenser	condenser heat exchanger		1	0.270	1.0	1.0	1.0	1.0	1.0	0.9	0.243	4115
30	Condenser	ducting ducting general		6	.002	1.2	1.0	1.5	1.0	1.0		.0036	277,778
31	Condenser	water cooling supply lines	manifold, submarine	1	.014	0.8	1.0	1.2	1.0	1.0		.0134	74,627
32	Condenser	water cooling pump	pump, condenser centrifugal destroyer	1	.039	1.0	1.0	1.0	1.0	1.0	0.9	.0351	28,490
33	Condenser	water cooling heat exchanger	cooling coil, in hull	1	.028	0.8	1.0	1.2	1.0	1.0		.027	37037
34	Condenser	main condensate feed pump	pump, main condensate, destroyer	1	0.128	1.0	1.0	1.0	1.0	1.0	0.9	.1251	7994
35	Condenser	water supply lines	manifold, water, submarine	1	0.014	0.8	1.0	1.2	1.0	1.0		.0134	74627
36	Condenser	feed pump	turbine, main condenser pump, destroyer	1	0.059	1.0	1.0	1.0	1.0	1.0	0.9	.0531	18832
37	Condenser	ducts & valves, ducts and co/from turbine valves, general		6	.002	1.5	1.0	1.5	1.0	1.0		.004	250,000
38	Ejector	air ejector	air ejector destroyer	1	.147	1.0	1.0	1.0	1.0	1.0	0.9	0.132	7576

TABLE A-2 (Cont'd)
STEAM SYSTEM COMPONENT FAILURE RATE ESTIMATION CALCULATION SHEET

Normal Configuration (Undegraded)				Reference Failure Rate, No/1000 Hrs				Adjustment Factors			Estimated Failure Rate No/1000 Hrs		Mean Time Between Failures, Hrs
Block #	Subsystem Name	Component Description		Reference Design	Source	Rate	Design	Duty Cycle	Environment	State-of-Art			
		New Design	Old Design										
39	Ejector	gland exhaust condenser	condenser distillation destroyer	1	0.250	1.2	0.8	1.0	0.9	.0216	4630		
40	Ejector	ducts, valves to/from ejector	ducts general	6	.002	1.0	1.0	1.5	1.0	.001	333,333		
41	Ejector	gland condenser pump	pump, main condenser destroyer	1	0.119	1.0	1.0	1.0	0.9	.125	8000		
42	Ejector	ducts to/from deaerator	ducts general	6	.002	1.0	1.0	1.5	1.0	.003	333,333		
43	Ejector	deaerating feedwater heater	deaerating feedwater heater, destroyer	1	0.192	1.0	1.0	1.0	0.9	.0173	5780		
44, 45	Boiler Feed Pumps	main boiler booster feed pump	pump, main feed booster, destroyer	1	0.282	1.0	1.0	1.0	0.9	.265	3774		
46, 47	Boiler Feed Pumps	lines to/from feed pump	manifold submarine	1	0.014	0.8	1.0	1.2	1.0	.013	76,923		
48, 49	Boiler Feed Pumps	main feed booster pump drive turbine	turbine main feed booster pump drive	1	0.056	1.0	1.0	1.0	0.9	.050	20,000		
50, 51	Boiler Feed Pumps	lines & ducts to/from main feed pump	manifold submarine	1	0.014	0.8	1.0	1.2	1.0	.013	76,923		
52, 53	Boiler Feed Pumps	main feed valve	steam control valve, destroyer	1	.010	1.0	1.0	1.0	0.9	.009	111,111		

STEAM SYSTEM COMPONENT FAILURE RATE ESTIMATION CALCULATION SHEET

Normal Configuration (Undegraded)

Block #	Subsystem Name	Component Description	Reference Failure Rate, No./1000 Hrs			Adjustment Factors			Estimated Failure Rate No./1000 Hrs	Mean Time Between Failures, Hrs
			Reference Design	Source	Rate	Design Duty Cycle	Environment State-of Art			
54, 55	Boiler Feed Pumps, etc	main boiler feed pump	Design	1	0.303	1.0	1.0	1.0	.273	3663
56, 57	Boiler Feed Pumps, etc	feed pump lines & valves	Design	6	.003	1.0	1.0	1.5	1.0	222,222
58, 59	Boiler Feed Pumps, etc	main feed pump drive	Design	1	0.040	1.0	1.0	1.0	0.9	.036
60, 61	Boiler Feed Pumps, etc	turbine drive	Design	6	.001	1.5	1.0	1.5	1.0	.002
62, 63	Boiler Feed Pumps, etc	turbine valves, steam control	Design	1	.010	1.0	1.0	1.0	0.9	.009
64, 65	Boiler Feed Pumps, etc	water check valve	Design	4	.002	1.0	1.0	1.5	0.9	.003
66, 67	Boiler Feed Pumps, etc	feed water lines & ducts	Design	6	.001	1.0	1.0	1.5	0.9	1,000,000
68, 69	Boiler Fuel Supply System	fuel supply valves	Design	1	.028	0.8	1.0	1.5	0.9	.030
70, 71	Boiler System	economiser included in boiler heat exch.	Design	1	10000-2500	-	-	-	-	included in boiler heat exch.
72, 73	Boiler System	main heat exchanger	Design	1	0.400	1.0	1.0	1.0	0.9	2,778

TABLE A-2 (Cont'd)
STEAM COMPONENT FAILURE RATE ESTIMATION CALCULATION SHEET

Normal Configuration (Undegraded)

Block <u>#</u>	Subsystem Name	Component Description	Reference Failure Rate, No./1000 Hrs			Adjustment Factors			Estimated Failure Rate No./1000 Hrs	Mean Time Between Failures, Hrs
			Reference Design	Source	Rate	Duty Cycle	Environment	State-of Art		
New Design										
74, 75	Boiler System	air blower	boiler soot blower, destroyer	1	.019	1.2	1.5	1.0	.9	.031
76, 77	Boiler System	blower drive turbine	turbine, accessory steam destroyer	1	0.048	1.0	1.0	0.9	.043	23,256
78, 79	Boiler System	blower drive turbine ducts & valves	ducts & valves General	1, 6	.002	1.0	1.0	1.5	1.0	.003
80, 81	Boiler System	superheater	included in boiler heat exchanger		NA	NA	NA	NA	NA	Included in boiler heat exch.
82, 83	Boiler System	steam drum	steam drum destroyer		.005	1.0	1.0	1.0	1.0	0.005
84, 85	Boiler System	ducts from superheater	ducts, general	6	.001	1.5	1.0	1.5	1.0	.002
86, 87	Boiler System	valve, main steam stop	unloading valve, destroyer	1	0.008	1.0	1.0	1.0	0.9	.007
88, 89	Auxiliary Steam System	valve, aux. steam control	steam supply regulator destroyer	1	0.014	1.0	1.0	1.0	0.9	.013
90, 91	Auxiliary Steam System	fuel-oil heater	lube-oil cooler destroyer	1	0.011	1.2	1.2	1.0	0.9	.014
92, 93	Auxiliary Steam System	fuel-oil service pump	pump, fuel feed, aircraft carrier	1	0.358	1.0	1.2	1.0	0.9	.387
94, 95	Auxiliary Steam System	turbine, fuel oil pump drive	turbine, fuel-oil drive	1	0.057	1.0	1.0	1.0	0.9	.051

STEAM SYSTEM COMPONENT FAILURE RATE ESTIMATION CALCULATION SHEET

Normal Configuration (Undegraded)

Block <u>#</u>	Subsystem Name	Component Description	Reference Failure Rate, No./1000 Hrs.		Adjustment Factors		Estimated Failure Rate No./1000 Hrs.	Mean Time Between Failures, Hrs.			
			Reference Design	Source	Rate	Beskin Duty Cycle	Environment	State-of Art			
96, 97	Auxiliary ducts to/ Steam System	ducts from fuel-oil pump drive turbine	general	6	.001	1.0	1.0	1.5	1.0	.0015	666,667
98, 99	Auxiliary Steam System	main lube oil pump	pump, main lube oil, destroyer	1	0.132	1.0	1.0	1.0	0.9	.119	8,403
100, 101	Auxiliary Steam System	turbine, main lube pump drive	turbine fuel-oil feed destroyer	1	0.057	0.8	1.0	1.0	0.9	.041	24,390
102, 103	Auxiliary Steam System	air ejector,	air ejector, destroyer	1	0.147	1.0	1.0	1.0	0.9	.0132	7,576
104, 105	Auxiliary Steam System	air ejector ducts	general	6	.001	1.0	1.0	1.5	0.9	.001	1,000,000
106, 107	Auxiliary Steam System	ducts, aux. steam exhaust	general	6	.001	1.5	1.0	1.5	1.0	.002	500,000
108, 109	Auxiliary Steam System	ducts, aux. steam unloading	valve destroyer	1	.008	1.0	1.0	1.0	0.9	.007	142,857
110, 111	Auxiliary Steam System	valves & ducts accessory power bleed	valves & ducts general	1, 6	.010	1.2	1.0	1.2	0.9	.013	76,973
112	Propulsion main steam Turbines	strainer, distiller, strainer	strainer, distiller, submarine	1	0.004	2.0	1.5	1.5	0.9	.016	62,500
113	Propulsion ducts, to/ Turbines	from steam strainer	ducts general	6	0.001	1.2	1.0	1.5	1.0	.002	500,000
114	Propulsion guarding Turbines	steam supply regulator, destroyer	steam supply regulator, destroyer	1	0.014	1.0	1.0	1.0	0.9	.213	76,923
115	Propulsion cross-over Turbines	casings, main steam, valves	casings, main steam, valves destroyer	1	0.074	0.5	1.0	1.0	1.0	.037	27,027

TABLE A-2 (Cont'd)
STEAM COMPONENT FAILURE RATE ESTIMATION CALCULATION SHEET

Normal Configuration (Undegraded)

Block #	Subsystem Name	Component Description	Reference Failure Rate, No/1000 Hrs		Adjustment Factors		Estimated Failure Rate No/1000 Hrs	Mean Time Between Failures, Hrs
			Reference Design	Source	Design Rate	Duty Cycle	Environment	State-of-Art
116, 117	Propulsion turbines	valves & ducts, cruise turbine control	1, 6	0.010	1.5	1.0	1.2	1.0
118	Propulsion turbines	turbine, electric gen. drive	7	0.070	1.0	1.2	0.9	.091
119	Propulsion turbine, turbines	high pressure	1	0.20	1.0	1.0	0.9	.018
120	Propulsion duct to turbines	casing, main steam, destroyer	1	0.074	0.3	1.0	1.0	.022
121	Propulsion turbine, turbines	low pressure	1	0.200	1.0	1.0	0.9	.018
122	Propulsion duct from turbines	turbine, low pressure, main stream, destroyer	1	0.074	0.3	1.0	1.0	.022
123	Propulsion bypass system, turbines	ducts, high press. turbine	6	.001	1.5	1.0	1.5	.002

TABLE A-3

LWSP ALTERNATE CONFIGURATION RELIABILITY EQUATIONS SET 2

. NO REPAIR/REPLACEMENT ALLOWED

$$* \text{Note } R_O = (R_{CS}) (R_{RH}) (R_{PC}) (R_{IV}) (R_{LC}) (R_{IC}) (R_{RC}) (R_H) (R_{CD}) (R_{PT})$$

Configuration #	Description	Changover Time	Maximum Power Attainable / Installed	Reliability Equation (Probability of Config. Operation)	Probability of Operation Reliability
IIIA-1	Basic power system with routine repair/replacement practices	0	100	$R_{IIIA-1} = (R_{IIIA}) (R_O) =$.41781
IV-1	Heater capacity reduced 20%	5	100	$R_{IV-1} = (R_{IV}) \left \frac{R_O}{R_H} \right =$.06030
V-1	Precooler bypassed	60	60	$R_{V-1} = (R_V) \left \frac{R_O}{R_{PC}} \right =$.01624
VI-1	Intercooler bypassed	60	60	$R_{VI-1} = R_{VI} \left \frac{R_O}{R_{IC}} \right =$.01634
VIIA-1	Regenerator cold-side bypassed	180	60	$R_{VIIA-1} = R_{VIIA} \left \frac{R_O}{R_{RC}} \right =$.02150
VIB-1	Regenerator totally bypassed	180	60	$R_{VIB-1} = R_{VIB} \left \frac{R_O}{R_{RH}} \right =$.00210
VIII-1	Heater capacity degraded by 40%	5	60	$R_{VIII-1} = R_{VIII} \left \frac{R_O}{R_H} \right =$.06190
IX-1	Cross-connection of heater rooms	180	40	$R_{IX-1} = R_{IX} \left \frac{R_O}{R_H} \right =$.05874
X-1	Cross-connection of compressor turbomachinery	180	40	$R_{X-1} = R_X \left \frac{R_O}{R_{CD}} \right =$.11291
XI-1	Heater capacity degraded by 60%	5	40	$R_{XI-1} = R_{XI} \left \frac{R_O}{R_H} \right =$.06354
XII-1	Single propeller shaft operation	5	40	$R_{XII-1} = \left R_{IIIA-1} \right \left 1 - R_{IIIA-1} \right =$.24324

TABLE A-4
LMSP ALTERNATE CONFIGURATION RELIABILITY EQUATIONS SET #3
• MAJOR ON-BOARD REPAIR ALLOWED

Configuration #	Description	Changeover Time	Maximum Power Attainable % Installed	Reliability Equation (Probability of Config. Operation Reliability Ri)	Probability of Operation Reliability
IIIIC	Basic power system with routine repair/replacement practices	0	100	$RIIIIC-2 = (RIIIA/RXH) X$.85019
IV-2	Not applicable since heater is assumed maintained at 100% capacity	5	100		
V-2	Not applicable since PC is totally maintained	60	60		
VI-2	Not applicable since heater is totally maintained	60	60		
VIIA-2	Not applicable since recuperator is totally maintained	180	60		
VIIIB-2	Not applicable since recuperator is totally maintained	180	60		
VII-2	Not applicable since heater is maintained at 100% capacity	5	60		
IX-2	Cross-connection of heater rooms	180	40	$RIX-2 = (RIX)/(RXH) =$.10362
X-2	Cross-connection of compressor turbomachinery	180	40	$RX-2 = (RX)/(RXH) =$.22586
XI-2	Not applicable	5	40		
XII-2	Single propeller shaft operation	5	40	$RXII-2 = (RIIIC) [1-(RIIC)] =$.12737

NOTE: $RXH = (R30)(R31)(R38)(R39)(R40)(R66)(R67)X$
 $(R68)(R74)(R76)(R85)(R90)(R91)(R100) = .87201$

TABLE A-5
STEAM POWER SYSTEM ALTERNATE CONFIGURATION RELIABILITY EQUATIONS SET 3
• NO REPAIR/REPLACEMENT PRACTICES

Configuration #	Description	Changeover Time	Maximum Power Attainable % Installed	Reliability Equation (Probability of Contig. Operation) Ri	Probability of Operation Reliability
A-i	Baseline configuration, all subsystems capable of installed capacity, liberal at sea repair allowed	0	100	$RA-i = (RA) (RSO)^* =$.09397
A1-i	One boiler inoperative on single shaft	60	100	$RI-i = (RAI) (RSI)^* =$.01117
AII-i	Condenser capacity reduced 20% (blockage, etc.)	5	100	$RAII-i = (RAII) (RSO)^* =$.02337
AIII-i	Condenser capacity reduced 40%	5	60	$RAIII-i = (RAIII) (RSO)^* =$.02457
AIV-i	Condenser capacity reduced 60%	5	40	$RAIV-i = (RAIV) (RSO)^* =$.02608
AV-i	Bypass of inoperative high pressure turbine	60	60	$RAV-i = (RAV) (RSO)^* =$.01851
AVI-i	Bypass of inoperative low pressure turbine	60	60	$RAVI-i = (RAVI) (RSO)^* =$.01854
AVII-i	Cross-connection with other shaft boiler room	180	45	$RAVII-i = (RAVII) (RSO)^* =$.01508
AVIII-i	Bypass of both high & low pressure turbines only cause turbine operating	180	30	$RAVIII-i = \frac{(RAVIII) (RSO)^*}{(RHPT) (RLPT)} =$.0416
AIX-i	Single propeller operation limited to speeds of 20 knots or less	5	20	$RAIX-i = (RA-i) (1-RA-i) *$.08514

*NOTE: $RSO = (RCSS)(RSC)(RSR) [1 - (1-RBFA)^2] [1 - (1-RB)^2] \times$

$$[1 - (1-RAS)^2] (RHPT) (RLPT) = .29765$$

$$RSI = (RCSS) (RSC) (RSR) (RBEP) (RB) (RAS) (RHPT) (RLPT) = .12371$$

TABLE A-6

STEAM POWER SYSTEM ALTERNATE CONFIGURATION RELIABILITY EQUATIONS SET 3
 • MAJOR REPAIR/REPLACEMENT PRACTICES ALLOWED

Configuration #	Description	Changeover Time	Maximum Power Attainable % Installed	Reliability Equation (Probability of Config. Operation) R_i	Probability of Operation Reliability
A-2	Baseline configuration, all subsystems capable of installed capacity, liberal at sea repair allowed	0	100	$RA-2 = (R119)(R121) =$.69773
AI-2	Not applicable	60	100		
AI1-2	Not applicable	5	100		
AI11-2	Not applicable	5	60		
AI4-2	Not applicable	5	40		
AV-2	Bypass of inoperative high pressure turbine	60	60	$RAV-2 = \frac{(RA-2)(1-R119)}{(R119)} =$.13757
AVI-2	Bypass of inoperative low pressure turbine	60	60	$RAVI-2 = \frac{(RA-2)(1-R121)}{(R121)} =$.13757
AVII-2	Not applicable	180	45		
AVIII-2	Bypass of both high & low pressure turbines only cruise turbine operating	180	30	$RAVIII-2 = \frac{RA-2}{(R121)(R119)} \left \frac{1-(R119)(R121)}{(R121)(R119)} \right (R118) = .27600$	
AIX-2	Single propeller operation limited to speeds of 20 knots or less	5	20	$RAIX-2 = (RA-2)(1-RA-2) =$.21090

TABLE A-7

LWSP MISSION RELIABILITY CALCULATION SHEET #2
 • ONLY CONFIGURATIONS ALLOWED WHICH MIGHT
 REQUIRE 5 MINUTES OR LESS FOR CONVERSION
 • ROUTINE REPAIR/REPLACEMENT PRACTICES
 • HI-SPEED DESTROYER MISSION

Power Level % Max	Allowable Configurations	Reliability Equation Qi = 1-Ri = Unreliability	Reliability at Power Level Rp	Time at Power Level		MTBF at Constant Power Level Setting $\frac{1}{\lambda_p t_p}$ 1000's hrs
				Effective Failure Rate, λ_p per 1000 hrs	t_p 1000's hrs	
100	IIIA, IV	R100% = 1-(Q111A)(Q1V) =	.7654	.2674	.006	.0016
55	IIIA, IV, VIII	R55% = 1-(Q100Z)(QVIII) =	.7877	.23864	.011	.00262
38	IIIA, IV, VIII	R38% = 1-(Q55%) =	.7877	.23864	.017	.00406
26	Same as 38%	R26% = R38% =	.7877	.23864	.017	.00406
16	Same as 38%	R16% = R26% =	.7877	.23864	.017	.00406
10	Same as 38%	R10% = R16% =	.7877	.23864	.011	.00262
7	All above plus XII	R7% = 1-(Q38%)(Q38%) =	.9549	.04615	.006	.00028
4	Same as 7%	R4% = R7% =	.9549	.04615	.006	.00028
3	Same as 7%	R3% = R4% =	.9549	.04615	.009	.00042

MISSION AS STATED ABOVE R = $e^{-\lambda_m t}$ where $\lambda_m = \sum \lambda_p t_p$

$$R = e^{-\sum \lambda_p t_p} = .9802$$

$$\sum \lambda_p t_p = .02$$

TABLE A-8

LWSP MISSION RELIABILITY CALCULATION SHEET #3
 • ONLY CONFIGURATIONS ALLOWED WHICH MIGHT
 REQUIRE 60 MINUTES OR LESS FOR CONVERSION
 • ROUTINE REPAIR/REPLACEMENT PRACTICES
 • 11-SPEED DESTROYER MISSION

Power Level % Max	Allowable Configurations	Reliability Equation Q1 - 1-Ri = Unreliability	MTBF at Constant Power Level Setting $\frac{1}{\lambda_p} 1000's \text{ hrs}$		
			Reliability at Power Level R_p	Effective Failure Rate, $\lambda_p \text{ per } 1000 \text{ hrs}$	Time at Power Level t_p $1000's \text{ hrs}$
100	IIIA, IV	$R100\% = 1 - (Q1 IIIA) (QIV) =$.7654	.2674	.006
55	IIIA, IV, V, VI, VII	$R55\% = 1 - (Q1 100\%) (QV) (QVI) (QVII) =$.7994	.22389	.011
38	IIIA, IV, V, VI, VIII, XI	$R38\% = 1 - (Q55\%) (QXI) =$.81901	.19966	.017
26	Same as 38%	$R26\% = R38\% =$.81901	.19966	.017
16	Same as 38%	$R16\% = R26\% =$.81901	.19966	.017
10	Same as 38%	$R10\% = R16\% =$.81901	.19966	.011
7	All above plus XII	$R7\% = 1 - (Q38\%) (Q38\%) =$.96724	.03331	.006
4	Same as 7%	$R4\% = R7\% =$.96724	.03331	.006
3	Same as 7%	$R3\% = R4\% =$.96724	.03331	.009

MISSION AS STATED ABOVE $R = e^{-\lambda_m t}$, where $\lambda_m = \sum \lambda_p t_p$

$$R = e^{-\sum \lambda_p t_p} = .9830$$

$$\sum \lambda_p t_p = .01713$$

TABLE A-9

STEAM POWER SYSTEM MISSION RELIABILITY CALCULATION SHEET #2
 • ONLY CONFIGURATION CONVERSIONS ALLOWED WHICH
 • MIGHT TAKE 5.0 MINUTES OR LESS
 • ROUTINE REPAIR/REPLACEMENT PRACTICES

Speed Knots	Power Level % Max	Allowable Configurations	Reliability Equations		Reliability at Power Level	Effective Failure Rate	Time at Power Level		MTBF at Constant Power Level $MTBF = \frac{1}{\lambda_p}$
			$Q = 1 - R_1$	$Q = 1 - R_1$			t_p	1000's hrs	
35 + 30	100	A, AII	$R100\% = 1 - (Q_A)(Q_{AII}) =$.36942	.99582	.0028	.00279	1.0042
30 + 25	58	A, AII, AIII	$R58\% = 1 - (Q_A)(Q_{II})(Q_{AIII}) =$.23037	1.46807	.0066	.00969	.68117
25 + 20	30	A, AII, AIII, AIV	$R30\% = 1 - (Q58\%)(Q_{V1})(Q_{V1})(Q_{V1}) =$.37491	.98107	.0530	.0520	1.0193
20 + 15	14	A, AII, AIII, AIV, AIX	$R14\% = 1 - (Q30\%)(Q_{IX}) =$.50995	.67344	.0640	.0431	1.48491
15 + 0	20	Same as 14%	$R2\% = R14\% =$.50995	.67344	.0736	.04957	1.48491

MISSION AS STATED ABOVE R_m = Mission Reliability

$$R_m = e^{-\lambda_m t}$$

$$\lambda_m = \sum \lambda_{ptp} = \text{Mission Failure Rate}$$

$$\sum \lambda_{ptp} = 1.5715$$

$$R = e^{-\sum \lambda_{ptp}} = .85458$$

TABLE A-10

STEAM POWER SYSTEM MISSION RELIABILITY CALCULATION SHEET #3

- ONLY CONFIGURATION ALLOWED WHICH MIGHT TAKE 60 MINUTES OR LESS FOR CONVERSION
- ROUTINE REPAIR/REPLACEMENT PRACTICES

Speed Knots	Power Level % Max	Allowable Configuration	Reliability Equations $Q_1 = 1 - R_1$	MTBF at Constant Power Level 1000's hrs		
				Reliability at Power Level	Effective Failure Rate	Time at Power Level 1000's hrs
35 + 30	100	A, AI, AII	R100% = 1 - (Q _A)(Q _{AII}) =	.42636	.85247	.00239
30 + 25	58	A, AI, AII, AIII, AV	R58% = 1 - (Q _A)(Q _{AII})(Q _{AIII})(Q _V) =	.50427	.68464	.0066
25 + 20	30	A, AI, AII, AIII, AIV, AV, AVI	R30% = 1 - (Q58%)(Q _{V1}) =	.57589	.55184	.053
20 + 15	14	A, AI, AII, AIII, AIV, AV, AVI, AVX	R14% = 1 - (Q30%)(Q _{IX}) =	.66751	.4042	.064
15 + 0	2.0	Same as 14%	R2% = R15% =	.66751	.40420	.0736
						.02975

MISSION AS STATED ABOVE R_m = Mission Reliability

$$R_m = e^{-\lambda_m t}$$

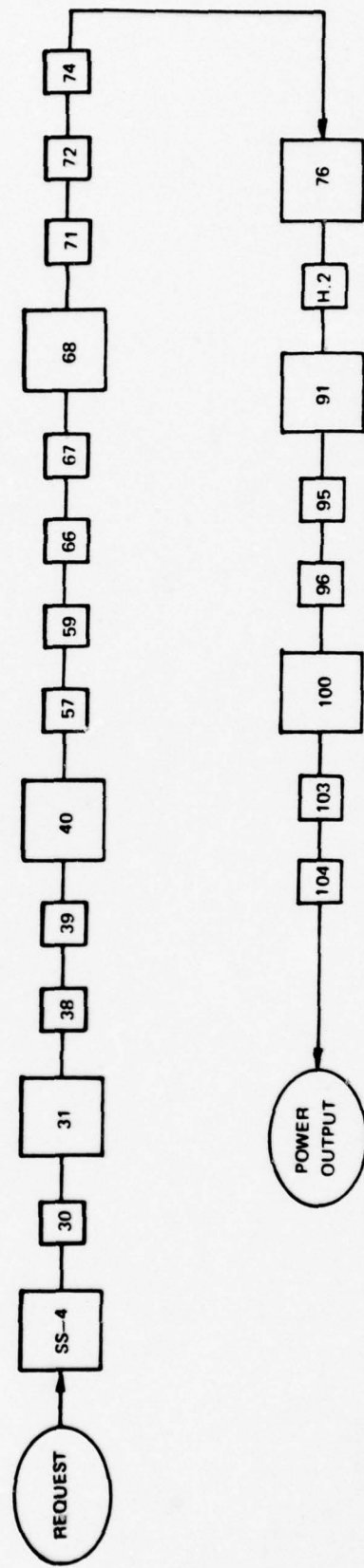
 $\lambda_m = \sum \lambda_{ptp}$ = mission failure rate

$$R = e^{-\sum \lambda_{ptp} t} = .9123$$

$$\sum \lambda_{ptp} = .09178$$

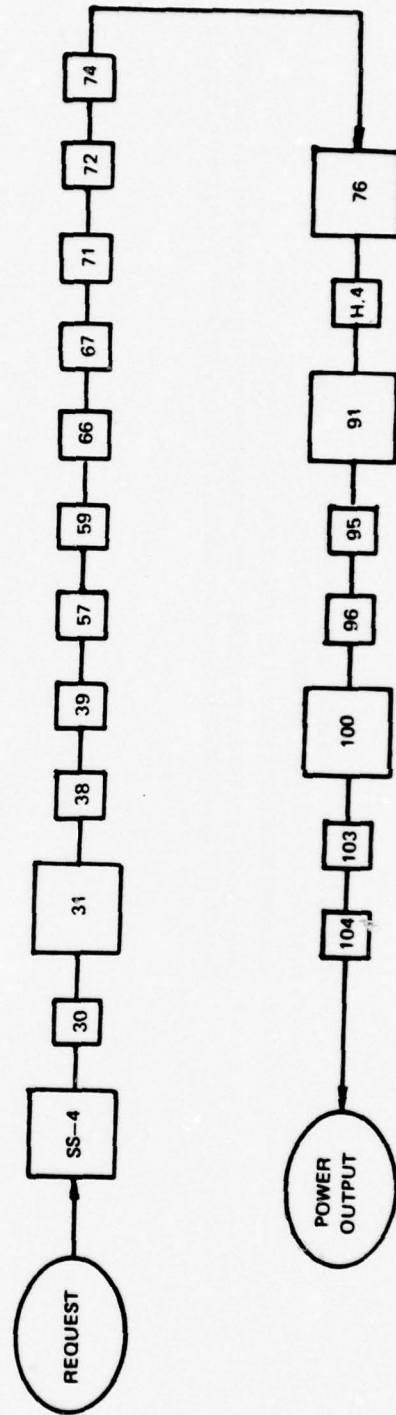
RELIABILITY BLOCK DIAGRAM FOR ALTERNATE LWSP-CCGT CONFIGURATION IV

- HEATER CAPACITY REDUCED TO 80% OF INSTALLED LEVEL
- ROUTINE REPAIR/REPLACEMENT PRACTICES
- MAXIMUM POWER ATTAINABLE IS 100% OF INSTALLED LEVEL
- LARGE BLOCKS REPRESENT GROUPS OF COMPONENTS WHICH CAN BE REPAIRED/REPLACED
EXCEPT FOR ALL HEATER SUBSYSTEM COMPONENTS WHICH ARE REPRESENTED BY BLOCK H.2



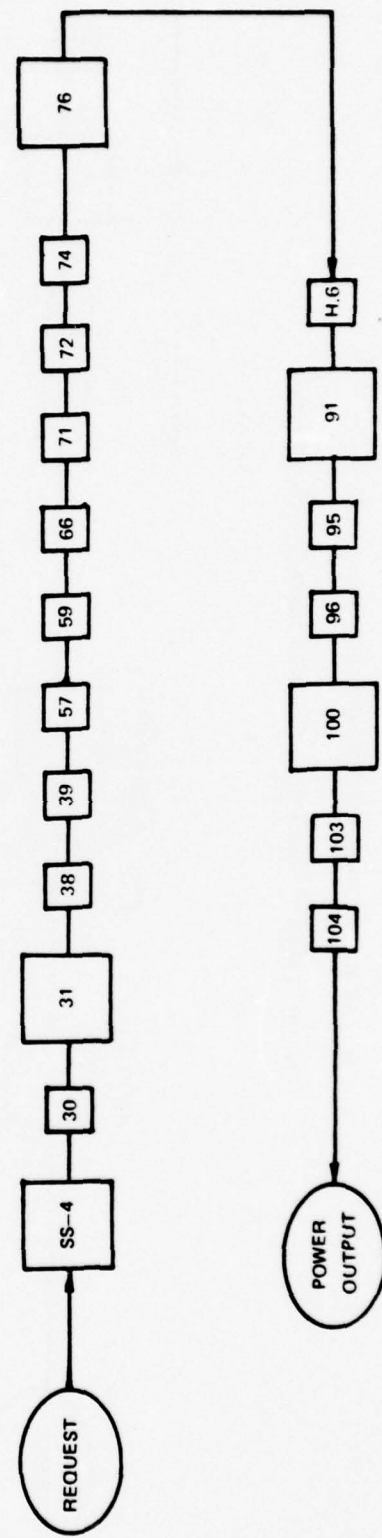
RELIABILITY BLOCK DIAGRAM FOR ALTERNATE LWSP-CCGT (CONFIGURATION VIII)

- HEATER CAPABILITY REDUCED TO 60% OF INSTALLED CAPABILITY
- ROUTINE REPAIR/REPLACEMENT PRACTICES
- MAXIMUM POWER ATTAINABLE IS 60% OF INSTALLED LEVEL
- LARGE BLOCKS REPRESENT GROUPS OF COMPONENTS WHICH CAN BE REPAIRED/REPLACED
- SS-4 REPRESENTS SUBSYSTEM COMPONENTS WHICH CAN BE REPAIRED IN-SERVICE EXCEPT FOR ALL HEATER SUBSYSTEM COMPONENTS WHICH ARE REPRESENTED BY BLOCK H.4



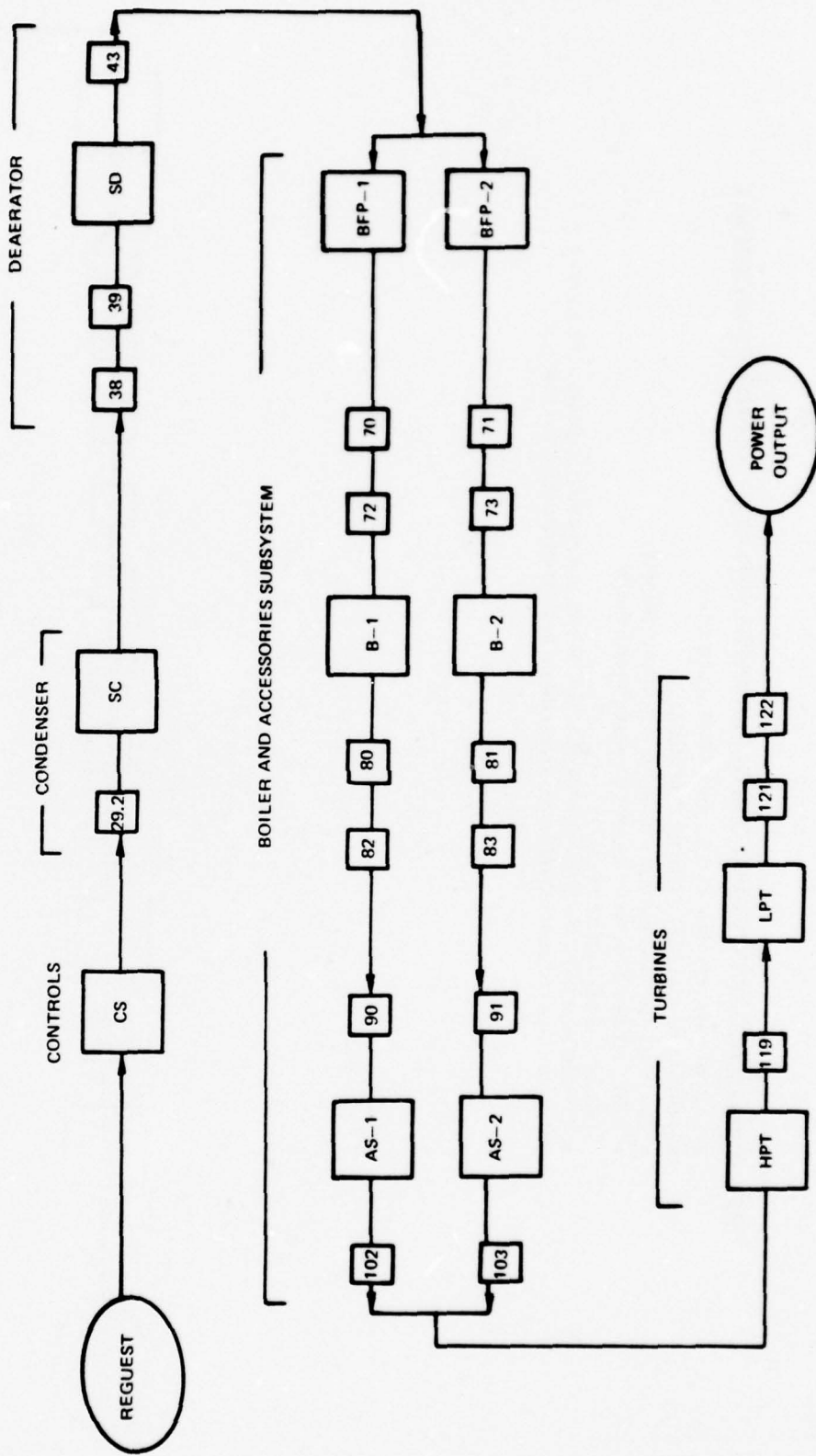
RELIABILITY BLOCK DIAGRAM FOR ALTERNATE LWSP-CCGT (CONFIGURATION XI)

- HEATER CAPACITY REDUCED TO 40% OF INSTALLED LEVEL
- ROUTINE REPAIR/REPLACEMENT PRACTICES
- MAXIMUM POWER ATTAINABLE IS 40% OF INSTALLED CAPACITY
- SMALL BLOCKS REPRESENT GROUPS OF COMPONENTS WHICH CAN NOT BE REPAIRED/REPLACED
- SS-4 REPRESENTS SUBSYSTEM COMPONENTS WHICH CAN BE REPAIRED OR REPLACED EXCEPT FOR ALL HEATER SUBSYSTEM COMPONENTS WHICH ARE REPRESENTED BY BLOCK H.6



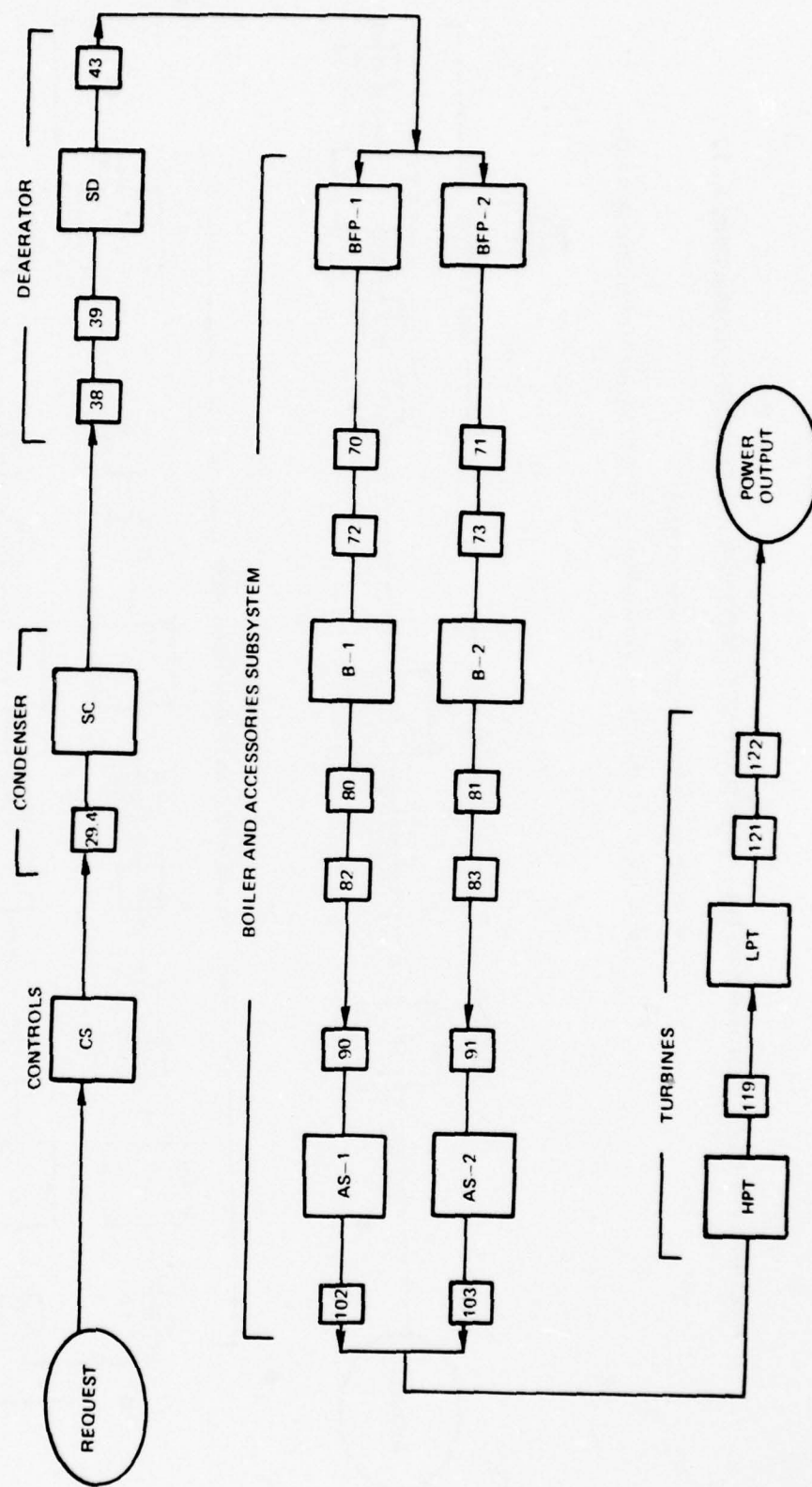
RELIABILITY BLOCK DIAGRAM FOR ALTERNATE STEAM POWER SYSTEM (CONFIGURATION A-II)

- ROUTINE REPAIR/REPLACEMENT PRACTICES
- MAIN CONDENSER (REDUCED TO 80% OF INSTALLED CAPABILITY)



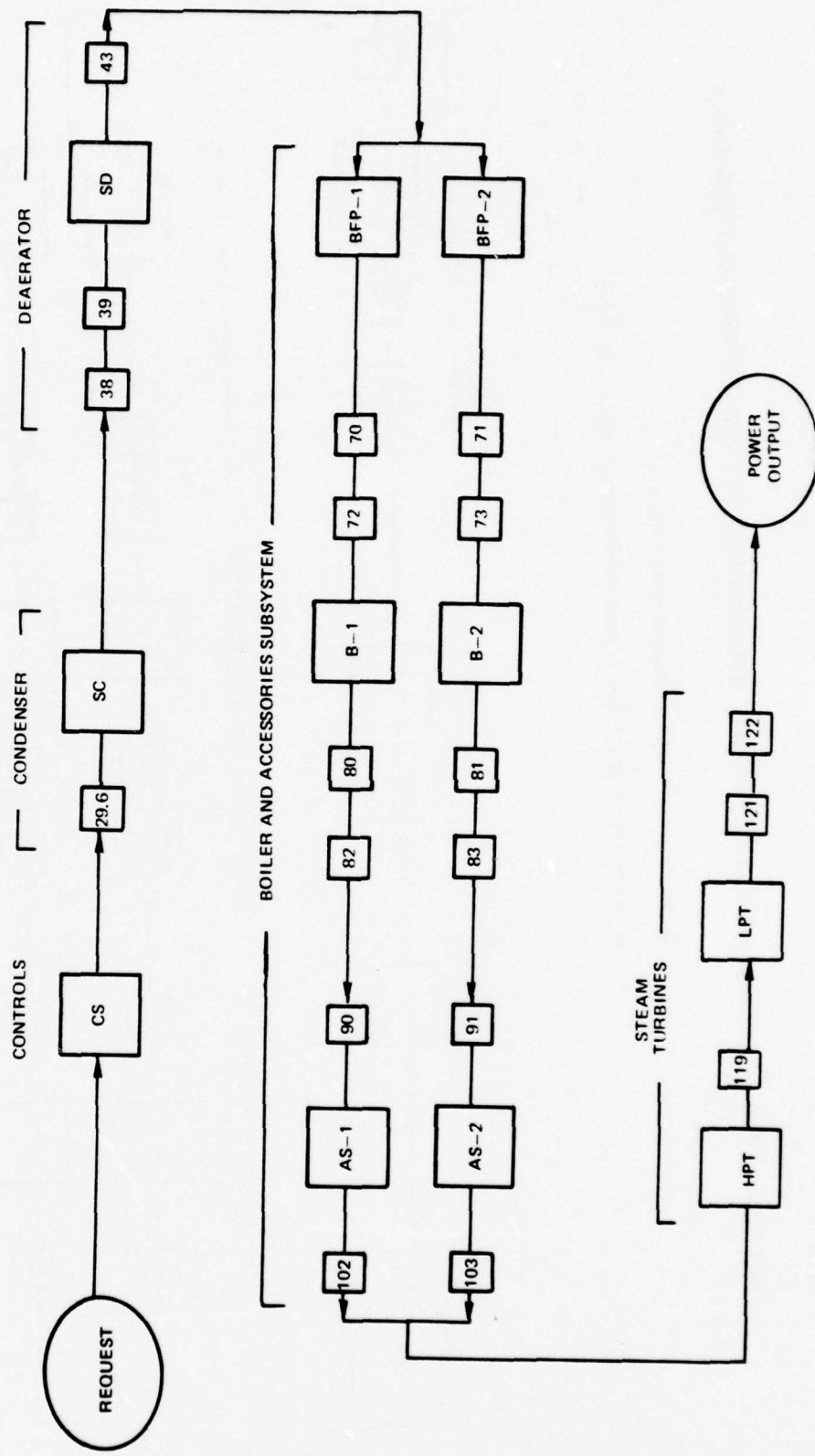
RELIABILITY BLOCK DIAGRAM FOR ALTERNATE STEAM POWER SYSTEM (CONFIGURATION A-III)

- ROUTINE REPAIR/REPLACEMENT PRACTICES
- MAIN CONDENSER CAPACITY REDUCED TO 60% OF INSTALLED LEVEL



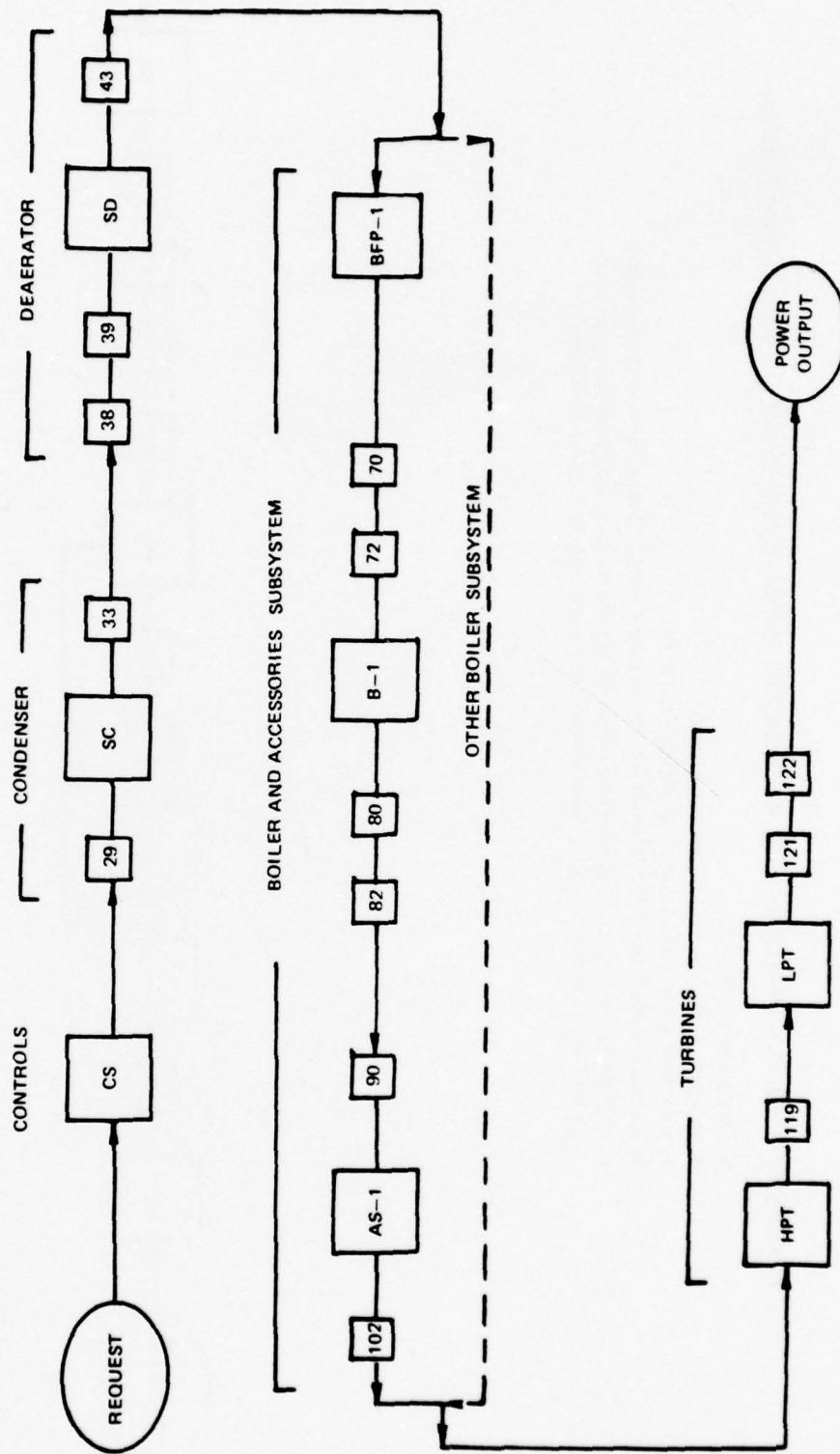
RELIABILITY BLOCK DIAGRAM FOR ALTERNATE STEAM POWER SYSTEM CONFIGURATION A-IV

- ROUTINE REPAIR/REPLACEMENT PRACTICES
- MAIN CONDENSER CAPACITY REDUCED TO 40% OF INSTALLED CAPABILITY LEVEL



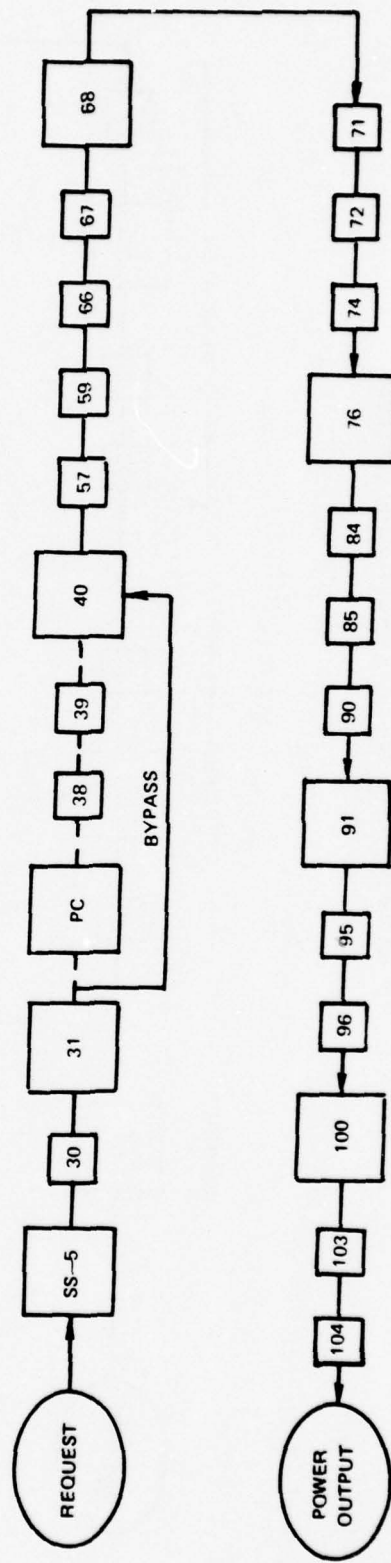
ALTERNATE STEAM POWER SYSTEM-CONFIGURATION A-2

- ONE BOILER IN SAME SYSTEM BYPASSED
- ROUTINE REPAIR/REPLACEMENT PRACTICES
- MAXIMUM POWER POSSIBLE IS 100 % OF INSTALLED LEVEL



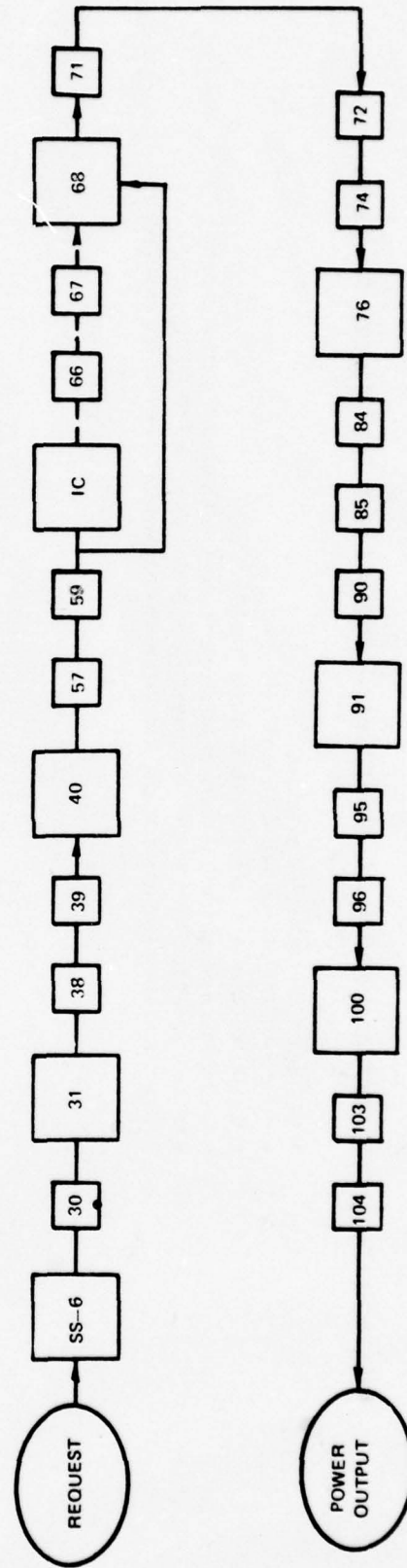
RELIABILITY BLOCK DIAGRAM FOR ALTERNATE LWSP-CCGT SYSTEM (CONFIGURATION V)

- PRECOOLER BYPASSED
- ROUTINE REPAIR/REPLACEMENT PRACTICES
- MAXIMUM POWER ATTAINABLE IS 60% OF INSTALLED
- LARGE BLOCKS REPRESENT GROUPS OF COMPONENTS WHICH CAN BE REPAIRED/REPLACED
- SS-5 REPRESENTS OTHER SUBSYSTEM COMPONENTS WHICH CAN BE REPAIRED/REPLACED EXCEPT FOR THE PRECOOLER COMPONENTS (PCI) WHICH ARE BYPASSED AS SHOWN



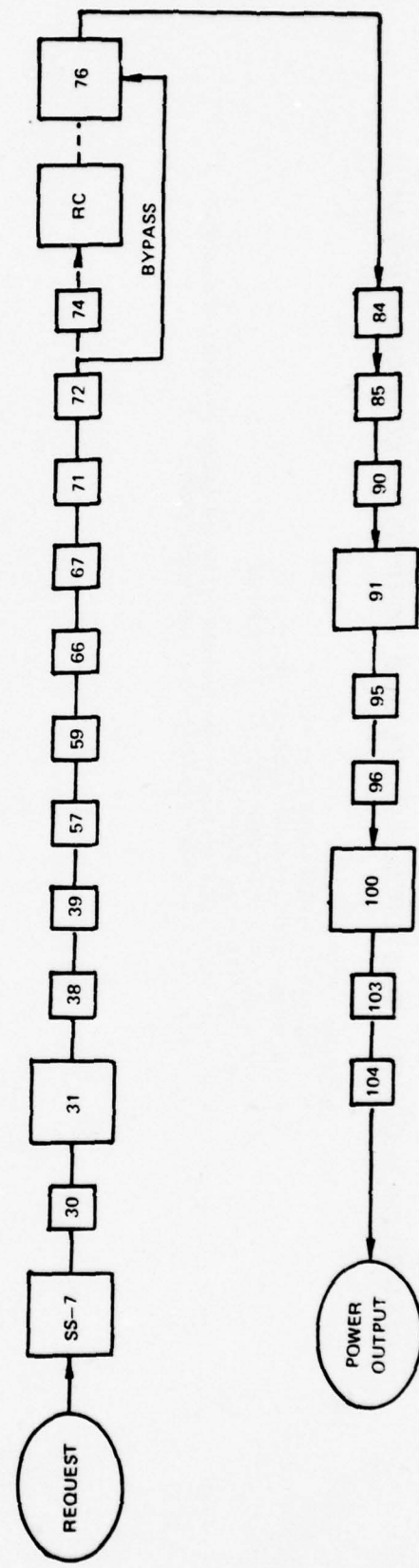
RELIABILITY BLOCK DIAGRAM FOR ALTERNATE LWSP-CCHT SYSTEM CONFIGURATION VI

- INTERCOOLER BYPASSED
- ROUTINE REPAIR REPLACEMENT PRACTICES
- MAXIMUM POWER ATTAINABLE IS 60% OF INSTALLED
- LARGE BLOCKS REPRESENT GROUPS OF COMPONENTS WHICH CAN BE REPAIRED/REPLACED
- SS- 6 REPRESENTS OTHER SUBSYSTEM COMPONENTS WHICH CAN BE REPAIRED/REPLACED EXCEPT FOR THE INTERCOOLER WHICH IS BYPASSED AS SHOWN



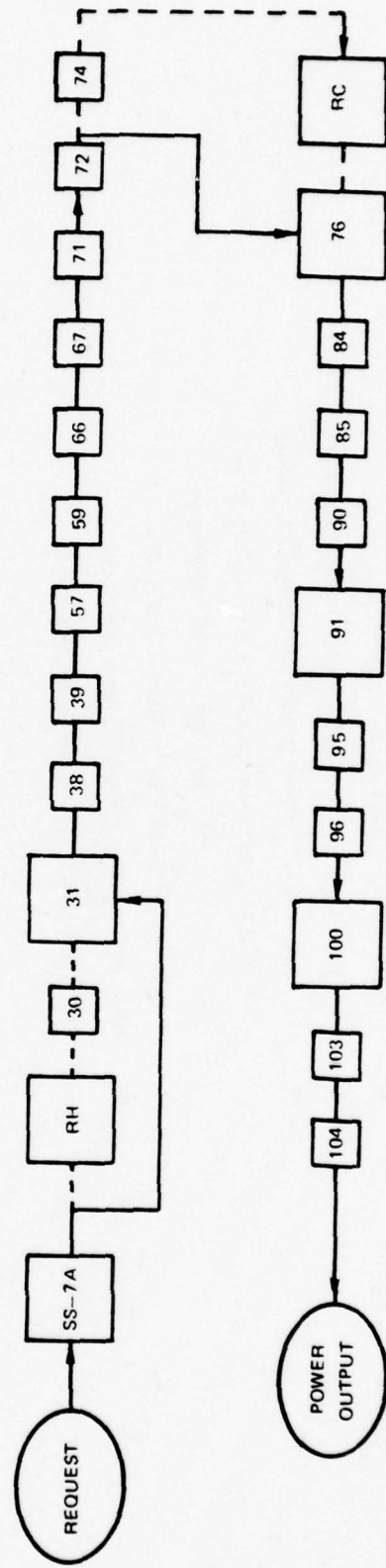
RELIABILITY BLOCK DIAGRAM FOR ALTERNATE LWSP-CCGT SYSTEM (CONFIGURATION VIIA)

- REGENERATOR COLD-SIDE BYPASSED
- ROUTINE REPAIR/REPLACEMENT PRACTICES
- MAXIMUM POWER ATTAINABLE IS 60% OF INSTALLED
- LARGE BLOCKS REPRESENT GROUPS OF COMPONENTS WHICH CAN BE REPAIRED/REPLACED
- SS-7 REPRESENTS OTHER SUBSYSTEM COMPONENTS WHICH CAN BE REPAIRED/REPLACED EXCEPT FOR THE REGENERATOR COLD-SIDE COMPONENTS WHICH ARE BYPASSED AS SHOWN



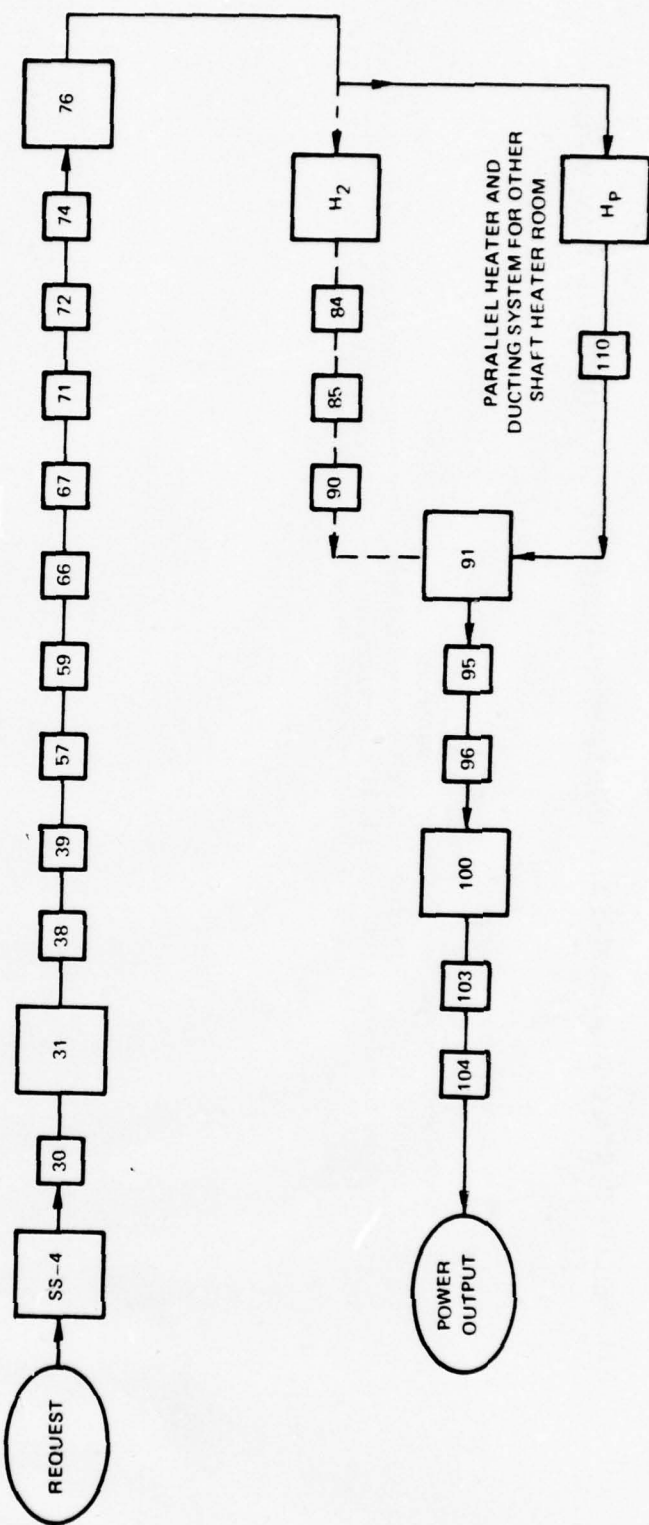
RELIABILITY BLOCK DIAGRAM FOR ALTERNATE LWSP-CCGT SYSTEM (CONFIGURATION VIIIB)

- TOTAL REGENERATOR BYPASS
- ROUTINE REPAIR/REPLACEMENT PRACTICES
- MAXIMUM POWER ATTAINABLE IS 60% OF INSTALLED
- LARGE BLOCKS REPRESENT GROUPS OF COMPONENTS WHICH CAN BE REPAIRED/REPLACED
- SS-7A REPRESENTS OTHER SUBSYSTEM COMPONENTS WHICH CAN BE REPAIRED/REPLACED EXCEPT FOR THE RECUPERATOR HOT AND COLD SIDE COMPONENTS WHICH ARE BYPASSED AS SHOWN



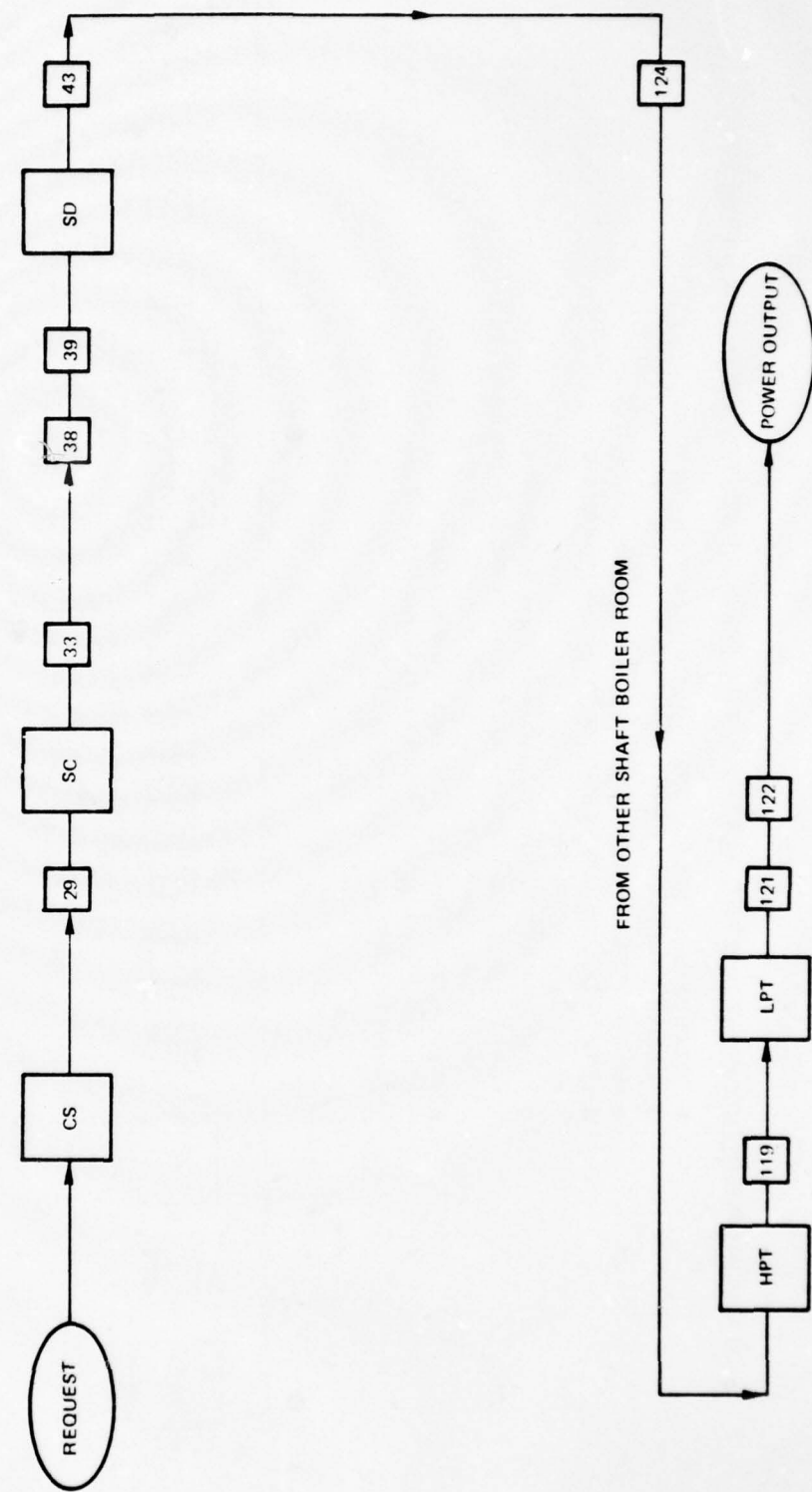
RELIABILITY BLOCK DIAGRAM FOR ALTERNATE LWSP-CCGT (CONFIGURATION IX)

- CROSS- CONNECTION BETWEEN ENGINE ROOM HEATER SYSTEMS
- ROUTINE REPAIR/REPLACEMENT PRACTICES
- MAXIMUM POWER ATTAINABLE IS 40% OF INSTALLED LEVEL
- SS-4 REPRESENTS OTHER SUBSYSTEM COMPONENTS WHICH CAN BE REPAIRED/REPLACED EXCEPT FOR THE PRIMARY HEATER (H₁) AND PARALLEL HEATER (HP) COMPONENTS
- BLOCK #110 REPRESENTS THE SUMMATION OF ALL NON-REPLACEABLE COMPONENTS ASSOCIATED WITH THE PARALLEL HEATER (HP) CONNECTION



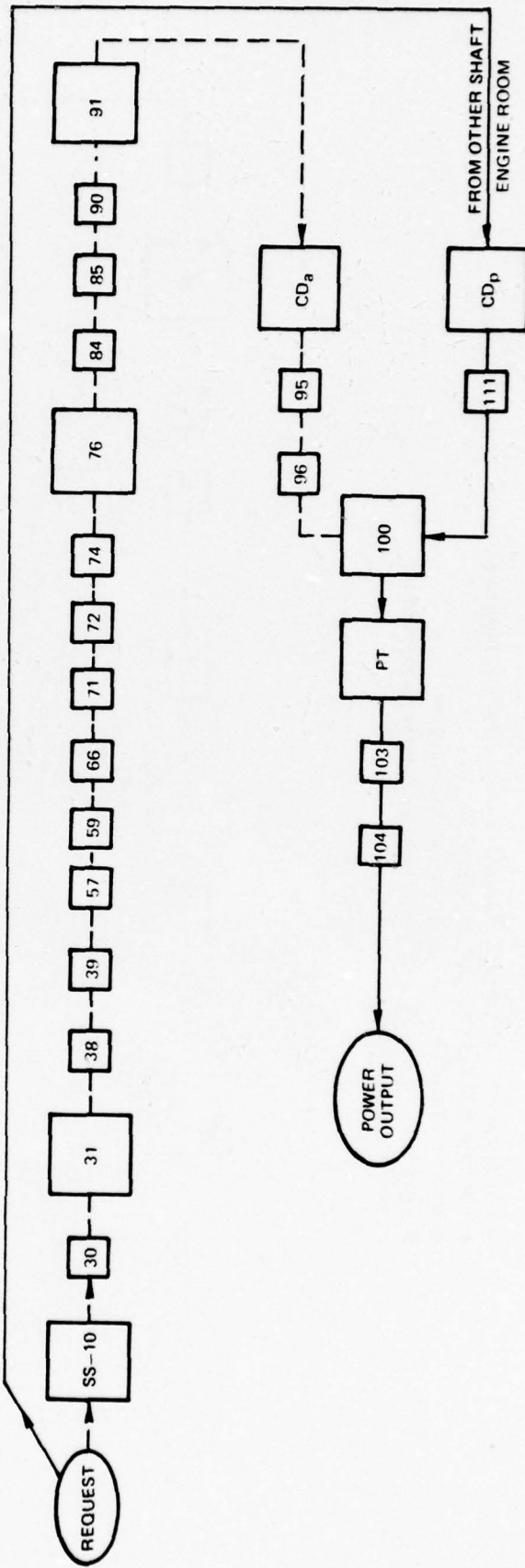
RELIABILITY BLOCK DIAGRAM FOR ALTERNATE STEAM POWER SYSTEM (CONFIGURATION A-VII)

- ONE ENTIRE BOILER ROOM BYPASSED BY CROSS CONNECTING WITH OTHER SHAFT BOILER ROOM
- ROUTINE REPAIR/REPLACEMENT PRACTICES
- MAXIMUM POWER POSSIBLY IS 45% OF INSTALLED LEVEL
- BLOCK #124 REPRESENTS AN ENTIRE BOILER SUBSYSTEM PRESENT IN THE OTHER SHAFT BOILER ROOM



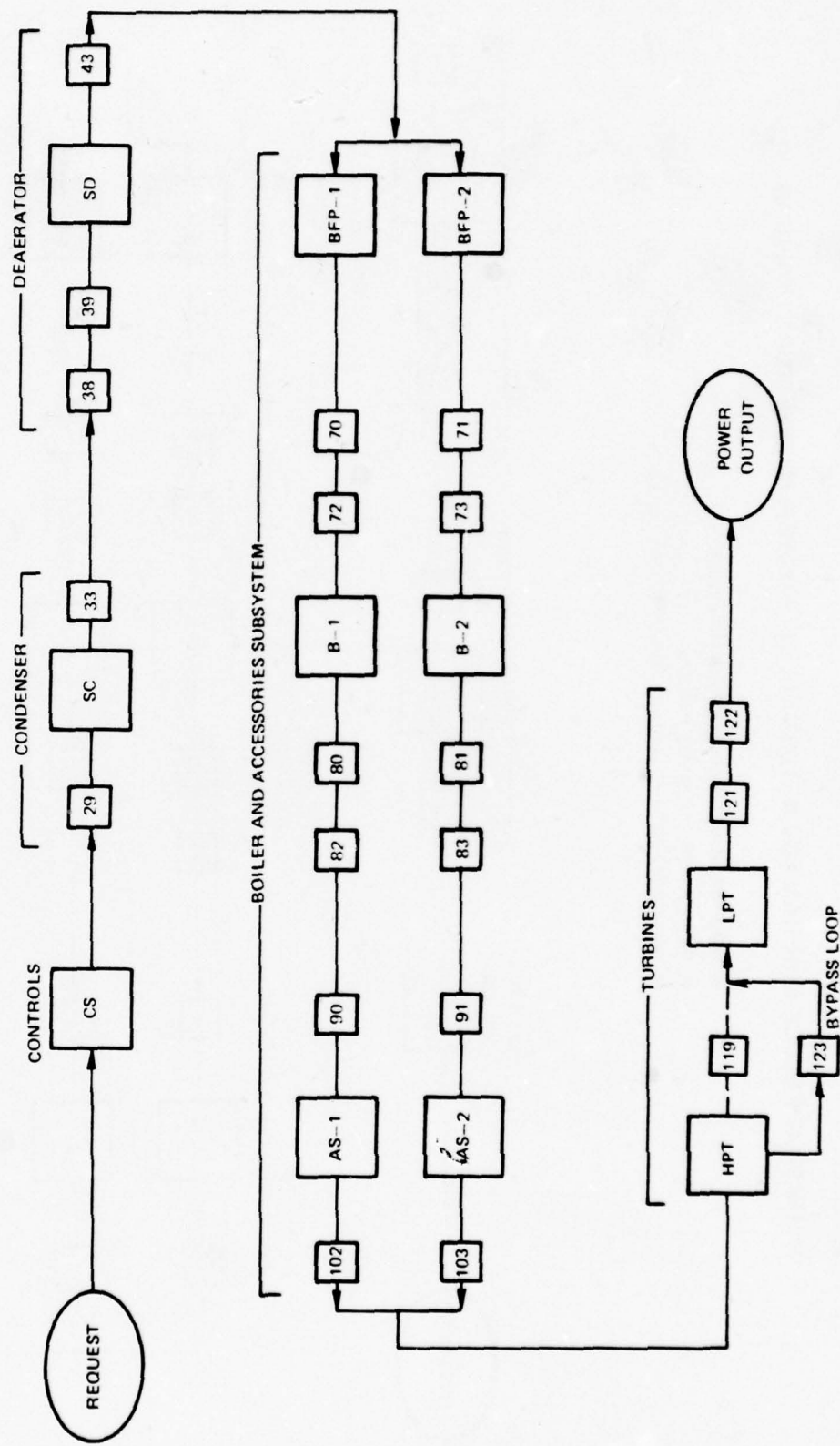
RELIABILITY BLOCK DIAGRAM FOR ALTERNATE LWSP-CCGT SYSTEM CONFIGURATION X

- CROSS-CONNECTION OF COMPRESSOR TURBOMACHINERY ALLOWED
- ROUTINE REPAIR/REPLACEMENT PRACTICES
- MAXIMUM POWER ATTAINABLE IS 40% OF INSTALLED LEVEL
- LARGE BLOCKS REPRESENT GROUPS OF COMPONENTS WHICH CAN BE REPAIRED ON-BOARD
- BLOCK #SS-10 REPRESENTS OTHER SUBSYSTEM COMPONENTS WHICH CAN BE REPAIRED/REPLACED EXCEPT FOR THE TURBOMACHINERY COMPRESSOR COMPONENTS, CD
- BLOCK #111 REPRESENTS THE SUMMATION OF ALL NON-REPLACEABLE ON-BOARD COMPONENTS ASSOCIATED WITH THE PARALLEL COMPRESSOR (CD_p) CONNECTION



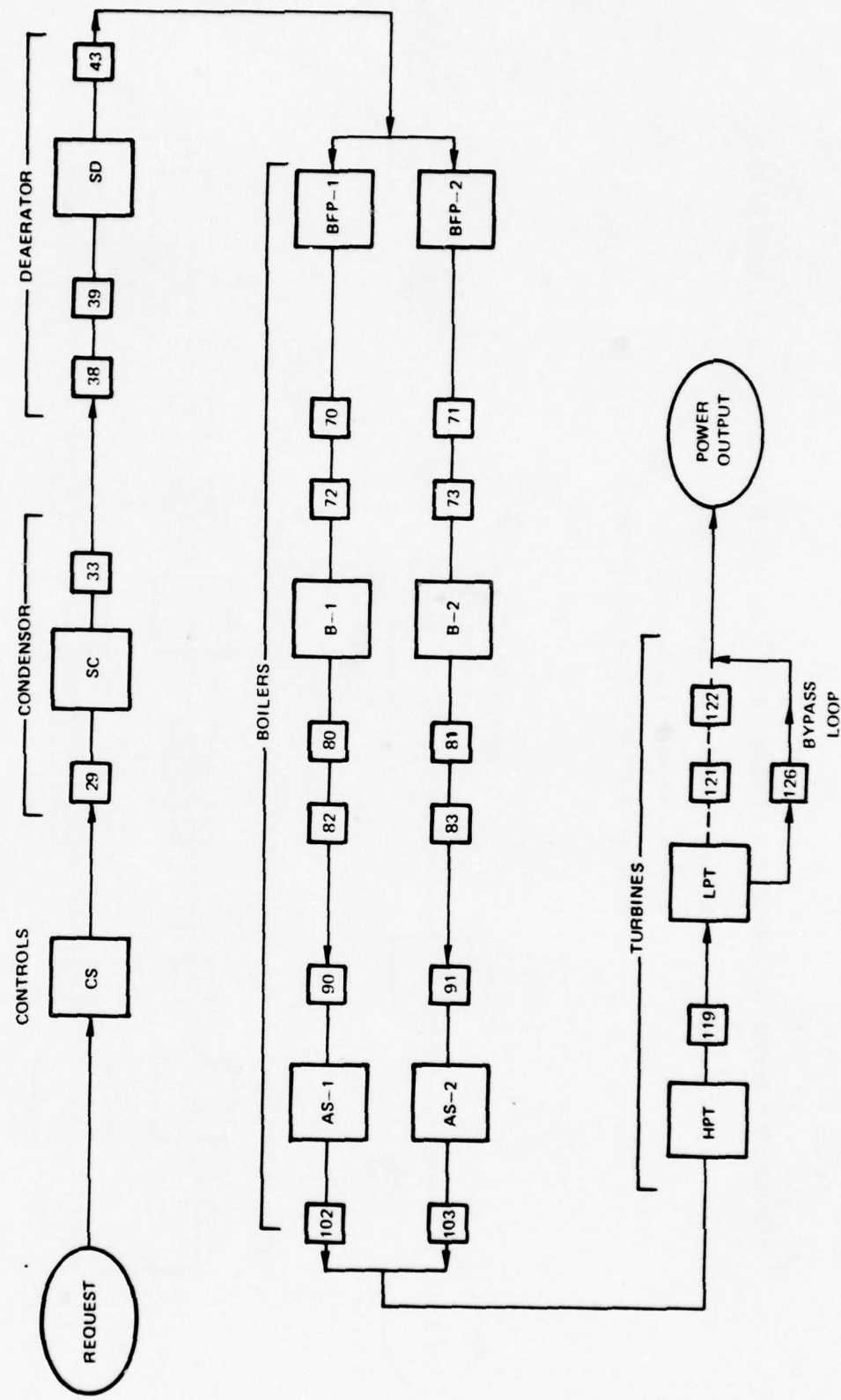
RELIABILITY BLOCK DIAGRAM FOR ALTERNATE STEAM POWER SYSTEM CONFIGURATION A-V

- ROUTINE REPAIR/REPLACEMENT PRACTICES
- BYPASSING HIGH PRESSURE TURBINE
- MAXIMUM POWER POSSIBLE IS 60% OF INSTALLED VALUE



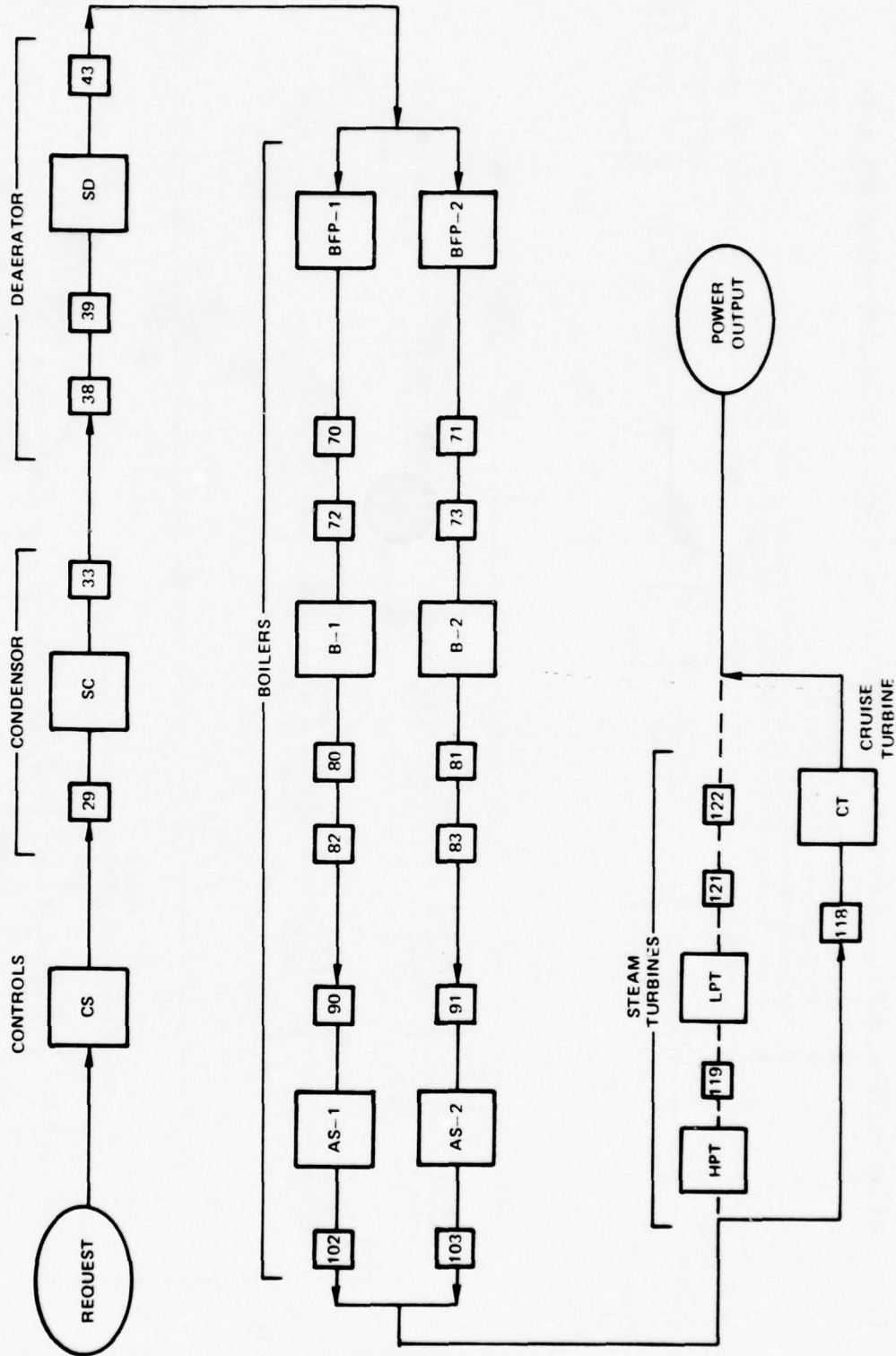
RELIABILITY BLOCK DIAGRAM FOR ALTERNATE STEAM SYSTEM CONFIGURATION A-VI

- ROUTINE REPAIR/REPLACEMENT PRACTICES
- BYPASS LOW PRESSURE TURBINE
- MAXIMUM POWER POSSIBLE IS 60% OF INSTALLED LEVEL



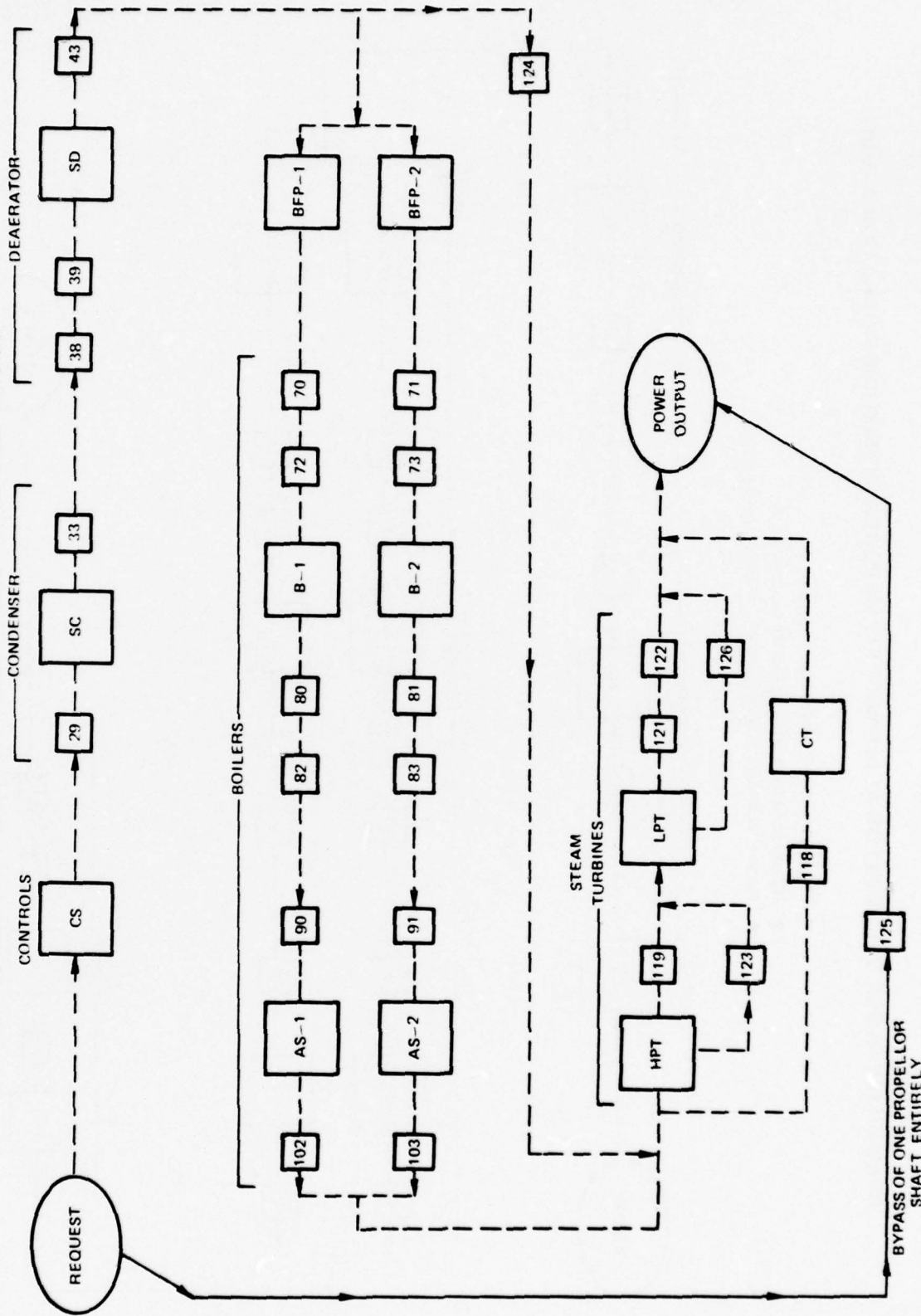
RELIABILITY BLOCK DIAGRAM FOR ALTERNATE STEAM POWER SYSTEM CONFIGURATION A-VIII

- OPERATING ONLY ON CRUISE TURBINE
- ROUTINE REPAIR/REPLACEMENT PRACTICES
- MAXIMUM POWER POSSIBLE IS 30% OF INSTALLED LEVEL



RELIABILITY BLOCK DIAGRAM FOR ALTERNATE STEAM POWER SYSTEM CONFIGURATION A-IX

- ONE PROPELLOR SHAFT OPERATING
- ROUTINE REPAIR/REPLACEMENT PRACTICES
- MAXIMUM POWER POSSIBLE IS 20% OF INSTALLED LEVEL (OR 20 KNOTS MAX SPEED)
- BLOCK 125 REPRESENTS THE ENTIRE PARALLEL PROPELLOR SHAFT SYSTEM



APPENDIX B

Status of Technological Development of Gas Turbines,
Nuclear Reactors, and Naval Shipbuilding in Japan

The executive summary which presents the major observations and technical findings from an October 1-23, 1977 fact-finding trip to Japan is included in this report in its entirety as Appendix B which follows.

UTRC Report R77-952972-1

**Status of Technological
Development of Gas Turbines,
Nuclear Reactors, and Naval
Shipbuilding in Japan**

AN EXECUTIVE SUMMARY

Simion C. Kuo

November 1977

**Prepared for
The Office of Naval Research
Arlington, Virginia 22217**

Contract N00014-77-C-0735

**UNITED TECHNOLOGIES
RESEARCH CENTER**



EAST HARTFORD, CONNECTICUT 06108

77-12-12-1

UTRC Report R77-952972-1

**Status of Technological
Development of Gas Turbines,
Nuclear Reactors, and Naval
Shipbuilding in Japan**

AN EXECUTIVE SUMMARY

Simion C. Kuo

November 1977

**Prepared for
The Office of Naval Research
Arlington, Virginia 22217**

Contract NOOO14-77-C-0735

**UNITED TECHNOLOGIES
RESEARCH CENTER**



EAST HARTFORD CONNECTICUT 06108

R77-952972-1

Status of Technological Development of Gas Turbines,
Nuclear Reactors, and Naval
Shipbuilding in Japan

TABLE OF CONTENTS

	<u>Page</u>
FOREWORD	i
SUMMARY	ii
SECTION I - MAJOR OBSERVATIONS AND CONCLUSIONS	I-1
1.0 General	I-1
2.0 Closed-Cycle Gas Turbine Systems	I-2
3.0 Marine Propulsion Systems	I-4
4.0 Aircraft and Industrial Gas Turbines	I-5
5.0 Nuclear Reactor Development	I-7
6.0 Shipbuilding	I-7
7.0 Energy Research	I-8
SECTION II - SUPPORTING REMARKS AND COMMENTS	II-1
REFERENCE	
TABLES	
FIGURES	

FOREWORD

This executive summary presents major observations and technical findings from an October 1-23, 1977 fact-finding trip to Japan, made for the purpose of discussing the latest developments and crucial technical problems associated with open- and closed-cycle gas turbines, gas-cooled nuclear reactors, and ship propulsion systems at major heavy industry corporations and selected government agencies.

The trip was made by Dr. Simion C. Kuo, Chief, Nuclear and Solar Power Systems, United Technologies Research Center (UTRC) for the benefit of both United Technologies Corporate-funded programs and for work being performed for the Office of Naval Research (ONR) under Contract N00014-77-C-0735 between UTRC and ONR on lightweight ship propulsion systems. Dr. Kuo is Program Director for this Contract. Assistance received from the New York Offices of the Japanese companies visited, the ONR-Tokyo, and United Technologies International (Tokyo) in planning for the trip itinerary are gratefully acknowledged. Questions regarding this trip may be directed to Dr. Kuo, telephone (203) 565-8758.

Two additional technical reports providing details for the specific technology areas of closed-cycle gas turbines and gas-cooled nuclear reactors will be issued to the Office of Naval Research (ONR) for publication in the ONR-Tokyo Quarterly.

R77-952972-1

Status of Technological Development of Gas Turbines,
Nuclear Reactors, and Naval Shipbuilding in Japan

SUMMARY

A fact-finding trip to Japan was made to collect information on the latest developments and to review crucial technical problems relating to open- and closed-cycle gas turbine ship propulsion systems utilizing fossil or nuclear heat sources. During the three-week trip, approximately twenty meetings were held at selected major Japanese heavy industrial corporations and government agencies. In this report, the major observations and conclusions for the trip are summarized, with supporting remarks and comments also provided. A summary of the trip itinerary is provided in Table I.

This trip was made as part of the ONR-sponsored study on lightweight ship propulsion systems under Contract N00014-77-C-0735 and as part of the Corporate-funded program in energy research. Funding was provided jointly by the ONR and United Technologies.

SECTION I - MAJOR OBSERVATIONS AND CONCLUSIONS

1.0 General

- 1.1 In order to put the extremely diversified Japanese industrial enterprise in good perspective, attempts were made to identify and rank the major corporations for each of the selected industrial technologies relevant to the trip objectives. The results are shown in Table II. It should be noted that ranking of industrial corporations is often difficult and inconclusive (particularly without detailed statistical data), and as such the results must be regarded as an aid to facilitate the reading of this summary report only.
- 1.2 The Japanese industrial strength is built on several major industrial/financing corporations, similar to that of the preWorld-War-II era; however, technological excellence and aggressive yet effective international trade strategy can be attributed to making Japan one of the major economic powers in the world today.
- 1.3 The relatively low Japanese defense R&D expenditures can be attributed to the existing US-Japanese mutual defense treaties and the supply of defense-related technologies and equipment by the United States. This, in turn, has enabled the Japanese to allocate sizable R&D funds for such exportable high-technology commercial products as electronic (e.g., TV, HiFi, calculator, and computer) and optical (camera) equipment and automobiles, which has contributed to their current trade surplus of over \$6 billion with the United States.
- 1.4 Due to the abrupt worldwide cutback in the shipbuilding business during the past few years, the demand for steel plates in Japan, particularly of those thicker plates needed for shipbuilding, also decreased substantially, thus necessitating a search for foreign markets for the surplus, including the United States.
- 1.5 Although the naval ships and aircraft types used by the Marine Self Defense Force (MSDF) of the Japan Defense Agency (JDA) generally reflect a strong US Navy influence, their procurement of equipment seems to depend on the availability of reasonable licensing agreements which can be negotiated with the foreign countries.
- 1.6 The existing major turbomachinery licensing agreements between Japanese companies and foreign manufacturers include:

Hitachi - GE (Industrial, Frame 5 & 7)
Kawasaki - Rolls Royce (Marine, Olympus & Tyne)
IHI - GE (Marine, LM2500)
MHI - Westinghouse (Industrial)
Toshiba - BBC (Industrial, old design)
MHI-UTC - (Aircraft, JT8D)

1.7 The potential need for Marine gas turbines with output capacities under 20,000 shp and land-based gas turbines (peaking) in the 35,000- to 40,000 shp range were voiced by the Japanese at different occasions.

2.0 Closed-Cycle Gas Turbine Systems

2.1 The MITI (Ministry of International Trade and Industry) officials indicated that they are unaware of any past effort in developing CCGT power systems. However, it was revealed later from industry sources that in 1973 MITI and the Electric Industry Research Institute (EIRI, a research arm of the electric utility and equipment manufacturers in Japan) sponsored a joint study program involving Hitachi, MHI, Fuji Electric, Mitsui, Sumitomo, IHI and National Aerospace Laboratory to review the General Atomic GT-HTGR program, the HHT Project in West Germany and the joint European Dragon Project, in order to shape up development programs and an appropriate time table for developing the CCGT system. The study program was suspended in 1975 after GA cancellation of the commercial HTGR plant contracts.

2.2 Three fossil-fired closed-cycle air gas turbines designed by Escher Wyss, including two land-based power plants (2-MWe and 12-MWe) and one 10,000-shp naval propulsion engine were built, tested, and operated commercially (except the 10,000-shp engine) between the late 1950s and mid 1970s.

2.3 The only closed-cycle gas turbine ever built for marine propulsion application in Japan or elsewhere was a Diesel-oil-burning 10,000-shp unit designed by Escher Wyss and built by Mitsui Engineering and shipbuilding company under contract from MSDF/TRDI* of the Japan Defense Agency (JDA). The unit which was built in 1960 underwent subsequent land testing from 1961 to 1963 but never installed aboard a ship for sea test.

2.4 The 2-MWe natural-gas-fired Toyotomi plant built by Fuji Denki for Hokkaido Electric was commissioned in November 1957 and operated reliably until it was shut down in 1976 for lack of natural gas supply. The plant which resembled the German Ravensburg plant (see Ref. 1) utilized radial compressors

*Marine Self Defense Force/Technology Research and Development Institute.

with one intercooling and an axial-flow turbine in a single-shaft rotor assembly with turbine inlet conditions of 27 atm (383 psi)/660 C (1220 F).

2.5 Based on the satisfactory performance of the Toyotomi plant, a second plant of 12-MWe capacity built by Fuji Denki for Nippon Kokan started operation by burning blast furnace gas available at the Kawasaki Iron Works until 1972 shut down, again for lack of fuel supply. This unit used three radial-flow compressors with double intercooling and a 6-stage turbine with 29 atm (423 psi)/680 C (1256 F) inlet conditions.

2.6 At a design turbine inlet temperature of approximately 700 C (1292 F), the major technical problem encountered during testing of the Mitsui CCGT engine was the air heater and it was said that although the engine demonstrated a specific fuel consumption of 338 g (0.745 lb/shp-hr) but could not achieve the maximum design output of 10,220 shp. Table III summarizes the major design specifications for this CCGT propulsion system while Fig. 1 depicts the flow diagram and machinery arrangement.

2.7 The oil-fired 10,000-shp closed-cycle marine engine apparently encountered more technical problems than the two gas-fired land-based engines previously mentioned but all of them had severe problems with the air heater. Some of the problems mentioned are:

- . corrosion of air heater tubing caused by impurities resulted in tubing rupture.
- . "hot stress" caused by deformation attributable to residual stress in heater and heat exchangers.
- . increasing system pressure loss with operation time and subsequent pressurization beyond the design level causing broken blades and other mechanical defects.
- . erosion of turbine blades caused by powdered insulation material, vapor droplets, and metallic oxide particles.
- . breakage of high-pressure compressor blades.

2.8 Due to the minor set-backs in the early 1960s on the Escher Wyss/Mitsui CCGT marine engine, the reaction of MSDF/TRDI on the feasibility of such propulsion systems appeared somewhat reserved. However, they indicated very strong interest in the results of the UTRC systems study, and also the potential improvement possible by utilizing advanced technologies as well as design concepts of aircraft-derivative origin.

- 2.9 Helium test facilities of modest scale compared to the German HHV have been built at IHI-Yokosuga, MHI-Nagasaki, Hitachi, and also at JAERI (said to have 3 ~ 4 loops) for fluid flow (including noise), heat transfer (including high-temperature insulation), and material testing purposes. The Hitachi facility uses an electric heat source for heating 20-atm helium to 1000°C, circulated by a 45-kW motor-driven reciprocating compressor.
- 2.10 Development and testing of heat-resisting materials for use in the HTGR gas turbine and heat exchangers are being conducted by Toshiba R&D Center, including molybdenum alloys, high chromium alloys, and directionally solidified eutectics.
- 2.11 No significant materials research related to preventing self-welding at the blade or disks was noticed during the trip, although use of molybdenum sulfide coatings to avoid sliding surfaces from becoming sticky was mentioned.

3.0 Marine Propulsion Systems

- 3.1 The Japanese Defense Agency has recently chosen the Rolls-Royce Olympus and Tyne marine gas turbines proposed by KHI over the GE LM2500 proposed by IHI for the first gas turbine-powered destroyer (2900 tons) and frigate (1250 tons) to be built by Sumitomo Heavy Industry. The destroyer (DD) will use COGOG arrangement with 2 x Olympus TM3B (28,000 shp) for boost and 2 x Tyne RMIC (5340 shp) for cruise while the frigate (DE) will use CODOG arrangement with single Olympus engine for boost.
- 3.2 The gas turbine-powered DD ship to be built will have a maximum/cruise speed of 32/10 knot using two identical units of COGOG propulsion systems each using one shaft in/one shaft out gearbox to drive a CRP propeller at 300 rpm.
- 3.3 The possibility of using more powerful engines (such as FT9) for increasing the maximum speed or displacement or both for the future DD ships have been mentioned by the Japanese shipbuilders. Similar possibilities for the DDH ships were also mentioned.
- 3.4 The Japanese reaction on the use of combined gas turbine and steam turbines (COGAS) power system for naval ship propulsion was generally negative; they are primarily concerned with the compatibility of the complex control system required for such propulsion system with the stringent operational requirement for the naval ships.

- 3.5 IHI has looked into the possibility of installing marine gas turbines vertically but neither significant advantage nor inherent problems prohibiting such installation method was indicated.
- 3.6 The largest marine Diesel engine being built in Japan is approximately 40,000 shp with a specific weight of approximately 60 lb/shp; KHI is manufacturing approximately 60 Diesel engines (all sizes) per month.
- 3.7 KHI is currently capable of manufacturing offset gearboxes using 1/1, 1/2 and 2/1 shaft arrangements with maximum capacity of 45,000 shp and epicyclic gearboxes up to 28,000 shp capacity; their feasibility studies indicate that an offset gearbox of 2/1 shaft arrangement with reversing capability can be built today for capacities up to 60,000 shp. KHI also has built CRP propellers of up to 45,000-shp capacity.

4.0 Aircraft and Industrial Gas Turbines

- 4.1 The manufacturing and marketing of industrial-type gas turbines in Japan depend heavily on the licensing agreements between the Japanese companies and the major turbomachinery manufacturers abroad. The existing licensing agreements listed in descending order of their market shares are:

Hitachi - GE for Frame 5 and 7
MHI - Westinghouse
Toshiba - BBC turbines of older models
Kawasaki - Rolls-Royce
Mitsui -

- 4.2 Among the several industrial gas turbine manufacturers in Japan mentioned above, only Hitachi has been selling a respectable number of units (approximately 250 units to date), particularly the GE Frame-5 type with a handful of Frame-7 units. Currently Hitachi sells approximately four units per month on the average.
- 4.3 MHI has built, under licensing agreement with UTC/P&WA, approximately 60 JT8D engines, and has sold 79 Westinghouse industrial gas turbines.
- 4.4 Some notable IHI activities related to jet engines are summarized as follows:
 - . 1700 jet engines built to date, including 200 Adour engines of 7000-lb thrust
 - . 800 JT8D engines overhauled

- . three MOD-15 development engines of 2640 lb thrust built, including one sold to JDA
- . six FJR710 development engines built, including two units shipped to England for altitude test
- . six more redesigned FJR710/20 engines to be built under a joint effort involving IHI, MHI, KHI/MITI/NAL.
- . a 3000-lb thrust F3 turbofan engine being developed for JDA
- . possible licensing agreement with UTC/P&WA to manufacture F-100 engines for the Japanese F-15 plane has been proposed by IHI through JDA.

4.5 Partial list of aircraft airframe capabilities in Japan include MHI for fighter planes, KHI for naval patrol planes; and MHI/KHI/Fuji for commercial airplanes.

4.6 Aircraft engine test cells located at IHI include:

4 test cells for jets	2 x 20,000 lb 1 x 30,000 lb 1 x 100,000 lb
5 cells for turboprops	2 x 5,000 lb 3 x 3,000 lb

Since no altitude test facility is available, they often ship their engines to England for such testing.

5.0 Nuclear Reactor Development

- 5.1 The Advanced Nuclear Reactor program in Japan is a government-sponsored program with emphasis placed on the High-Temperature Reactor (HTR), particularly the gas-cooled Very-High Temperature Reactor (VHTR) for process-heat application in nuclear steel making. An organization chart indicating the government sponsors and industrial participant in this program and its relations to other nuclear reactor programs is depicted in Fig. 2.
- 5.2 The major effort within the HTR program includes fundamental R&D on VHTR conducted by JAERI and the Nuclear Steel Making R&D conducted by ERANS as one of the future applications of VHTR. The overall schedules for these programs have not been finalized yet, but tentative proposed schedules are given in Fig. 3. The annual budget for the VHTR program is now said to be approximately \$12 million a year.
- 5.3 The six industrial participants in the VHTR program can be divided into four groups, as follows:

Fuji-Kawasaki group, Mitsubishi group, Toshiba - IHI group, and Hitachi group. While the Fuji - Kawasaki group appeared to be leading the program, Toshiba has been conducting feasibility studies, and helium test facilities have been built at IHI (Yokosuga), Hitachi, and MHI (Nagasaki).

- 5.4 The basic design conditions and the vertical cross sectional view of the VHTR plant are given in Table IV and Fig. 4, respectively. JAERI's original plan on the VHTR program was for multi-purpose application including power generation by the closed-cycle helium gas turbines. However, the current efforts seem to focus on the reactor itself and a steam generator coupled with an intermediate heat exchanger.

6.0 Shipbuilding

- 6.1 The major Japanese destroyer types, their acronym, and number of ships in active duty include:

Destroyer	DD	23
Helicopter Destroyer	DDH	2
Guided Missile Destroyer	DDG	1
All Purpose Destroyer	DDA	4
Escort Vessel	DE	<u>14</u>
		44 (92,000 tons)

- 6.2 Currently, DD and DE types are receiving more attention because they outnumber other ship types, and because they will be powered by gas turbines for the first time in Japan.
- 6.3 The largest destroyer built in Japan after World War II is the helicopter Destroyer DDH; two such DDH of 4700-ton displacement, each carrying three helicopters have been built, the first by Sumitomo and the second by IHI. New orders for two larger (5200 tons) DDH's each powered by two coal-fired 35,000-shp steam turbines have been issued to IHI recently for delivery of the first ship in September 1979.
- 6.4. There was a general consensus among the MSDF officials and shipbuilders that improvements for future naval ships should take the form of lower capital cost and/or higher speeds.
- 6.5 Japanese capabilities in building submarines are located at MHI and KHI, both in Kobe; currently there are 15 submarines, typically 800-ton and 1700-ton displacements. Total displacement in active duty is approximately 22,000 tons.
- 6.6 Modern shipbuilding facilities for large tankers, up to one-million-ton displacement, were built in the early 1970s by MHI (Nagasaki), IHI (Yokohama), and Kawasaki (Kobe).
- 6.7 Like other major shipbuilding countries of the world, the Japanese ship-building industry is suffering from the most serious setback in demand in recent decades; the largest ships being built are 20,000-ton class multipurpose (MHI) and hybrid (KHI) cargo ships typically powered by 2 x 18,000-shp diesel engines.
- 6.8 Japanese shipbuilders can build a destroyer hull in three to four months, with an additional four months needed to complete the ship for sea testing.

7.0 Energy Research

- 7.1 The National Research and Development Program launched in 1966 was a totally government-financed program aimed at developing new and original technologies for preserving the environment and promoting efficient utilization of natural resources. The research capabilities of the Government, academic institutions and industry were mobilized in conducting the following projects:

MHD - \$25 million, 1966-75
Desalination - \$20 million, 1969-75
Deep Sea Drilling - \$20 million, 1970-75
Electric Car - \$20 million, 1971-75
Information Processing - \$140 million, 1971-78

Jet Engines \$27 million, 1971-75
Nuclear Steel Making - \$29 million, 1973-78
High Performance Computer - \$40 million, 1966-71
Resource Recovery - \$64 million plus, 1973-75

- 7.2 The latest Japanese efforts in energy R&D are contained in their two national energy projects called "Sunshine Project" and "Moonlight Project"; the former which emphasizes development of alternative energy source involves work on solar energy, geothermal energy, coal gasification, and hydrogen fuel production while the later emphasizes conservation and involves development of high-temperature gas turbines, MHD power, and waste heat recovery systems.
- 7.3 As part of the Moonlight Project, research on high-temperature gas turbines for combined gas turbine and steam (COGAS) power system applications is being initiated. This research program, which somewhat resembles the HTTT program in U.S. sponsored by the USDOE, will be started in early 1978 and a goal of powerplant efficiency of 60 percent.
- 7.4 The Japanese work on MHD has been emphasizing the open-cycle system powered by low-grade fuels. Some successful testing have been achieved with the 100-kWe class Mark 6, which has operated 200 hours to date.
- 7.5 Despite the nearly total dependence on imported fuels to meet their energy demands, the Japanese effort to harness solar energy seems to be less aggressive than the U.S. programs. Their solar energy effort constitutes an important part within the national Sunshine Project which was launched shortly after the 1973 Arab oil crisis, for harnessing alternative and new energy sources.
- 7.6 Two major solar energy programs noticed are located at Hitachi and MHI; the Hitachi program is based on low-temperature distributed-type solar collectors for heating and cooling of buildings and auxiliary power generation while the MHI program is based on the tower-top central-receiver approach utilizing steam turbines for solar power generation. Design work is said to be underway for an 0.5-MWe system at IHI and a 1-MWe plant at MHI.

SECTION II - SUPPORTING REMARKS AND COMMENTS

1. Japanese engineers are quite ingenious in designing special machining tools for "reproducing" various complex mechanical parts, such as three-dimensional fuel control valves or turbine blades to original specifications within reasonable machining time.
2. Wages for engineers in Japan compare slightly over half that of U.S. engineers, but their managers are often subsidized with an "expense account" which can be more than their annual salary.
3. While the prices of Japanese goods in Japan are no longer bargains for the American visitor, the prices for US-produced goods are two to three times higher in Japan than in the United States.
4. Traffic noise control seems to receive considerable attention and enforcement, as can be seen from the noise-absorbing barriers built along many major highways through the residential areas in Tokyo.
5. The major Japanese nuclear reactor manufacturers and their market shares are:

Toshiba	(45%)	}	For Boiling Water Reactors
Hitachi	(20%)		
MHI	(35%)	for Pressurized Water Reactors	

6. The major supplier of steam turbines in Japan is Toshiba Company which captures approximately 80% of the market followed by MHI and Hitachi which share the remaining 20% market; current Toshiba sales of steam turbines amount to approximately 3500 MWe per year.
7. Toshiba built a 10-kW experimental fuel cell unit for the Japan Defense Agency, and is conducting a research program on a 6-MWe superconducting alternator in cooperation with MHI.
8. Electric power generated by a future powerplant in Hokkaido will be transmitted by direct-current transmission lines to Tokyo area before inverted to alternating current for distribution to power grids.
9. The three MHI technical institutes and their major activities are listed as follows:
 - Nagasaki - Marine Propulsion and Power Stations;
 - Takasago - Steam and Industrial Gas Turbines, and Hydroelectric Plant;
 - Hiroshima - Steel Structure and Chemical Plants

10. MHI capabilities in aircraft systems are located in Nagoya area, including two airframe plants and two jet engine plants.
11. The IHI is one of the three largest heavy industry companies in Japan and is a sister company of Toshiba Electric Company. Among their main business areas are: shipbuilding, jet engines, steel making, process industry, fossil and nuclear plant equipment, floating platforms, among others. They have built 1700 jet engines and 500 marine boilers to date, and are overhauling P&WA JT8D engines for airlines in the far east.
12. While shipbuilding is still the main business for Mitsui, its share in the company is expected to drop from the current 50 percent to 35 percent when other lines of business in chemical plants, steel structures, and offshore drilling platforms are expected to expand gradually; they manufacture the latest design SB-900 industrial gas turbines, and they are licensee for the Foster Wheeler boilers.
13. KHI is a major Japanese manufacturer of transportation equipment including commercial and military aircraft and ships, gearboxes and thrusters, helicopters (14,000 units built), and the bullet train. Among other major products are: steel-making furnaces, rocket launchers, environment abatement equipment, boilers, incinerators, cement plants (sold to Iran and Algeria), steel mills (to Brazil), sugar plants and also a motorcycle plant built in Lincoln, Nebraska.
14. Intensified technical discussions with the key personnel involved in the design, fabrication and testing of the 10,000-shp closed-cycle gas turbine marine engine built by Mitsui could be extremely useful. Among the key personnel recently identified are Professor (Emeritus) Koyzumi of Tokyo University who was the chief engineer for the project, and Mr. Nakashima who was involved in the design and fabrication of the CCGT marine engine.

REFERENCE

1. Kuo, Simion C.: Recent Development of Closed-Cycle Gas Turbines and Gas-Cooled Nuclear Reactors in West Germany and Switzerland. UTRC Report R76-952566-2, October 1976, and ONR-London Report R-3-77, March 11, 1977.

TABLE I

ITINERARY FOR THE ONR-SPONSORED FACT-FINDING TRIP TO JAPAN
By Dr. Simion C. Kuo, UTRC

Date	AM	PM	Hotel*
9-30 F	--	Lv. Kennedy 12:00 noon via Pan Am 801	
10-1 S	--	Ar. Tokyo 2:40 PM	Imperial
2 S	Orientation/Detailed Trip Planning	Additional Reservations	"
3 M	ONR-Tokyo (US Embassy)	MITI (Ministry of Int. Trad. & Ind.)	"
4 T	IHI Head Office (Tokyo)	IHI Tokyo Shipyard	"
5 W	IHI Tanashi Aero Engine Plant	IHI Mizuho Aircraft Engine Plant	"
6 Th	Maritime Self Defense Force	MHI Head Office (Tokyo)	"
7 F	JAERI (Tokyo)	Mitsui Eng. & Shipbuilding Co. (Tokyo)	"
8 S	--	--	"
9 S	--	--	"
10 M	Japan National Holiday	Toshiba Turbine Works	"
11 T	Toshiba (Tokyo or Kawasaki Office)	Lv. Tokyo for Hitachi City	Open
12 W	Fuji Electric (Tokyo or Kawasaki)	Lv. Hitachi City for Tokai	Open
13 Th	Hitachi Research Laboratories	Lv. Tokai for Tokyo	"
14 F	Tokai Research Establishments	--	"
15 S	--	--	Nagoya Castle
16 S	Lv. Tokyo for Nagoyz by Kikari Train	Lv. Nagoya for Kobe	Oriental (Kobe)
17 M	MHI-Nagoya Aircraft Work	--	"
18 T	Kawasaki Heavy Ind. (Kobe)	--	Nagasaki Tokyu
19 W	Lv. Kobe for Nagasaki via Osaka by Air	--	"
20 Th	MHI-Nagasaki Techn. Inst.	--	--
21 F	Lv. Nagasaki for Tokyo followed by One Week Vacation	Ar. Kennedy 5:45 PM	
31 M	Lv. Tokyo 6:15 PM for US via Pan AM 800		

* Hotel expenses will be paid by UTRC.

TABLE II
MAJOR HEAVY INDUSTRIAL CORPORATIONS AND
THEIR RANKING IN JAPAN

Technology Area	Ranking	1	2	3	4
Closed-Cycle Gas Turbine	Fuji	Mitsui	—	—	—
Marine Gas Turbine	IHI	MHI	KHI	Hitachi Ship	
Industrial Gas Turbine	Hitachi	MHI	Toshiba	Mitsui	
Jet Engine	IHI	MHI	KHI	—	
Steam Turbine	Toshiba	Hitachi	MHI	Fuji	
Marine Transmission	MHI	IHI	KHI	—	
Marine Propeller	MHI	KHI	—	—	
Marine Boiler	Hitachi (B&W)	MHI (CE)	IHI (F&W)	KHI	
Nuclear Reactor	Toshiba/IHI	MHI	Hitachi	Fuji	
Shipbuilding	MHI	IHI	KHI	Mitsui	
Heavy Electric Equipment	Toshiba	Hitachi	Mitsubishi Electric	Fuji	
Hydroplant	Hitachi	MHI	Toshiba	Fuji	

TABLE III
MAJOR DESIGN FEATURES OF MITSUI 10,000-SHP CCGT MARINE PROPULSION SYSTEM

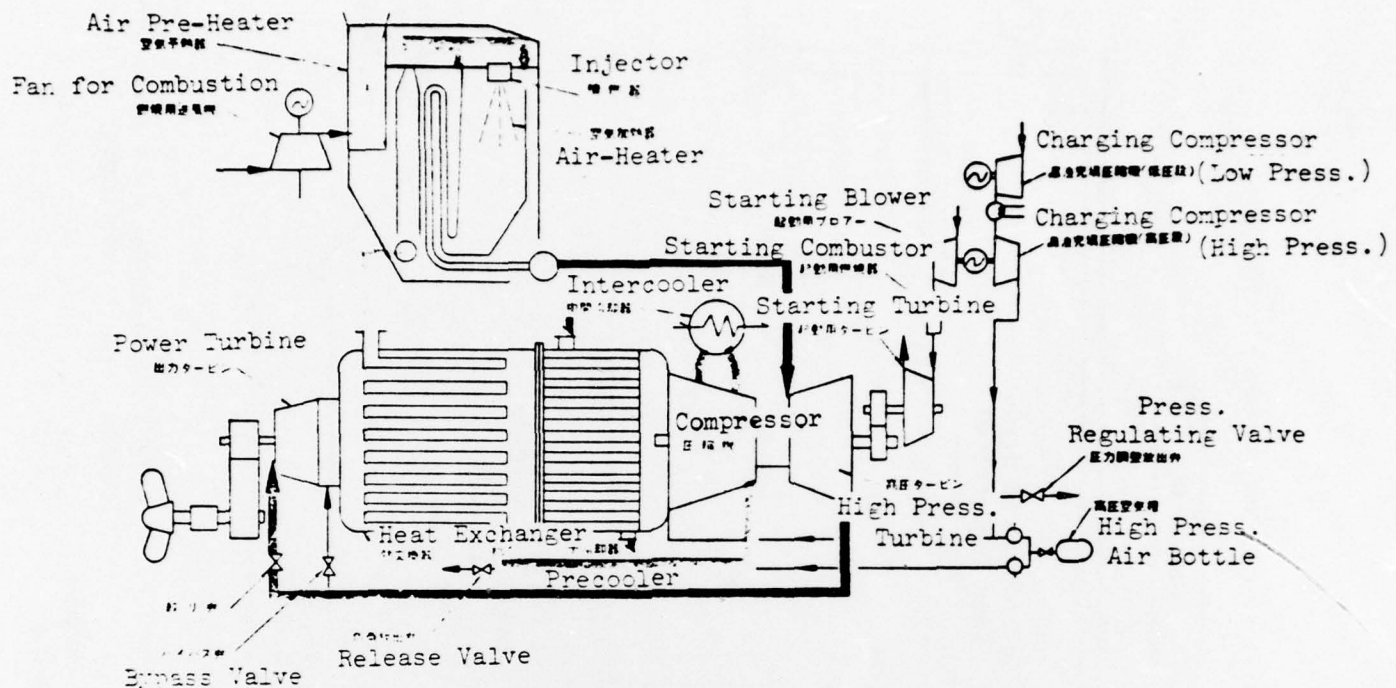
Cycle:	Closed-Cycle Air Turbine with Regeneration and Precooling				
Turbomachinery:	Two-Shaft with Low-Pressure Power Turbine				
Air Heater:	Indirect Heating Vertical Tubular Type				
Fuel:	Diesel Oil				
Compressor:	Centrifugal Type, 3 stages, 8500 ~ 8700 rpm				
Comp. Turbine:	Axial Flow, 4 stages				
Power Turbine:	Axial Flow, 3 stages, 7760 ~ 4550 rpm				
	1/10 Load (Cruising)		Full Load		
Shaft Horsepower	1,170 shp				10,220 shp
Pressure Ratio	4.4				3.9
Air Flow	8.5 kg (18.7 lb)/sec				94 kg (207.3 lb)/sec
TIT	725 C (1337 F)				670 C (1238 F)
Max. Pressure	6.1 kg/cm ² (86.7 psi)				64.5 kg/cm ² (917.2 psi)
Propeller RPM	205				350
Reduction Gear	Single Helical Dual Tandem Articulated Type				
Propeller	Mitsui/Eshier Wyss	Controllable Reversible			

TABLE IV
BASIC DESIGN CONDITIONS FOR THE VENUS-II
TEMPERATURE REACTOR

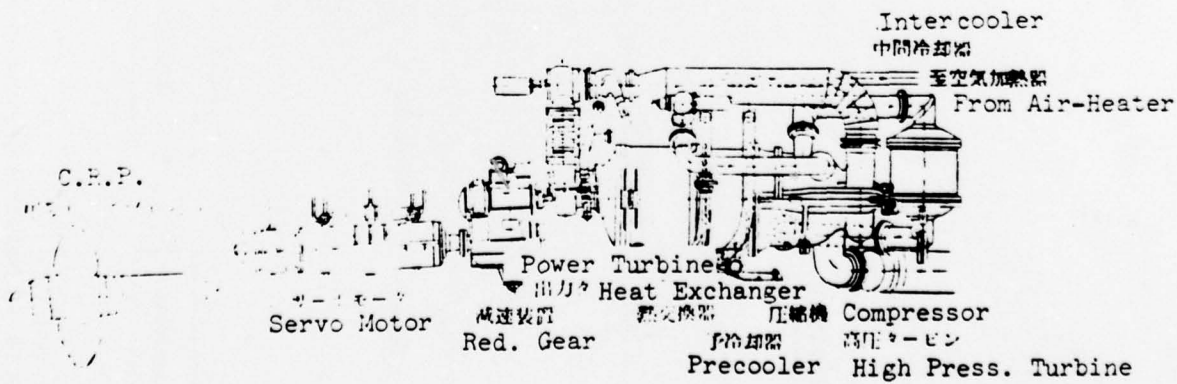
Main items	Basic design conditions
1 Reactor thermal output (nominal)	50MW
2 Reactor outlet coolant temperature	1,000°C
3 Reactor inlet coolant temperature	The temperature must be determined with regard to specifications of the reactor vessel and helium circulator, as well as to thermal characteristics of the core
4 Fuel	UO ₂ kernel coated fuel particle, graphite matrix, dispersion type
5 Fuel element type	Pin-in-block type
6 Direction of coolant flow	Downward flow through the core
7 Pressure vessel	Steel
8 Number of primary coolant circuits	2
9 Heat transmission	Indirect (Addition of IHX)
10 Primary coolant pressure	40kg/cm ² G
11 Secondary coolant pressure	Higher than that of the primary coolant
12 Components in the secondary circuit	Heat removal components Heat utilizing components
13 Containment	Reactor and primary cooling system are adopted in the containment building.

ESHER WYSS/MITSUI 10,000 shp CLOSED-CYCLE AIR GAS
TURBINE MARINE PROPULSION SYSTEM

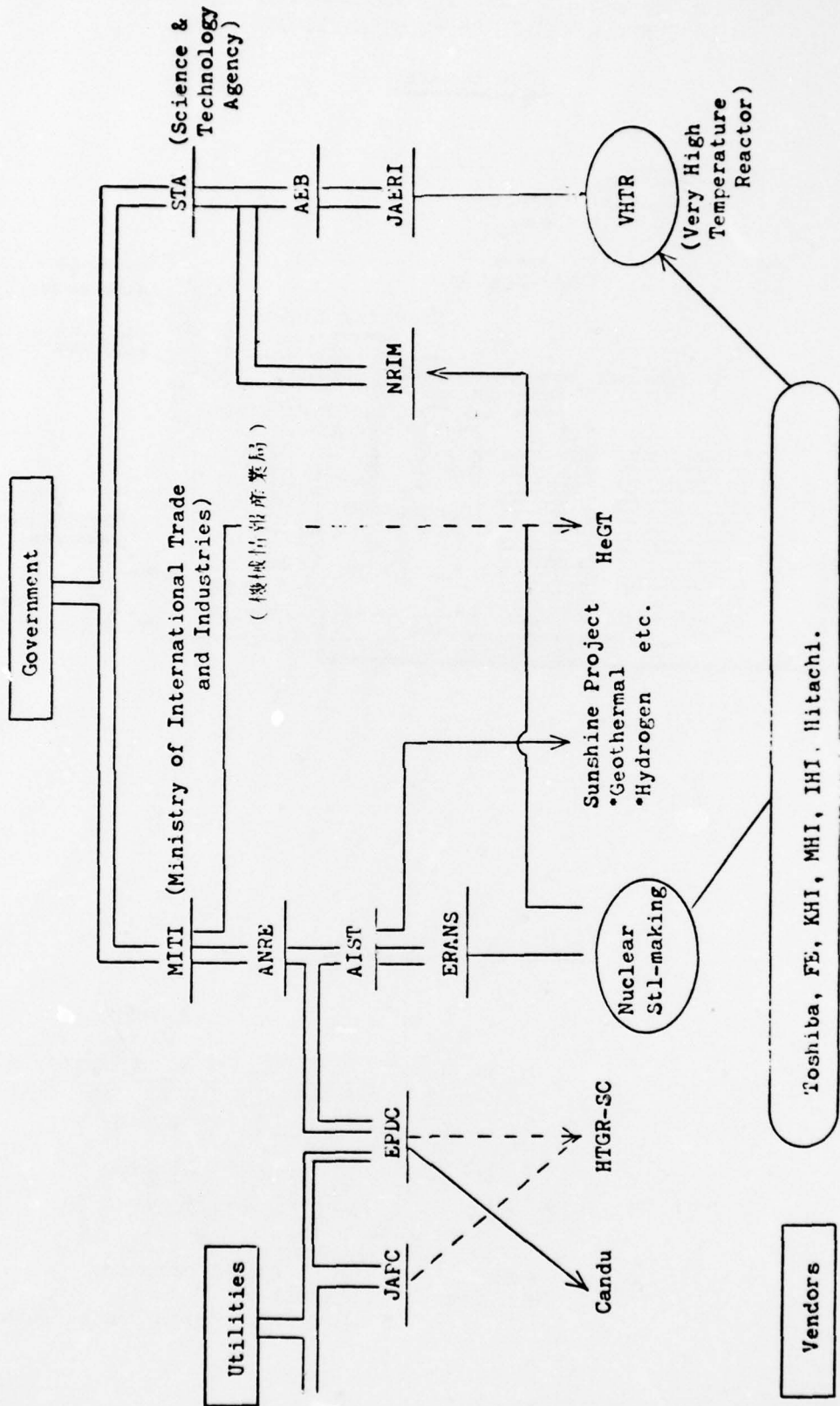
Flow Diagram



Machinery Arrangement



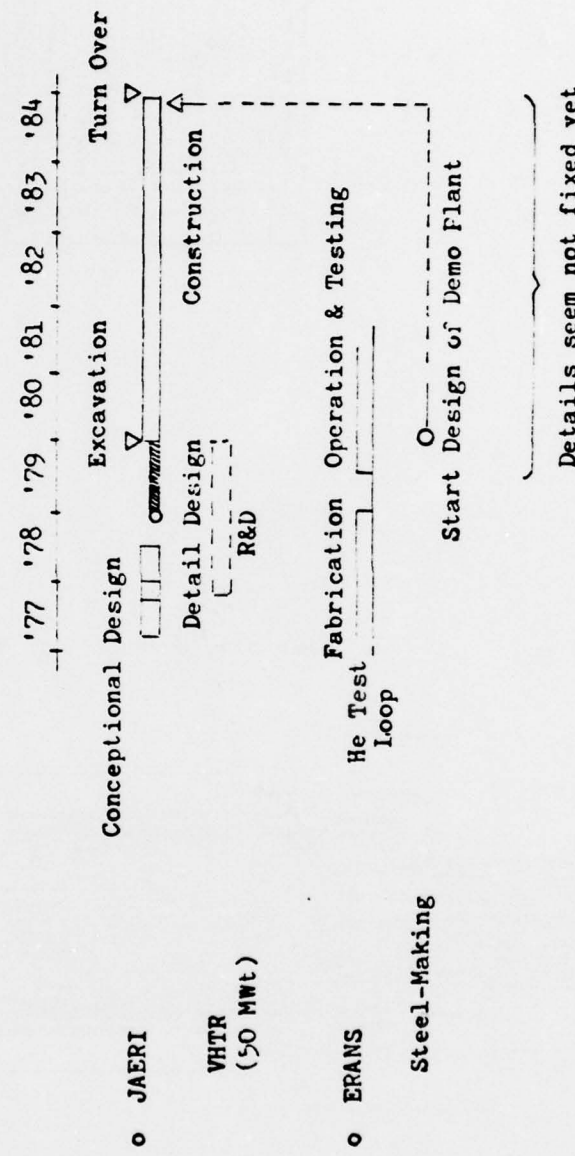
ORGANIZATION CHART FOR THE ADVANCED NUCLEAR REACTOR PROGRAM IN JAPAN



ANRE : Agency of Natural Resources & Energy
 AIST : Agency of Industrial Science & Technology
 ERANS: Engineering Research Association for Nuclear Steelmaking
 AEB : Atomic Energy Bureau of Science and Technology Agency

NRIM : National Research Institute for Metals
 JAERI: Japan Atomic Energy Research Institute
 EPUC: Electric Power Development Co.
 JAFC: Japan Atomic Power Co.

PROPOSED SCHEDULE FOR DEVELOPMENT OF ADVANCED
NUCLEAR REACTOR IN JAPAN



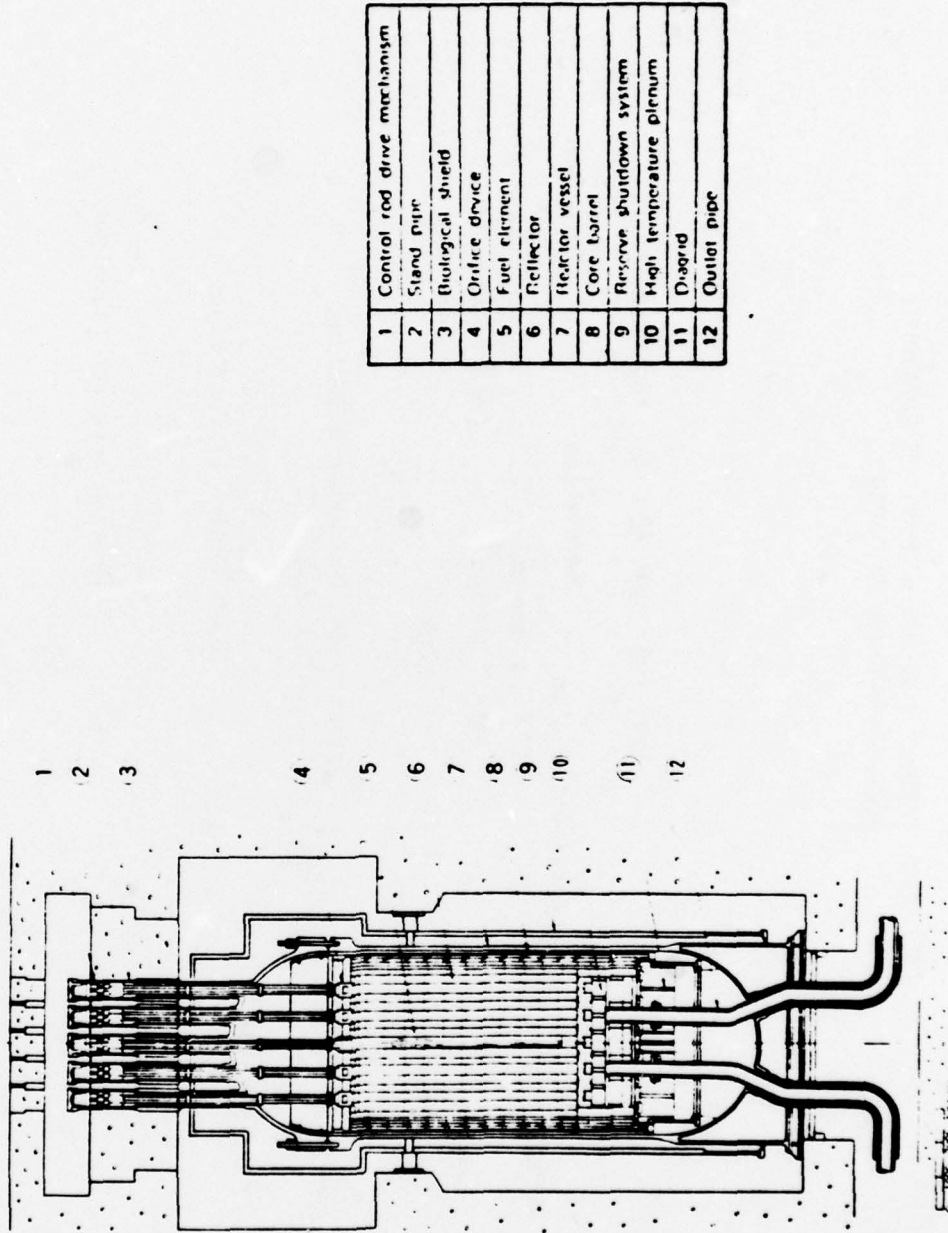
JAERI: Japan Atomic Energy Research Institute

VHTTR: Very High Temperature Reactor

ERANS: Engineering Research Association for Nuclear Steelmaking

NUCLEAR POWER SYSTEM OF REACTOR,
WAKI AND HIGH TEMPERATURE REACTOR,
TOKAMAK

FIG. 4. Cross-sectional view by WAKI, Japan



DISTRIBUTION LISTS

Mr. M. Keith Ellingsworth (6)
Program Monitor
Office of Naval Research
800 North Quincy Street
Arlington, VA 22217

Defense Advanced Research Projects Agency (1)
Attn: CAPT Cox
1400 Wilson Blvd.
Arlington, VA 22209

Mr. John A. Sackowski (1)
Director, Power Program
Office of Naval Research
800 North Quincy Street
Arlington, VA 22217

United States Coast Guard Research & Technology
Attn: CAPT D. B. Flanagan
400 7th Street SW
Washington, DC 20590

Commander, Defense Contract Admin. (1)
Services District, Hartford
96 Murphy Road
Hartford, CT 06114

Director, Naval Research Lab. (6)
Attn: Code 2627
Washington, DC 20375

Defense Documentation Center (12)
Bldg. #5, Cameron Station
Alexandria, VA 22314

Office of Naval Research Branch Office
495 Summer Street
Boston, MA 02201

Commanding Officer (1)
Office of Naval Research Branch Office
495 Summer Street
Boston, MA 02201

United States Naval Post Graduate School (1)
Dept. of Mechanical Engineering
Attn: Dr. R. H. Munro
Monterey, CA 93940

Defense Advanced Research Projects Agency (1)
Director of Tactical Technology
Attn: Dr. Robert Moore
1400 Wilson Blvd.
Arlington, VA 22209

Mr. Carey Kinney
Department of Energy
6000 1st Street NW
Room 408-RB
Washington, DC 20545

Mr. E. F. Brady
Ingalls Shipbuilding
Advanced Engineering Program Directorate
P. O. Box 149
Pascagoula, MS 39567

Mr. Robert Allen (1)
David W. Taylor
Naval Ship Research & Development Center
Code 012
Bethesda, MD 20884

Dr. Earl Quandt (1)
David W. Taylor
Naval Ship Research & Development Center
Code 272
Annapolis, MD 21402

Mr. F. R. Riddell (1)
Institute for Defense Analyses
Room 9A11
400 Army & Navy Drive
Arlington, VA 22202

Mr. James Remain (1)
Headquarters, Naval Material Command
(NAT) 033
Washington, DC 20360

Mr. Zel Lavine, Director (1)
Office of Advanced Ship Development
Department of Commerce
Maritime Administration
Box 4610, Code 920
14th & E Street, NW
Washington, DC 20230

Mr. Frank Hellriegel (1)
NSFC, 2011
3700 East-West Highway
Prince Georges Plaza
Hyattsville, MD 20782

Mr. Colin F. McDonald
Manager, Gas Turbine Preliminary Design Branch
General Atomic Company
P. O. Box 81608
San Diego, CA 92138